READING THE RAINBOW:

TAILORING THE PROPERTIES OF ELECTROCHROMIC POLYMERS

A Dissertation
Presented to
The Academic Faculty

by

Justin Adam Kerszulis

In Partial Fulfillment
of the Requirements for the Degree
Doctor of Philosophy in the
School of Chemistry and Biochemistry

Georgia Institute of Technology
December 2014

READING THE RAINBOW:

TAILORING THE PROPERTIES OF ELECTROCHROMIC POLYMERS

Approved by:

Dr. John R. Reynolds, Advisor
Schools of Chemistry and Biochemistry;
Materials Science and Engineering
Georgia Institute of Technology

Dr. Samuel Graham
School of Mechanical Engineering
Georgia Institute of Technology

Dr. David Collard
School of Chemistry and Biochemistry
Georgia Institute of Technology

Dr. Vladimir Tsukruk
School of Materials Science and Engineering
Georgia Institute of Technology

Dr. Christine Payne
School of Chemistry and Biochemistry
Georgia Institute of Technology

Date Approved: October 22nd 2014

“Why do two colors, put one next to the other, sing? Can one really explain this? No. Just as one can never learn how to paint.”
-Pablo Picasso

“He who cannot paint must grind the colours.”
-German Proverb

To my family, friends, and Natasha

ACKNOWLEDGEMENTS

It’s a strange feeling to end the journey of a PhD. If one assumes to live 100 years, the average time of graduate studies is ~5-6% of a lifetime. With that in mind, make the most of it but not only through hard work and production of knowledge but also through building relationships and forming memories. This is one of the grandest periods of intellectual and personal growth where the evenings of failures and struggles are just as important as those of success and celebration. It is also an experience that should not be endured alone and here I would like to recognize those that inspired to get me here or helped me along the way because we only go as far in life as others around us allow.

I first want to thank the professors at Florida State that showed me what I was capable of and inspired me to acquire a PhD. Thank you to Dr. Hilinski, whose teaching methods instilled good academic habits and made a tangible sense of chemistry; to Dr. Zhu for giving me my first research experiences as an undergrad; and to Dr. Goldsby for motivating me to finish the language requirements and switch to the chemistry major.

As I was always attracted to colors, I want to thank Dr. Reynolds for giving me the opportunity to be a part his group at the University of Florida and at the Georgia Institute of Technology. His dedication to students, discipline and thoroughness in science molded me to not only be an expert in a large scientific field but also allowed me to be free and enthusiastic in all of my graduate endeavors. I also want to thank him for surrounding me with an army of expert senior graduate students, post-docs, and research scientists that allowed me to ask the questions that yielded a successful graduate career.

I would like to also thank the authors of the referenced publications herein from the Reynolds group. Without their diligence, intelligence, and work ethic, these projects would not have the firm scientific footing to succeed.

Moving from the University of Florida to the Georgia Institute of Technology was an incredibly stressful but valuable experience that presented many unique opportunities. It allowed me to experience two different universities, different plans of action, how to build and set up a lab, how to disassemble a lab, and how to deal with an influx of academic and personal challenges. It also allowed me to have two committees. Thank you to Dr. Wagener, Miller, Toth, and So, the committee at the University of Florida which granted me PhD candidacy and thank you to Dr. Collard, Payne, Tsukruk, and Graham for the collaborations and allowing me to complete this dissertation.

I was lucky to join the group when I did. I was able to interact with the largest and most unique group of individuals and learned immensely from all of them. Thank you to Rayford Bulloch for allowing me to rope him into the group, catalyzing the endless memories of simultaneous productivity and lunacy; a true friend and colleague. To Coralie Richard for a humor I still do not fully understand but undoubtedly agree with. Pho, Toan for his keen sense of direction, I truly appreciate it. To Chi Kin Lo, mainly for his planning of many after lab events. Sorry that you could not move with us but thank you to Brendan Sweeny, a man of many hats and genius wit.

A special thank you to Chad Amb for mentoring me in my first years of graduate school, a post-doc that somehow knew the answer to every conceptual question or how to solve every experimental problem; to Mike Craig for the many late night synthetic discussions, unique humor, and a constant willingness to discuss new ideas; and to

Aubrey Dyer for her expert counseling in electrochemistry and guidance through the vastness of the literature. Thank you to Sai Shum for all the advice and guidance in the professional world and for making program reviews exciting. Thank you to all of the graduate students and post-docs that I had the fortune of spending time with: David Liu, Frank Arroyave, Pengjie Shi, Ken Graham, Egle Puodziukynaite, Andy Spring, Dan Patel, Leandro Estrada, Eric Shen, Gaëlle Deshayes, Caroline Grande, Jacob Jensen, Anna Österholm, James Ponder, and Rylan Wolfe; many habits, discussions, and nuggets of knowledge stuck with me as well as the memories from extracurricular activities. Thank you to Eric Knott, Emily Thompson, and Andy Chilton, a group of intelligent undergrads while at the University of Florida and to Keith Johnson at Georgia Tech, one of the most impressive undergraduates I've met. I regret the inability to articulate my gratitude for all the memories and experiences I shared with everyone.

On a more personal note I want to thank those that remained very close to me. To Michael Richards for his invaluable friendship, insight, and its effect on my personality while remembering how to make 2/3 of a cup. Good luck in the Navy and I wish you and Dani the best. Thank you to my dear friends Ryan Cook, Elliott Monroe, and Joseph Sottilare for bringing home to me throughout undergrad and graduate school. A heartfelt thank you to Natasha for her patience, thoughtfulness, kindness, support, and for putting up with my décor at inappropriate times of the year. Thank you to my brother, sister-in-law, niece and new nephew for the pumpkin patches and Easter egg colorings. Finally, thank you to my parents Joanne and Walter for supporting me in every possible way. Thank you dad for giving me your sense of humor and mom for your appreciation of color and beautiful things. I hope I can repay you with more than a box in the future.

TABLE OF CONTENTS

LIST OF TABLES

LIST OF FIGURES

LIST OF SCHEMES

LIST OF EQUATIONS

LIST OF SYMBOLS AND ABBREVIATIONS

a*	greenness or redness
AcDOT	Acyclic DOT; 3,4-(2-ethylhexyloxy)thiophene
ACN	Acetonitrile
b*	blueness or yellowness
BTD	Benzothiadiazole
CB	Conducting Band
CBz	Carbazole
CE	Counter electrode
CIE	International Commission on Illumination
CMY	Cyan-magenta-yellow
CT	Charge transfer
CV	Cyclic voltammetry
D50	Standard illuminant, white light at 5000 kelvin
D-A	Donor-Acceptor
DCM	Dichloromethane
DMA/DMAc	*N*,*N*-dimethylacetamide
DMF	*N*,*N*-dimethylformamide
DOT	3,4-dioxythiophene
DPV	Differential pulse voltammetry
E_g	Band Gap
E_{ox}	Oxidation Potential
EBE	EDOT-BTD-EDOT

ECD	Electrochromic Device
ECP	Electrochromic Polymer
EDOT	3,4-ethylenedioxythiophene
EtOAc	Ethylacetate
GPC	Gel permeation chromatography
HOMO	Highest Occupied Molecular Orbital
ITO	Indium Tin Oxide
JND	Just noticeable difference
L*	Lightness
LiBTI	Bis(trifluoromethyl)sulfonylimide
LUMO	Lowest Unoccupied Molecular Orbital
M_n	Number-average molecular weight
M_w	Molecular weight average
MCCP	Minimally Color Changing Polymer
NBS	*N*-bromosuccinimide
NIR	Near-infra-red
NMP	*N*-methylpyrrolidone
PC	Propylenecarbonate
PDI	Polydispersity index
PEDOT	3,4-polyethylenedioxythiophene
Ph	Phenylene
PivOH	Pivalic acid
P3MT	Poly-3-methylthiophene
PPy	Polypyrrole
PS	Polystyrene

PT	Polythiophene
ProDOT	3,4-propylenedioxythiophene
RE	Reference electrode
RYB	Red-yellow-blue
SEC	Size exclusion chromatography
SpecEchem	Spectroelectrochemistry
$TBAPF_6$	Tetrabutylammonium hexafluorophosphate
TCB	1,3,5-trichlorobenzene
THF	Tetrahydrofuran
VB	Valence Band
WE	Working electrode
X_n	Number-average degree of polymerization

SUMMARY

Electrochromism is defined as the change in the color of a material as a result of an applied voltage. This color change can be defined as switching when the charge states (oxidized and reduced) are alternately cycled. When color is generated upon oxidation, the material is anodically coloring, while color generation upon reduction, is termed cathodic coloration. In this dissertation, the properties of 3,4-dioxythiophene (DOT)-based π-conjugated electrochromic polymers (ECPs) are explored with a focus on using synthetic methods to control structure-property relationships to achieve desired light absorption across the visible region of the spectrum with the goal of attaining desired color neutral states. Because of the electron rich nature of the DOT moieties, these polymers are able to switch to highly transmissive oxidized states, allowing these materials to be utilized in full color window or non-emissive display applications. Chapter 1 begins with an introduction to optics, how the human eye perceives color, the background of conjugated polymers and electrochromism, and ultimately a discussion on the applications of these materials. In Chapter 2, comparisons of the various methods to synthesize ECPs are taught and then the synthetic procedures for this dissertation are detailed. Following this, Chapter 3, details a discussion concerning the proper processing and characterization of ECPs, ranging from film casting, electrochemistry, spectroscopy, colorimetry, to photography and is taught to ensure high quality and consistency of data. With these introduction and experimental tutorials in mind, Chapter 4 overviews the completion of the color palette with the discovery of ECP-Yellow-1 (P2.1), an ECP that first allowed full color displays and windows to be realized. Unfortunately, this polymer

possessed a high oxidation potential (500 mV with respect to Ag/Ag^{+}), leading to the need to apply high potentials to attain the most transmissive oxidized state (1100 mV), harmful to more easily oxidizable polymers. To amend this, work was conducted to understand the structure-property relationships required to maintain high gap electrochromic polymers (> 2.25 eV) with the ability to be fully oxidized at lower potentials (≤ 800 mV). This work resulted in the final optimization of yellow ECPs with ECP-Yellow-2 (P2.9). With the challenge of achieving high gap, electron rich ECPs overcome, further work was directed to developing methods to affect the broadness of the absorption spectrum of ECPs to achieve new neutral state hues. In Chapter 5 detailed studies were conducted to understand subtle steric interactions along the polymer backbone and its effect on the neutral state visible light absorption and how it can be manipulated to achieve new magenta and blue hued ECPs that are all donating and electron rich with highly transmissive oxidized states (%T > 70). These methods were then applied to prototype ProDOT-EDOT/AcDOT and ProDOT-EDOT/Ph random copolymers in an attempt to produce broadly absorbing ECPs with black-to-transmissive coloration without acceptors. It was discovered that these materials could not achieve the required extents of conjugation necessary to absorb long wavelength light, yielding polymers that were still highly colored (magenta, purple, and orange) in the neutral state. This proved the need for donor-acceptor interactions in random copolymers in order to produce dark or black (low L*) ECPs with contrast greater than 50%. Chapter 6 takes the concepts learned in Chapter 5 and applies polymer backbone steric strain and relaxation to improve the contrast of black ECPs. A subtle increase in strain through the introduction of AcDOT units gave a broader neutral state absorption spectrum in the

visible by absorbing more short wavelength light, making the material more black to the eye. However, when fully oxidized, this polymer exhibited tailing absorption of long wavelength visible light (600-720 nm). To depress this residual absorption in the fully oxidized state, a sterically relaxed donor-acceptor-donor (EDOT-BTD-EDOT) monomer was utilized in random copolymerizations. In these polymerizations, strain was varied to affect the broadness of absorption in the visible spectrum. This gave a polymer that achieved the broadest absorption with the highest electrochromic contrast. The content of the relaxed donor-acceptor was then steadily increased until a new black ECP was produced where the neutral state color was the lowest achieved (L*:45, a*:5, b*:3), appearing black to the eye. It was then able to be switched to a fully oxidized state with minimal color (L*:88, a*:-4, b*:-3), completing Chapter 6, rendering much understanding in producing high contrast black-to-transmissive ECPs.

CHAPTER 1

INTRODUCTION

Electrochromism is a change in the color of a material upon the application of a voltage. In a way, it is the science of light and color, and therefore it is necessary to understand fundamental optics, how your eye perceives color, how conjugated materials behave to allow this phenomenon to occur, and how it can be applied in the world.

1.1. Fundamental Optics

There are four important aspects of optics to understand when concerning the systems discussed herein: absorption, transmission, reflection, and scattering. These are fundamental to how light behaves with respect to ECPs in solutions and thin films.

1.1.1. Absorption, Transmission, Reflection, and Scattering

In this field (and dissertation) we deal with the passage of light through solutions or films. Aside from a polymer's ability to absorb or transmit incident light, the nature of the film or solution can affect the spectra acquired and subsequent data interpretation. Here we will discuss some basic, fundamental optics behind absorption, transmission, reflection, and scattering.

First we will address *transmission* and *absorption* as they are interrelated. Let's concern ourselves with a beam of monochromatic light with radiant power P_0 passing through a medium. When absorption takes place, the beam of light leaving the sample has less radiant power (P). This and the interconversion between transmission and absorption are expressed in Figure 1.1.1.1.

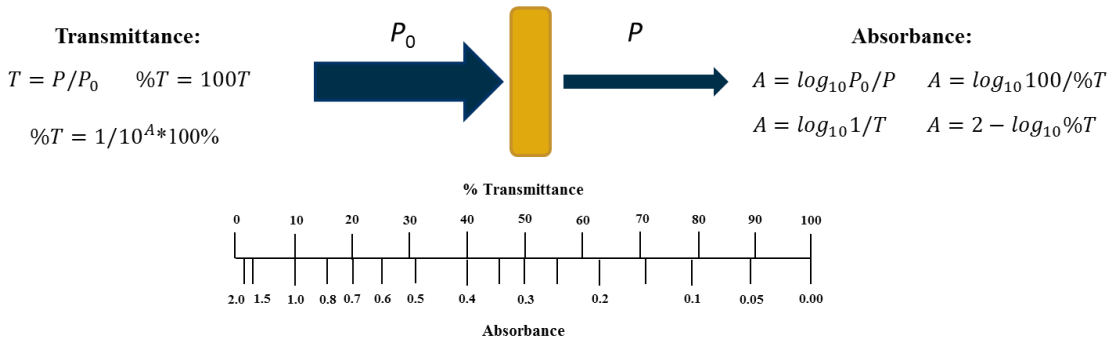

Figure 1.1.1.1: Illustration of the absorption of light in a sample and conversions between absorption and transmission. Concepts adapted from Tipler and Mosca's Physics for Scientist and Engineers.[1]

The absorption of light in ECPs is due the π to π* transition, donor-acceptor (D-A) interactions, or a combination of the two from moieties installed in the polymer backbone (discussed in section 1.3.5).

When light passes through a medium, it is *transmitted* and the material is *transparent*. If a medium has no color, all the light has been transmitted with the exception of a small percentage of light that is *reflected* between the material of one medium and another. The *refractive index* describes how light slows down in a medium relative to speed in air of the two or more different media. The difference in this index can also change the direction of a transmitted beam of light.[2] Small, localized non-uniformities in or on the surface of a medium can change the trajectory of light, causing *scattering*.[3] As illustrated in Figure 1.1.1.2, when light crosses from one medium to another, at the boundary light will change its speed and a fraction of light will be reflected and the beam will have a slight change in direction unless the incident light hits perpendicular to the boundary at *normal incidence*. Light striking non-uniformities scatters in different directions.

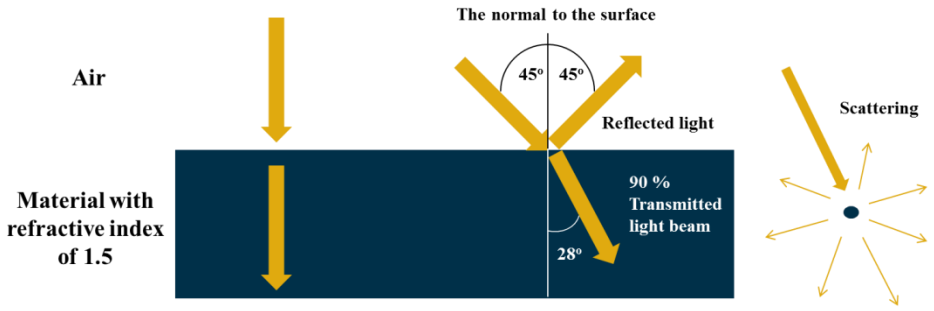

Figure 1.1.1.2: Illustration of index of refraction, reflection, and scattering of light between media.

Concerning reflection once more, there is total reflectance (referred to as *specular reflectance*) and *diffuse reflectance* (can be described as *scattering*);[2,3] this is illustrated in Figure 1.1.1.3. Specular reflectance means that there is perfect reflection of all light where the angle of incidence is equal to the angle of reflection ($\theta_i = \theta_r$) and is accessible through highly uniform, smooth surfaces. Diffuse reflectance occurs when there is a heterogeneity and roughness (non-uniformity) of a surface and the reflected light rays scatter in all directions. This is what causes the difference between a mirror like and opaque surface.

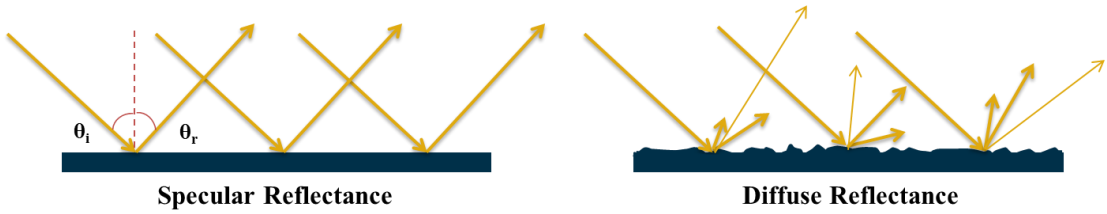

Figure 1.1.1.3: Illustration of specular or diffuse reflectance.

We address this because the ECPs are measured as solutions or solutions cast onto a substrate (glass coated with a thin electrically conducting layer) to form thin films which are then immersed into an electrolyte solution. This introduces multiple layers of different media where the index of refraction changes. As demonstrated in Figure 1.1.1.4, these materials, solutions, and processing methods are not perfect. In solution, aggregation can occur and cause small particles to form where they can cause the

scattering of light. For thin films made *via* spray casting, voids of air can form which create cavities or surface roughness and subsequent index matching issues, scattering light; these films can be described as "hazy" or "rough".

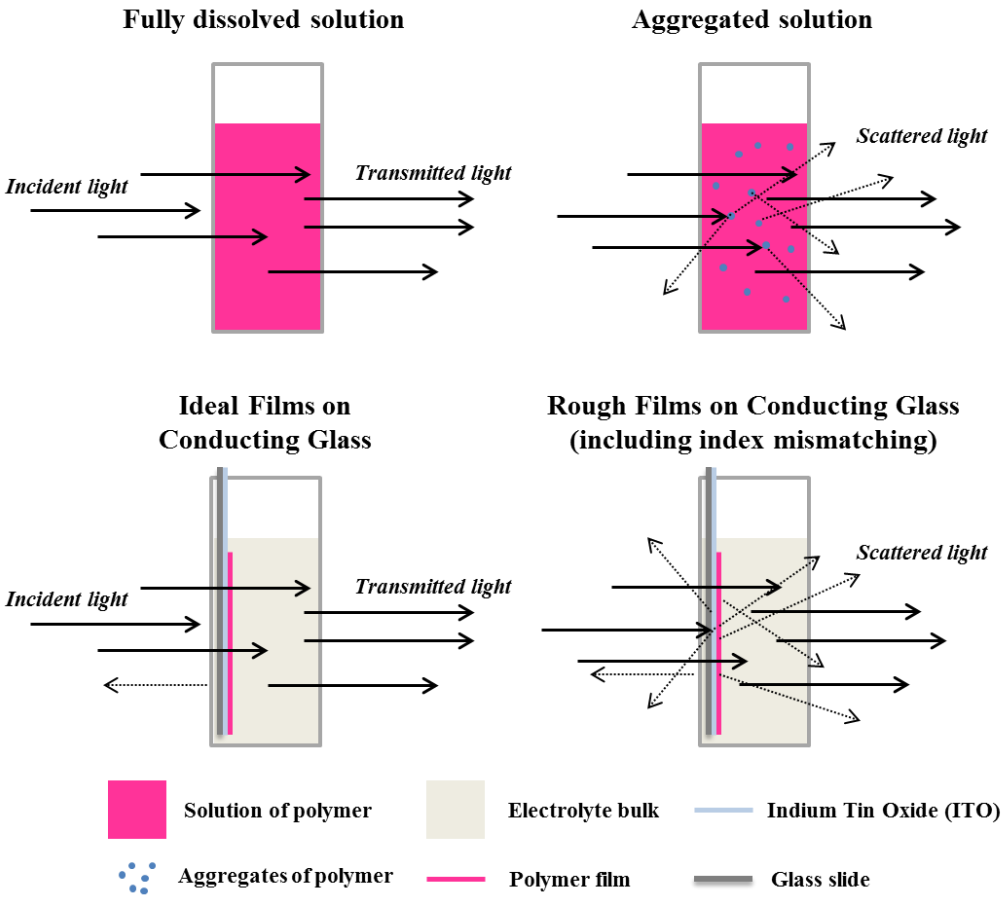

Figure 1.1.1.4: Comparison between the trajectory of light in fully dissolved and aggregated polymer solutions (top) and ideal films of polymer on glass and rough films on glass with index mismatching (bottom).

In a typical measurement setup, the path of light begins at the lamp of an instrument then travels through the cuvette wall, electrolyte (or air), glass slide, conducting surface (ITO), polymer layer, electrolyte (or air), cuvette wall again, and finally into the detector. When light is scattered there will be less light reaching a detector and can commonly be identified as an increase in absorption across the spectrum being observed.

Often times, these ECP films and layers of media can act as anti-reflective coatings at longer wavelengths, giving transmittance values above 100% (absorbance below 0). A

description of this phenomenon is described in Figure 1.1.1.5. In essence certain polymers (or processing conditions) can afford active layers that will cause internal reflection of light allowing more light to reach the detector relative to the baseline.[4,5]

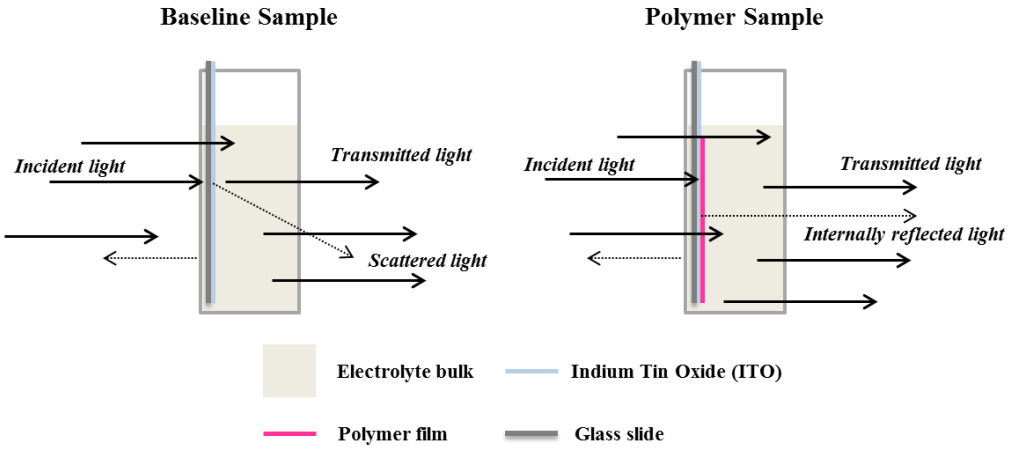

Figure 1.1.1.5: Comparison of light trajectories between baseline and polymer sample.

1.2. Colorimetry and How the Eye Perceives Color

The human eye is typically sensitive in the visible range of 390 nm-720 nm.[6] It is the detector that is essential to our ability to see color. Because the ability to perceive color is subjective and can vary between individuals, the quantification of color is absolutely necessary in electrochromism. The science of this color quantification is colorimetry and was developed extensively by The International Commission on Illumination (CIE)[7] and explained at length by Billmeyer and Saltzman's Principles of Color Technology.[6]

1.2.1. Color Vision and the Anatomy of the Eye

To appropriately quantify color one must understand that the eye detects light with rod and cone cells. There are three types of cone cells each detecting wavelengths that the brain then interprets as color, while there is only one type of rod cell that is more sensitive to low intensity light but serves no known function in color vision. Both the rods and cones reside in a portion of the eye known as the fovea. The highest

concentration of cone cells is located in the center of the fovea, as evident from Figure 1.2.1.1. This is known as the 2^{o} observer in colorimetry and is the center of vision. As the angle from the fovea becomes greater, the distribution of cones drops dramatically while rods increase; this is known as the periphery.

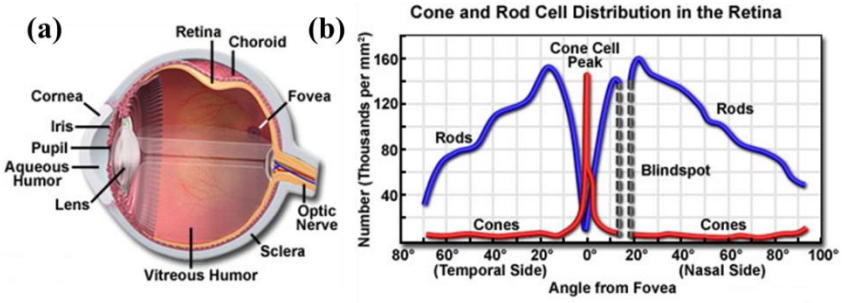

Figure 1.2.1.1: (a) Vertical sagittal section of an adult human eye. (b) Distribution of rod and cone cells relative to the center of the Fovea. Figure adapted with permission from the Florida State University website: Optical Microscopy Primer, the Physics of Light and Color.[8]

In humans, there are three cone cells and they are sensitive to long wavelength light (L-cone, peak sensitivity range: 564–580 nm), medium wavelength light (M-cone, peak sensitivity range: 534–545 nm), and short wave light (S-cone, peak sensitivity range: 420–440 nm), these cones can be thought of as three parameters of stimulus. Their spectral sensitivities can be seen in Figure 1.2.1.2. Rod cells are most sensitive at 498 nm.

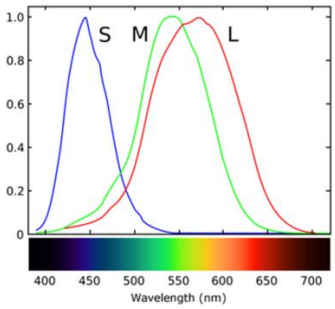

Figure 1.2.1.2: The normalized spectral sensitivities of cone cells.

If the total light power spectrum is weighted by the individual spectral sensitivities of the three types of cone cells, one will get three effective stimulus values and, thus, we have formed the basis of the three values of tristimulus specification for the objective color of light: X, Y, and Z.

1.2.2. CIE Standard Observers

Because of the distribution of cones in the eye, tristimulus values are dependent on the observer's field of view. Since a majority of the cones reside in the 2^o arc of the fovea, the 2^o standard observer color matching functions are used to better quantify the cone response in the human eye.[9] The color matching function curves for the standard observers can be seen in Figure 1.2.2.1 and are analogous to the spectral sensitivities of the L ($\bar{x}$), M ($\bar{y}$), and S ($\bar{z}$) cones.

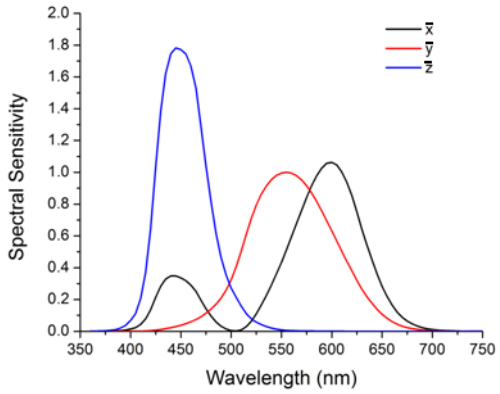

Figure 1.2.2.1: The distribution functions for the standard observers $\bar{\mathbf{x}}$, $\bar{\mathbf{y}}$, and $\bar{\mathbf{z}}$.

Considering the luminance or brightness of a color, if light is of equal power, humans tend to perceive green light as brighter than red or blue. To quantify the relative luminance (brightness) of colors under bright conditions (photopic vision), a standard observer ($\bar{y}$) is used to establish a luminosity function to properly differentiate color values on a given color space. This function is similar to the peak spectral sensitivity of the M cone which provides a maximum efficacy of 683 lm/W at a wavelength of 555 nm

(green). This is why yellow is always perceived as "bright" (high L*), due to the maximum stimulation of $\bar{y}$ from reflected or transmitted medium and long wavelengths of light.

1.2.3. Calculating Colorimetry Values

The tristimulus values calculated for color quantification depends upon an observer's field of view; this variable was eliminated when the CIE defined standard observers to represent cone stimulus in a 2^o arc inside the fovea of the eye. The equations to quantify the color of an object (where the object reflects light given off from a source) or a source (colored light being emitted) can be seen in Equation 1.2.3.1.

$$X = K\int_{380}^{780} S(\lambda)\bar{x}(\lambda)R(\lambda)d\lambda \qquad Z = K\int_{380}^{780} S(\lambda)\bar{z}(\lambda)R(\lambda)d\lambda$$

$$Y = K\int_{380}^{780} S(\lambda)\bar{y}(\lambda)R(\lambda)d\lambda \qquad K = \frac{100}{\int_{380}^{780} S(\lambda)\bar{y}(\lambda)R(\lambda)d\lambda}$$

Equation 1.2.3.1: Equations to calculate tristimulus values to quantify color.

For calculating tristimulus values for color, $S(\lambda)$ is the relative spectral power distribution of a standard illuminant (e.g., illuminant A, D65, D50, etc.), as provided by CIE. $\bar{x}(\lambda)$, $\bar{y}(\lambda)$, $\bar{z}(\lambda)$ are the CIE 1931 spectral tristimulus values and are constant, and $R(\lambda)$ is the measured spectral reflectance (or transmittance) of an object. If one is measuring light coming directly from a source, not passing through a filter, $R(\lambda)$ is not used. K is a normalization constant and depends upon what is being measured. If one is measuring the color of a primary light source K=683 lm/W. If one is measuring an object, the K factor described in Equation 1.2.3.1 is used. Once tristimulus values are calculated they can be plotted into a color space.

A color space displays a gamut, or all possible colors in a quantitative form. Two color spaces are commonly used in electrochromics: they are the xyY and the L*a*b*. Artistic renditions of the two spaces can be found in Figure 1.2.3.1. The xyY color space has a

gamut that is horse-shoe shaped and the edge of the gamut is the spectral locus and all colors along the edge are spectral colors (monochromatic light of single wavelengths). The flat edge is the line of purples and is not monochromatic but rather a mixture of blue and red light. White and less saturated colors appear towards the center of the gamut.

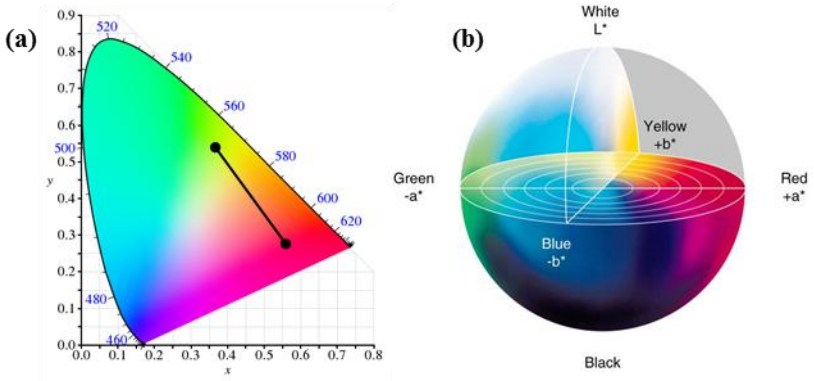

Figure 1.2.3.1: (a) xyY color space. (b) Artist rendition for L*a*b* color space.[6]

A straight line between two points within the gamut represents all possible colors through mixing the extremes of the line, as shown in Figure 1.2.3.1a. Though xyY is widely used, it lacks uniformity in geometric distance between color points, for example the space of greens is much larger than for yellow. The L*a*b* color space allows for 3 dimensional uniformity in color points. In this color space, the L* represents the brightness of a color with 0 being black and 100 being white, a* represents greens and reds while b* represents blues and yellows for negative and positive values respectively. As values of a* or b* progress farther from the origin, the greater the saturation (chroma). As values of a* or b* travel around the circumference of the sphere, hue changes in a uniform manner.

(a) $$y = \frac{Y}{X+Y+Z} \qquad x = \frac{X}{X+Y+Z}$$

(b) $$L^* = 116\left(\frac{Y}{Y_n}\right)^{\frac{1}{3}} - 16 \qquad a^* = 500\left[\left(\frac{X}{X_n}\right)^{\frac{1}{3}} - \left(\frac{Y}{Y_n}\right)^{\frac{1}{3}}\right] \qquad b^* = 200\left[\left(\frac{Y}{Y_n}\right)^{\frac{1}{3}} - \left(\frac{Z}{Z_n}\right)^{\frac{1}{3}}\right]$$

Equation 1.2.3.2: Calculations for color values in xyY (a) or L*a*b* (b).

Using the conversions shown in Equation 1.2.3.2, one can determine the color values of an object or a source. For either color space, one needs to use the tristimulus numbers calculated from Equation 1.2.3.1 to acquire color values using the functions in Figure 1.2.3.2 for xyY (Figure 1.2.3.2a) or L*a*b* (Figure 1.2.3.2b) where X_n, Y_n, and Z_n are the tristimulus values of the illuminant.

1.2.4. Relationship of Absorption, Observers, and the Eye

Since we have examined how the eye perceives color and its quantification, let us examine a practical example as this form of data will be repeated many times in this dissertation. For electrochromic polymers, a spectroelectrochemistry experiment will yield the colorimetry values as a function of oxidation state attained with an applied potential (as detailed in Chapter 3). A spectrum taken at each voltage is converted into tristimulus values and color coordinates using the equations described above[10] and then plotted into a color space. L*a*b* is used as there is geometric uniformity between points, enabling the visual comparison of different values of various hues or shades of the same color with little confusion.

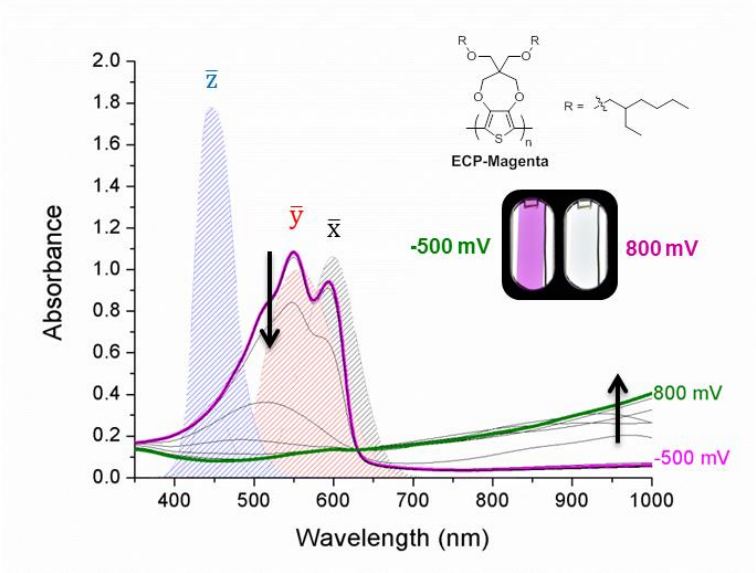

Figure 1.2.4.1: Spectroelectrochemistry of ECP-Magenta with standard observers $\bar{x}$, $\bar{y}$, and $\bar{z}$ overlaid as shaded curves. Structure of ECP-Magenta and photographs of neutral and oxidized states are inset.

Looking to Figure 1.2.4.1, for the polymer known as ECP-Magenta, observe that as the polymer is progressively electrochemically oxidized from a vibrant magenta neutral state (-500 mV) to a transmissive oxidized state (800 mV), there is a progressive loss in absorption that overlaps with the standard observers. This leads to a loss in color and is referred to as "bleaching". The spectra at each state can be converted into colorimetry values using the methods described above (more on how experimentally in Chapter 3) and plotted in the L*a*b* color space, as shown in Figure 1.2.4.2.

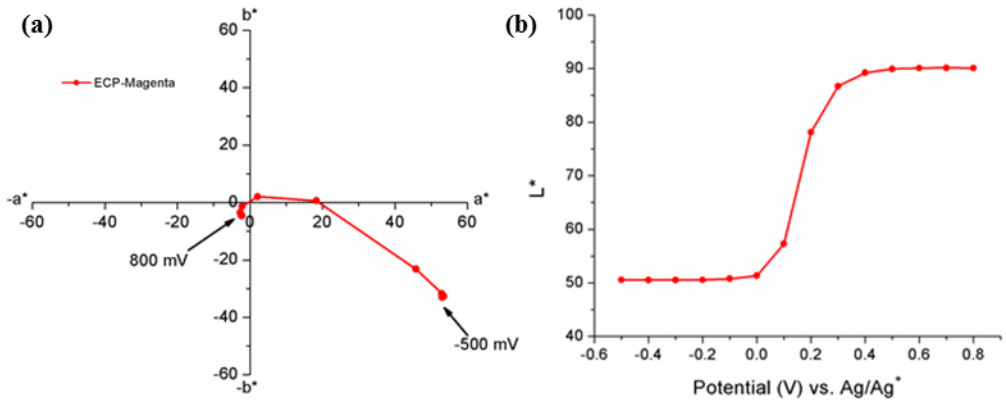

Figure 1.2.4.2: (a) a*b* and (b) L* color coordinates for ECP-Magenta electrochromism.

With the quantification of the color for the electrochromism of ECP-Magenta in hand, at a potential of -500 mV the polymer exhibits a vibrant magenta with values of L*=51.0, a*=51.7, and b*=-32.2. The polymer is then incrementally oxidized to 800 mV where it is transmissive with color values of L*=90.0, a*=-2.4, and b*=-4.2 (fully bleached). Now that we have a grasp on how the eye functions and perceives color, let's discuss the theory of conjugated polymers and how these materials behave and are designed.

1.3. Introduction to Conjugated Polymers, Electrochromism

The discovery of polypyrrole[11] and polyacetylene[12,13] started the field of conjugated polymers. Over time these polymers have structurally evolved to fit numerous applications but in this dissertation we examine the practical application of the theory of conjugated polymers in electrochromism.

1.3.1. Theory of Conjugated Polymers

To understand conjugated polymers, one needs to understand the origin of the band structure. Using polyacetylene as a model, as the number of π bonds increase, there is a proportional growth in the number of new energy levels. These new states are stabilized by an increasing amount of electron delocalization (double bond alternation). With a greater number of π bonds, energy bands arise from the hybridization of an increasing amount of π orbitals, illustrated in Figure 1.3.1.1. The 'distance' between bands (where the HOMO is known as the valence band (VB) and the LUMO is known as the conduction band (CB)) gives rise to an energy or band gap (E_g) and is the source of the properties of conjugated materials, giving rise to the term *band gap engineering*.

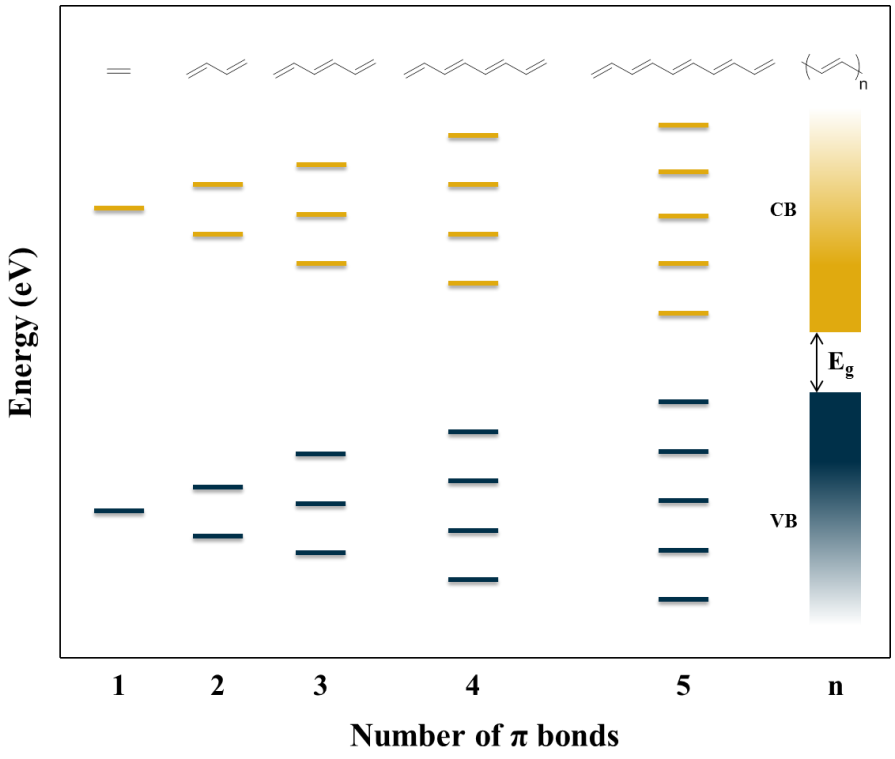

Figure 1.3.1.1: Schematic representation of the evolution of the band gap (E_g) with the extent of conjugation in π-conjugated polymers. Blue energy levels are "filled" (HOMO), gold energy levels are "empty" (LUMO). Adapted from Salzner *et al*.[14]

Ideally, this increasing π electron delocalization would be even along the conjugated backbone and eventually through more and more π bonds, the E_g would close (VB and

CB would touch) and the material would be an intrinsic metal or metallic. In reality, this is not the case as electronic repulsions analogous to those observed in cyclobutadiene, create a geometrical distortion in the conjugated backbone known as Jahn-Teller distortion (or Peierls distortion if you are a condensed matter physicist). This distortion prevents evenly spaced, alternating double and single bonds and thus, the bands push apart, giving rise to the band gap. This model for polyacetylene (which has alternating bond lengths of 1.35 and 1.45 Å) applies for aromatic rings such as phenylenes, pyrroles, or thiophene, where the growing number of rings, bond length alternation, and steric interactions prevent infinitely planar structures and gives rise to the E_g. This is advantageous for electrochromism because this gap can be structurally tuned to give rise to a desired color in one state and then bleached away when doped or oxidized.

It can be generally stated that for conjugated polymers in their neutral forms, the E_g arises from the effective π-conjugation length which is a result of an equilibrium geometry from twisting along the backbone. High degrees of twist will decrease conjugation and yield high gaps (high energy absorption, giving yellow, orange, or red colors) while low degrees of twist will increase the effective conjugation length, yielding low gaps (low energy absorption, giving magenta, purple, or blue colors). Greens and cyans can be achieved by simultaneous absorption in the high and low energy regions of the visible.

Upon progressive oxidation or doping, new equilibrium geometries are achieved. The formation of radical cations (polarons) form localized distortions on the conjugated backbone in the form of relaxation. These mid-gap states possess lower energy absorption transitions. Further oxidation or doping gives rise to a dication (bipolaron), since the localized chain relaxation around two charges (bipolaron) at one point on a polymer chain is stronger than around only one charge (polaron) at two points, and mid-gap states form with even narrower gaps.[15,16] The more relaxed or planar a dication from complete oxidation or doping, the more transmissive the state will become due to the narrower gap.

1.3.2. A Colorful Peculiarity in Polypyrrole and Polythiophene

Polyaromatics were polymerized and studied alongside polyacetylenes to achieve electrically conducting plastics. When films of these materials were produced and then doped, there was a color change associated with an increase in conductance and this change was reversible. As we established, the color of the neutral (undoped) state is dependent on the extent of conjugation which is directly affected by steric effects in the polymer backbone. X-Ray diffraction of polypyrrole (PPy) oligomers suggest the rings are coplanar[17] however, as shown in Scheme 1.3.2.1, substitution at the nitrogen or the β-position introduces greater steric repulsion and a twist is induced along the backbone eliminating the zero dihedral angle θ (θ≠0 when R_1≠H and R_2≠H).

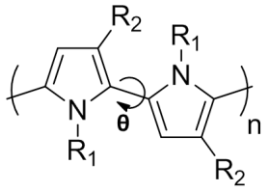

Scheme 1.3.2.1: Twist in the backbone of polypyrrole represented by dihedral angle θ.

Films of PPy[18,19,20] and polythiophenes (PTs)[20,21] expressed electrochromism, the colors and structures of the extreme states are illustrated in Scheme 1.3.2.2. PPy in the neutral state when dopant ions are fully removed (only accomplished in films thinner than 1 μm) is yellow-green in color (due to structural defects upon polymerization, reducing extent of conjugation)[22,23] switching to a blue-violet oxidized state. This was not a practical color change and the films would decompose over repeated cycling due to the electron rich nature of PPy causing over oxidation.

To attenuate this, PT was utilized as it is less electron rich, inhibiting over oxidation. However, like PPy, electropolymerized unsubstituted PT suffers from α-β, β-β coupling defects. To amend this, methyl groups were installed onto the 3-position of poly(3-methylthiophene) (P3MT). The methyl groups also had the effect of increasing conjugation (slightly red shifting optical transitions), attributed to the statistical decrease

in insulative α-β couplings.[21] This helps to stabilize oxidized states, hence the slight difference in color between PT and P3MT in their extreme states.

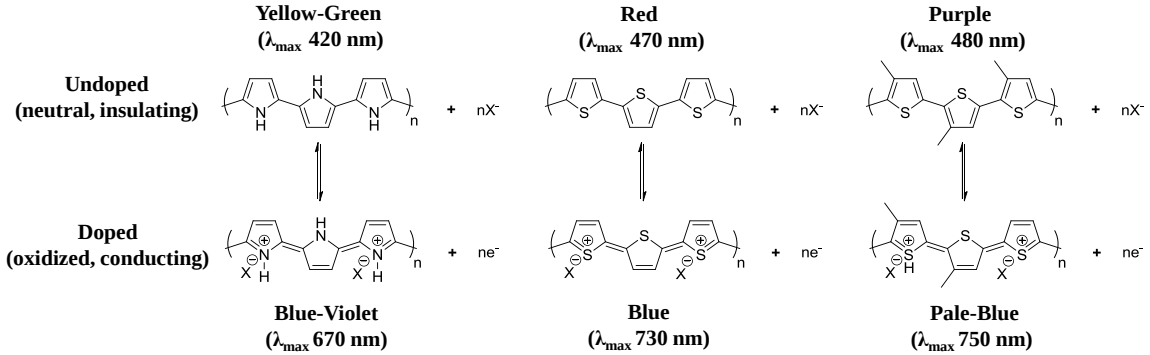

Scheme 1.3.2.2: Schematic representation of the doped and undoped forms of polypyrrole and polythiophenes and their colors in either state.

1.3.3. Discovery of PEDOT

Given that unsubstituted heterocycles are prone to structural defects at the β position during polymerization, Heywang and Jonas reported the synthesis and characterization of a 3,4-ethylenedioxythiophene (EDOT)-based polymer (PEDOT).[24] This material was cathodically switching and exhibited a neutral state λ_{max} of 621 nm (2.0 eV) giving a blue color. Upon oxidation, a sky blue near transmissive color was observed due to tailing absorption into the long wavelength portion of the visible. The discoloration was due to increasing absorption in the near-infra-red (NIR) while a decrease in absorption occurred at 621 nm.

The success of PEDOT was due to the addition of a dioxyethylene bridge between the 3 and 4 positions of the thiophene ring, making it the first dioxythiophene (DOT). Aside from effectively blocking the β positions, protecting them during polymerizations, the oxygen atoms donate π-electron density into the heterocycle, making the ring electron rich and easier to oxidize. This effect raises the HOMO of the subsequent polymer, imparting these types of materials with low oxidation potentials (E_{ox}). This architecture is able to stabilize bipolarons to such a degree that they absorb energy far outside of the

visible and into the NIR making them highly transmissive and nearly colorless when fully oxidized. This makes DOTs attractive to electrochromic applications as you want materials that can achieve vibrant colored states with high absorption in the visible and can then switch to colorless, transmissive states with high absorptions outside of the visible. PEDOT kicked off a colorful race to achieve all colors of the rainbow to transmissive electrochromic polymers for use in devices such as smart windows and nonemissive displays.

1.3.4. Chemistry of Dioxythiophenes

Dioxythiophenes have high utility in the field of electrochromism. They possess low oxidation potentials imparted by electron donation from oxygen π-electrons on the β positions of the thiophene ring. They are relatively air stable and can be handled under ambient conditions with little degradation. The 2 and 5 positions are readily exploitable for a variety of reactions. DOTs can be produced using straight forward synthesis starting from thiodiglycolic acid for the production of 3,4-dimethoxythiophene in Scheme 1.3.4.1a.[25,26] These first methods however, required multiple steps. To favor industrial resynthesis, a one-step route towards 3,4-dimethoxythiophene was reported in 2004[27] and is shown in Scheme 1.3.4.1b. The cyclization gives the product in high yield with distillation as the only purification step. A third and viable route starting from thiophene is also possible shown in Scheme 1.3.4.1c. The thiophene is completely brominated to tetrabromothiophene[28] which is then subsequently and selectively dehalogenated with zinc metal in glacial acetic acid.[29] The final step utilizes Ullmann etherification with a copper (I) catalyst.[30]

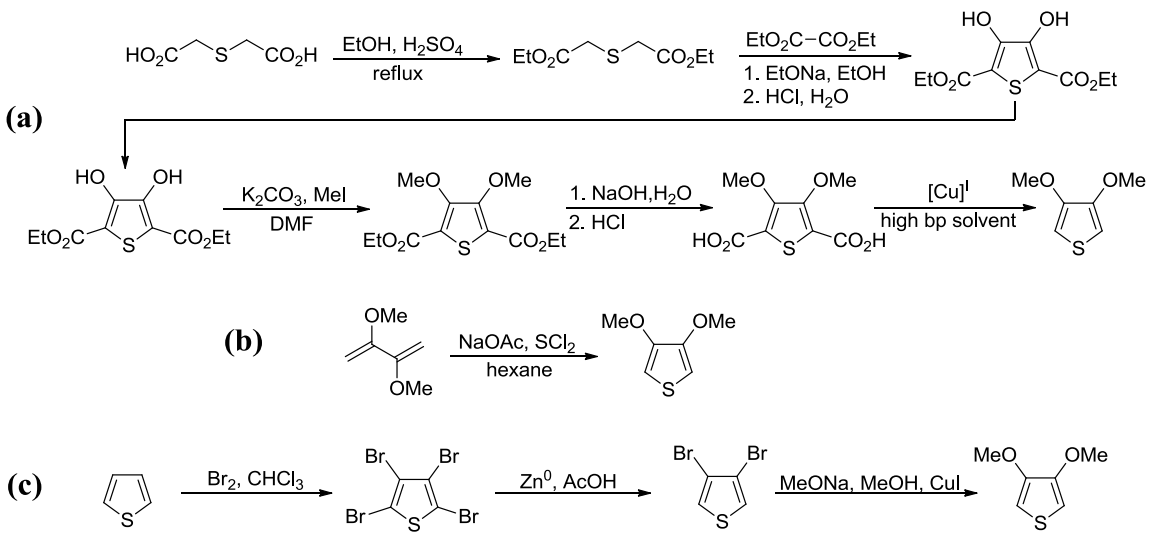

Scheme 1.3.4.1: (a) Total synthesis of 3,4-dimethoxythiophene starting from thiodiglycolic acid. (b) Once-step route for synthesis of 3,4-dimethoxythiophene. (c) Alternate route starting from thiophene.

The 3,4-dimethoxythiophene starting material can then be modified *via* acid catalyzed transetherification and Williamson etherification to yield substituted monomers for polymers to achieve a number of properties such as solubility for processing from organic or aqueous solvents[31] or to tune optical properties.[32,33,34] Just a few examples of these reactions are shown in scheme 1.3.4.2 and are all high yielding and do not require complex purification methods beyond distillation, recrystallization, or flushing through pads of silica. The brominations to form **C** and **E** are quantitative in yield and the products are stable under ambient conditions. Molecules **A**, **B**, **D**, and **F** can be dimerized using Ullman-like copper or iron catalyzed conditions[35,36] to access structures to tune the absorbance or electrochemical properties of subsequent polymers. These reactions are also scalable, capable of being produced in kilogram quantities; suitable for industrial reproduction.

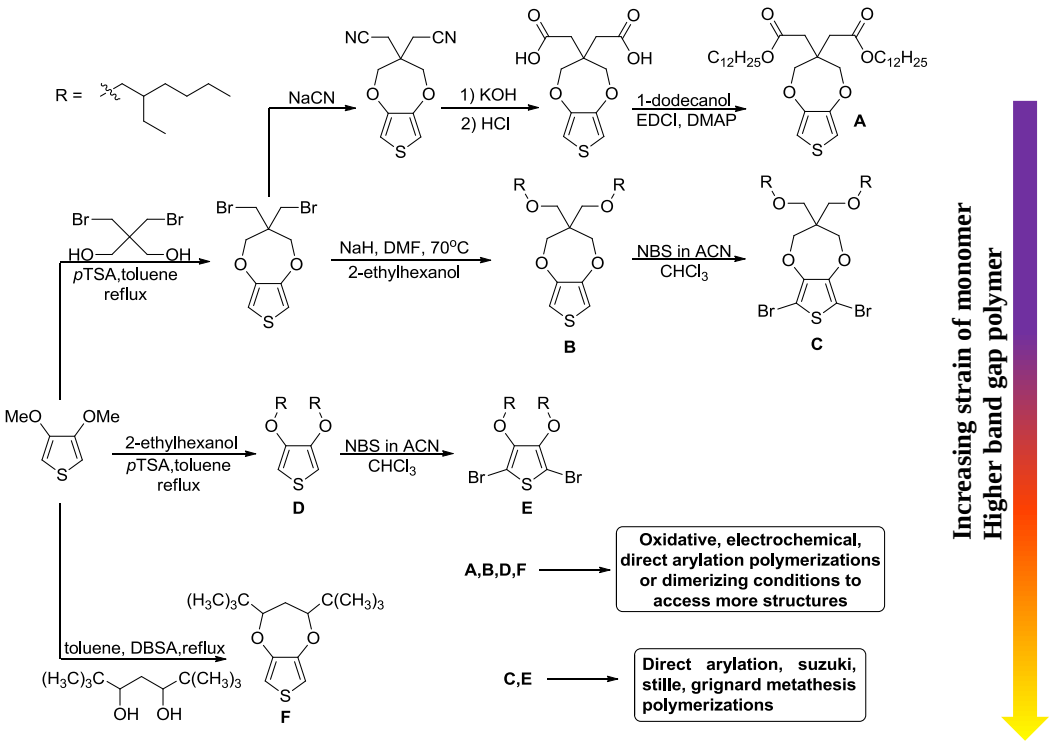

Scheme 1.3.4.2: Typical synthetic routes to achieve monomers for DOT based ECPs and what polymerization methods are appropriate for the indicated monomer.

To form polymers, **A**, **B**, **D**, and **F** can be polymerized using oxidative (iron(III) based),[37] electrochemical,[38] or direct arylation (palladium based) polycondensation conditions.[39,40] Molecules **C** and **E** can be used in a variety of transition metal cross coupling polycondensation reactions to form polymers using Suzuki,[41] Stille,[42] direct arylation,[39,40] and Grignard metathesis conditions.[33] These polycondensations are typically high yielding and give M_n greater than 10 kDa. All of the polymers formed from monomers above are organic soluble and can be cast into films using organic solvents with the exception of **F**. The ester side chains in the homopolymer of **A** can be hydrolyzed under basic conditions to yield a water soluble polymer that can be cast into films from water and rendered insoluble with treatment with acid. This and general polycondensation

conditions for Stille, Suzuki, and direct arylation can be found in scheme 1.3.4.3. These polycondensation reactions will be discussed in greater detail in chapter 2.

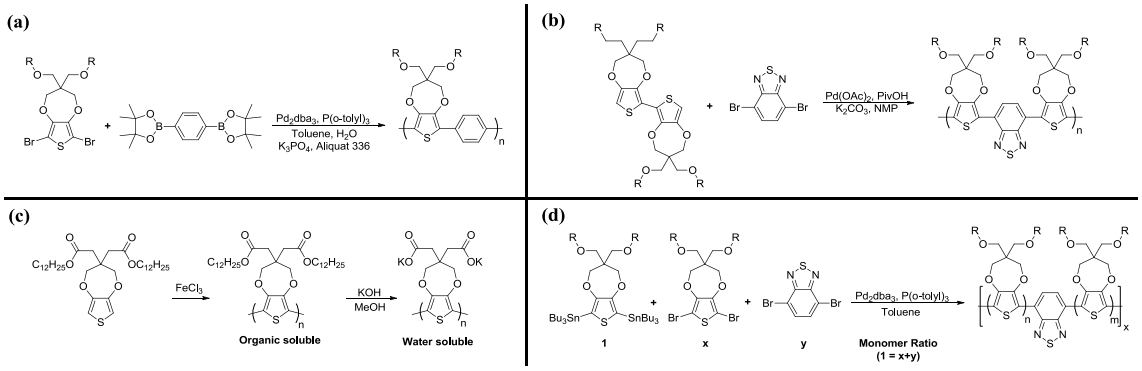

Scheme 1.3.4.3: General polycondensation schemes for Suzuki (a), direct arylation (b), oxidative (c), and Stille (d).

1.3.5. A Completed Color Palette of ECPs

The nature of the E_g directly affects the optical or color properties of a designed polymer; this is why we care to *engineer* band gaps. The method to tune optoelectronic properties in ECPs is broken down into the model shown in Figure 1.3.5.1. Coarse control is accomplished with the appropriate selection of heterocyclic backbone (for these discussions, thiophene). The addition of oxygens in the β positions not only lowers the E_{ox} of the polymer, but the nature of the dioxy groups can fine tune optical properties.[43] From smaller to larger rings bonded to the β positions, the E_g will increase; the largest gaps can be achieved with acyclic dioxy systems.[32] The nature of the size of the side chains can also affect the E_g. With smaller, unbranched alkyl groups allowing greater relaxation along the backbone giving lower band gaps while larger, branched chains give higher band gaps from increased torsional strain along the conjugated backbone.[34] The nature of the chains can be tuned to achieve solubility in desired solvents;[31] if you find a polymer is insoluble in organic solvents, a good rule of thumb is to increase the size and bulk of the solubilizing chains. Finally, the optoelectronic properties can be further tuned

by the use of another aryl ring in an alternating or random fashion; the electron richness or poorness can affect the redox properties.

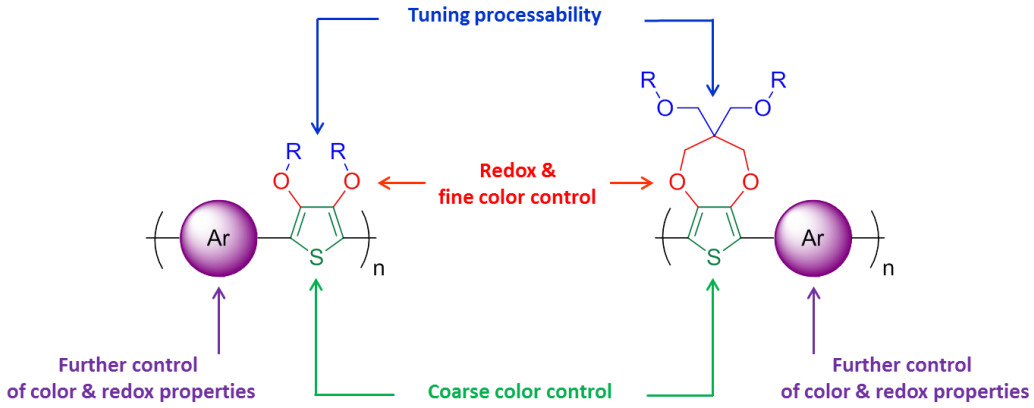

Figure 1.3.5.1: Model for tuning optoelectronic properties in ECPs.

Using this model, our group has been able to access a full color palette of ECPs.[44] As complex as conjugated polymers are, this was and still is accomplished through coarse color control using steric interactions along the backbone or donor-acceptor effects. The structures of polymers and their respective colors are shown in Figure 1.3.5.2.

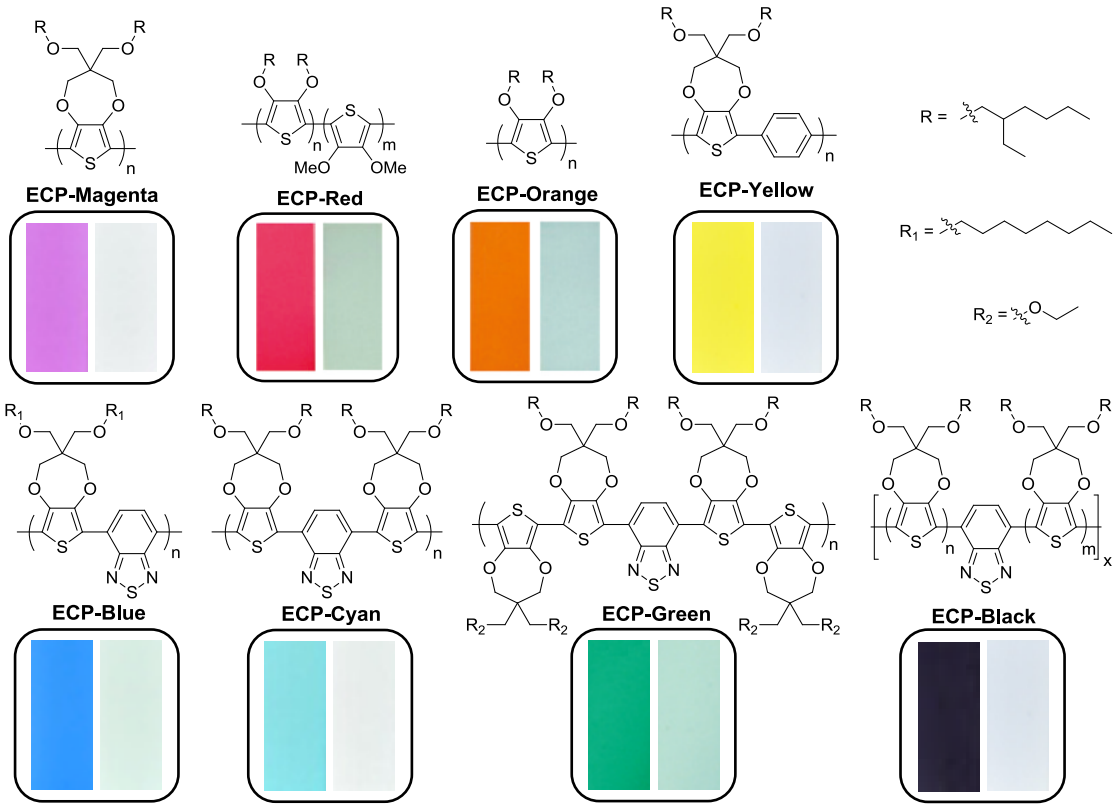

Figure 1.3.5.2: Structures for all soluble, DOT based ECPs produced in the Reynolds group that complete the color palette.

To relate the structure-property relationships, the spectra of each polymer (except for ECP-Black) and color coordinates at various potentials are shown in Figure 1.3.5.3. Steric effects tuning the π to π* transition have allowed access to magenta,[33] red, orange,[32] and yellow;[45,46] from low to high strain shifting the absorption to progressively shorter wavelengths of light respectively. Donor-acceptor effects have allowed access to blue,[41,47] cyan,[48] and green[49,50] where the variation in the dual band absorption is a result of π to π* from varying level of donor content (absorbing short wavelength light) and D-A interactions (absorbing long wavelength light), the λ_{max} of this can be shifted to longer wavelengths with increasing relaxation or number/electron richness of the donors.[49,51]

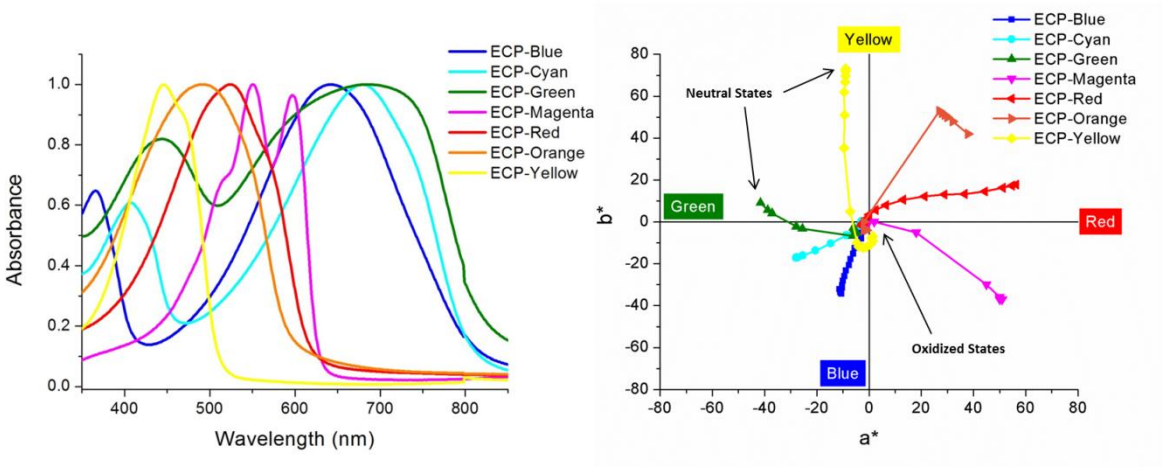

Figure 1.3.5.3: Spectra (left) and color coordinates (right) of DOT based ECPs produced in the Reynolds group that complete the color palette.

ECP-Black is a random copolymer; this randomness is what imparts its color properties as illustrated in Figure 1.3.5.4. The polymer was made using a complex balance of the two methods. The first employs random lengths of D-A, which yields low energy transitions absorbing long wavelength light; the stronger or greater the D-A interaction, the lower the energy transition. The second employs random runs of donors along the backbone affording varying extents of conjugation and giving rise to moderate and higher energy transitions, absorbing short and medium wavelengths of light; short extents of conjugation give rise to high energy transitions and longer extents give rise to moderate energy transitions. The random nature of the polymer gives a nearly even distribution that enables it to absorb broadly across the visible spectrum, giving a material that is black in color.[42,51]

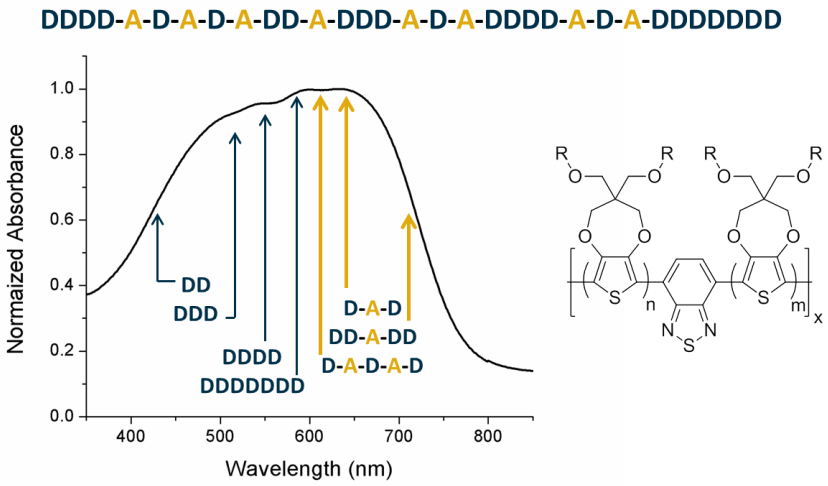

Figure 1.3.5.4: Illustration of various optical transitions that give rise to total absorption across the visible.

A colorless to colorless ECP based on a dioxypyrrole (dubbed, minimally color changing polymer (MCCP)) has been utilized as a counter electrode material for charge balance in devices.[52] For a more detailed analysis on dioxypyrroles please see the dissertations by Ryan Walczak[53] and Frank Arroyave.[54]

As was noted with the small molecule reactions, the polycondensation conditions to produce these ECPs are scalable, capable of producing polymer in the tens of grams or greater. To emphasize scalability, Figure 1.3.5.5 is a photograph of a 6 g standing film of ECP-Magenta and a 300 g scale of ECP-Yellow.

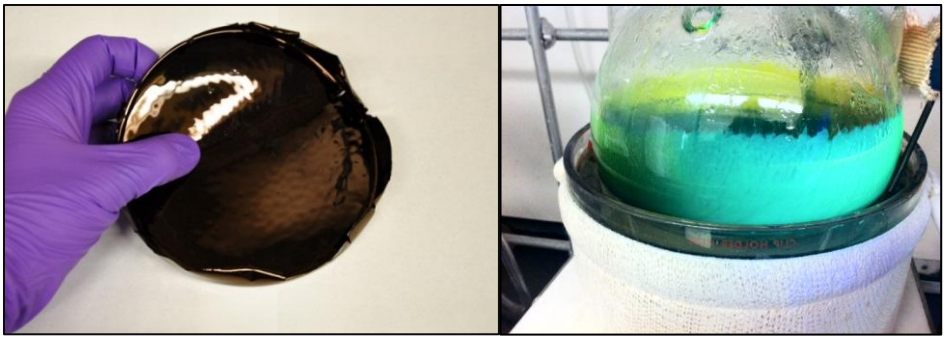

Figure 1.3.5.5: A cast film of ~6 g of ECP-Magenta (left). Suzuki polycondensation, 300 g scale (right).

1.4. Out of the Cuvette and Towards Applications

Here we will address electrochromic applications, not limiting ourselves to conjugated polymers. There are several classifications of electrochromic materials: inorganic (Prussian blues and metal oxides), organic small molecule (viologens and dimethylterephthalates) and polymeric (based on polypyrrole and polythiophene). These materials have demonstrated the possibilities in a range of applications.

1.4.1. General Electrochromic Device Architecture

In order to realize applications of electrochromics, we shall briefly discuss the architecture of electrochromic devices (ECDs) based on polymers, but this is generally the same for other materials.[55,56] For a typical ECD, the layers of activity from closest to the eye to furthest are as follows: Glass, ITO, ECP, Gel Electrolyte, ECP, ITO, and Glass where the glass/ITO layer has conducting metal contacts to a power source. There are two forms of ECDs, reflective and transmissive. A pictorial representation of a reflective ECD is shown in Figure 1.4.1.1. In a reflective ECD, The same ECP is deposited on each ITO/Glass layer to maintain a charge balance. The boundary between layers possesses a white, diffuse reflecting gel electrolyte by utilizing titanium dioxide passivated with other insulating metals.[57,58,59,60] This same concept can be utilized with porous reflective metals.[61,62] On either side of the reflecting electrolyte layer, each polymer is in an extreme state opposite to the other. When electrochromic switching occurs, you will only

see the color change of the front most ECP layer and the color change behind the reflecting gel electrolyte is of no consequence.

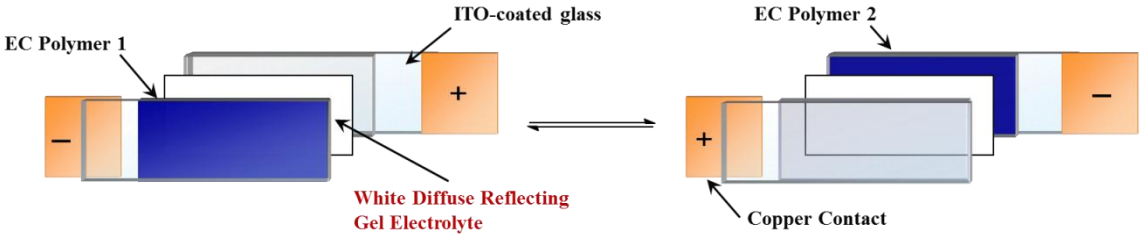

Figure 1.4.1.1: Schematic of a reflective ECD. Adapted from the dissertation of Aubrey Dyer.[63]

The architecture for a transmissive ECD is very similar to the reflective with the exception that the gel electrolyte possesses no reflective material; this is illustrated in Figure 1.4.1.2. Since you are now seeing *through* all of the layers, the color change at the two electrodes matters. To provide charge balance during electrochromic switching, non-color changing materials are required to act as counter electrode materials; as mentioned at the end of section 1.3.5, MCCP can be used.[52,64]

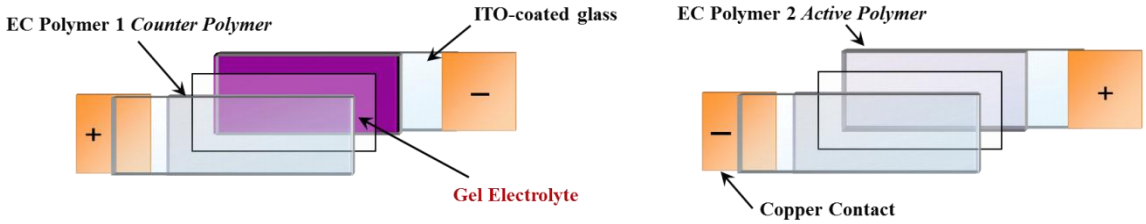

Figure 1.4.1.2: Schematic of a transmissive ECD. Adapted from the dissertation of Aubrey Dyer.[63]

1.4.2. Applications of Electrochromism

- Mirrors

Our first application is mirrors which are essentially reflective ECDs. These are devices that are capable of self-darkening for automotive applications whilst driving at night. These would prevent the dazzling of drivers *via* reflection of headlights by neighboring cars off of the various mirrors around the vehicle. In essence an electrochromic material

is coated over a conventional mirror and acts as a color filter to reduce the intensity of the reflected light.[65,66,67,68,69]

- Transmissive ECDs for Windows in Buildings, Aircraft, and Eyewear

The second application is general windows for buildings and aircraft. In 1985 "smart window" was coined by Svensson and Granqvist as a term for windows that electrochromically change transmission.[70] In these devices, the electrochromic layer acts as a light filter, and rather than having shutters, you are able to select "tint" settings to eliminate or allow as much light as desired. These devices can have an impact on the environment and structure running cost as these devices can filter out much solar radiation from an enclosed space, eliminating the need to constantly apply climate control while enhancing comfort.[71,72,73,74,75] View Inc. and Sage Glass have installed electrochromic windows in building across North America and parts of the world.[76,77]

For aircraft applications, these devices could be installed with sensors or manual controls to turn them on (colored) or off (transmissive), allowing them to completely darken or allow all light to pass. Through cooperation between the Gentex Corporation, PPG Aerospace, and Boeing, electrochromic windows have been installed on the Boeing 787 "Dreamliner".[78,79] A personal favorite example is in military applications where either a pilot's helmet visor or cockpit canopy would darken when a fighter rises above clouds and then becomes transmissive when it flies below clouds, relieving the pilot's eyes and concentration during operations as they would no longer need manually lift or lower the current tinted visors. This same idea for helmet visors has been attempted for generic eyewear. Electrochromic eyewear is different from photochromic as photochromic materials change color based on the intensity and wavelength of ambient light. EC eyewear has been explored in the past, but yielded little business success and is an area for improvement in the future.[80,81,82,83]

- Nonemissive Image and Data Displays

Operating in either a reflective or transmissive mode (majority being reflective),[84,85,86] ECDs would be able to display full color information using a subtractive color mixing scheme.[87,88,89] Initial applications for such displays were suggested as watch faces[90] but now they can be utilized in data and advertising boards, and indicators on security cards or banknotes.[91,92,93,94]

Electrochromic displays are referred to as "passive" since they do not emit light and would not be subject to issues of glare from outdoor sunlight like emissive display systems. Some have felt that electrochromics "definitely exceeded the original iPod [screen] in crispness and brightness.[95] Since they do not emit light, and are capable of electrochromic memory meaning power is not required for prolonged periods of time to maintain a state. Though these ECDs do rely on an external light source, limiting their use to well-lit applications, to get around this, a white back light beneath the electrochromic layer can be utilized. However, another route has shown that EC materials can be utilized in dual use emissive/nonemissive systems, allowing day and night applications.[96,97] Research has been rather imaginative in the use of substrate for these displays, giving rise to ECDs based on paper or cloth.[98,99,100,101] These and various niche applications are discussed at length by Monk *et al.*[102]

1.5. Dissertation Thesis

Herein encompasses the synthesis and characterization of electrochromic polymers, with the goal of controlling light absorption to acquire desired colors and redox properties. As we saw, Chapter 1 introduced concepts of optics, human color vision, conjugated polymers, electrochromism, and applications. Chapter 2 overviews the primary polycondensation methods used to synthesize ECPs, and establishes a set of guidelines to produce the polymers weighing the pros and cons of the polycondensation methods. Chapter 3 contains all experimentals in conducting processing and characterization of ECPs and will be established as a guide for new students to follow. Chapter 4 details the

introduction of yellow-to-transmissive ECPs through utilizing subtle *ortho* C-H phenylene interactions neighboring DOTs to achieve polymers with band gaps higher than 2.25 eV, where ECP-Yellow-2 (P2.9) optimizes yellow in the completed color palette of ECPs. Chapter 5 presents trends in modulating steric effects in alternating all donor ECPs to tune hues of magenta and blues through subtle increases in strain and relaxation respectively. As these polymers are all donors they achieve bleached states with transmittance values greater than 70%. With these trends in hand, random copolymers based on ProDOT-Ph/EDOT and ProDOT-AcDOT/EDOT were produced in an attempt to give broad visible absorptions with neutral state colors at low L*a*b* values without the use of acceptors. These random copolymers could not achieve the required extents of conjugation necessary to absorb long wavelength visible light to give black ECPs as evident by their highly color neutral states. Because acceptors need to be employed to achieve black-to-transmissive ECPs, Chapter 6 focuses on the use of steric strain of main chain donors and steric relaxation around acceptor moieties to enhance the broadness and contrast of black ECPs. This was ultimately achieved with a new black ECP where the neutral state color was the lowest achieved (L*:45, a*:5, b*:3), appearing black to the eye and was then able to be switched to a fully oxidized state with minimal color (L*:88, a*:-4, b*:-3).

CHAPTER 2

CONDUCTING CONJUGATED POLYMER SYNTHESIS

Polymer synthesis is no easy task; it can be nerve-wracking to conduct polymerizations using precious monomers that have taken much effort to synthesize and purify. Therefore to prevent wasted effort in conducting polymerizations that fail to reach an acceptable degree of polymerization and conjugation lengths, we will discuss the main methods that are used to produce conjugated polymers, with ECPs being the focus. We will discuss the mechanisms and examples of each polymerization, compare the methods to give the best information available to make educated decisions on polymerization choice, review purification, and close with synthetic methods used to make the materials in this dissertation.

2.1. Conjugated Polymerizations

The number-average degree of polymerization (X_n) refers to the number of monomer units in a polymer or oligomer chain. For a homopolymer, X_n is described by Equation 2.1.1 where M_n refers to the number-average molecular weight distribution of a polymer, as measured by GPC (interchangeably referred to as size exclusion chromatography (SEC) and gel permeation chromatography (GPC)) and M_0 refers to the molecular weight of the monomer repeat unit. For example, a polymerization yielding ECP-Magenta with a M_n of 32,000 Da, gives a X_n of ~73, or 73 repeat units.

$$X_n = \frac{M_n}{M_0}$$

Equation 2.1.1: Number-average degree of polymerization.

For an alternating copolymer M_0 can be found by combing the total weight of both repeat units while for a random copolymer, M_0 can be found by averaging repeat unit ratios based on the initial equivalencies used for polymerization. For number-average degree of

polymerization M_n is chosen as it represents the weight of the chains that are most prevalent, not a polymer molecular weight average (M_w, includes all chains, of all lengths).

In the field of industrial thermoplastics, good mechanical properties such as high melt temperature or mechanical strength increase with X_n (thousands or tens of thousands are desired), while in the realm of π-conjugated polymers it affects optoelectronic properties by relation to the *maximum effective conjugation length* (high X_n in conjugated polymers also yield more desirable mechanical properties such as the ability to form solid, continuous surface electrodes). This "length" is based on the number average of repeat units which can be identified through Equation 2.1.1 and the maximum effective conjugation length is typically achieved at M_n's of 10,000 Da. As illustrated in the simplistic Figure 2.1.1, as the number of repeat units (rings) increases, the effective conjugation length increases to a point of saturation (maximum effective conjugation length) and shows little change in absorption (λ_{max}) with a corresponding increase in M_n (and subsequently, X_n).

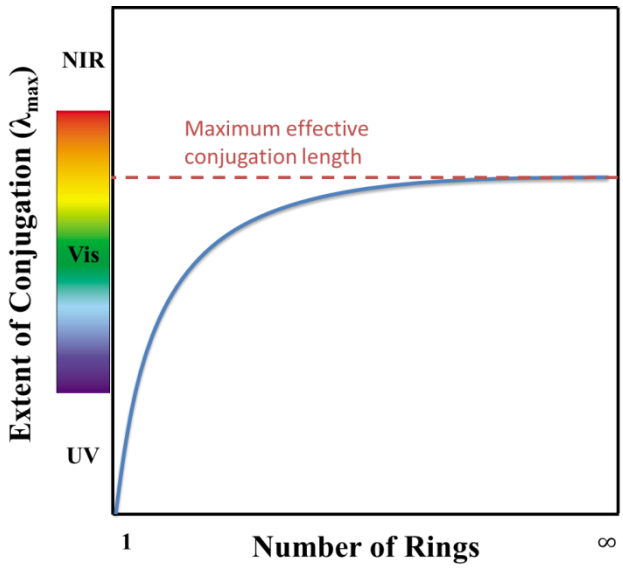

Figure 2.1.1: Extent of conjugation with increase in the number of rings (M_n).

λ_{max} is often used as it represents the largest density of absorption transitions. In thin films, one can optically measure the onset of absorption which can then be coupled with electrochemistry to reveal the HOMO level (top of VB) of a polymer. As mentioned in Section 1.3.1, this can be tuned by either increasing steric repulsion in the backbone to push the onset to higher energies (shorter wavelengths) or through relaxation to absorb lower energies (longer wavelengths).

The saturation of conjugation length varies between the polyaromatic systems. Some studies for polythiophene (PT), poly-*p*-phenylenevinylene (PPV), polyfurans (PF), and ProDOT have found the effective saturated conjugation length with regard to the number of rings to be slightly over 11,[103] 20,[104] 16,[105,106] and 12[35] repeat units respectively. Others have found the saturation of conjugation length for PT, PPV, PPy to be greater than 20 repeat units.[107] Meier *et al* compiled a series of studies concerning the effect on the extent of conjugation with respect to the number of repeat units for a variety of polyaromatic systems, which have been condensed in Figure 2.1.2 where λ_{∞} represents the maximum effective conjugation length for each oligomer.

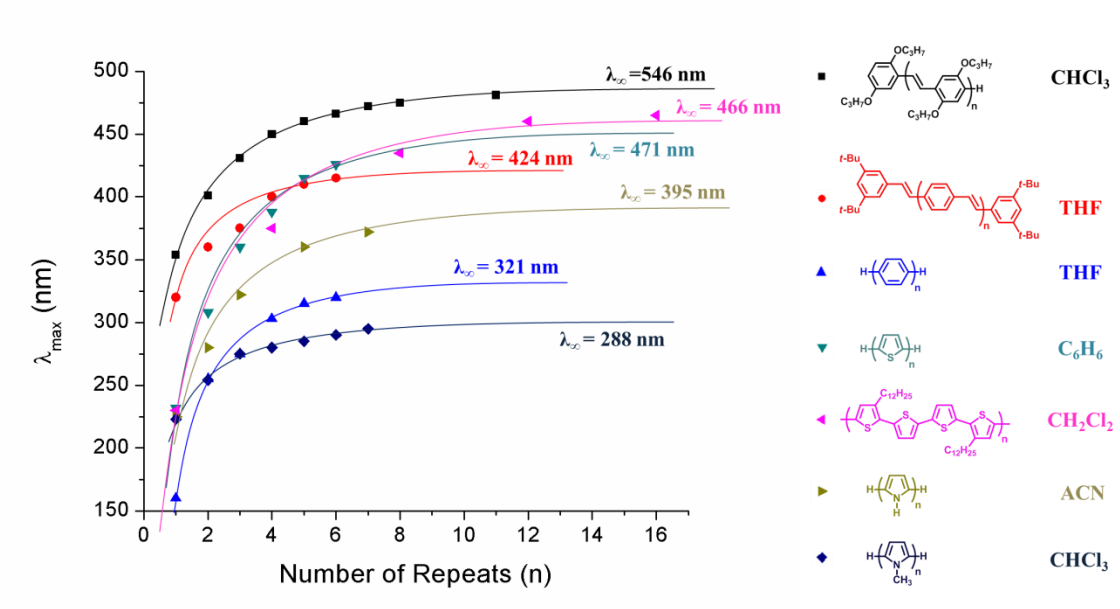

Figure 2.1.2: Change in the extent of conjugation with an increase in the number of rings as measured by solution spectroscopy. Adapted from Meier *et al*.[107]

Interestingly 48, 72 and 96-mer PT systems have been synthesized and it was found that there was a continuing and slight redshift with increasing weight (~2 nm between the 72 and 96-mer).[108,109]

In a study by Jin *et al*,[110] two batches of poly(3-hexylthiophene) (P3HT) were produced. The low molecular weight batch had a weight of M_n: 2,200 Da, M_w: 3,146 Da and exhibited a λ_{max} of 450 nm. The high-molecular weight batch (M_n: 19,000 Da; M_w: 25,650 Da) exhibited a λ_{max} of 555 nm, showing the dependence of conjugation (and properties) on the chain length. With a repeat unit weight of P3HT being 166.28 g/mol; the low weight batch has ~13 rings while the high weight batch has ~114 rings, showing different effects on the absorption spectra. Now that we understand the importance of conjugation length in polymers of sufficient weight (M_n > 10,000 Da), let us discuss common polymerization methods with suggestions on how they be performed.

2.2. Oxidative

This is the most simplistic method to produce conjugated polymers. It can be used for making homopolymers from one monomer that is electron rich or random copolymers from multiple monomers. These types of polymerizations can be conducted chemically using oxidants such as ferric chloride ($FeCl_3$) or electrochemically to deposit films onto electrodes. Dioxythiophenes (β-substituted heterocycles in general) work well for this method as they are electron rich and the dioxy-substituents completely prevent defects from forming in the β positions of the rings, allowing only α-α couplings.

The suggested general mechanism for oxidative polymerization is not very well known but believed to be identical for chemical and electrochemical processes; it is illustrated in Scheme 2.2.1. The initial DOT monomer (ProDOT($OEtHex_2$) for ECP-Magenta) is oxidized by a chemical oxidant ($FeCl_3$) or at the working electrode in an electrochemical cell; the more electron rich a monomer, the lower the oxidation potential and the easier to oxidize. The resulting radical cation monomer is stabilized through aromatic resonance

and by the dioxy-substituents in the β positions. Chemically, two radical cation monomers will bond together, followed by deprotonation to produce HCl in the reaction mixture, and should be bubbled away by a carrier gas. As couplings progress, a radical cation monomer and a radical cation dimer or radical cation oligomers will bond together forming polymer chains. Electrochemically, the mechanism is the same.[111] This process repeats as long as the oxidant is present in excess or potential cycling continues until the polymer precipitates out of solution forming a thin film or monomer/low weight oligomers are completely consumed.

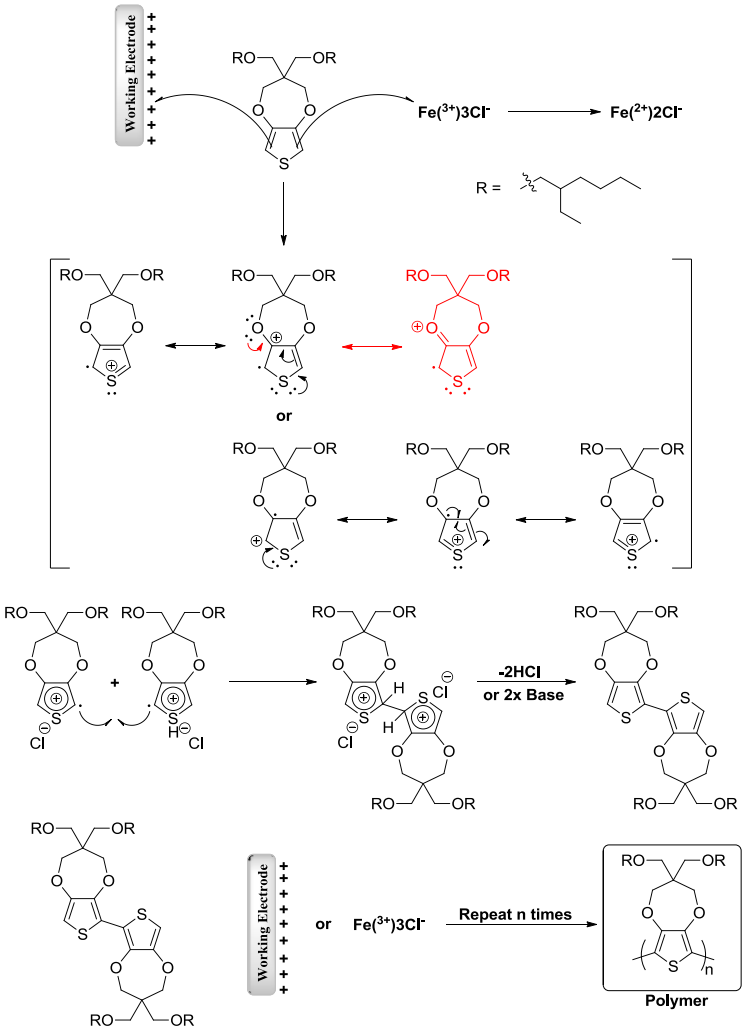

Scheme 2.2.1: Mechanism for oxidative polymerization, chemical or electrochemical, where R can be any alkyl or solubilizing chain (typically 2-ethylhexyl).

Chemical oxidative polymerizations are to be performed on monomers with solubilizing chains. Typical synthetic examples are presented in Scheme 2.2.2. Both are entirely viable but have differences. Method (a) uses a good polymer solvent but the $FeCl_3$ is not soluble thus, nitromethane or methanol are used but retardation of polymerization is possible.[112,113] Method (b,c) uses a moderate polymer solvent that can also dissolve $FeCl_3$ providing a homogeneous polymerization yielding adequate molecular weights using ProDOTs and high molecular weights for acyclic DOTs. For chemical methods, the end polymer is partially in an oxidized state (radical cation/polaron) and protonated yielding a black, blue, to green mass. The mixture or dispersion is precipitated into methanol and washed with copious amounts of methanol to remove iron salts. The filtered mass is then dissolved into a good polymer solvent (toluene or chloroform) as best as possible and then a small volume of hydrazine (1-5 mL) is added to reduce the doped and protonated polymer and a beautiful dark to vibrant neutral state color change occurs, thus allowing the polymer to be further purified.

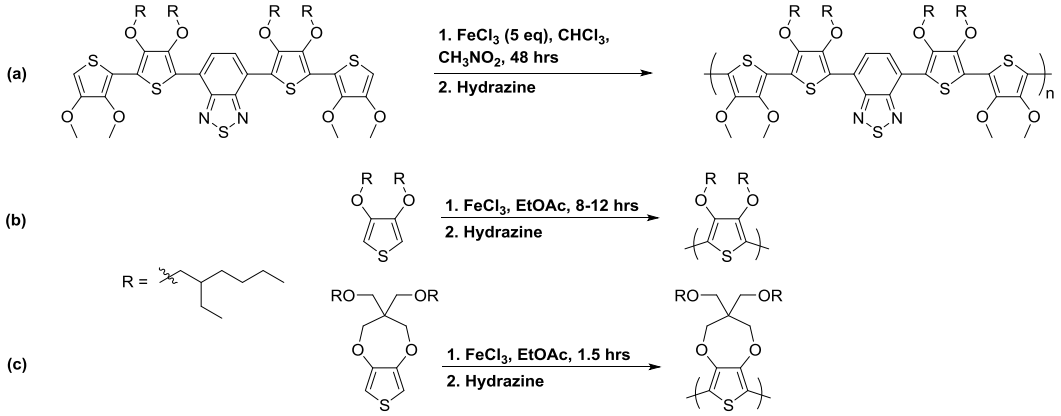

Scheme 2.2.2: Three synthetic oxidative routes. All carried out at room temperature.[32, 49]

These polymerizations on smaller scales (up to 5 g) are best performed in a single neck, round bottom flask with as large of a stir bar as possible to enable adequate mixing of the solution during the rapid increase in viscosity (an overhead stirrer would be ideal but was not appropriate for the scales discussed herein). The monomer and solvent are added

together and degassed by bubbling with an inert gas such as argon (typically for 45 minutes) and then constantly bubbled during polymerization to remove HCl. Do not use a metal syringe as it will corrode or dissolve from the oxidant and produced HCl during the duration of the polymerization; I recommend using a shortened pipette made of thick glass with wide internal diameter (prevents breakage, blockage and allows for high rate of gas flow). The oxidant is typically added as a concentrated solution using EtOAc, methanol, or nitromethane. This step is where there is the greatest level of risk as the oxidant solution can get quite hot. On small scales (requiring $FeCl_3$ solution concentrations of 4.5M (0.7 mg/ml), 15 mL or less) this is manageable and the oxidant can be added to an adequately sized vial of solvent, degassed *via* sparging with inert gas (5 minutes to minimize needle corrosion), and injected drop wise (3-5 drops/second, rapid) using a syringe. For larger volumes it is best to use a separate round bottom flask and cannula to avoid injury from the exothermic oxidant solution (a cannula is acceptable as the oxidant solution will not significantly corrode the metal due to short exposure time followed by rapid cleaning). Finally the polymerization flask should be lowered into an ice bath to cool and to prevent solvent from evaporating from the inert gas bubbling. After oxidant addition, the vessel can be allowed to warm to room temperature.

If a monomer lacks solubilizing chains, it should be used as a co-monomer to produce random copolymers; if homopolymers are desired, electrochemical methods are to be used. A thorough explanation on performing electrochemical oxidative polymerization can be found in the dissertation of Ryan Walczak beginning on page 17.[53] If the monomer contains functional groups that are acid sensitive or is a heterocycle that is also sensitive to acid (such as furan), chemical oxidation as a polymerization method should be avoided.

2.3. Stille

This method of polymerization is one of the most common in the field of organic electronics. It can access polymers in good yield with adequate molecular weights and is capable of utilizing a variety of monomers with minimal adjustments in reaction conditions. Two advantages over oxidative polymerization is that it can be used to achieve alternating polymer repeat units and is selective only at positions that have been activated by a halide (typically bromide) and organotin, allowing monomers with unsubstituted β positions to be utilized with no fear of defects. A thorough review on this chemistry is presented by Carsten *et al*.[114]

Shi *et al*, utilized Stille polymerization for the synthesis of ECP-Black.[42] This produced a polymer with a more even absorption across the visible spectrum, giving a material that possesses a lower L* value (darker) than what was afforded by Beaujuge *et al* using oxidative methods.[51] A mechanism of Stille polymerization is presented in Scheme 2.3.1 with ECP-Black as an example. The palladium catalyst $Pd_2(dba)_3$ with the bulky phosphine ligand P(*o*-tolyl)$_3$ is used in favor of $PdCl_2(PPh_3)_2$ or $Pd(PPh_3)_4$ as the same $Pd^{(0)}$ state can be achieved with a complex that can be stored in air for long periods of time. After oxidative addition of a dibromide monomer (or dibromide terminated oligomer as reaction progresses), the subsequent diorganotin or tin terminated oligomer under goes transmetallation with the palladium catalyst. The purpose of the bulky ligand is to aid in the *trans-cis* isomerization of the palladium complex to facilitate reductive elimination, minimizing coupling by-products that would otherwise lower molecular weight, increase PDI, and deplete yields. As this is a palladium-mediated-step-growth polymerization, great care must be taken in monomer ratio and purity to maximize yield and M_n while also ensuring an oxygen free environment to maintain catalyst lifetime.

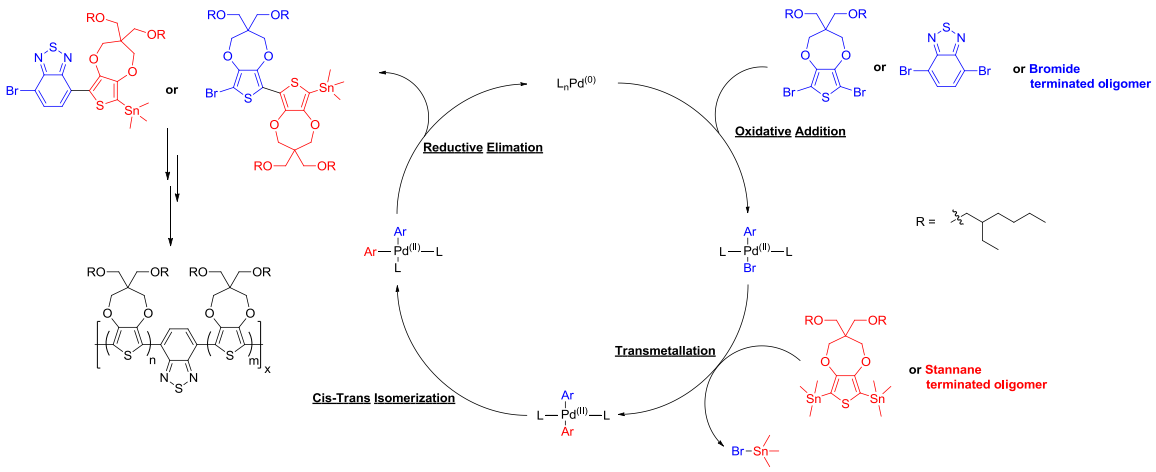

Scheme 2.3.1: Stille polymerization mechanism with ECP-Black as example.

Typical Stille polycondensation conditions are shown in Scheme 2.3.2. These polymerizations are best conducted in Schlenk tubes or flasks (or any vessel that maintains an oxygen free environment) with as large of a stir bar as possible to ensure thorough and homogenous stirring of the solution. Before the reaction is set up, solvent should be stored in a Schlenk flask and degassed by at least three freeze-pump-thaw cycles. Monomers are added carefully and separately to ensure proper weight (to within ∓0.5 mg of needed amount). If the monomers are solids this is a relatively simple task with the exception of ensuring all monomer has been removed from weighing paper and joint of reaction vessel. Oil or liquid monomers should be added to a vial and then dissolved in hexane and transferred to the reaction flask followed by washing the vial with hexanes three times where after the hexane is gently removed *in vacuo*. Because of the toxicity of organotins, these should be weighed out in a fume hood if they are volatile. Catalyst and ligand are added directly to the flask and followed by the vessel and contents being vacuum purged for at least 45 minutes, followed by three purge and argon back-fill cycles. Finally the solvent is then added to the vessel and it is immersed into an oil bath held at the reaction temperature, typically below solvent reflux.

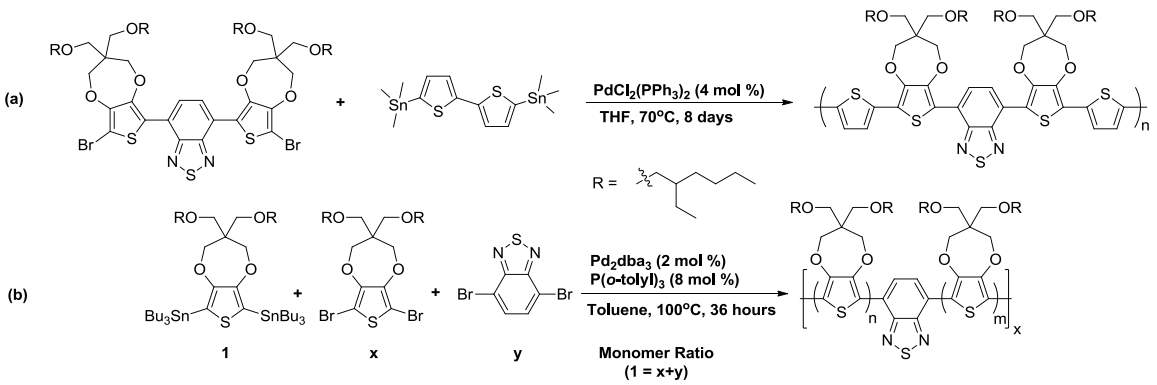

Scheme 2.3.2: Two different methods for Stille polymerization.[42,48]

Organotins are well known to be neurotoxic[115] and great care must be taken to handle the monomers and by-products of reactions. Organotin exposure is not only a hazard to you but also to others around the lab as vapors can be inhaled and residues can be absorbed through the skin. Because of this, take care that organotins are handled in a fume hood as much as possible and that all exposed labware is properly labeled with warnings; a base bath is suitable enough to hydrolyze organotin residues, mitigating dangers. Organotin by-products from polymerizations or monomer synthesis can be removed by first end-capping the polymer followed by precipitation into methanol, Soxhlet extraction, or passing the polymer solution through a thin pad of silica. Do not be frightened over the health hazards of this method for Stille polymerization is a proven and viable route in polymer synthesis, but as with any chemistry, proper safety and awareness is the key to success and health.

2.4. Suzuki

Suzuki is a safer alternative to Stille. It utilizes boronic acids or esters as the activating group on the aromatic monomer and can give polymers in high yield, good M_n, and boronic esters are generally environmentally benign. Overall it is nearly the same with regards to reaction conditions, catalyst loadings, and temperature with the exception that a Lewis base is needed to facilitate transmetallation. Original mechanisms presented in a

variety of organic chemistry textbooks shed little light as to the reductive elimination and transmetallation steps; merely that transmetallation involves a Lewis base of hydroxide or fluoride forming a negatively charged tetrahedral boronate intermediate $ArB(OR)_3^-$ or $ArB(OR)_2F^-$ as the active species. The reductive elimination step was assumed to pass through the same route as mentioned for Stille. However, a thorough study by Amatore *et al*, of both processes now show that the steps are not as simple as portrayed in the past and through their work a new mechanism has been presented, and is adapted for the polymerization of ECP-Yellow shown in Scheme 2.4.1.[116,117]

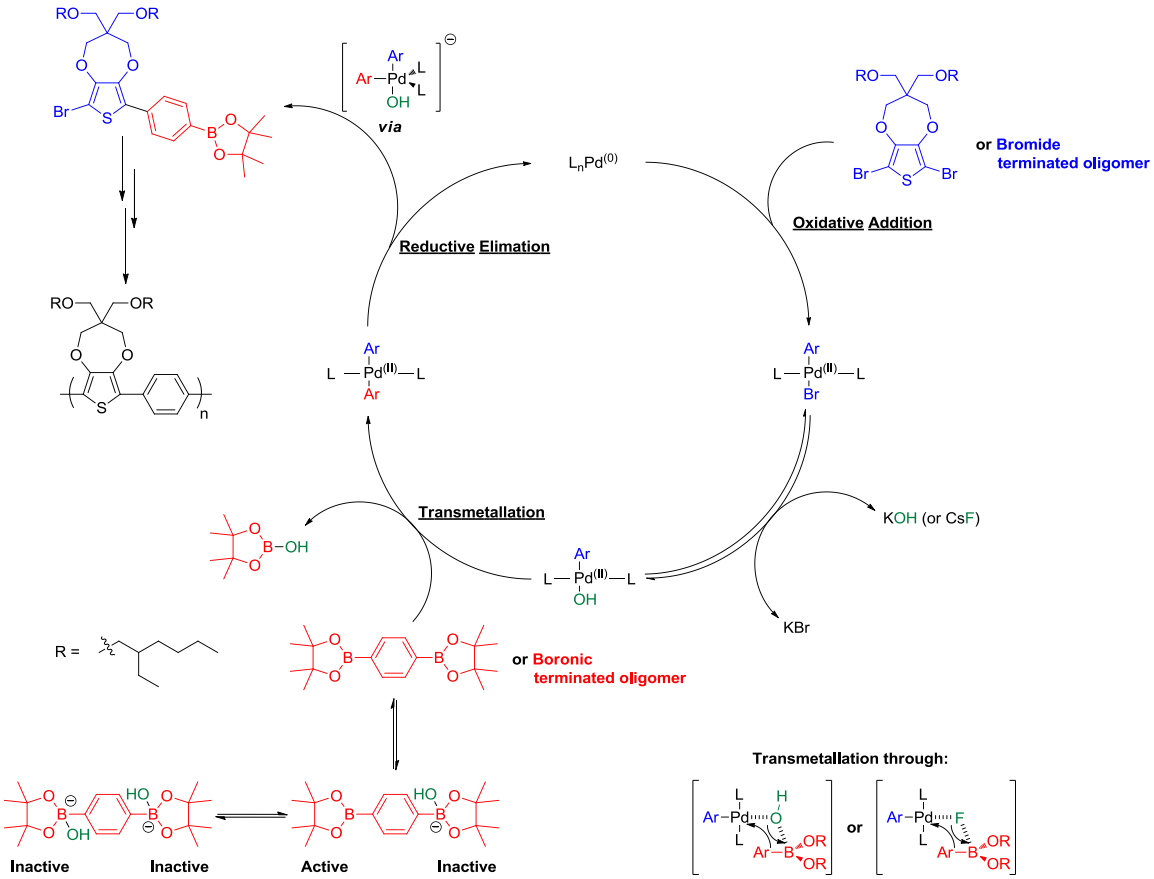

Scheme 2.4.1: Mechanism for Suzuki polycondensation with hydroxide (or fluoride).

In this scheme, hydroxides can be exchanged for fluorides if conditions necessitate (more below). Oxidative addition of a dibromide monomer or bromide terminated oligomer occurs and is followed by an equilibrium exchange reaction between hydroxide (or

fluoride) and bromide on the palladium complex. The transmetallation step as discovered by Amatore *et al*, will not proceed if the negatively charged tetrahedral boronate intermediate is formed, or if the hydroxide (or fluoride) is not a part of the Pd complex. Only a neutral, trigonal planar boronic ester will undergo transmetallation. This enlightened mechanism is due to the empty p-orbital on boron behaving as a Lewis acid, allowing electrons to be accepted from the lone pairs on O or F, guiding the aryl-boron species to the Pd complex. The authors then discovered an unexpected role of the Lewis base in promoting the faster reductive elimination through a stable *trans*-bis-(aryl)Palladium complex with hydroxide (or fluoride) as a fifth ligand[118,119,120] over the slower *trans-cis* isomerization that was seen with Stille.

The type of aryl boronic species is important. Free aryl boronic acids (aryl-$B(OH)_2$) are prone to hydrolysis from Lewis bases. In the work of this dissertation, bulkier pinacol esters were chosen because the excess steric hindrance from the tetramethyl substituted bridge slows this process, increasing the stability of the boron activated aryl monomer. If aryl boronic acids or esters are electron rich, the rate of hydrolysis increases, to mitigate this, fluorides can be utilized over bases that produce hydroxide in equilibrium; this knowledge was utilized to produce yellow ECPs with electron rich dimethoxyphenylene monomers using CsF over K_3PO_4. These fluorides are also functional group tolerant and can be used to produce polymers with base sensitive side chains.[121,122]

Typical Suzuki polymerization schemes are presented in Scheme 2.4.2 and in general the setup is nearly the same as for Stille. The major difference is the addition of a Lewis base (a source of hydroxide or fluoride) and a phase transfer catalyst Aliquat 336 which is used to help homogenize the biphasic solution formed upon the addition of water. To eliminate the use of water which forms a biphasic polymerization mixture, tetrabutylammoniumhydroxide can also be used.[123] The Lewis base and phase transfer catalyst are added prior to vacuum purging and water is free-pump-thawed alongside toluene. It is recommended that toluene be added before water to better dissolve organic

monomers, freeing the stir bar. When the vessel is added to the heated oil bath, stirring should be conduct in such a manner that the two phases are indistinguishable.

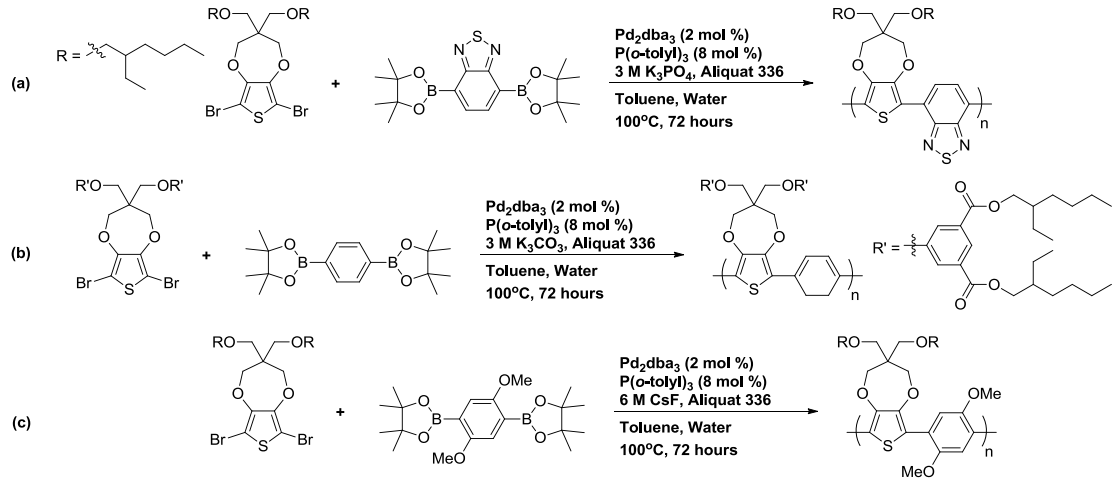

Scheme 2.4.2: Typical Suzuki conditions with strong base (a), moderate base (b), and base free (c).[47,45,46]

Suzuki methods often suffer from the inability to utilize monomers that are electron rich or have sterically hindered active centers. A report by Liu *et al* synthesized electron rich and bulky ligands to allow such polymers to be realized.[124] Typically aryl boronate monomers are solids and can be recrystallized. If column chromatography is required, silica can decompose such monomers however, there is a method utilizing treated silica to enable safe purification with minimal decomposition.[125]

2.5. Direct Arylation

The method of direct (hetero)arylation is a relatively new route of forming polymers. Direct arylation has existed in the world of small molecule synthesis[126,127] with near equal fame as the "click" reaction. However, direct arylation took time to mature into a method of polymer synthesis that is capable of giving good yields and adequate M_n; it is still being actively explored and understood.[128,129]

The major advantage the lack of a monomer that needs an activated center using tins, borons, or triflates. These couplings can occur directly at unsubstituted hydrogen and

bromide centers of aryl rings, hence direct arylation. This means that there are less synthetic steps, no need to brominate a monomer to prepare for lithium-halogen exchange for stannylation or Miyaura borylation and the subsequent and sometimes arduous purifications. The catalyst materials are commercially available, economical, air stable, and relatively nontoxic. Polymerizations can be run from 1 to 24 hours, meaning degassing of solvents is not as vital; bubbling of the solvent with inert gas is suitable. The method is not perfect however, polymerizations must be run at high temperature to facilitate oxidative addition (most efficient found to be +120^{o}C) or in pressure vessels, the solvent that best supports the catalyst systems is often a poor polymer solvent (polar aprotic) which can result in premature termination of the polymerization as molecular weight increases, and finally there is a possibility of nonselective couplings at unsubstituted positions on electron rich rings and the risk of incorporating aromatic rings from solvents like toluene or chlorobenze. These issues are being addressed with time: The Leclerc group has reported extensive work in utilizing new catalysts, solvents, and temperatures to fit a variety of rings,[130,131] the Thompson group has explored the use of neodecanoic acid (NDA) in place of pivalic acid and temperature variations to mitigate cross-linking of thiophene monomers during polymerization,[132,133] and the Kanbara group has studied the use of fluorine atoms, methyl groups, or pyrimidinyl directors and ruthenium catalysts to prevent α-β defects.[134,135,136] For the majority of this dissertation, DOT monomers are ideal for this chemistry as there is no chance of cross linking due to the oxygen atoms occupying the β positions, the protons in the α positions are sufficiently acidic, and the polymers are adequately soluble during polymerization reaching desired M_n, requiring little deviation from previous literature conditions.[39]

The mechanism at the writing of this dissertation is in a state of debate but much work by the Fagnou (who is now deceased) group has shed sufficient light to give a general mechanism known as concerted-metalation-deprotonation (CMD). The polymerizations generally work best with the carboxylate additive pivalic acid[137,138] but can function

without.[139] For the purpose of this dissertation we will discuss the mechanism with pivalic acid; an explanation on the mechanism without the additive can be found by Mercier and Leclerc[128] but many of the transition states are similar. The mechanism is adapted for the synthesis of ECP-Black in Scheme 2.5.1 (note the difference between Stille in Scheme 2.3.1). In essence the mechanism is believed to have two similar routes, Pathway A and B. Both follow traditional oxidative addition followed by a halogen-carboxylate ligand exchange. The carboxylate ligand simultaneously acts to support the complex and to deprotonate the di-hydrogen-DOT species.[140] The ligands (carboxylate, solvent, or phosphine if needed) can then recoordinate with the catalyst center following Pathway A or remain coordinated during the entirety of the cycle for Pathway B.

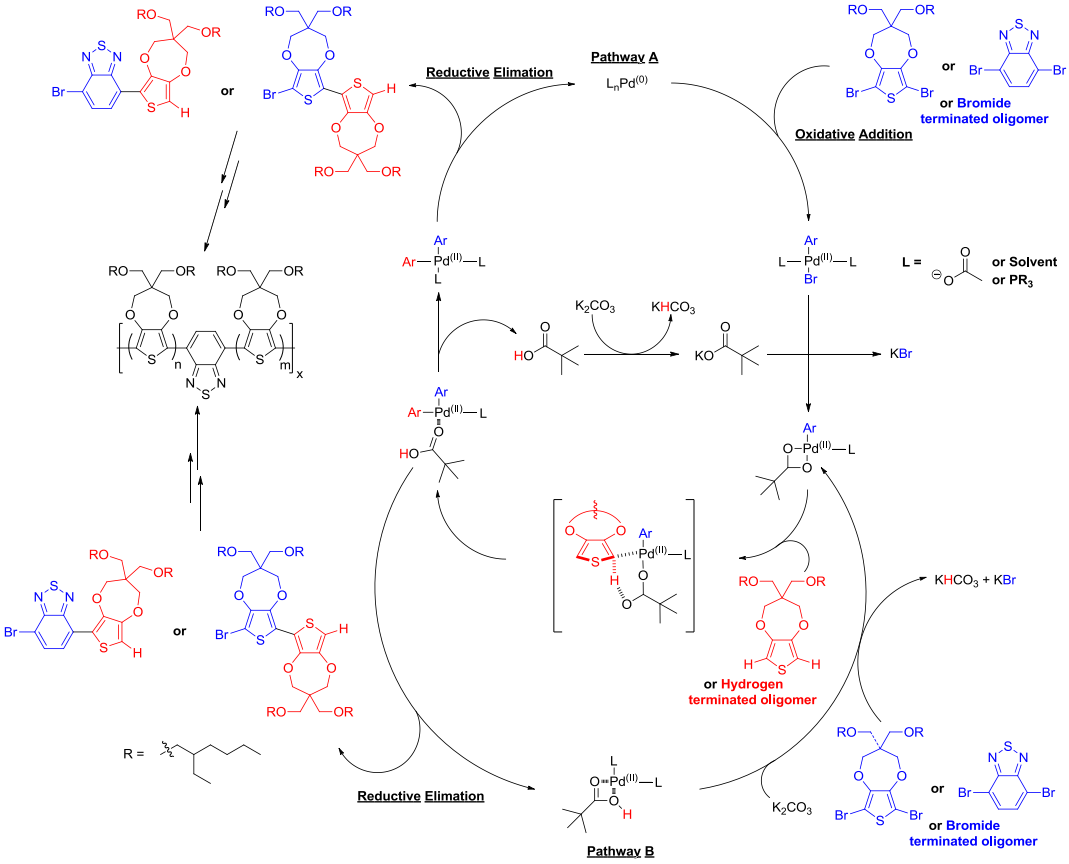

Scheme 2.5.1: Proposed mechanism for direct arylation using a carboxylate additive.

This cycle will continue until the polymer precipitates out of solution which may be a disadvantage as the weight might not be adequate; if this is the case, new solvents need to be explored that will maintain polymer solubility. Compare the two polymerization routes of ECP-Orange in Scheme 2.5.2. Direct arylation (a) gives an orange oil with a M_n that satisfies the requirement for weight but it was unable to form a continuous electrode surface. The low weight is due to a viscous precipitate that was observed after 3 hours of stirring. However, using oxidative methods (b) the polymer had a considerably high M_n on the order of ~10 greater as the polymer was continually soluble in ethylacetate; though the polymer is tacky it is able to produce a fixed continuous electrode surface.[32] Conditions using the Herrmann-Beller Catalyst system[139] had little effect on weight due to insufficient stirring, a result of the pressure vessel architecture required for such methods.

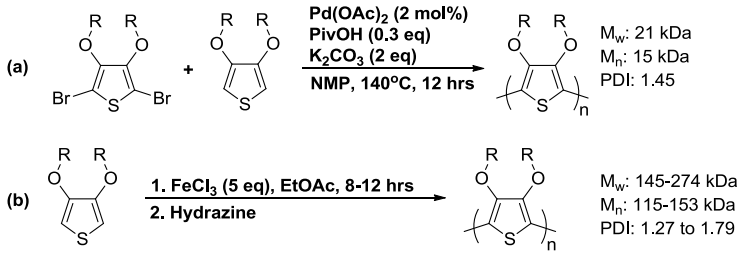

Scheme 2.5.2: Comparison of direct arylation (a) and oxidative addition (b) for the production of ECP-Orange.

Palladium acetate conditions can be performed in similar glassware (Schlenk tubes and flasks) with the same general procedure as seen for Stille and Suzuki polymerizations with the exception that solvent merely requires bubbling with inert gas. Typical solvents for this method are dimethylacetamide (DMA/DMAc), *N*-methylpyrrolidone (NMP), or dimethylformamide (DMF) as they are polar aprotic solvents with high boiling points. Direct arylation as a polymerization method can quickly result in high solution viscosities and polymer precipitation such that stirring becomes impossible as demonstrated in Figure 2.5.1.

Figure 2.5.1: Polymer precipitation completely covering stir bar and adhering to the vessel wall, preventing stirring.

To amend this, a new vessel architecture was explored using an appropriately sized one neck round bottom flask to allow the largest stir bar possible. A variety of conditions and catalyst loadings is presented in Scheme 2.5.3. Monomers and catalysts are added directly to the flask and then a claisen head is attached, followed by one vacuum adapter for purging and inert gas flow and one rubber septum for injection of degassed solvent. The contents of the flask are vacuum purged for 45 minutes then back filled with argon and purged three times finally followed by the addition of solvent. The round bottom and setup is lowered into an oil bath held at 140^{o}C. Color change is rapid, almost immediate and the larger stir bar allows for complete solution homogenization even with the intense increase in viscosity and polymer precipitation. An overhead stirrer would have been ideal but was not appropriate for the scales discussed herein.

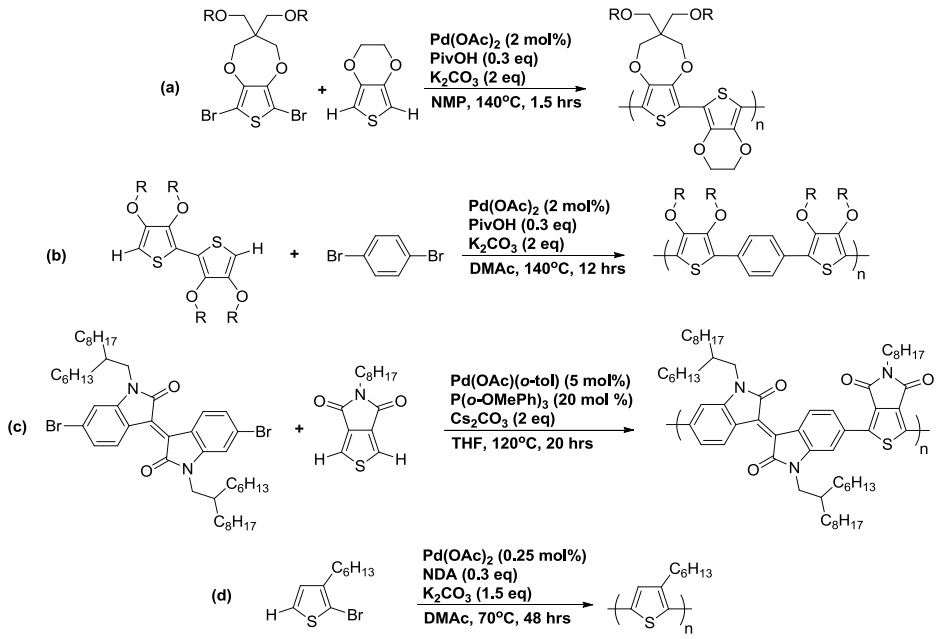

Scheme 2.5.3: Direct arylation methods with similar catalyst loadings but at different run times (a,b), Herrmann-Beller catalyst (c), and NDA (d).

If Palladium acetate conditions are insufficient, the Herrmann-Beller catalyst system may be required (bulky aryl bromide centers, exotic acceptors such as thienopyrrolodione (TPD))[130,131] using tetrahydrofuran (THF) in which a reinforced-glass walled pressure vessel is utilized rather than a schlenk tube or round bottom flask. If this does not achieve the desired polymer, Stille or Suzuki methods may need to be pursued.

2.6. Comparison of Methods; Pros, Cons, Successes, Failures

Careful consideration needs to be made in the selection of a polymerization method. Table 2.6.1 assembles the methods discussed above and compares them as a road map in selecting the appropriate coupling for certain types of general monomers.

Table 2.6.1: Table comparing the discussed polymerization methods.

Coupling Method	**Monomer Type**	**Advantages**	**Disadvantages**
Chemical Oxidation	• Electron Rich • With solubilizing chains • Without solubilizing chains (as comonomer)	○ No synthesis to activate monomer ○ Straightforward set-up ○ Economical reagents ○ Air tolerant ○ Scalable ○ Reliable	❖ Incompatible with acid sensitive monomers ❖ Cannot achieve perfectly alternating structures ❖ Can induce β defects in heterocycles ❖ Subsequent polymers must be soluble
Electrochemical Oxidation	• Electron Rich • With solubilizing chains • Without solubilizing chains	○ Control of film thickness/morphology ○ Access polymers with no solubilizing chains ○ Reliable	❖ Cannot achieve perfectly alternating structures ❖ Can induce β defects in heterocycles ❖ Not scalable in laboratory setting
Stille	• Electron rich • Electron Poor • π-Bridges • With solubilizing chains • Without solubilizing chains (as comonomer)	○ Well understood ○ Straightforward set-up ○ Reliable ○ Scalable ○ Can achieve perfectly alternating structures	❖ Toxic monomers ❖ Toxic by-products ❖ Air sensitive ❖ Requires at least two different activated monomers
Suzuki	• Electron Poor • π-Bridges • With solubilizing chains • Without solubilizing chains (as comonomer)	○ Nontoxic monomers ○ Well understood ○ Straightforward set-up ○ Scalable ○ Reliable ○ Can achieve perfectly alternating structures	❖ Electron rich monomers require condition probing ❖ Air sensitive ❖ Biphasic ❖ Requires at least two different activated monomers
Direct Arylation	• Electron rich • Electron Poor • π-Bridges • With solubilizing chains • Without solubilizing chains (as comonomer)	○ Only one activated monomer required ○ Straight forward set-up ○ Scalable ○ Air tolerant ○ Can achieve perfectly alternating structures	❖ Not fully understood ❖ Requires condition probing ❖ Poor polymer solvents

Referring to the table, electron rich monomers include ring systems such as thiophenes, dioxythiophenes, pyrroles, or dialkoxybenzenes; otherwise known as donors. Electron poor monomers can consist of benzothiadiazoles, isoindigo, thienopyrrolodione, or quinoxaline; otherwise known as acceptors. The moieties known as π-bridges can consist of phenylenes, fluorenes, vinylenes, naphthalenes, or pyrenes; common electron neutral

systems. Solubilizing chains are typically 6 carbons or longer; as length or branching increases, solubility increases.

During Stille polymerizations, it is recommended that the organotins be on the least sterically hindered monomer to facilitate synthesis and transmetallation. For Suzuki the boronate esters should be on the most electron poor, neutral, or least sterically hindered site to simplify synthesis and minimize hydrolysis by Lewis bases. When using direct arylation the dibromides should be on the least sterically hindered site to stabilize oxidative addition and the proposed transitions states mentioned above.

2.7. Polymer Workup and Purification

To attain the highest M_n possible and remove unwanted small weight oligomers and impurities, we will briefly discuss the purification process. When a polymerization is terminated it is precipitated into a methanol solution. Stille polymerizations should be end capped to remove tin groups prior to precipitation into pure methanol. Chemical oxidative polymerizations should be precipitated into pure methanol to remove iron salts. Suzuki and direct arylation polymerizations should be precipitated into methanol solutions containing dilute HCl to eliminate salts. Once the precipitates have stirred for at least 45 minutes, the dispersion can be poured directly into a cellulose soxhlet thimble. As mentioned above, oxidative precipitates must be filtered, washed with methanol, dissolved in toluene or chloroform and reduced with hydrazine before soxhlet can be pursued. Some polymers may behave like viscous oils or tacky substances and won't form uniform dispersions of polymer particles in methanol, easily collected by filtration, if this occurs it is best to decant off the liquor, leaving the tacky mass. Using the stir bar and a magnet akin to a squeegee, the mass can be collected onto the stir bar and dropped directly into the thimble. If there is concern for the molecular weight if this happens, look above at the discussion on Scheme 2.5.2. If a cloudy precipitate or "mist" is acquired, adding small amounts of 1 M HCl can expedite precipitation.

Once the polymer has been poured into the cellulose thimble, Soxhlet extraction can be conducted. The general set up is presented in Figure 2.7.1. The polymer is washed with various solvents, extracting small to higher molecular weight oligomers and byproducts from methanol to hexane respectively. The polymer is finally removed from the thimble using chloroform, leaving behind insoluble organics, metals, or salts.[141] If a narrower PDI is desired, solvents like DCM or THF can be used before final dissolution of product polymer but the choice of solvent depends on polymer structure. If a polymer is soluble enough, final extraction can occur with hexane or even acetone (as the case for ECP-Orange) so ensure the cleanliness of collection flasks and stir bars.

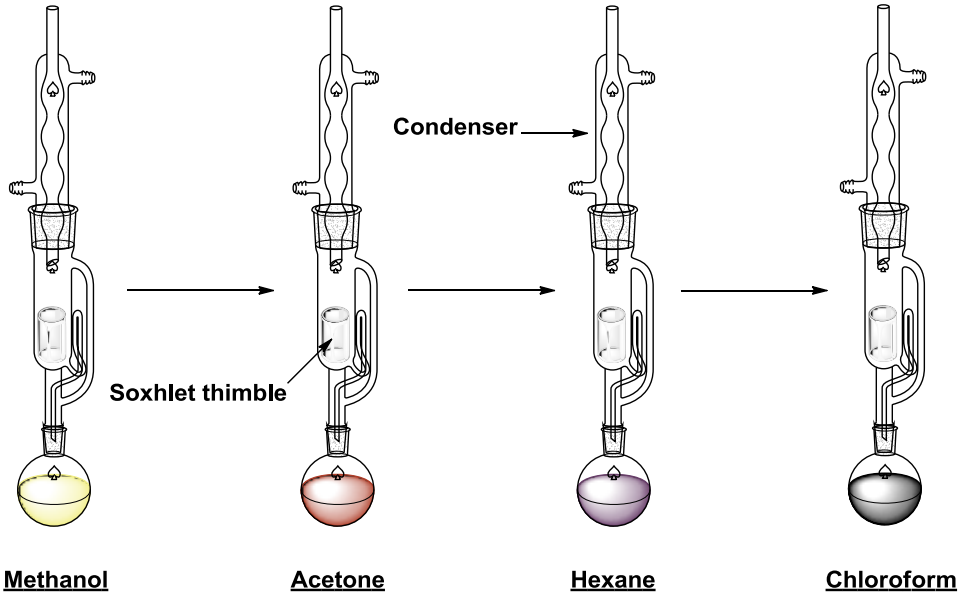

Figure 2.7.1: Soxhlet extraction of ECP-Black made from direct arylation methods.

An alternative to Soxhlet extraction is the use of a stirred ultrafiltration cell. This is a more active purification method. It differs from Soxhlet extraction in that the solvent is not heated, the polymer-solvent slurry is stirred during the entire process, and the contents are under pressure when final filtration occurs through a nylon membrane.

Once the polymer has been extracted from Soxhlet apparatus (or ultrafiltration cell), the solvent is removed entirely. The solid polymer film is then best dissolved in

chlorobenzene followed by the addition of 18-Crown-6 and palladium scavenger (diethylammonium diethyldithiocarbamate) to remove metal ions like potassium and palladium respectively.[142] Take care adding the crown ether as it can affect your nervous system by interfering with potassium ions, preventing communication between neurons. The solution will then be stirred at 60^{o}C for at least 6 hours.[39]

Once cooled to room temperature the final polymer solution can be precipitated into methanol, stirred for 45 minutes then filtered over a 0.45 μm nylon pad. The filtrate will be a pale yellow color from the extracted ions and metals washing thoroughly with methanol will remove any that remain. If filtration is slow, be careful not to disturb the nylon pad as it can tear, it is recommended that you use a large, smooth, glass stirring rod to gently agitate any polymer layers that form on the filter, inhibiting solvent flow. Once the filtration is complete, the polymer cake can be dried, collected, and stored for later characterization.

2.8. Synthetic Experimentals and Procedures

This section details the synthesis of all monomers and polymers discussed throughout this thesis. Reaction is presented first followed by the procedure.

Toluene and water for Suzuki polycondensations were degassed using the freeze-pump-thaw method five times prior to reaction. *N*,*N*-Dimethylacetamide for direct arylation polymerizations was degassed *via* bubbling with argon for 45 minutes. All reagents and starting materials were purchased from commercial sources and used without further purification, unless otherwise noted.

Gel-Permeation Chromatography (GPC) acquired at Georgia Tech was utilized to estimate molecular weights were determined at 35 °C in THF. A combination of Waters HPLC pump 1515, UV-Vis Detector 2487, and a Refractive Index Detector 2414 were used. A Waters column (4.6 mm × 300mm; Styragel HR 5E) and polystyrene standards from Fluka were used. The polymer solution (1 mg/mL in THF) was prepared and

filtered through a Mini-UniPrep PTFE vial with a 0.45 μm filter. 20 μL of each polymer solution was injected and molecular weights were calculated using Waters Breeze II software.

GPC data acquired at 135^{o}C in 1,3,5-trichlorobenzene at MPI were determined by PSS-WinGPC (PSS) (pump: allianceGPC 2000) GPC equipped with an RI detector using a PLgel MIXED-B column (particle size: 10 mm, dimension: 0.8 x 30 cm) calibrated against polystyrene standards.

^{1}H-NMR and ^{13}CNMR spectra were collected on a Varian Mercury Vx 300 Mhz instrument using $CDCl_3$ as a solvent and the residual $HCCl_3$ peak as references (^{1}H: δ = 7.26 ppm, ^{13}C: δ = 77.23 ppm).

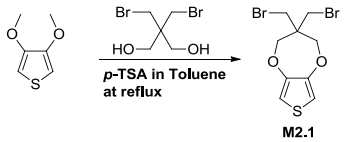

M2.1

3,3-bis(bromomethyl)-3,4-dihydro-2H-thieno[3,4-b][1,4]dioxepine (M2.1)

In a 1000 mL round bottom flask with magnetic stirbar, dimethoxythiophene (21.1 g, 0.15 mol), 2,2-bis(bromomethyl)propane-1,3-diol (42.1 g, 0.16 mol), and *p*-toluenesulfonic acid (2.78 g, 0.015 mol) were added under argon followed by anhydrous toluene (600 mL). The flask was attached to a soxhlet apparatus and an appropriate cellulose thimble was filled with activated molecular sieves (3Å) to remove methanol. The reaction was refluxed overnight after which the reaction was quenched with 175 mL of DI water followed by 25 mL of a saturated $NaHCO_3$ solution. The organic layer was extracted 3 times into diethyl ether then passed over a silica plug using 4:1 hexanes:dichloromethane and evaporated to yield a green solid. The solid was purified by recrystallization using minimal methanol to yield large white crystals in 82% yield. MP: 68^{o}C. ^{1}H-NMR (500 MHz, $CDCl_3$); δ 6.47 (s, 2H), 4.08 (s, 4H); 3.59 (s, 4H). ^{13}C-NMR (125 MHz, $CDCl_3$); δ 148.1, 104.2, 74.4, 46.1, 35.7.

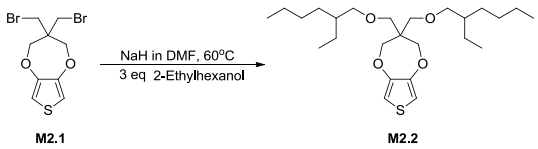

3,3-bis(((2-ethylhexyl)oxy)methyl)-3,4-dihydro-2H-thieno[3,4-b][1,4]dioxepine (M2.2)

To a three-neck 500 mL round bottom flask fitted with a magnetic stir bar and condenser, NaH (6.54 g, 0.27 mol, 10.9 g with oil) was added then purged by vacuum and filled with argon 3 times. After, 120 mL of hexanes were added and allowed to stir for 30 minutes after which the hexanes were washed off *via* cannula. Anhydrous-amine free DMF (300 mL) was added followed by 2-Ethylhexanol (17.7 g, 0.15 mol, 21.3 mL) drop wise at a rate of 0.5 mL/sec at 40^{o}C. The temperature of the mixture was increased to 70^{o}C and stirred for at least 6 hours after which **M2.1** (15.52 g, 0.05 mol) was added in one portion. The reaction was stirred for 2 days at 70^{o}C, then allowed to cool to r.t. and then quenched over 15 minutes with 150 mL of brine and stirred for 30 min. The reaction was added to a separatory funnel with 400 mL of DI water and the organic layer was extracted with 250 mL of hexanes 4 times then dried over $MgSO_4$, filtered, and evaporated down to a colorless oil and vacuum dried overnight with 97% yield. ^{1}H-NMR (500 MHz, $CDCl_3$); δ 6.44 (s, 2H), 4.01 (s, 4H), 3.47 (s, 4H), 3.28 (d, 4H, J= 5.0 Hz), 1.48 (m, 2H), 1.39-1.21 (m, 16H), 0.89 (m, 12H). ^{13}C-NMR (125 MHz, $CDCl_3$); δ 149.9, 105.2, 74.0, 70.1, 48.1, 39.8, 29.4, 23.3, 14.4, 11.4.

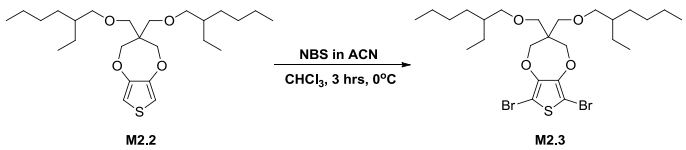

6,8-dibromo-3,3-bis(((2-ethylhexyl)oxy)methyl)-3,4-dihydro-2H-thieno[3,4-b][1,4]dioxepine (M2.3)

To a dry 500 mL round bottom flask with magnetic stirbar, **M2.2** (9.75 g, 0.22 mol) was added and dissolved in 200 mL of chloroform then bubbled with argon for 10 minutes.

To a 250 mL addition funnel, *N*-bromosuccinimide (NBS, 9.84 g, 0.055 mol) was dissolved in a minimal amount of acetonitrile and then bubbled with argon for 10 minutes. Once bubbling was complete, the addition funnel was attached to the flask and the temperature was lowered to 0^{o}C. The solution of NBS was added drop wise at a rate of 2 drops/sec. The entire system was covered in foil to avoid light exposure. After all NBS was added, the reaction temperature was raised to r.t. and allowed to stir for 3 hours where the reaction was determined complete by TLC using 4:1 hexanes:dichloromethane. The mixture was added to a separatory funnel where 300 mL of DI water was added and the organic layer was extracted with dichloromethane 3 times. The organic layer was then dried over $MgSO_4$, filtered, and evaporated to a pale yellow oil. The product was purified by Silica chromatography using 4:1 hexanes: dichloromethane. Product was evaporated down at room temperature and vacuum dried overnight covered in aluminum foil yielding a colorless oil in 95% yield. ^{1}H-NMR (500 MHz, $CDCl_3$); δ 4.08 (s, 4H), 3.48 (s, 4H), 3.27 (d, 4H, J= 2.45 Hz), 1.52 (m, 2H), 1.43-1.21 (m, 16H), 0.84 (m, 12H). ^{13}C-NMR (125 MHz, $CDCl_3$); δ 147.3, 91.1, 74.6, 70.0, 48.3, 39.9, 30.9, 29.4, 24.3, 22.9, 14.4, 11.4.

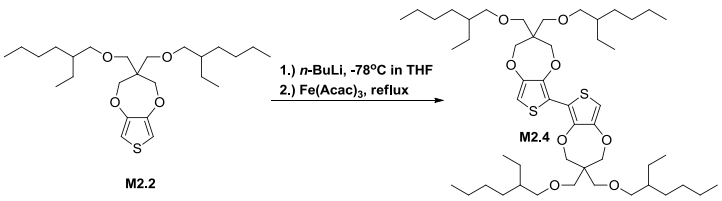

3,3,3',3'-tetrakis(((2-ethylhexyl)oxy)methyl)-3,3',4,4'-tetrahydro-2H,2'H-6,6'-bithieno[3,4-b][1,4]dioxepine (M2.4)

To a dry 500 mL round bottom flask with stirbar, ProDOT monomer **M2.2** (12.5 g, 0.028 mol) was dissolved in 300 mL of dry THF and then bubbled with argon for 30 minutes then lowered to -78^{o}C where *n*-butyl lithium (2.5 M, 0.03 mol) in hexane was added. After stirring for 45 min while warming to r.t. after addition of *n*-BuLi, the solution was transferred into a dry-degassed THF solution (80 mL) of $Fe(acac)_3$ (10.3 g, 0.03 mol)

under argon at r.t *via* cannula and the reaction mixture was refluxed for 48 hours. Volatiles were evaporated, and the residue was purified by standard column chromatography through silica using 3:1 hexane:dichloromethane to give **M2.4** in 80% yield as pale yellow-green viscous oil; ^{1}H-NMR (300 MHz, $CDCl_3$); δ 6.36 (s, 2H), 4.10 (s, 4H), 4.05 (s, 4H), 3.51 (s, 8H), 3.26 (d, 8H, J= 1.25 Hz), 1.47 (m, 4H), 1.03-1.40 (m, 32H), 0.91-0.98 (m, 24H); ^{13}C-NMR (75 MHz, $CDCl_3$); δ 147.3, 143.6, 114.0, 91.8, 69.6, 48.1, 39.8, 31.4, 29.6, 23.9, 23.5, 14.0, 11.5.

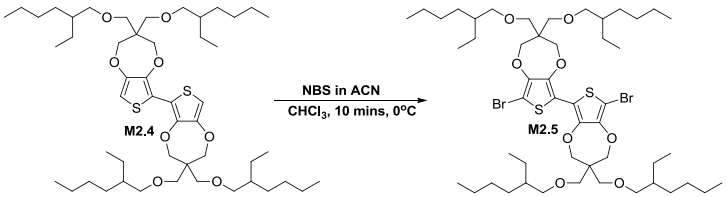

8,8'-dibromo-3,3,3',3'-tetrakis(((2-ethylhexyl)oxy)methyl)-3,3',4,4'-tetrahydro-2H,2'H-6,6'-bithieno[3,4-b][1,4]dioxepine (M2.5)

To a dry 50 mL round bottom flask with stirbar, **M2.4** (1 g, 1.14 mmol) was added and dissolved in 15 mL of chloroform then bubbled with argon for 10 minutes. To a 10 mL addition funnel, *N*-bromosuccinimide (NBS, 503.5 mg, 2.84 mmol) was dissolved in a minimal amount of chloroform and then bubbled with argon for 10 minutes. Once bubbling was complete, the addition funnel was attached to the flask and the temperature was lowered to 0^{o}C. The solution of NBS was added drop wise at a rate of 0.5 drops/sec. The entire system was covered in foil. After all NBS was added, the reaction was stirred for 10 minutes at 0^{o}C where the reaction was determined complete by TLC using 5:1 hexanes:dichloromethane. All volitiles were evaporated yielding a blue oil. The crude product was purified by Silica chromatography using 5:1 hexanes: dichloromethane. Product was evaporated to dryness at room temperature and vacuum dried overnight covered in foil yielding a yellow oil in 90% yield. ^{1}H-NMR (300 MHz, $CDCl_3$); δ 4.07 (d, 8H, J= 3 Hz), 4.53 (s, 8H), 3.32 (d, 8H, J= 6 Hz), 1.47 (m, 4H), 1.21-1.42 (m, 32H), 0.94-0.98 (m, 24H); ^{13}C-NMR (75, $CDCl_3$) δ 147.3, 143.6, 114.0, 91.8, 69.6, 48.1, 39.8,

31.4, 29.6, 23.9, 23.5, 14.0, 11.5. HRMS (EI-FTICR): *m/z* calcd for $C_{50}H_{84}Br_2O_8S_2$ (M^+) 1034.3974, found 1034.3995.

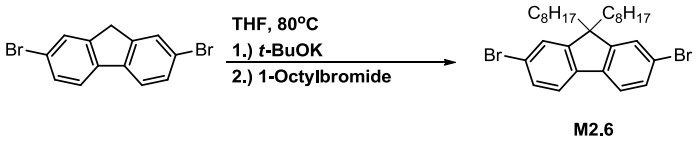

M2.6

2,7-dibromo-9,9-dioctyl-9H-fluorene (M2.6)

To a 500 mL three-neck round bottom flask with condenser affixed and magnetic stirbar, 2,7-dibromo-9*H*-fluorene (7.00 g, 0.22 mol) was added and then vacuum purged and filled with argon 3 times. Anhydrous tetrahydrofuran (250mL) was added by cannula to the flask followed by 2 eq. of 1-octylbromide (7.50 mL, 0.44 mol) and allowed to stir for 1 minute. Then, 2 eq. potassium tert-butoxide was added to the flask and allowed to stir for 30 minutes. The reaction was warmed to 80^{o}C and then 2 more eq. of 1-octylbromide was added followed by 2 eq. of potassium tert-butoxide and allowed to stir for 30 minutes. A final 2 eq. of 1-octylbromide was added followed by 2 eq. of potassium tert-butoxide and allowed to stir for 8 hours after which the reaction was allowed to cool to r.t. The THF was evaporated. The remaining solid was dissolved in hexanes with 200 mg of *t*-Butyl hydroxide and passed over an alumina plug using 500 mL of hexanes which was then evaporated to dryness and recrystallized using minimal ethanol giving white crystals in a 84% yield. MP: 50-52^{o}C. ^{1}H-NMR (500 MHz, $CDCl_3$); δ 7.50 (d, 2H, J= 7.8 Hz), 7.45 (d, 4H, J= 8.4 Hz), 1.90 (m, 4H), 1.39-1.04 (m, 20H), 0.92 (m, 6H), 0.81 (bs, 4H). ^{13}C-NMR (125 MHz, $CDCl_3$); δ 152.8, 139.4, 130.2, 128.6, 125.2, 56.7, 40.5, 34.6, 32.1, 31.1, 23.4, 22.2, 18.3.

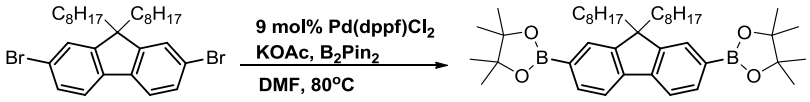

M2.6 M2.7

2,2'-(9,9-dioctyl-9H-fluorene-2,7-diyl)bis(4,4,5,5-tetramethyl-1,3,2-dioxaborolane) (M2.7)

To a dry 250 mL round bottom flask with magnetic stirbar, 4 g of **M2.6** (4 g, 0.0073 mol), 4,4,4',4',5,5,5',5'-octamethyl-2,2'-bi(1,3,2-dioxaborolane) (9.30 g, 0.04 mol), and oven dried potassium acetate (6.20 g, 0.63 mol) were added and then vacuum purged and filled with argon 3 times. Anhydrous-amine free DMF (120 mL) was added by cannula to the flask. The solution was bubbled with argon for 45 minutes whilst stirring. After degassing, 9 mol% of $Pd(dppf)Cl_2$ (537 mg, 0.66 mmol) was added rapidly while an argon atmosphere was maintained. The solution was then heated to 80^{o}C and allowed to stir for 24 hours after which the reaction was cooled to r.t. and the DMF was removed *in vacuo* yielding black crystals. The crystals were recrystallized twice from hexanes giving white crystals in 75% yield. MP:123-124^{o}C. ^{1}H-NMR (500 MHz, $CDCl_3$); δ 7.81 (d, 2H, J= 7.2 Hz), 7.75 (d, 4H, J=7.0 Hz), 2.00 (m, 4H), 1.38 (s, 24H), 1.21-1.05 (m, 20H), 0.82 (bs, 6H), 0.61 (bs, 4H). ^{13}C-NMR (125 MHz, $CDCl_3$); δ 153.2, 139.4, 130.6, 128.4, 125.2, 56.1, 40.7, 34.8, 32.2, 31.1, 23.4, 22.3, 18.5.

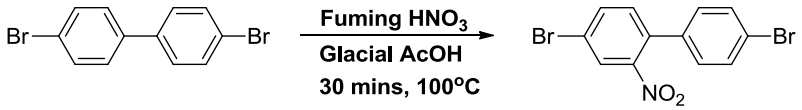

M2.8

4,4'-dibromo-2-nitro-1,1'-biphenyl (M2.8)

4,4'-dibromo-1,1'-biphenyl (20 g, 64 mmol) was added to a 500 mL Erlenmeyer flask with stirbar. Then 300 mL of glacial acetic acid was added and the mixture was stirred and heated to 120^{o}C. Once the solid fully dissolved, 100 mL of 90% nitric acid was added at a rate of 2 drops/sec. After addition, the solution was stirred at 120^{o}C for 30 minutes where the flask was removed from heat and allowed to cool to room temperature. The resulting yellow precipitate was vacuum filtered and then washed three times with cold ethanol. The product was collected as a pale yellow solid in 70% yield with a melting point of 122-125^{o}C. ^{1}H-NMR (300 MHz, $CDCl_3$) δ 8.03 (d, 1H, J= 3.0 Hz), 7.75 (dd, 1H, J= 2 Hz, 8 Hz), 7.56 (ABq, 2H), 7.28 (d, 1H, J= 8 Hz), 7.16 (ABq, 2H); ^{13}C-NMR (75 MHz, $CDCl_3$) δ 135.6, 135.3, 134.18, 133.0, 132.0, 129.4, 127.3, 123.1, 121.8.

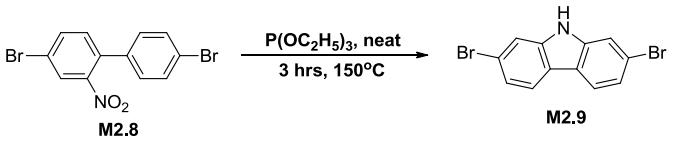

M2.8 M2.9

2,7-dibromo-9H-carbazole (M2.9)

4,4'-dibromo-2-nitro-1,1'-biphenyl (16.64 g, 41 mmol of) was added to a 250 mL one neck round bottom flask with stirbar. After a condenser was affixed to the flask, the system was vacuum purged and filled with argon three times. Using a syringe, 100 mL of triethylphosphite was added rapidly. The dispersion was stirred and heated to 65^{o}C to dissolve the solid. The solution was then stirred and refluxed for three hours, after the flask was removed from heat and allowed to cool to room temperature. The triethylphosphate was then evaporated off with rotovap, yielding a dark brown oil which was then dissolved into DCM and then extracted. The organic layer was dried over magnesium sulfate, filtered, and the solvent was evaporated off. The resulting orange oil was purified *via* silica gel chromatography using 25% ethylacetate in hexanes. The product was collected as a white solid in 55% yield with a melting point of 234-236^{o}C.. ^{1}H-NMR (300 MHz, $CDCl_3$) δ 8.06 (bs, 1H), 7.88 (d, 2H, J= 9 Hz), 7.58 (d, 2H, J = 1.6 Hz), 7.36 (dd, 2H, J = 1.6 Hz, 8.5 Hz); ^{13}C-NMR (75 MHz, $CDCl_3$) δ 140.2, 123.3, 121.7, 121.5, 119.7, 113.8.

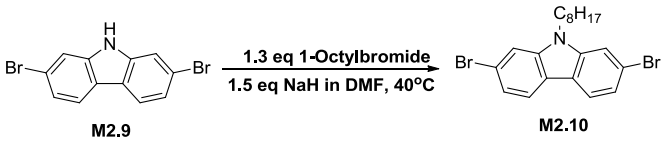

M2.9 M2.10

2,7-dibromo-9-octyl-9H-carbazole (M2.10)

To a 500 mL two neck round bottom flask with stirbar, 2,7-dibromo-9-octyl-9H-carbazole, (7.00 g, 21.6 mmol) was added and then vacuum purged and filled with argon three times. Anhydrous DMF (70mL) was then added and the solution was stirred followed by the onetime addition of sodium hydride (60% in mineral oil) (1.30 g, 32.4 mmol). The solution was then stirred for 45 minutes, after 1-octylbromide (5.42 g, 28.1

mmol) was added *via* syringe at a rate of 2 drops a second. The solution was then warmed to 40°C for and allowed to react overnight where after the solution was then quenched with 400 mL of deionized water and then extracted with ethyl acetate. The organic layer was washed four times with water and then once with a saturated solution of ammonium chloride, dried over magnesium sulfate, filtered, and then the solvent was evaporated off. The resulting yellow oil was vacuumed purged at 70°C until a yellow solid resulted which was then recrystallized with methanol yielding white needles (70%) with a melting point of 59-60°C. ^{1}H-NMR (300 MHz, $CDCl_3$) δ 7.89 (d, 2H, J= 6 Hz), 7.53 (d, 2H, J= 3 Hz), 7.33 (dd, 2H, J= 1.5 Hz, 9 Hz), 4.19 (t, 2H, J= 9 Hz), 1.83 (m, 2H), 1.35-1.19 (bm, 10H), 0.87 (t, 3H, J= 6 Hz); ^{13}C-NMR (75 MHz, $CDCl_3$) δ 141.3, 122.5, 121.4, 121.2, 119.7, 112.0, 43.3, 31.8, 29.3, 29.2, 28.8, 27.2, 22.6, 14.1. HRMS (EI-FTICR): *m/z* calcd for $C_{20}H_{23}Br_2N(M^+)$ 435.0197, found 435.0203.

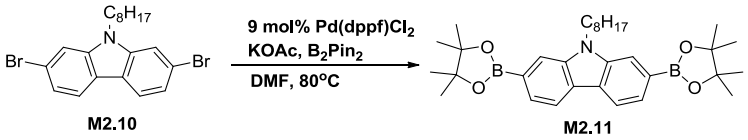

M2.10 M2.11

9-octyl-2,7-bis(4,4,5,5-tetramethyl-1,3,2-dioxaborolan-2-yl)-9H-carbazole (M2.11)

To a 500 mL one neck round bottom flask with stir bar, 2,7-dibromo-9-octyl-9H-carbazole (5 g, 11.4 mmol), 4,4,4',4',5,5,5',5'-octamethyl-2,2'-bi(1,3,2-dioxaborolane) (14.5 g, 57.2 mmol), and oven dried potassium acetate (9.51 g, 97 mmol) was added and vacuum purged then filled with argon 3 times. Once purged, 380 mL of DMF was added, the solution was stirred and bubbled with argon for 45 minutes where after, 9 mol% $Pd(dppf)Cl_2$ (838 mg, 11.4 mmol) was added. The reaction was heated to 80°C over night. After the solution was allowed to cool to r.t. and then the solvent was evaporated off. The black solid was dissolved in 10% ethyl acetate in hexanes and passed through a short silica plug. The solution was evaporated down to an orange residue which was then recrystallized twice from ethanol giving white needles (80%) with a melting point of 182-184°C. ^{1}H-NMR (300 MHz, $CDCl_3$) δ 8.12 (d, 2H, J= 9 Hz), 7.88 (s, 2H), 7.67 (d, 2H, J=

9 Hz), 4.38 (t, 2H, J= 6 Hz), 1.88 (m, 2H), 1.39 (s, 24H), 1.26-1.22 (m, 10H), 0.87 (t, 3H, J= 6 Hz); ^{13}C-NMR (75 MHz, $CDCl_3$) δ 140.4, 125.0, 124.8, 120, 115.2, 83.7, 31.8, 29.3, 29.2, 27.1, 24.9, 22.6, 18.4, 14.1. HRMS (EI-FTICR): *m/z* calcd for $C_{32}H_{47}B_2NO_4$ (M^+) 531.3691, found 531.3696.

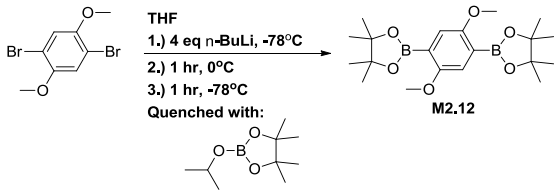

2,2'-(2,5-dimethoxy-1,4-phenylene)bis(4,4,5,5-tetramethyl-1,3,2-dioxaborolane) (M2.12)

To a 250 mL round bottom flask with magnetic stirbar, 1,4-dibromo-2,5-dimethoxybenzene (2.9g, 0.01 mol) was added and vacuum purged and filled with argon 3 times. Anhydrous THF (100 mL) was then added and the solution was stirred and cooled to -78^{o}C. After, *n*-butyl lithium (*n*-BuLi, 16 mL, 0.04 mol) was added as a 2.5 M solution in hexanes slowly at a rate of 0.5 mL/sec. Once *n*-BuLi was added, the mixture was warmed to 0^{o}C and allowed to stir for 1 hour and was then cooled back down to -78^{o}C where 2-isopropoxy-4,4,5,5-tetramethyl-1,3,2-dioxaborolane (7.44 g, 0.04 mol) was added at a rate of 1 mL/sec. The reaction was then allowed to warm to r.t. and stirred for 8 hours. The reaction was quenched with 30mL of 0.05 M HCl and immediately extracted with ethylacetate 3 times. The organic layer was dried over $MgSO_4$, filtered, and evaporated down to a pink crystalline solid which was then recrystallized using minimal hexanes to yield white crystals in 57% yield. MP: 185-187^{o}C. ^{1}H-NMR (500 MHz, $CDCl_3$); δ 7.15 (s, 2H) 3.82 (s, 6H), 1.35 (s, 24H). ^{13}C-NMR (125 MHz, $CDCl_3$); δ 207.1, 158.3, 119.1, 83.8, 57.2, 25.1. HRMS (ESI–FTICR): *m/z* calcd for $C_{20}H_{32}B_2O_6$($M+H^+$) 390.2385, found 390.2268. Anal. calcd. for $C_{20}H_{32}B_2O_6$ C 61.58, H 8.27, Found C 61.66, H 8.46.

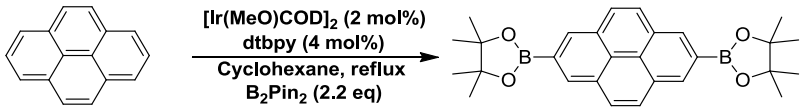

M2.13

2,7-bis(4,4,5,5-tetramethyl-1,3,2-dioxaborolan-2-yl)pyrene (M2.13)

To a 250 mL round bottom flask with stirbar, Pyrene (5 g, 0.0247 mol), 4,4,4',4',5,5,5',5'-octamethyl-2,2'-bi(1,3,2-dioxaborolane) (13.83 g, 0.054 mol) and 4,4'-di-*tert*-butyl-2,2'-bipyridine (4 mol%, 265 mg, 1 mmol) were all dissolved in cyclohexane (100 mL). The mixture was bubbled with argon for 45 minutes. Bis(1,5-cyclooctadiene)di-μ-methoxydiiridium(I) (2 mol%, 327 mg, 0.5 mmol) was added rapidly and then an oven dried condenser was affixed to the flask. The mixture was allowed to stir at 80^{o}C for 20 hours after which, the volatiles were evaporated leaving a red-black solid. The crude solid was washed with ethanol, dissolved in toluene and then precipitated twice using ethanol, yielding white needles in 60% yield. MP: 344-346^{o}C. ^{1}H-NMR (300 MHz, $CDCl_3$) δ 8.62 (s, 4H), 8.08 (s, 4H), 1.46 (s, 24H); ^{13}C-NMR (75 MHz, $CDCl_3$) δ 131.2, 130.9, 127.6, 126.3, 84.2, 24.9. HRMS (EI-FTICR): *m/z* calcd for $C_{28}H_{32}B_2O_4$ (M^+) 454.2487, found 454.2491.

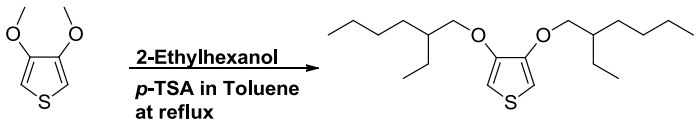

M2.14

3,4-bis((2-ethylhexyl)oxy)thiophene (M2.14)

In a 1000 mL round bottom flask with magnetic stir bar, dimethoxythiophene (17.0 g, 0.117 mol), 2-ethylhexanol (40.0 g, 0.304 mol), and *p*-toluenesulfonic acid (2.2 g, 0.012 mol) were added under argon followed by anhydrous toluene (500 mL). The flask was attached to a soxhlet apparatus and an appropriate cellulose thimble was filled with activated molecular sieves (3Å) to remove methanol. The reaction was refluxed overnight after which the reaction was quenched with 300 mL of a saturated $NaHCO_3$ solution. The organic layer was extracted 3 times into DCM then passed over a silica plug using

hexanes and evaporated to yield a green oil. The oil was purified by distillation (180°C @ 1 torr) giving a colorless oil in 75% yield. ^{1}H-NMR (300 MHz, $CDCl_3$); 6.19 (s, 2H), 3.86 (d, 4H, J= 6 Hz), 1.77 (m, 2H), 1.60-1.31 (m, 16H), 0.94 (t, 12H, J= 7 Hz). ^{13}C-NMR (125 MHz, $CDCl_3$); 147.2, 97.4, 73.3, 39.4, 30.8, 29.5, 24.1, 23.0, 14.2, 11.4.

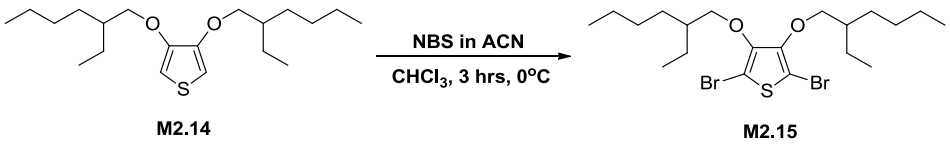

M2.14 M2.15

2,5-dibromo-3,4-bis((2-ethylhexyl)oxy)thiophene (M2.15)

To a dry 500 mL round bottom flask with magnetic stir bar, **M2.14** (10.0 g, 0.029 mol) was added and dissolved in 350 mL of chloroform then bubbled with argon for 45 minutes. To a powder addition funnel, *N*-bromosuccinimide (NBS, 13.1 g, 0.073 mol) was added and left under an argon blanket. The funnel was attached to the flask and the temperature was lowered to 0°C. The NBS was completely added over a 10 minute period. The entire system was covered in foil to avoid light exposure. After all NBS was added, the reaction temperature was raised to r.t. and allowed to stir for overnight where the reaction was determined complete by TLC using 4:1 hexanes:dichloromethane. The solvent was stripped off *via* rotovap and the crude was purified by Silica chromatography using hexanes. Product was evaporated down at room temperature and vacuum dried overnight covered in aluminum foil yielding a pale green-yellow oil in 96% yield. ^{1}H-NMR (300 MHz, $CDCl_3$); δ 3.96 (d, 4H, J= 7 Hz), 1.47 (m, 2H), 1.66-1.27 (m, 16H), 0.93 (t, 12H, J= 7 Hz); ^{13}C-NMR (75 MHz, $CDCl_3$); δ 147.8, 94.8, 40.1, 30.1, 28.9, 23.9, 23.0, 14.1, 11.1. HRMS (EI-FTICR): *m/z* calcd for $C_{20}H_{34}Br_2O_2S$ (M^+) 496.0650, found 496.0646.

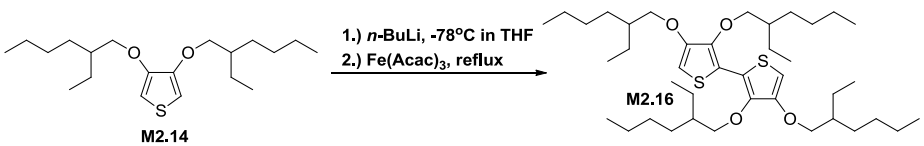

M2.14

3,3',4,4'-tetrakis((2-ethylhexyl)oxy)-2,2'-bithiophene (M2.16)

To a dry 1000 mL round bottom flask with stir bar **M2.14** (20.4 g, 0.06 mol) was dissolved in 500 mL of dry THF and then bubbled with argon for 45 minutes then lowered to -78^{o}C where *n*-butyl lithium (2.5 M, 0.06 mol) in hexane was added. After stirring for 45 min at -78^{o}C from final addition of *n*-BuLi, the solution was transferred into a dry-degassed THF solution (80 mL) of $Fe(acac)_3$ (21.2 g, 0.06 mol) under argon at r.t *via* cannula and the reaction mixture was refluxed for 72 hours until determined complete by TLC using 4:1 hexanes:dichloromethane. Volatiles were evaporated, and the residue was purified by column chromatography through silica using 6:1 hexane:dichloromethane to give **M2.16** in 70% yield as pale yellow-green viscous oil; ^{1}H-NMR (300 MHz, $CDCl_3$); δ 6.06 (s, 2H), 3.98 (d, 4H, J= 6 Hz), 3.85 (d, 4H, J= 5 Hz), 1.84 (m, 2H), 1.72 (m, 2H), 1.45-1.03 (m, 32H), 0.98-0. 98 (m, 24H); ^{13}C-NMR (75 MHz, $CDCl_3$); δ 149.7, 142.1, 117.6, 94.3, 75.6, 71.8, 40.5, 39.5, 30.7, 30.0, 29.0, 24.3, 23.5, 22.8, 14.1, 11.1. HRMS (EI-FTICR): *m/z* calcd for $C_{40}H_{70}O_4S_2$ (M^+) 678.4697, found 678.4716.

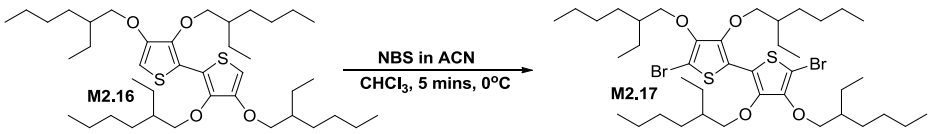

5,5'-dibromo-3,3',4,4'-tetrakis((2-ethylhexyl)oxy)-2,2'-bithiophene (M2.17)

To a dry 250 mL round bottom flask with stir bar, **M2.16** (3 g, 4.42 mmol) was added and dissolved in 40 mL of chloroform then bubbled with argon for 30 minutes. In an iodometric flask, *N*-bromosuccinimide (NBS, 1.95 g, 0.011 mol) was dissolved in 40 mL of 1:1 chloroform:acetonitrile and then bubbled with argon for 30 minutes. Once bubbling was complete, the flask containing the solution of **M2.16** was lowered to 0^{o}C. The solution of NBS was added in one portion. After all NBS solution was added, the reaction was stirred for 5 minutes at 0^{o}C where the reaction was determined complete by TLC using 9:1 hexanes:dichloromethane. All volatiles were evaporated yielding a purple oil. The crude product was purified by Silica chromatography using hexanes. Product was

evaporated to dryness at room temperature and vacuum dried overnight covered in foil yielding a yellow oil in 92% yield. ^{1}H-NMR (300 MHz, $CDCl_3$); δ 3.93 (m, 8H), 1.80 (m, 2H), 1.69 (m, 2H), 1.49-1.31 (m, 32H), 0.96-0.88 (m, 24H); ^{13}C-NMR (75, $CDCl_3$) δ 147.5, 144.5, 116.8, 96.1, 40.2, 30.0, 29.5, 23.9, 23.0, 14.2, 11.1. HRMS (EI-FTICR): *m/z* calcd for $C_{40}H_{68}Br_2O_4S_2$ (M^+) 834.2900, found 834.2926.

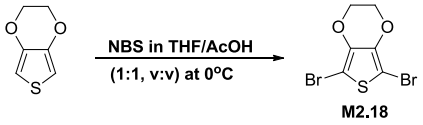

5,7-dibromo-2,3-dihydrothieno[3,4-b][1,4]dioxine (M2.18)

To a dry 100 mL two-neck round bottom flask with stir bar, EDOT (5 g, 0.035 mol) was added and dissolved in 40 mL of THF:glacial acetic acid (1:1 by volume), cooled to 0^{o}C then bubbled with argon for 45 minutes. NBS (13.7 g, 0.077 mol) was added in small portions over 10 minutes. After all NBS solution was added, the reaction was stirred for 2 hours at while warming to r.t. under foil and argon. The crude was then poured into 200 mL of D.I. water and stirred for 30 minutes. The dispersion was poured over qualitative filter paper until pH 6 was achieved by washing with D.I. water, yielding a black precipitate. Crude was passed through silica using ethylether and rotovapped down to a pale pink solid which was then recrystallized three times using methanol and isopropyl alcohol yielding off-white needles in 60% yield. ^{1}H-NMR (300 MHz, $CDCl_3$); δ 4.28 (s, 4H); ^{13}C-NMR (75, $CDCl_3$) δ 140.3, 85.2, 65.6.

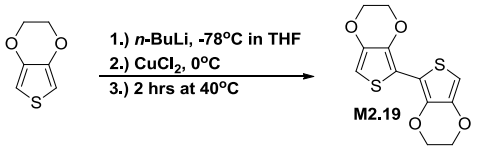

2,2',3,3'-tetrahydro-5,5'-bithieno[3,4-b][1,4]dioxine (M2.19)

To a dry 300 mL two-neck round bottom flask with stir bar, EDOT (5.0 g, 0.035 mol) was dissolved in 150 mL of dry THF and then bubbled with argon for 30 minutes then lowered to -78^{o}C where *n*-butyl lithium (2.5 M, 0.035 mol) in hexane was added drop-wise. After stirring for 45 min at 0^{o}C from final addition of *n*-BuLi, the solution was

cooled back down to -78°C where $CuCl_2$ (4.7 g, 0.035 mol) was added in one portion. The reaction was then warmed to 40°C and stirred for 2 hours and then poured into 500 mL of D.I. water and stirred for 30 minutes. The pale green precipitate was filtered over coarse filter paper, washed with 600 mL of water and then 600 mL of hexane and dried. The green-blue crude was purified through a thin pad of silica using chloroform. The final solution was concentrated and precipitated into methanol, stirred for 45 minutes and then filtered and vacuum dried to give **M2.19** in 42% yield as off-white-powder; ^{1}H-NMR (300 MHz, $CDCl_3$); δ 6.26 (s, 2H), 4.28 (dm, 8H); ^{13}C-NMR (75 MHz, $CDCl_3$); δ 139.7, 85.5, 64.9.

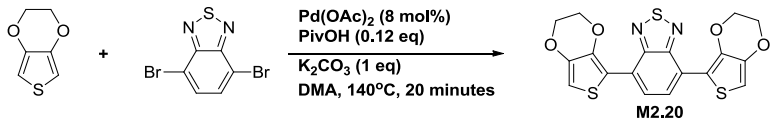

4,7-bis(2,3-dihydrothieno[3,4-b][1,4]dioxin-5-yl)benzo[c][1,2,5]thiadiazole (M2.20)

To a dry 100 Schlenk flask with stir bar, EDOT (10.2 g, 0.072 mol) and 4,7-dibromobenzo[c][1,2,5]thiadiazole (2.9 g, 0.012 mol), 8 mol% palladium acetate (0.22 g, 1.0 mmol), pivalic acid (0.15 g, 1.4 mmol), and potassium carbonate (1.7 g, 0.012 mol) were added and vacuum purged for 45 minutes followed by three purge and argon back-fill cycles. *N*,*N*-dimethylacetamide was degassed by bubbling with argon for 45 minutes then injected into the flask to dissolve the contents. The flask was lowered into an oil bath held at 140°C. The reaction was monitored by TLC in DCM and was determined to be complete at 20 minutes where the mixture was poured into 600 mL of methanol and stirred for 45 minutes then filtered over qualitative filter paper giving a dark purple-red solid which was suction dried to give the crude product in 90% yield. The solid was purified by sublimation and the acquired red solid was washed with excess methanol over fine filter paper, dissolved into DCM and reduced down to give **M2.20** as red crystals in 40% yield. ^{1}H-NMR (300 MHz, $CDCl_3$); δ 8.39 (s, 2H), 6.57 (s, 2H), 4.40 (m, 4H), 4.33 (m, 4H). *m/z* calcd for $C_{20}H_{34}Br_2O_2S$ (M^+) 415.9959, found 415.9959.

Typical Suzuki polycondensation procedure to yield polymers

Compound **M2.3** or **M2.5** (0.0012 mol) was added precisely *via* pipette to within 0.4 mg to a small vial. Then **M2.3** or **M2.5** was completely dissolved in 10-20 mL of hexanes and pipetted into a 50 mL schlenk tube with magnetic stir bar. The solution was stirred while the hexanes were gently removed *in vacuo*. Two drops of Aliquat 336 were added followed by 1.005 eq. of **1,4-Benzenediboronic acid dipinacol ester, M2.7, M2.11, M2.12, or M2.13**, 3 mol% P(*o*-tol)$_3$, K_3PO_4 (0.015 mol, 3M) or CsF (0.03 mol, 6M), and 1 mol% Pd_2dba_3. The schlenk tube was capped with a septum and then wired shut. The contents of the tube were vacuum pumped for 45 minutes. After which the contents of the tube were filled with argon then vacuum purged and filled with argon 3 times. Degassed toluene (15 mL) was added followed by 5 mL of degassed water. The mixture was then stirred to ensure complete mixing of phases, heated to 90^{o}C, and covered with aluminum foil for 72 hours. The mixture was then cooled to r.t., precipitated into methanol, allowed to stir for one hour. The solid was filtered into a soxhlet extraction thimble and washed with methanol, hexanes, and chloroform respectively. The washings were conducted until color was no longer observed during extraction. After the chloroform wash, the resulting solution was concentrated down to *ca.*30 mL and stirred with 200 mg of the palladium scavenger diethylammonium diethyldithiocarbamate for 6 hours at 50^{o}C then precipitated into 300 mL of methanol. The precipitate was filtered over a 20 μm Nylon pad and washed with 300 mL of pure methanol and allowed to dry. The dried material was collected into a tared vial and vacuum dried.

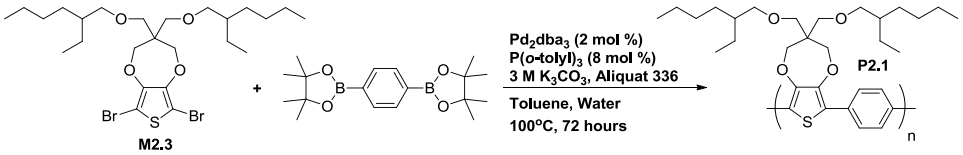

P2.1: Yellow solid in 80% yield (860 mg). ^{1}H-NMR (500 MHz, $CDCl_3$): δ 7.78 (br s, 4H), 4.20 (br s, 4H), 3.58 (br s, 4H), 3.36 (br s, 4H), 1.6-1.2 (br, 16H), 0.96 (br s, 12H) Anal. calcd. for $C_{38}H_{54}O_4S$ C 72.33, H 9.01, Found C 72.47, H 9.81. GPC: M_n: 20.2 kDa,

M_w: 34.4 kDa, PDI: 1.70, in THF vs PolyStyrene. M_n: 10.8 kDa, M_w: 31.2 kDa, PDI: 2.89, in TCB vs PS.

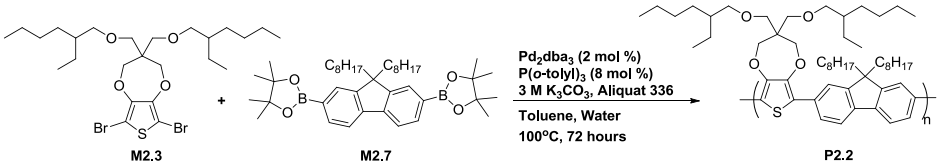

P2.2: Brown solid in 83% yield (773 mg). ^{1}H-NMR (500 MHz, $CDCl_3$): δ 7.81 (br s, 2H), 7.7 (br s, 4H), 4.24 (br s, 4H), 3.63 (br s, 4H), 3.36 (br s, 4H), 2.05-1.9 (br s, 4H), 1.4-1.25 (br s, 18H), 1.23-1 (br s, 20), 0.95-0.8 (br s, 14H), 0.79-0.6 (br s, 12H). Anal. calcd. for $C_{54}H_{82}O_4S$ C 78.42, H 9.99, Found C 78.81, H 10.22. GPC: M_n: 12.0 kDa, M_w: 17.6 kDa, PDI: 1.47, in THF vs PS.

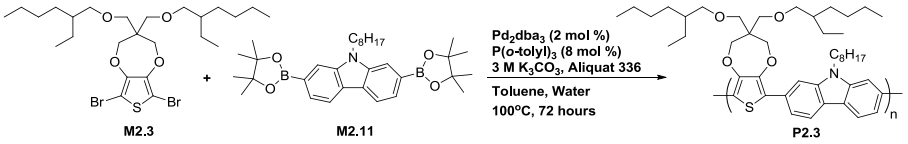

P2.3: Yellow solid in 95% yield (800 mg). ^{1}H-NMR (300 MHz, $CDCl_3$) δ 8.08 (br d, 2H, J= 9 Hz), 7.85 (br s, 2H), 7.67 (br d, 2H, J= 9 Hz), 4.54-4.06 (br m, 6H), 3.67 (br s, 4H), 3.37 (br d, 4H, J= 6 Hz), 2.06-1.92 (br s, 2H), 1.65-1.19 (br m, 34 H), 0.98-0.80 (br m, 15H). Anal. calcd. for $C_{45}H_{65}NO_4S$ C 75.48, H 9.15, Found C 75.49, H 9.24. GPC: M_n: 15.5 kDa, M_w: 42.3 kDa, PDI: 2.90, in TCB vs PS.

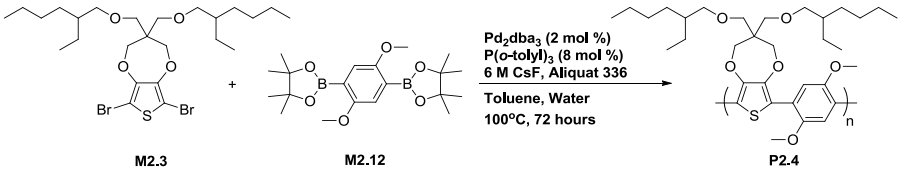

P2.4: Orange flakes in 38% yield (256 mg). ^{1}H-NMR (300 MHz, $CDCl_3$) δ 7.45 (br s, 2H), 4.17 (br s, 4H), 3.90 (br r, 6H), 3.56 (br s, 4H), 3.30 (br d, 4H, J= 3 Hz), 1.6-1.43 (br s, 2H), 1.42-1.19 (br m, 16 H), 0.98-0.80 (br m, 12H). Anal. calcd. for $C_{33}H_{50}O_6S$ C 68.95, H 8.77, Found C 69.19, H 8.64. GPC: M_n: 16.6 kDa, M_w: 24.4 kDa, PDI: 1.46, in THF vs PS.

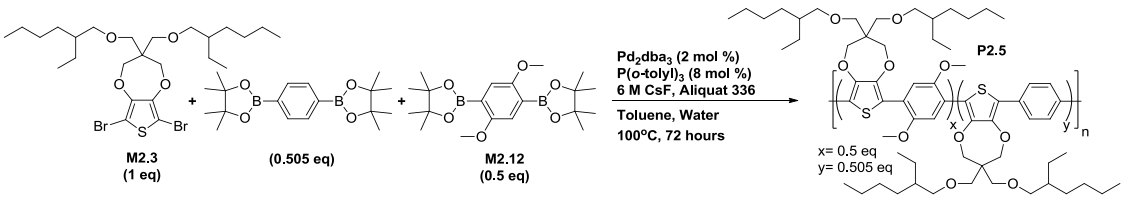

P2.5: Orange powder in 20% yield (125 mg). ^{1}H-NMR (300 MHz, $CDCl_3$) δ 7.7 (br s, 4H), 4.11 (br s, 2H), 3.83 (br s, 6H), 3.50 (br s, 4H), 3.24 (br s, 4H), 1.54-1.37 (br s, 2H), 1.36-1.12 (br m, 16 H), 0.91-0.75 (br m, 12H). Anal. calcd. for $C_{32}H_{48}O_5S$ C 70.64, H 8.89, Found C 71.09, H 9.00. GPC: M_n: 14.9 kDa, M_w: 22.4 kDa, PDI: 1.50, in THF vs PS.

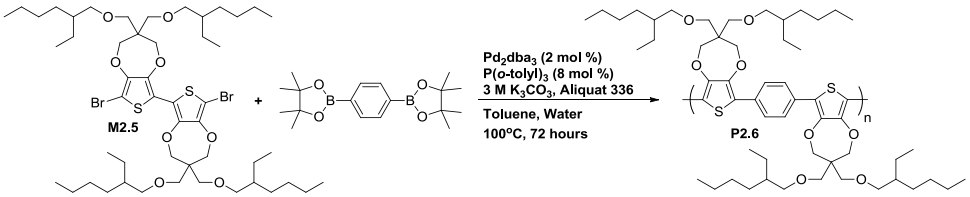

P2.6: Orange solid in 96% yield (640 mg). ^{1}H-NMR (300 MHz, $CDCl_3$) δ 7.7 (br s, 4H), 4.17 (br s, 4H), 3.60 (br s, 8H), 3.60 (br s, 8H), 3.35 (br d, 8H, J= 4 Hz), 1.60-1.41 (br s, 4H), 1.38-1.25 (br m, 32H), 1.05-0.85 (br m, 24H). Anal. calcd. for $C_{56}H_{88}O_8S_2$ C 70.55, H 9.30, Found C 69.67, H 9.21. GPC: M_n: 13.8 kDa, M_w: 26.3 kDa, PDI: 1.90, in THF vs PS.

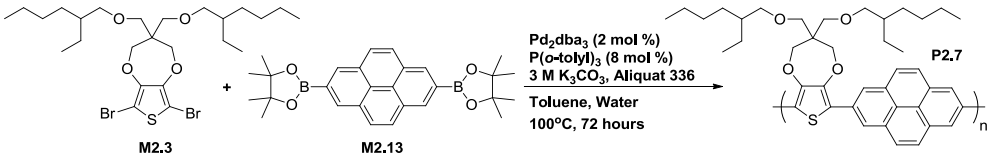

P2.7: Brown powder in 80% yield (343 mg). ^{1}H-NMR (300 MHz, *o*-DCB) δ 8.6 (br, 4H), 8.0 (br, 4H), 4.1 (br s, 4H), 3.56 (br s, 4H), 3.34 (br s, 4H), 1.6-1.2 (br, 16H), 0.96 (br s, 12H) Anal. calcd. for $C_{38}H_{54}O_4S$ C 72.33, H 9.01, Found C 72.47, H 9.81. Anal. calcd. for $C_{41}H_{50}O_4S$ C 77.08, H 7.89, Found C 74.27, H 7.48. GPC: M_n: 8.3 kDa, M_w: 24.9 kDa, PDI: 3.00, in TCB vs PS.

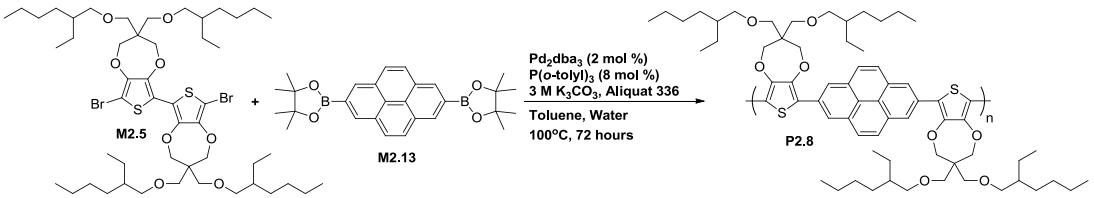

P2.8: Brown solid in 78% yield (573 mg). ^{1}H-NMR (300 MHz, *o*-DCB) δ 8.6 (br, 4H), 8.1 (br, 4H), 4.2 (br s, 4H), 3.57 (br s, 8H), 3.62 (br s, 8H), 3.38 (br, 8H), 1.60-1.41 (br s, 4H), 1.38-1.25 (br m, 32H), 1.05-0.85 (br m, 24H). Anal. calcd. for $C_{66}H_{92}O_8S_2$ C 73.56, H 8.61, Found C 72.3, H 8.49. GPC: M_n: 9.2 kDa, M_w: 39.1 kDa, PDI: 4.26, in TCB vs PS.

Typical direct arylation polycondensation procedure to yield polymers

To a 50 mL round bottom flask with stir bar, the dibromide monomer **1,4-Dibromobenzene, M2.3, M2.5, M2.15, M2.17, M2.18, 4,7-dibromobenzothiadiazole** (1.17 mmol, or appropriate equivalent listed below), dihydrin monomer **M2.2, M2.4, M2.14, M2.16, M2.19, M2.20** (1.17 mmol, or appropriate equivalent listed below), 8 mol% palladium acetate (5.3 mg, 0.023 mmol), pivalic acid (36.0 mg, 0.35 mmol), and potassium carbonate (0.323 g, 2.34 mmol) were added and a claisen head was affixed to the top of the flask and then vacuum purged for 45 minutes followed by three purge and argon back-fill cycles. *N*,*N*-dimethylacetamide was degassed by bubbling with argon for 45 minutes then injected into the flask to dissolve the contents. The flask was lowered into an oil bath held at 140^{o}C and allowed to stir vigorously from 1.5 hrs-24 hrs. After the flask was removed from the oil bath and allowed to cool to r.t. and the polymer dispersion was dissolved with chloroform and precipitated into methanol:1 M HCl (350 mL: 75 mL) and stirred for 45 minutes. The precipitate was filtered into a soxhlet extraction thimble and washed with methanol, acetone, hexanes, and chloroform respectively. The washings were conducted until color was no longer observed during extraction. After dissolution from the thimble, the solvent was removed *via* rotovap and then 50 mL of chlorobenzene was added followed by 200 mg of the palladium scavenger

diethylammonium diethyldithiocarbamate, 300 mg of 18-crown-6 and then stirred for 6 hours at 50°C then precipitated into 300 mL of methanol. The precipitate was filtered over a 20 μm Nylon pad and washed with 300 mL of pure methanol and allowed to dry. The dried material was collected into a tared vial and vacuum dried.

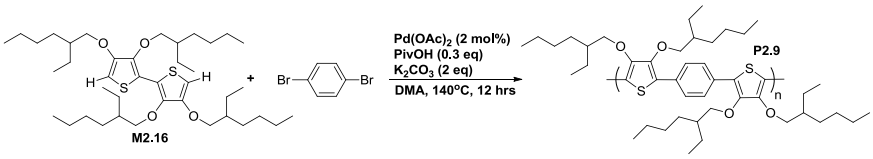

P2.9: Yellow solid in 96% yield (643 mg). ^{1}H-NMR (300 MHz, $CHCl_3$) δ 7.75 (br, 4H), 4.07 (br d, 4H, J= 6 Hz), 3.90 (br s, 4H), 1.95 (br s, 4H), 1.82-1.16 (br m, 34H), 1.08-0.85 (br m, 24H). Anal. calcd. for $C_{46}H_{72}O_4S_2$ C 73.35, H 9.64, Found C 72.84, H 10.09. GPC: M_n: 77.8 kDa, M_w: 261.4 kDa, PDI: 3.4, in THF vs PS.

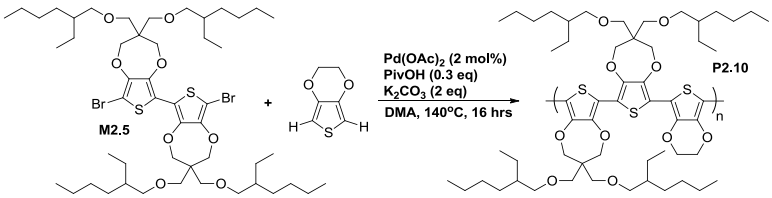

P2.10: Purple solid in 81% yield (1064 mg). ^{1}H-NMR (300 MHz, $CHCl_3$) δ 4.39 (br s, 4H), 4.15 (br s, 8H), 3.60 (br s, 8H), 3.32 (br, 8H), 1.6-1.25 (br m, 36H), 1.05-0.85 (br m, 24H). Anal. calcd. for $C_{56}H_{88}O_{10}S_3$ C 66.11, H 8.72, Found C 67.02, H 8.47.

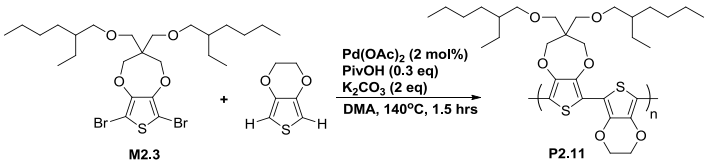

P2.11: Black solid in 23% yield (158 mg). ^{1}H-NMR (300 MHz, $CHCl_3$) δ 4.40 (br, 4H), 4.14 (br, 4H), 3.59 (br s, 4H), 3.29 (br s, 4H), 1.67-1.43 (br s, 2H), 1.42-1.00 (br m, 16H), 0.95-0.85 (br m, 12H). Anal. calcd. for $C_{31}H_{46}O_6S_2$ C 64.33, H 8.01, Found C 64.83, H 8.49.

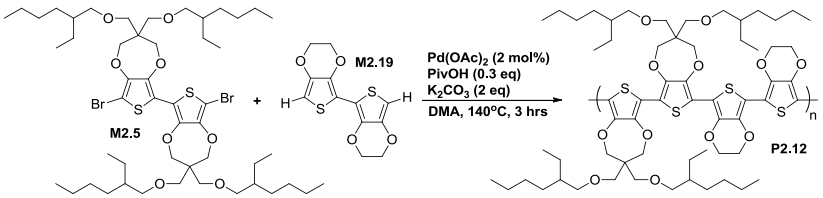

P2.12: Blue solid in 70% yield (621 mg). ^{1}H-NMR (300 MHz, $CHCl_3$) δ 4.39 (br s, 8H), 4.17 (br s, 8H), 3.59 (br s, 8H), 3.31 (br, 8H), 1.62-1.15 (br m, 36H), 1.05-0.85 (br m, 24H). Anal. calcd. for $C_{62}H_{92}O_{12}S_4$ C 64.33, H 8.01, Found C 63.98, H 7.94.

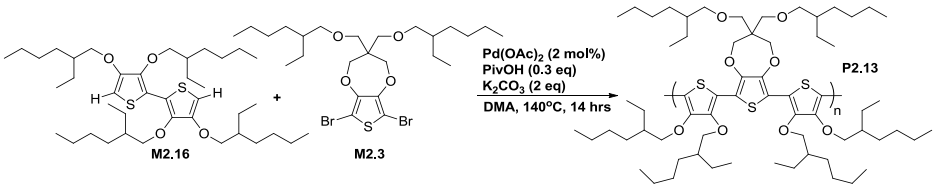

P2.13: Red solid in 82% yield (880 mg). ^{1}H-NMR (300 MHz, $CHCl_3$) δ 4.25 (br, 4H), 3.97 (br, 4H), 3.62 (br s, 4H), 3.29 (br s, 4H), 1.94 (br s, 2H), 1.79-1.27 (br s, 50H), 1.07-0.75 (br m, 36H). Anal. calcd. for $C_{65}H_{110}O_8S_3$ C 69.97, H 9.94, Found C 71.23, H 9.49. GPC: M_n: 176.0 kDa, M_w: 387.5 kDa, PDI: 2.2, in THF vs PS.

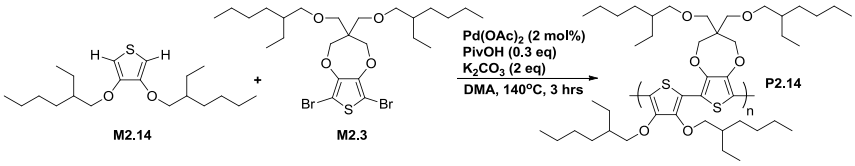

P2.14: Red solid in 97% yield (880 mg). ^{1}H-NMR (300 MHz, $CHCl_3$) δ 4.16 (br s, 4H), 3.96 (br s, 4H), 3.59 (br s, 4H), 3.31 (br, 4H), 1.86 (br, 2H), 1.71-1.14 (br s, 32H), 1.04-0.74 (br m, 24H). Anal. calcd. for $C_{45}H_{76}O_6S_2$ C 69.54, H 9.86, Found C 70.53, H 9.49. GPC: M_n: 51.8 kDa, M_w: 123.1 kDa, PDI: 2.37, in THF vs PS.

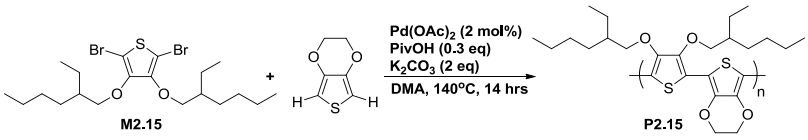

P2.15: Blue solid in 75% yield (420 mg). ^{1}H-NMR (300 MHz, $CHCl_3$) δ 4.37 (br, 4H), 3.96 (br, 4H), 4.2 (br s, 4H), 1.88 (br, 2H), 1.76-1.12 (br s, 16H), 1.07-0.67 (br m, 12H). Anal. calcd. for $C_{26}H_{38}O_4S_2$ C 65.24, H 8.00, Found C 66.08, H 8.66. GPC: M_n: 30.9 kDa, M_w: 37.4 kDa, PDI: 1.21, in THF vs PS.

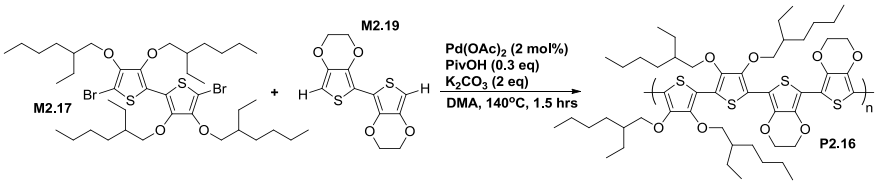

P2.16: Red solid in 65% yield (778 mg). ^{1}H-NMR (300 MHz, $CHCl_3$) δ 4.37 (br, 8H), 3.96 (br, 4H), 1.99 (br s, 2H), 1.73 (br s, 2H), 1.61-1.114 (br s, 32H), 1.08-0.72 (br s, 24H). Anal. calcd. for $C_{52}H_{76}O_8S_4$ C 65.24, H 8.00, Found C 66.82, H 8.51.

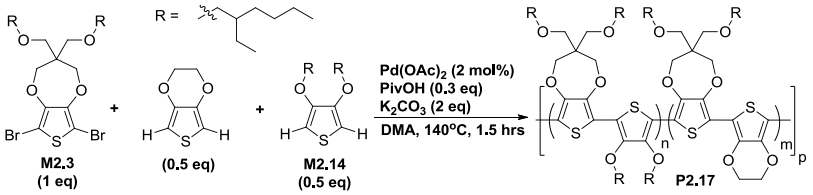

P2.17: Purple solid in 86% yield (686 mg). ^{1}H-NMR (300 MHz, $CHCl_3$) δ 4.39 (br s, 4H), 4.16 (br s, 8H), 3.97 (br s, 4H), 3.61 (br s, 8H), 3.32 (br s, 8H), 1.99 (br s, 2H), 1.87 (br s, 2H), 1.79-1.12 (br m, 50H), 1.05-0.71 (br m, 36H). Anal. calcd. for $C_{38.5}H_{62.5}O_8S_2$ C 68.22, H 9.29, Found C 69.01, H 9.72.

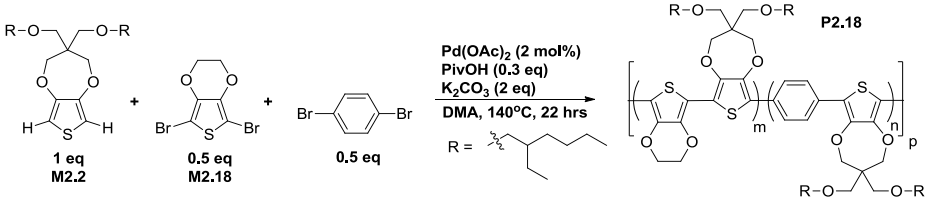

P2.18: Red solid in 88% yield (622 mg). ^{1}H-NMR (300 MHz, $CHCl_3$) δ 7.74 (br, 4H), 4.39 (br s, 4H), 4.16 (br s, 8H), 3.61 (br s, 8H), 3.32 (br s, 8H), 1.87 (br s, 4H), 1.79-1.12 (br m, 32H), 1.05-0.71 (br m, 24H). Anal. calcd. for $C_{31}H_{46}O_5S_{1.5}$ C 68.09, H 9.08, Found C 69.31, H 8.89. GPC: M_n: 46.8 kDa, M_w: 77.7 kDa, PDI: 1.65, in THF vs PS.

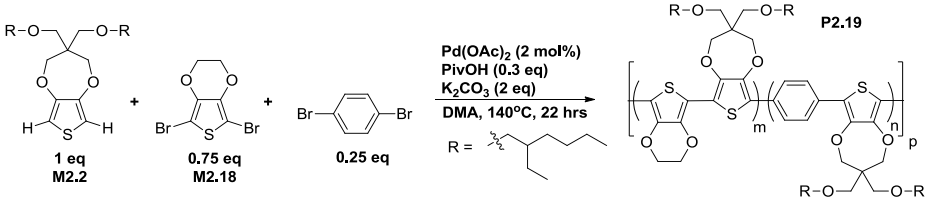

P2.19: Purple solid in 91% yield (662 mg). ^{1}H-NMR (300 MHz, $CHCl_3$) δ 7.73 (br, 4H), 4.38 (br s, 4H), 4.15 (br s, 8H), 3.63 (br s, 8H), 3.34 (br s, 8H), 1.90 (br s, 4H), 1.79-1.12

(br m, 32H), 1.05-0.71 (br m, 24H). Anal. calcd. for $C_{34}H_{46}O_{5.5}S_{1.75}$ C 72.55, H 8.24, Found C 72.83, H 8.50. GPC: M_n: 50.8 kDa, M_w: 80.2 kDa, PDI: 1.57, in THF vs PS.

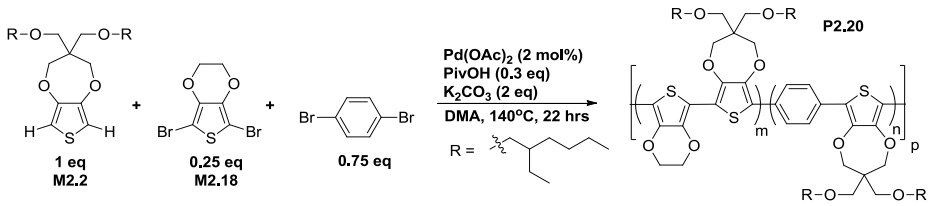

P2.20: Brown solid in 84% yield (587 mg). ^{1}H-NMR (300 MHz, $CHCl_3$) δ 7.71 (br, 4H), 4.40 (br s, 4H), 4.14 (br s, 8H), 3.63 (br s, 8H), 3.32 (br s, 8H), 1.86 (br s, 4H), 1.79-1.12 (br m, 32H), 1.05-0.71 (br m, 24H). Anal. calcd. for $C_{40}H_{46}O_{4.5}S_{1.25}$ C 90.51, H 8.73, Found C 89.20, H 8.49. GPC: M_n: 23.3 kDa, M_w: 40.0 kDa, PDI: 1.71, in THF vs PS.

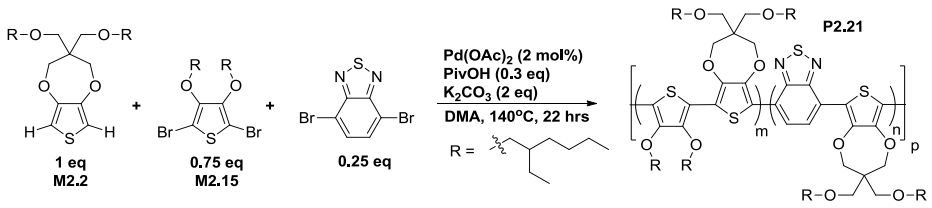

P2.21: Black solid in 89% yield (915 mg). ^{1}H-NMR (300 MHz, $CHCl_3$) δ 8.40 (br, 2H), 4.17 (br s, 4H), 3.97 (br s, 8H), 3.64 (br s, 8H), 3.32 (br s, 8H), 1.87 (br s, 2H), 1.68-1.14 (br m, 54H), 1.08-0.76 (br m, 36H). Anal. calcd. for $C_{44.5}H_{68}N_{0.5}O_8S_2$ C 73.45, H 9.42, N 0.96 , Found C 74.01, H 9.77, N 1.12.

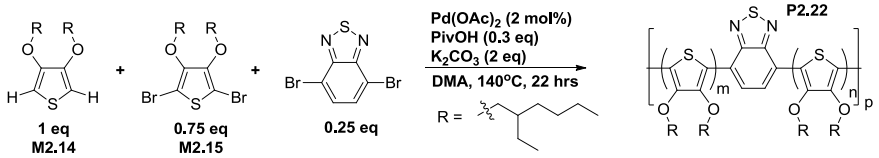

P2.22: Black oil in 92% yield (812 mg). 8.54 (br, 2H), 4.10 (br d, 4H, J= 6 Hz), 3.92 (br s, 4H), 1.94 (br s, 4H), 1.80-1.15 (br m, 34H), 1.07-0.80 (br m, 24H) Anal. calcd. for $C_{40.75}H_{60}N_{0.5}O_{3.5}S_2$ C 78.18, H 9.65, N 1.12, Found C 78.89, H 10.02, N 1.41.

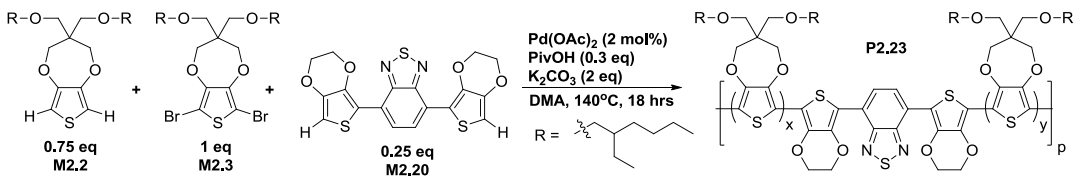

P2.23: Black solid in 56% yield (577 mg). ^{1}H-NMR (300 MHz, $CHCl_3$) δ 8.38 (br, 2H), 4.46 (br s, 8H), 4.15 (br s, 8H), 3.60 (br s, 8H), 3.32 (br, 8H), 1.68-1.14 (br m, 36H), 1.05-0.85 (br m, 24H). Anal. calcd. for $C_{48.25}H_{76}N_{0.5}O_8S_{2.5}$ C 66.56, H 8.80, N 0.80, Found C 67.44, H 8.23, N 1.08.

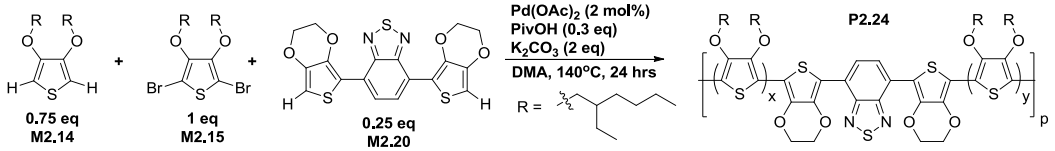

P2.24: Green solid in 53% yield (430 mg). ^{1}H-NMR (300 MHz, $CHCl_3$) δ 8.41 (br, 2H), 4.46 (br s, 8H), 3.94 (br s, 8H), 2.21 (br s, 2H), 2.02-1.17 (br m, 34H), 1.14-0.63 (br m, 24H). Anal. calcd. for $C_{39.5}H_{62}N_{0.5}O_{4.5}S_{2.5}$ C 68.22, H 8.99, N 1.01, Found C 70.30, H 9.22, N 1.24.

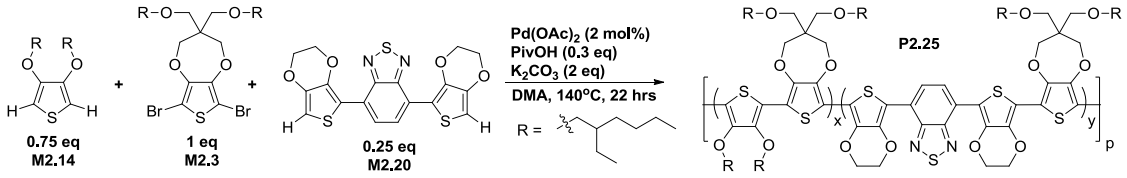

P2.25: Black solid in 75% yield (930 mg). ^{1}H-NMR (300 MHz, $CHCl_3$) δ 8.38 (br, 2H), 4.44 (br s, 8H), 4.14 (br s, 8H), 3.94 (br s, 4H), 3.59 (br s, 8H), 3.31 (br s, 8H), 1.99 (br s, 2H), 1.85 (br s, 4H), 1.66-1.12 (br m, 48H), 1.05-0.66 (br m, 36H). Anal. calcd. for $C_{44.5}H_{70}N_{0.5}O_{6.5}S_{2.5}$ C 67.19, H 8.87, N 0.88, Found C 67.40, H 8.64, N 1.15.

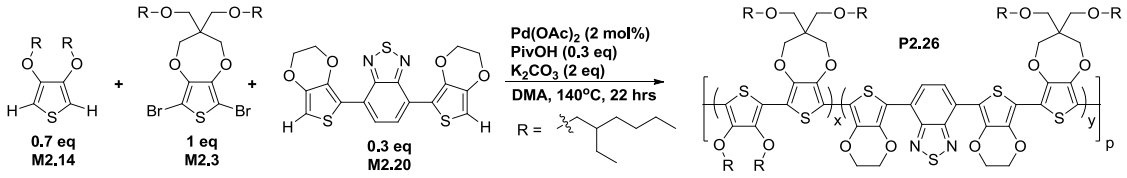

P2.26: Black solid in 77% yield (723 mg). ^{1}H-NMR (300 MHz, $CHCl_3$) δ 8.38 (br, 2H), 4.44 (br s, 8H), 4.16 (br s, 8H), 3.96 (br s, 4H), 3.60 (br s, 8H), 3.31 (br s, 8H), 2.01 (br s, 2H), 1.86 (br s, 4H), 1.66-1.13 (br m, 48H), 1.05-0.72 (br m, 36H). Anal. calcd. for $C_{44.4}H_{68.8}N_{0.6}O_{6.6}S_{2.6}$ C 66.72, H 8.68, N 1.05, Found C 67.21, H 8.94, N 1.57.

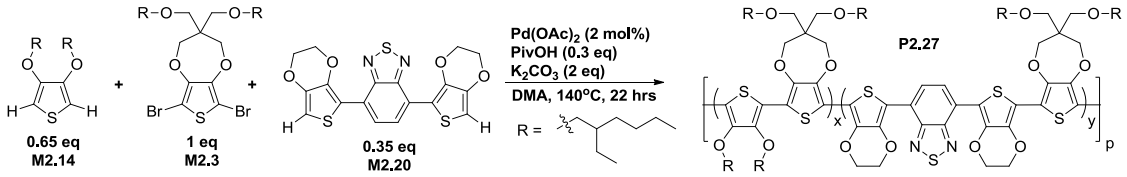

P2.27: Black solid in 82% yield (662 mg). ^{1}H-NMR (300 MHz, $CHCl_3$) δ 8.38 (br, 2H), 4.44 (br s, 8H), 4.15 (br s, 8H), 3.95 (br s, 4H), 3.62 (br d, 8H, J= 12 Hz), 3.32 (br s, 8H), 2.01 (br s, 2H), 1.86 (br s, 4H), 1.71-1.12 (br m, 48H), 1.06-0.71 (br m, 36H). Anal. calcd. for $C_{44.3}H_{67.6}N_{0.7}O_{6.7}S_{2.7}$ C 66.25, H 8.48, N 1.22, Found C 66.95, H 8.85, N 1.56.

CHAPTER 3

ELECTROCHROMIC POLYMER CHARACTERIZATION TECHNIQUES AND EXPERIMENTALS

Since we have discussed the background, theory, and synthesis of ECPs we will now detail the characterization of these materials to determine their optoelectronic properties. The electrochemical, spectroelectrochemical, kinetic, and colorimetric behavior must be determined rigorously and consistently to enable accurate comparison of different materials. Herein we will outline the methods and experiments that were employed to characterize ECPs. These are personal methods and experimentals I have developed and I offer this to future members in the field to use freely.

3.1. Procedures for Making Polymer Solutions and Preparing Films

The polymers have been spray cast into films using Anest Iwata airbrushes.[143] These are compatible with many organic solvents at room temperature. Small volumes of polymer solutions are required: 50 mg in 10 mL of toluene or chloroform is optimal. This amount is more than sufficient to cast eight to ten films of an area of ~2 cm^2 on ITO coated glass. The ITO electrodes were purchased from Delta Technologies, Ltd. (7 x 50 x 0.7 mm, sheet resistance, R_s 8-12 Ω/sq). Prior to spraying, the solution is to be filtered through a 0.45 μm PTFE syringe filter. If there is resistance the solution can be gently heated and if there is continued resistance the solution can be pre-filtered through a compacted cotton plug in a syringe to remove insoluble matter. Filtering acts to prevent clogging of the airbrush and to give homogenous film surfaces. To achieve films with clarity, the best conditions for flow pressure and solvent is 25 psi for toluene, 10 psi for chloroform and 40-50 psi for water. Solutions that must be continually heated to maintain solubility will be unsuitable for spray casting, if this is the case use spin casting or blade coating methods.

Before spraying, fresh ITO/glass slides must be cleaned; this is done by first removing the plastic film binding the slides together then identifying the conductive side and marking it or the non-conducting side with a small scratch that will not be readily visible and is outside the beam path of any instrument. Clean both sides of the slide by wiping with isopropyl alcohol, acetone, and finally toluene. If you are recycling slides, wipe clean the used polymer films with chloroform then sonicate the slides in chloroform. Then wipe both sides of the slides with acetonitrile (ACN), acetone, and finally toluene. If you are spraying an aqueous solution, it is best to finish wiping the slides with water. If you encounter beading of the spray solution, plasma clean the surface of the slides.

3.2. Performing Characterization of Electrochromic Polymers

To characterize the properties of ECPs the following experiments must be performed: profilometry, electrochemistry (cyclic voltammetry (CV) and differential pulse voltammetry (DPV)), spectroelectrochemistry (SpecEchem), chronoabsorptometry (kinetics), photography, and colorimetry. To begin characterization, you must identify the stable potential window of a polymer. The most efficient way to do this is by first taking a test film and performing initial CV from -500 mV to 600 mV and extending the potential to greater values incrementally in 25 mV steps for 5 cycles each until electrochromic failure occurs. This is demonstrated in Figure 3.2.1 with the polymer known as P2.1 (ECP-Yellow). The initial cycling window however is from -500 mV to 800 mV, ending at a more positive value than was stated above as this material exhibits little electroactivity below 800 mV. As cycling continues to higher potentials the current begins to stabilize and it was found that the most stable current corresponding to the greatest transmittance was at 1100 mV. Pushing the voltage cycling beyond 1100 mV, a new electrochemical process occurs as indicated by an increase in current. This results in an instability of the film, followed by degradation in the form of a loss in color of the neutral state and finally delamination and can be tracked as the overall loss in current

throughout the CV. Therefore this polymer is best switched from -500 to 1100 mV in later studies.

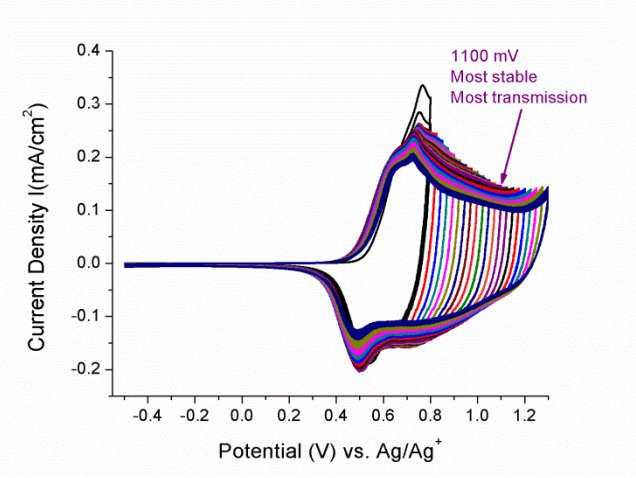

Figure 3.2.1: Potential probing for P2.1 *via* CV using 0.5 M $TBAPF_6$ in PC.

Once you have identified the stable switching regions for a new material, you can continue to characterize the cast films in the advisable order: profilometry, UV-VIS-NIR spectroscopy of the dry (without electrolyte) and wet pristine (with electrolyte) film, photography of the wet pristine film, break-in CV, photograph of the neutral and oxidized states (or intermediate states if interested), SpecEchem, chronoabsorptometry, and finally DPV on Pt buttons. This is to be conducted over a variety of thicknesses as measured by optical density (0.8, 1.0, 1.2 *a.u.* for the majority of this work). It is best if a single film can endure the battery of experiments as it would demonstrate a considerable degree of stability.

3.2.1. General Considerations (solubility, stability, storage)

Consider a polymer and its films. During purification of the material it is wise to take small portions (~5 mg or spatula tips worth) and experiment with the solubility as it will aid in the selection of solvents for film casting and ensure that the electrolyte solvent will

not dissolve your polymer. If these are water soluble polymers, be sure that the films are stored in a dry atmosphere if they are not yet protonated.

These materials are generally stable in the bulk, but recent studies have shown that they are light and air sensitive and will photoxidize or bleach while standing in air under illumination over prolonged periods of exposure.[144] More thorough studies performed by Rayford H. Bulloch have shed light as to possible degradation products and prevention with proper encapsulation under argon with judicious selection of sealants. Therefore it is best to store bulk polymers in the dark and film samples under inert atmosphere without exposure to light.

3.2.2. Profilometry

This enables you to attain an average thickness of a cast film. Because spray casting can result in subtle variations in thickness across the surface, it is best to take an average of multiple profilometry measurements at different points across a film. The physical thickness of a film can be compared to its optical density based on absorbance and can allow you to estimate electrochromic properties such as maximum contrast and absorption coefficients.[145,146] After washing electrolyte away the thickness can be measured post-electrochromic switching to investigate changes. Profilometry was performed on a Bruker dektakXT Profilometer using a standard scan, hill & valley profile, stylus force of 3 mg, and a run length of 3000 μm for a time of 10 seconds.

3.2.3. Electrochemistry (CV&DPV)

Due to slow relaxation effects in neutral conjugated polymers from intercalation of solvent and ions,[147,148,149] the properties of films such as redox potentials and absorption spectra can change upon doping and dedoping. Thus, cyclic voltammetry is utilized to break-in electrochromic polymer films in the cuvette set up shown below in Figure

3.2.3.1. The counter electrode (CE) can be either a platinum flag or wire. A wire is more advantageous as it can be easily positioned out of the path of a beam of a spectrometer and can make photographs more aesthetically appealing. If you find a CV is *leaning*, showing a high resistance with positive slope in the i-V curve, use a CE with a larger surface area which can simply be a longer or a coiled wire. The working electrode (WE) is your polymer film coating the ITO/Glass slide and a contact can be made using copper tape to affix wires. The reference electrode is typically a 10 mmol solution of $AgNO_3$ dissolved in 0.5 M of electrolyte solution in ACN, calibrated to Fc/Fc^+.[150] CVs can be performed on the bench top but it is easier to conduct the experiment in a cuvette holder within a photo booth as shown in Figure 3.2.3.1b. This is advantageous as you can perform two experiments (CV break-in and photography) at the same time or in close succession to one another using the same film and setup.

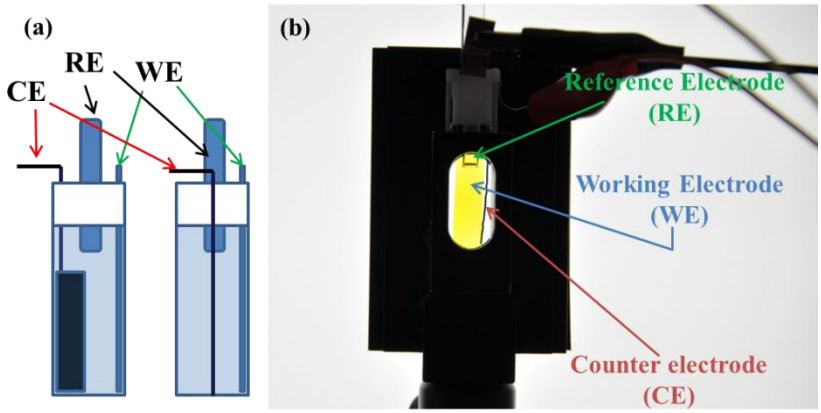

Figure 3.2.3.1: Cartoon of three-electrode setup in a cuvette (a). Electrochemistry setup held in a cuvette holder in a photo booth (b).

The break-in is performed in the materials most stable electrochromic switching window at a rate of 50 mV/s over 25 cycles where a stable and reproducible CV curve is achieved. Often, the optical properties of a polymer can change drastically upon break-in, the greatest being observed between the first and second potential sweep. In Figure 3.2.3.2, P2.10 and P2.11 are prime examples of this as they switch from vibrant purple pristine states to deep periwinkle-blue neutral states (discussed further in Chapter 5).

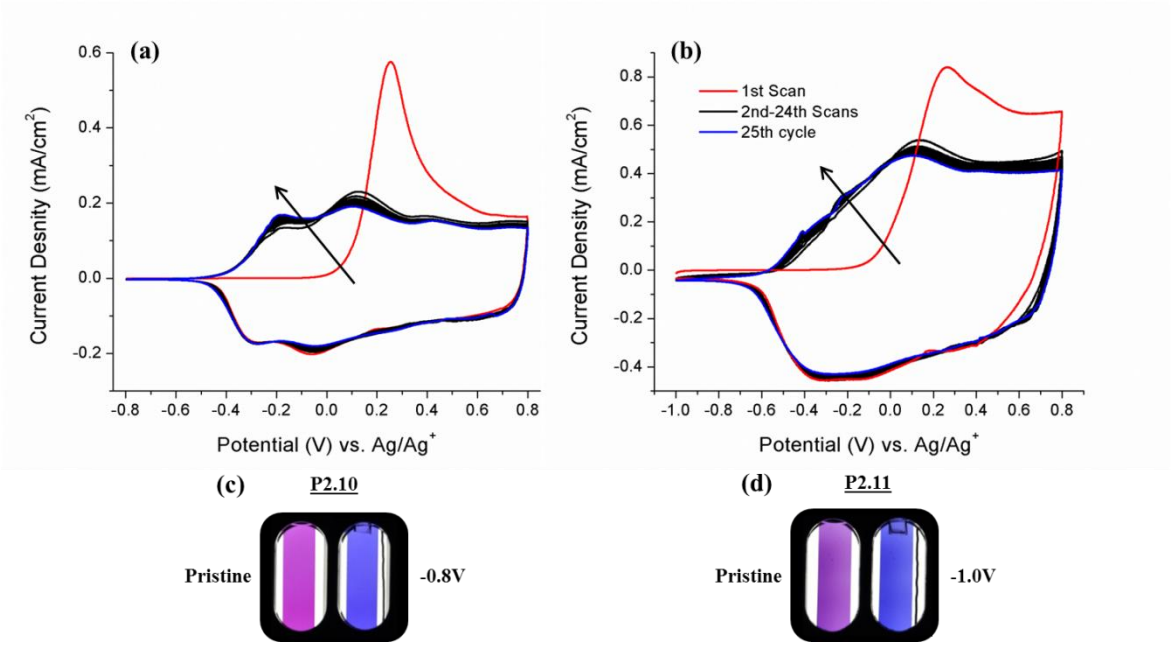

Figure 3.2.3.2: Break-in CV curves of P2.10 (a) and P2.11 (b) where the inset arrow indicates the progression of current between cycles. Photos of the pristine and broken in neutral states for P2.10 (c) and P2.11 (d).

Differential pulse voltammetry is used to determine the oxidation potential of a polymer. The setup is nearly the same for CV with the exception that the working electrode is typically a polymer film cast on a Pt button. The films are drop cast from filtered dilute solutions (~0.5 mg/mL) onto small Pt button electrodes. This method enables you to accurately determine a polymers oxidation or reduction potential for p-type and n-type materials respectively. The oxidation potential (E_{ox}) is determined as the onset for an increase in current as illustrated in Figure 3.2.3.3 for P2.9 and P2.11. The polymer film is held at the neutral state potential for one minute and then swept to the oxidized state voltage. This method has the advantage over CV because the sampling of the current before a potential change minimizes the effect of the charging/capacitive current. The films should be broken-in using the same conditions as for CV. If you are performing reduction the DPV must be done in a glovebox or under an argon atmosphere with degassed electrolyte to protect the radical anions and dianions from exposure to water or oxygen.

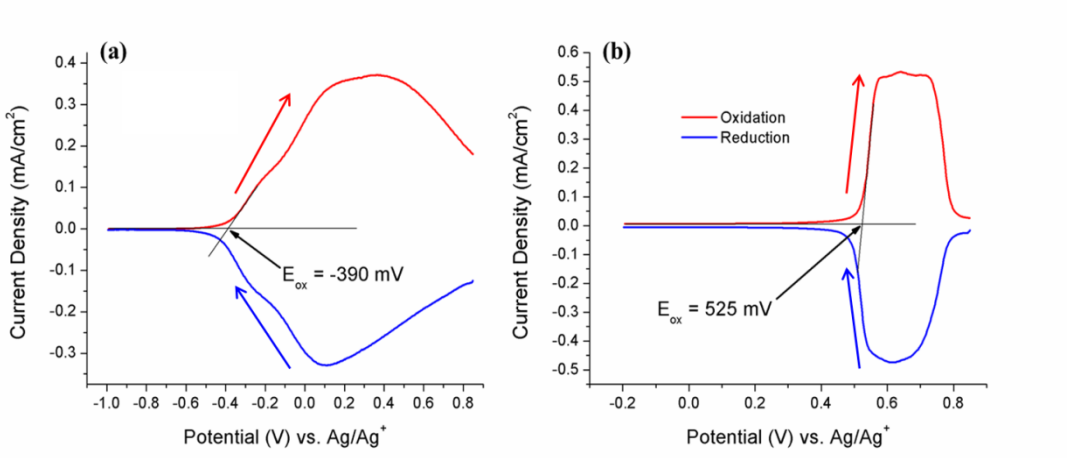

Figure 3.2.3.3: DPV curves of P2.11 (a) and P2.9 (b) where the E_{ox} is indicated by the onset. Red and blue arrows indicate the direction of the potential cycling.

Electrochemical measurements were carried out using an EG&G Princeton Applied Research model 273A potentiostat / galvanostat used under the control of Corrware II in a 3-electrode cell configuration, using ITO working electrodes, Ag/Ag^+ (used for non-aqueous solutions) reference electrodes, and Pt wire counter electrodes. Differential pulse voltammetry samples were prepared *via* drop casting a 0.5 mg/mL solution (pre-filtered with 0.45 μm PTFE syringe filters) onto Pt button electrodes with a surface area of 0.02 cm^2. An electrolyte system of 0.5 M tetrabutylammonium hexafluorophosphate ($TBAPF_6$) or 0.2 M lithium bis(trifluoromethyl)sulfonylimide (LiBTI) in propylene carbonate (PC) was used. CV and DPV curves were smoothed using the Corrview program High-Low filter tool.

Always ensure that before you begin either a CV or DPV experiment that you set the proper area of your active electrode. This is done in Corrware by clicking *experiment* then *cell setup* and typing in the measured area of your polymer film on ITO for CV or the area of the Pt button for DPV. If you encounter noisy signals or seemingly random voltage fluctuations of the curve and current, be sure that for a given selected experiment under *setup* you have set *Low Pass Filter* to auto and *Scan Interpolation* to on. If this continues, ensure that no portions of the wires are exposed and that the metal alligator clips are not touching anything conductive. If DPV curves continue to appear noisy or

give illogical data, or if a calibration of a reference electrode yields a large junction potential ($E_{1/2}$), the Pt button must be polished. For films, it is best for the copper tape to be affixed to the ITO/glass in such a way that it remains out of the cuvette and far from electrolyte. This is because through capillary action the electrolyte can climb up the front or back of the slide, through the cuvette cap and reach the tape causing corrosion (Standard electrode potential (E^o) for Cu^{+2}/Cu = +0.342 V). Take care that there is no voltage being held across the cell when wires are removed as this can destroy the film and harm the reference electrode. Take extra care of this electrolyte climbing for aqueous systems and it can short the circuit between the WE and CE, decomposing the film.

3.2.4. Photography

It is important that photographs be taken to aid in the illustration of color properties. When such photography is performed, careful consideration needs to be taken into account so that the colors are properly imaged in the photograph. The standard illuminant for calculating the color values needs to be used to back light films being photographed. There needs to be as little stray light as possible and no photo editing is to be performed with regards to brightening or contrast. These photos may however not be displayed in their true fashion when printed or displayed on a monitor or projector as the color values in the material studied may not be attainable in the gamut of the display media, hence the necessity of the quantification of color in electrochromic materials. Cropping is acceptable but you should not remove artifacts such as bubbles or other anomalies caused by spraying or device construction and they should be pointed out for explanation when published. If you do not wish to explain, spray new films and take greater care in cell or device setup for photography.

Before electrochemical break-in a photo should be taken. After break-in, a potentiostatic experiment is used and photos of the neutral and most transmissive oxidized states are taken. Intermediate state photographs should be taken if any interesting electrochromic

phenomena occurs and these can be correlated with the colorimetry data. When a series of photos for a polymer at a variety of thicknesses is complete, it is best to arrange them by increasing optical density from top to bottom and to show the pristine, broken-in neutral and oxidized states from left to right. An example of this is shown in Figure 3.2.4.1 with the photographical comparison of P2.12, P2.13, and P2.9 at three film thicknesses.

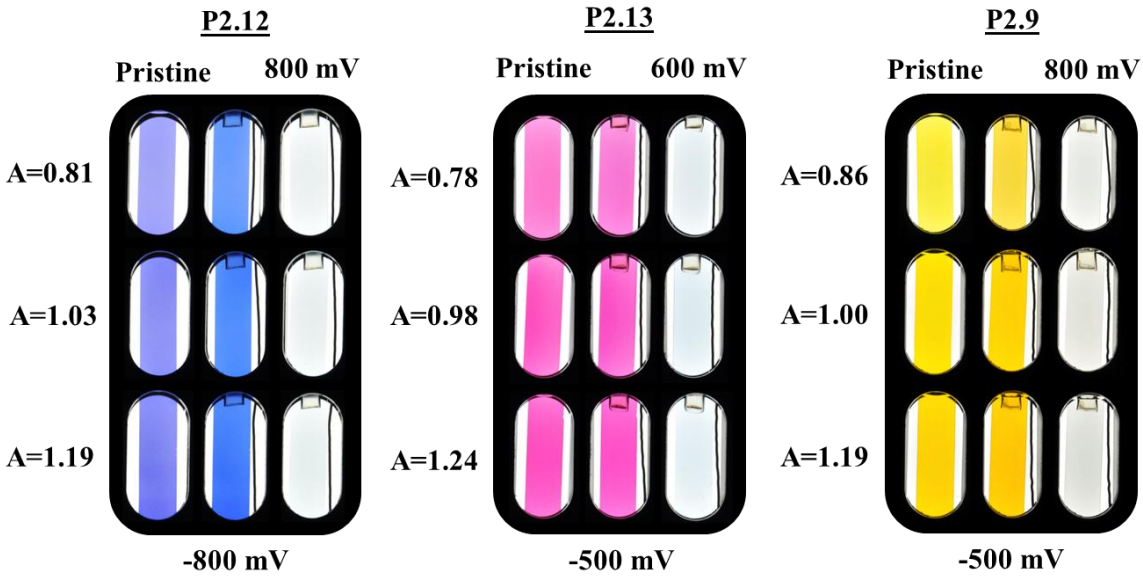

Figure 3.2.4.1: Photographs of P2.12 (left), P2.13 (center) and P2.9 (right) at three film thicknesses and in the pristine, neutral (broken in), and oxidized states.

3.2.5. Spectroelectrochemistry

Spectroelectrochemistry determines the spectral behavior of an ECP at incremental potentials across a switching window using an Agilent Cary 5000 UV-vis / NIR spectrophotometer. For new materials the entire spectrum needs to be collected across the NIR to visible to the UV, from 2000-300 nm. This range enables you to observe polaron or bipolaron oxidized states, D-A or π to π^* effects, or over oxidation in a conjugated polymer. When data is collected, it is advised to plot from 1600-350 nm, from the NIR the edge of the visible.

Once profilometry data is acquired, the pristine dry and wet spectra are captured to examine any changes in absorption intensity upon electrolyte wetting. After the initial electrochemical break-in is complete and photographs are taken the specEchem experiment is carried out using the same cell setup as shown in Figure 3.2.3.1. It is advisable to take spectra of the cell without wires attached and then again with wires as the cables can move the counter electrode into the path of the beam or move the cap which will reposition the working electrode and can affect data output. Make sure the spectra with and without wires match as close as possible before continuing. Once this is confirmed, using a potentiostatic experiment in Corrware, the most negative potential is applied and a scan is taken of the polymer in the neutral state. This is repeated in 50 mV steps until the highest stable potential is reached, correlating with the most transmissive oxidized state. This is exemplified in Figure 3.2.5.1 for P2.12, whereas the potential increases there is a loss in absorbance at the π to π* with a λ_{max} at 608 nm coupled with simultaneous growth and loss of a polaron band and overall increase in a bipolaron band in the NIR. The band gap is taken as the onset of absorption.

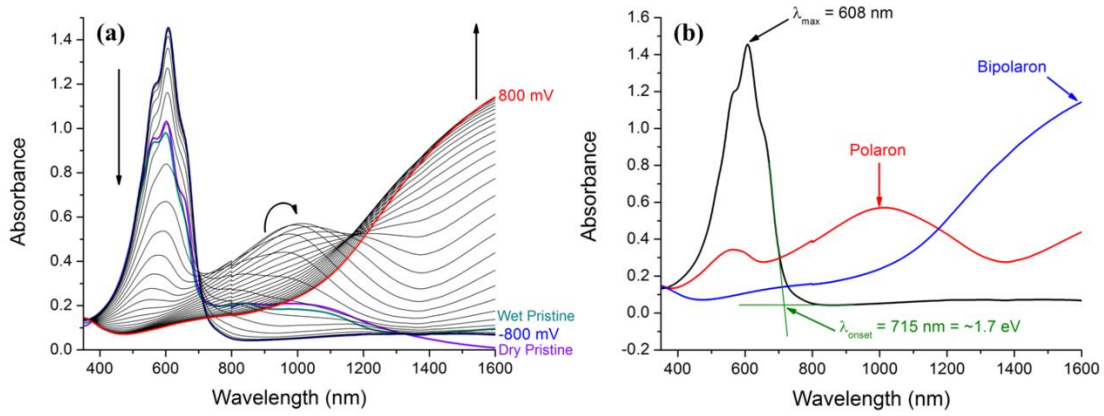

Figure 3.2.5.1: Full spectroelectrochemistry for a film of P2.12 sprayed to an optical density of 1.03 *a.u.* including pristine dry and wet spectra (a). Isolated spectrum for the neutral (-800 mV), polaron (-150 mV), and bipolaron (800 mV) states with the identification of the onset of absorption.

The absorbance values acquired for a spectroelectrochemistry experiment can be converted to % transmittance. The converted series for P2.12 is shown in Figure 3.2.5.2. The small *notch* at 800 nm is the detector change-over from NIR to UV-Vis and can be minimized with increasing film clarity (less haze). Such artifacts should not be electronically smoothed away. The stability to high applied potential beyond the value where the most transmissive oxidized state is accessed, can be measured as a steady loss in absorption attributed to over oxidation with increasing voltage.

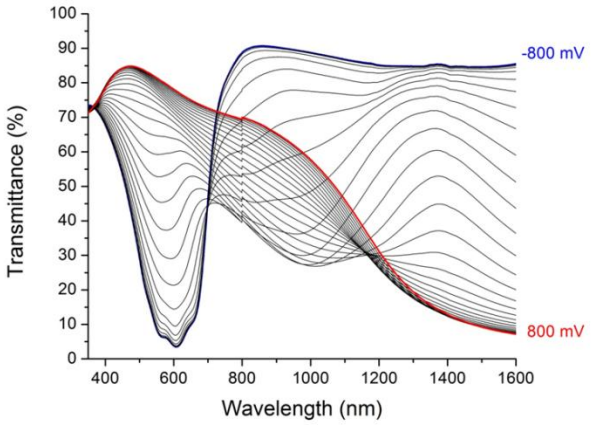

Figure 3.2.5.2: Full spectroelectrochemistry for P2.12 sprayed to an optical density of 1.03 *a.u.* in % transmittance.

3.2.6. Chronoabsorptometry

This is a technique that enables you to analyze the change in contrast (Δ%T) of an ECP at a variety of switching speeds and it is measured at the λ_{max} of a polymer system. It uses the same cell setup as SpecEchem in the Cary 5000 UV-Vis-NIR spectrometer but uses a potential square-wave Corrware experiment. While the spectrophotometer is allowing light of a single wavelength to reach the detector, the potential is switched repeatedly between the voltage for the neutral and most oxidized transmissive states and held at these two voltages for varying lengths of time. The typical data is as follows in Figure 3.2.6.1 for P2.12. The polymer is switched over gradual shorter time lengths starting with 60 s switches at the longest and ending at ¼ s cycles where after the film is then switched

at 2 s to demonstrate longevity of the film and the ability to endure a variety of speeds. The Δ%T is taken by subtracting the transmittance in the neutral and most oxidized form. At cycles of 60, 30, 10, and 2 seconds the Δ%T is ~75 %. At 1 s cycles the Δ%T is ~73 %. Due to diffusion limiting processes, at ½ and ¼ s switches the Δ%T drops dramatically to ~60 and ~42 % respectively but can be amended with device engineering. Switching seeds faster than ¼ s was not measured as the contrast drops significantly as extrapolated by Figure 3.2.6.1. Finally the film is able to rebound to Δ%T ~75 % at 2 s cycles. This is also the rate at which the polymer can switch the fastest with the highest contrast.

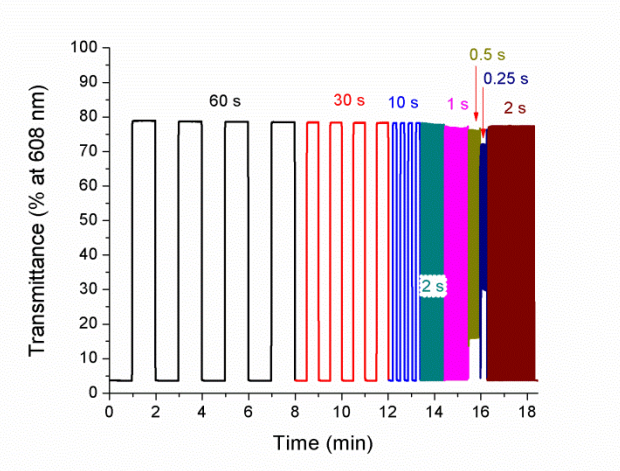

Figure 3.2.6.1: Chronoabsorptometry for a film of P2.12 sprayed to an optical density of 1.03 *a.u.* Switching times are colorized for ease of visualization.

Not all ECPs are as stable nor switch as rapidly as the example presented in Figure 3.2.6.1. Many may present progressive loss in contrast that is not dependent on switching time. Stability is generally a property of a material that varies from polymer to polymer where some materials simply are unable to withstand the stresses of switching at high speed and delamination can occur.

3.2.7. Colorimetry, From Minolta to Cary Conversions

In Chapter 1 we discussed colorimetry and how the eye perceives color. Here colorimetry data was acquired using Star-Tek colorimetry software using settings of a D50 illuminant, 2 degree observer, and L*a*b* color space; similar results can be obtained by the method reported by Varley and Mortimer.[10] After specEchem, the spectra attained at progressive voltage levels were converted using this software. This differs greatly from an older method using a Minolta CS-100A Luminance and Color Meter where a fresh film was progressively oxidized and xyY values were gathered at each potential and converted through a spreadsheet to L*a*b* values. This older method had the disadvantages of taking considerable time to complete, led to the possibility of transcription errors, and required additional electrolyte and films. The method utilizing the Star-Tek package is able to take all of the spectra and directly convert them into color values in a variety of spaces with different illuminants instantly. With color values calculated, photographs help correlate and visualize the colorimetry of ECPs as shown in Figure 3.2.7.1.

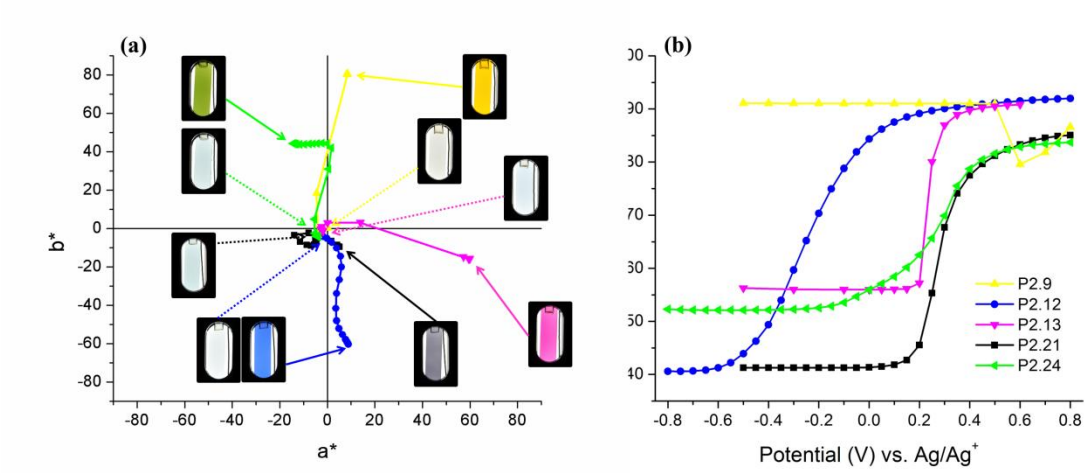

Figure 3.2.7.1: Colorimetry in a*b* (a) and L* (b) for P2.21, P2.12, P2.29, P2.13, and P2.24. Photographs of ECP extreme states are insets.

CHAPTER 4

COMPLETION OF THE COLOR PALETTE

To achieve full color electrochromic devises (ECDs), one requires polymers that complete the cyan-magenta-yellow (CMY) or red-yellow-blue (RYB) subtractive color sets. Red, blue, magenta, and cyan ECPs have been reported and discussed in chapter 1. Before 2011 however, there were no yellow-to-transmissive ECPs available. This chapter concerns the initial development and subsequent optimization of yellow ECPs.

4.1. Discovery of ECP-Yellow

In order for full color electrochromic devices to be realized, CMY and RYB subtractive color sets must be fulfilled. In this section we will discuss previous attempts in producing electrochromic materials with yellow and transmissive states, their shortcomings and the invention of ECP-Yellow-1 (P2.1).

4.1.1. Importance and Previous Known Attempts

Full color applications of electrochromics rely on the reflection or transmission of visible light and, as such, are dependent upon the subtractive color sets RYB or CMY shown below in Figure 4.1.1.1. The color yellow is typically produced in emissive displays by the stimulation of the eye with red and green light (affecting the L and M cones respectively). In non-emissive applications, a material that absorbs high energy light (violet/blue) is required as it will allow the passage of red and green light, stimulating the aforementioned cones and producing the sensation of yellow in the brain.

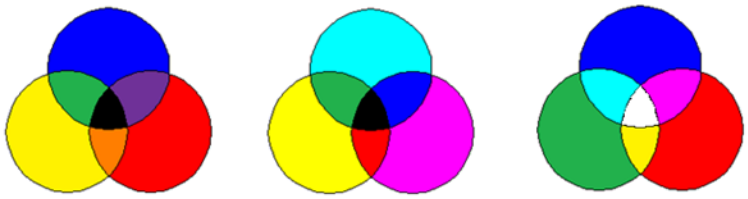

Figure 4.1.1.1: RYB (left) and CMY (middle) subtractive color sets. RGB (right) additive color set.

With the aim to produce electrochromic materials that complete the CMY color set, a series of cathodically coloring terephthalate based small molecules were reported in 2004[151] and as shown by Figure 4.1.1.2, they do complete the subtractive color set. These materials are clear in the neutral state and colored when reduced but unfortunately, the voltage to achieve these colors are of considerably high magnitude (> -2.0 V) and engineering colors in charged states is difficult to achieve and maintain as there is the potential for voltage drift, making desired colors difficult to target accurately upon repeated switches.

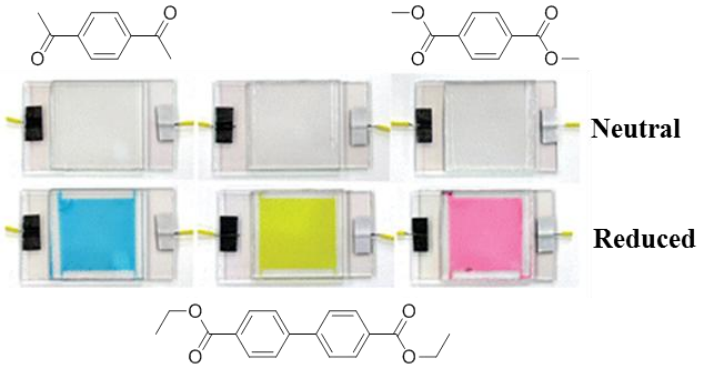

Figure 4.1.1.2: Terephthalate based small molecule electrochromes.

In 2008 a colorless to yellow ECP was reported through the synthesis and characterization of the anodically coloring poly(amine-amide) by Liou and Lin,[152] the structure and color states can be seen in Figure 4.1.1.3. The electron rich nature of the ECP structure allowed the material to be oxidized, making charges that are considerably more stable. However, like the example mentioned above, it is a material that is colorless

when neutral and then colored when charged meaning accurate potentials need to be maintained for desired coloration, exemplified by the drastic yellow to black-blue color change between 0.55 V and 0.80 V respectively.

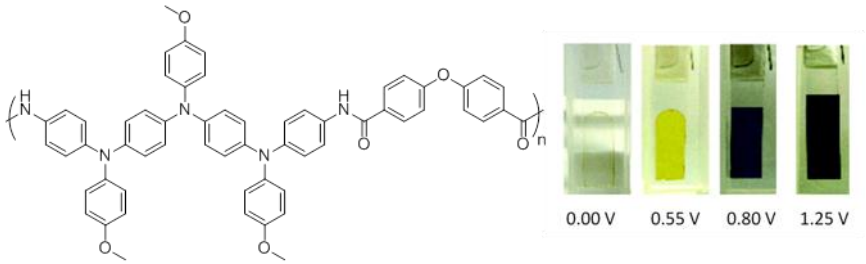

Figure 4.1.1.3: Poly(amine-amide) structure (left). Photos at various potentials (right).

A more recent report by Nielsen, *et al*[153] resulted in a material that was yellow when neutral and switched to a near transmissive oxidized state as shown in Figure 4.1.1.4. When patterned into films, the oligomer required crosslinking *via* UV exposure for several hours. Thin films had 38% transmittance over the course of 400 switches. Aside from the short life time, its slow switching speeds of 2.4 s for coloration and 10 s for bleaching prevented the use of this material in devices. Furthermore, thicker films took longer to colorize and to bleach.

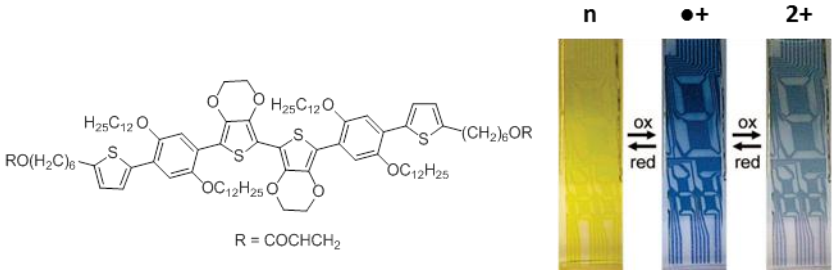

Figure 4.1.1.4: Structure of a cross-linkable yellow oligomer (left). Photos of cross-linked film in neutral, radical cation, and dication form (right).

Though yellow colors are achievable, the challenge lies in predictably engineering high gaps in the neutral state with transmissive oxidized states. These types of cathodically coloring materials are desirable as no voltage is needed to display color, positive charges

are more stable, and less accurate maintenance of applied positive potentials would still result in transmissive, colorless states.

Finally a publication from the Sotzing group reported the synthesis and characterization of a highly bulky, all DOT polymer film made by electropolymerization and is shown in Figure 4.1.1.5.[34] This was an insoluble polymer film and though in the neutral state it was a vibrant yellow color (E_g of 2.50 eV), it displayed a green transmissive oxidized state.

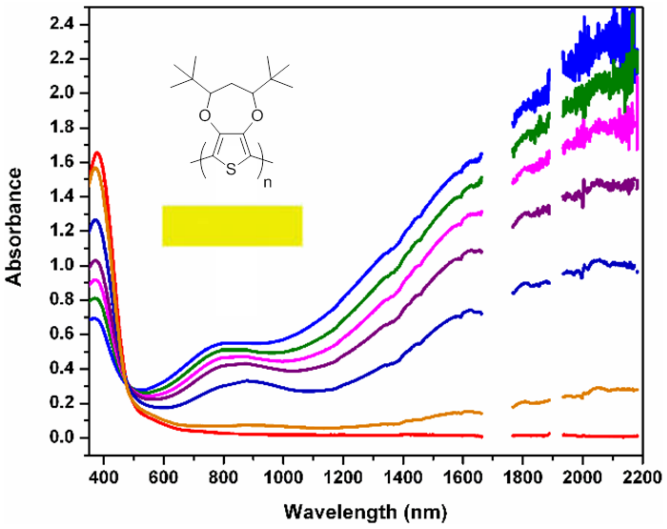

Figure 4.1.1.5: SpecEchem (from -1.1 V to 0.3 Ag/Ag+ reference (0.445V vs. NHE)) with structure and neutral state color as inset.

4.1.2. The Discovery of ECP-Yellow-1

In 2011, the world's first yellow-to-transmissive ECP was synthesized and characterized.[46] It is an alternating polymer consisting of a single 3,4-propylenedioxythiophene (ProDOT) in alternation with a single phenylene. The subtle *ortho* C-H interactions from the phenylene induce twisting with the neighboring ProDOT, giving a high gap material with a vibrant yellow color neutral state; the polymer is then able to reversibly achieve a transmissive oxidized state, imparted by the electron rich character of the ProDOT ring. The polymer structure and images of films in the extreme redox states are shown in Figure 4.1.2.1. In the neutral state (-0.5 V), it has color values of L*=95, a*=-6, b*=81, once fully oxidized (1.1 V) is has color values of L*=84, a*=1, b*=-6.

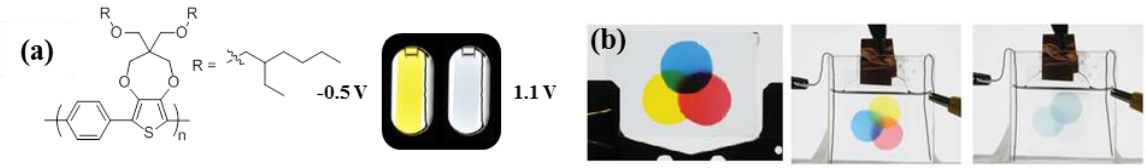

Figure 4.1.2.1: Structure of P2.1 (ECP-Yellow-1) (a, left). Photos of the neutral, colored and oxidized, transmissive states (a, right). Photo of colored ECPs to fulfill RYB color set (b, left). Photo of colored ECPs to fulfill CMY color set, in the neutral state (b, center). Photo of colored ECPs to fulfill CMY color set, in the oxidized state (b, right).

4.1.3. Challenges to Overcome in Future Yellow ECPs

P2.1 has allowed the completion of the color palette.[44] With its yellow neutral and transmissive oxidized (bleached) states, CMY or RYB non-emissive devices are now possible, as evident in Figure 4.1.2.1b and demonstrated by Bulloch *et al*.[87] However, the polymer exhibits a high potential in the bleached state, attributed to the high aromaticity of phenylene. This is an issue as it can negatively impact redox stability over long periods of time and if P2.1 is mixed with other polymers in solution and cast into films, the potential to bleach P2.1 is beyond the limits of redox stability of other more easily oxidizable polymers. Thus it was necessary to further study yellow ECPs to achieve lower bleached state potentials.

4.2. Modulating Electrochemical Properties While Maintaining Yellow

The high potential required to fully bleach P2.1 complicates the use of multiple ECPs on the same electrode as over-oxidation of more easily oxidized polymers can occur. This observation, along with recent reports of several electrochromic polymers[154,155,34,156] and small molecule esters[157] that possess yellow states, has motivated a detailed study in developing an understanding of structure-property relationships in a series of ProDOT-Arylene conjugated polymers with the goal of lowering the oxidation potential, allowing a higher level of transparency in the bleached state, while maintaining a vibrant yellow neutral state.

Through varying the choice of an arylene unit in alternation with ProDOT, dimers of ProDOT, or using a random copolymer with ProDOT, the oxidation potential of seven

new ECPs could be modified through structural modulation while maintaining yellow or near yellow neutral states that can switch to various transmissive or near transmissive oxidized states. This work has been published[45] but is described below.

4.2.1. Structures to Attain Yellows with Lower Potentials

In the quest to lower the oxidation potential of yellow ECPs, seven new polymers were synthesized and characterized. The polymers were based on repeat units of ProDOT in alternation with a variety of arylene units including 1,4-phenylene (P2.1), 2,7-fluorene (P2.2), 2,7-carbazole (P2.3), 2,5-dimethoxy-1,4-phenylene (P2.4), and 2,7-pyrene (P2.7). Additionally, a random copolymer containing ProDOT and two different arylene units was produced: ProDOT-phenylene-ProDOT-dimethoxyphenylene (P2.5). Also, two polymers with a ProDOT dimer in alternation with phenylene and pyrene composed $ProDOT_2$-phenylene (P2.6) and $ProDOT_2$-pyrene (P2.8) respectively. The structures are presented in Scheme 4.2.1.1.

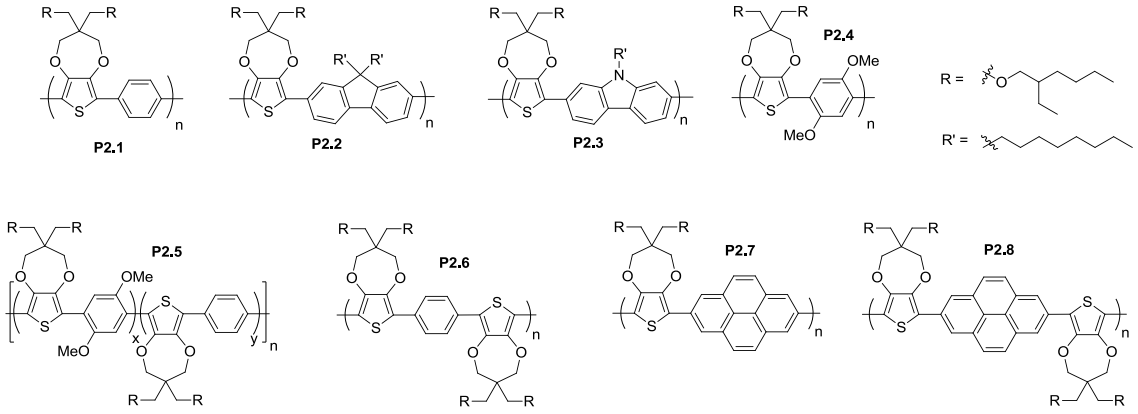

Scheme 4.2.1.1: Seven new polymers investigated for yellow ECPs with improved transmissive state potentials. P2.1 is used as a standard comparison.

4.2.2. Electrochemical and Spectroscopic Properties

Through the variation of the arylene, high gap polymers in the visible with a variety of oxidation potentials were produced. Steric hindrance along the backbone was maintained, giving materials that were yellow or near yellow in their neutral states. The arylene units were varied in electronic character, giving a variety of oxidation potentials (E_{ox}) which

affected the optical properties of the oxidized states. To investigate the effect on redox properties, differential pulse voltammetry (DPV) was performed. A comparison of the DPV oxidation scans for P2.1-8 is shown in Figure 4.2.2.1 where the trend of oxidation potential onsets (from highest to lowest) is as follows: P2.2 (650 mV) > P2.1 (500 mV) > P2.7 (460 mV) > P2.3 (450 mV) > P2.8 = P2.5 (320 mV) > P2.6 (300 mV) > P2.4 (270 mV).

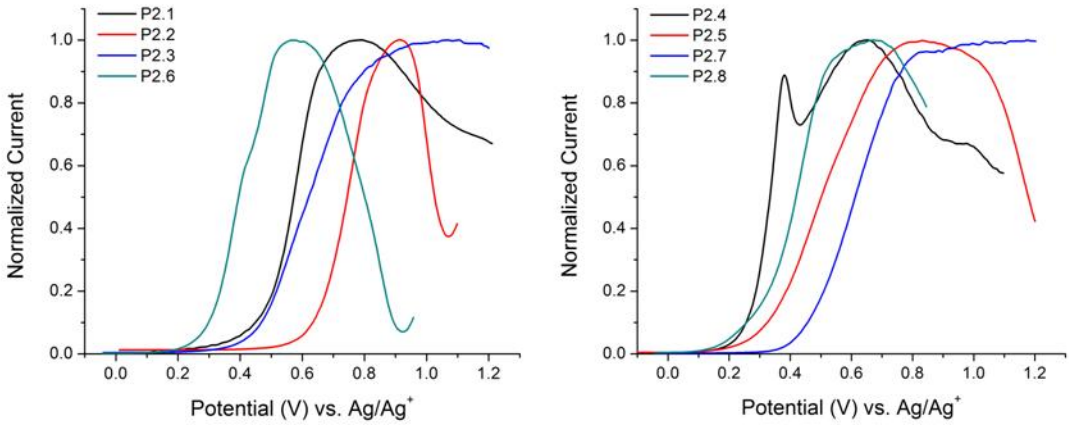

Figure 4.2.2.1: DPV curves for P2.1-8 where the current has been normalized.

It can be seen that P2.2 has the highest E_{ox}, a 150 mV increase compared to P2.1. This is attributed to the bridged biphenyl nature of the fluorene, where the additional phenylene ring decreases the HOMO level giving a higher oxidation potential. P2.1 has the second highest E_{ox} due to the high aromaticity of the phenylene unit, imparting a low lying HOMO. The E_{ox} for P2.7 is 190 mV less than P2.2 and 40 mV less than P2.1. For P2.3, the use of carbazole in the repeat unit gave a further decrease in the trend of oxidation potentials and can be attributed to the electron-donating ability of the nitrogen atom bridging the two phenylene rings, raising the HOMO. The random polymer, P2.5 and the alternating polymer, P2.8 both possess the same E_{ox}. This lowering of potential for P2.5 was achieved by randomly incorporating phenylene and electron rich dimethoxyphenylene into the repeat unit, raising the HOMO relative to P2.1. For P2.8,

the incorporation of an additional electron rich ProDOT in an alternating repeat unit with pyrene raised the HOMO relative to P2.7. The E_{ox} of P2.6 is the second lowest in the trend by similar reasoning with P2.8. The lowest E_{ox} of the series is for P2.4, achieved by adding a more electron rich arylene unit in alternation with a single ProDOT.

Unfortunately the materials containing pyrene are difficult to dissolve and cast into usable films and P2.7 exhibits poor switching stability. It should be noted that P2.8 is a modification of a previously reported yellow ECP where the connectivity of the system is at the 1,6 positions of the pyrene ring, giving it a considerably high E_{ox} value.[156] Here, the connectivity is through the 2,7 positions of the pyrene ring, affording greater conjugation as evident by the lower oxidation potential of P2.8.

UV/Vis spectroscopy of polymer solutions was performed to probe repeat unit structural effects on spectra. The normalized spectra of each solution are shown in Figure 4.2.2.2 with inset photographs of the solutions in vials under white light. When considering the λ_{max} of all polymers in solution (from shortest to longest), the trend is as follows: P2.7 (417 nm) < P2.4 (422 nm) < P2.2 (436 nm) < P2.5 (438 nm) < P2.3 (446 nm) < P2.1 (448 nm) < P2.8 (475 nm) < P2.6 (506 nm).

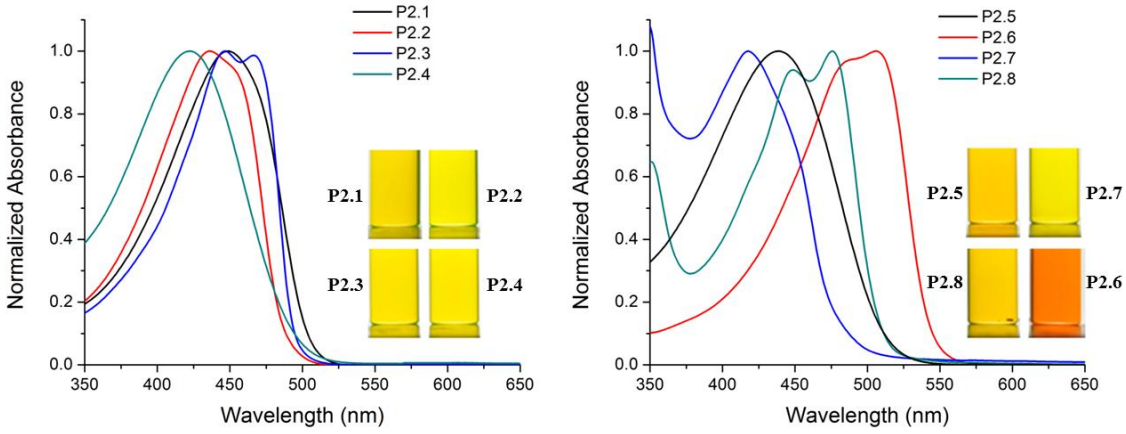

Figure 4.2.2.2: Normalized UV-Vis-NIR spectra of polymer solutions for P2.1-8 in chlorobenzene. Concentrations of solutions for spectra range from 0.05 mg/mL to 0.02 mg/mL. Photographs of polymer solutions are inset.

From the trend, P2.7 has the shortest λ_{max}. P2.4 has the second shortest λ_{max}, ascribed to the bulky methoxy units in place of the smaller hydrogen atom on the phenylene ring. An alternative possibility for this increase is the raised LUMO from the more electron rich arylene. P2.2 has the next red-shifted λ_{max}. P2.5 has an even longer λ_{max} attributed to backbone relaxation from randomly dispersed phenylene units that possess smaller hydrogen atoms, when compared to P2.4. P2.3 possesses a λ_{max} that is longer than P2.2, possibly from electron donation from the nitrogen atom bridging the biphenyl, raising the HOMO. The third longest λ_{max} is for P2.1, due to subtle *ortho* C-H interactions from a single phenylene in alternation with ProDOT. The second longest λ_{max} for P2.8 is believed to be due to the additional ProDOT ring in the repeat allowing S-O interactions between neighboring ProDOTs, facilitating planarity and increasing conjugation along the backbone.[35,43,153] Additionally, increased content of the electron rich ProDOT unit could serve to raise the HOMO of the polymer. The longest λ_{max} is exhibited by P2.6 as per the same reasoning discussed with P2.8 and has a solution spectral profile similar in shape and width to P2.3 and P2.1, but red-shifted by ~60 nm. The peaks at ~350 nm are typically observed for pyrene related materials.[158,159]

Probing the effect on optical properties in thin films in the neutral state, the spectra can be seen in Figure 4.2.2.3 where the polymers exhibited the following trend based on band gap (E_{gap}): P2.7 (2.59 eV) > P2.2 (2.51 eV) > P2.3 (2.48 eV) > P2.1 = P2.8 (2.42 eV) > P2.5 (2.26 eV) > P2.4 (2.25 eV) > P2.6 (2.23 eV).

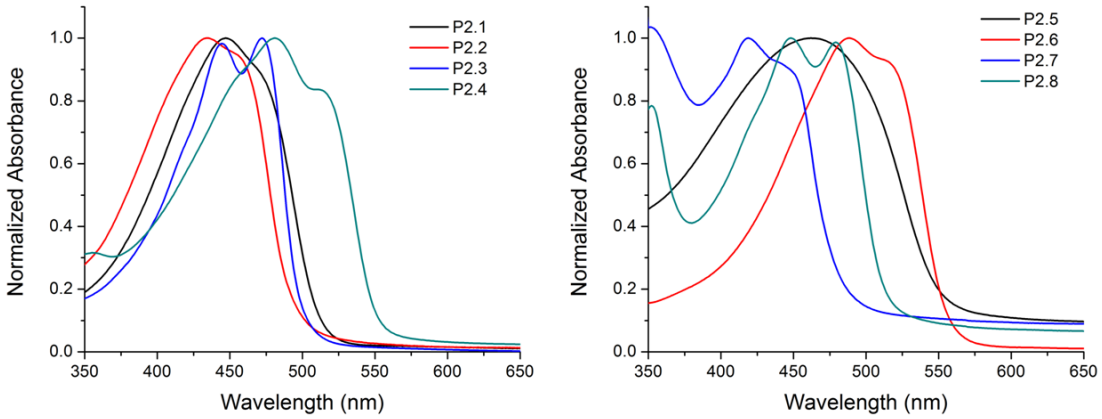

Figure 4.2.2.3: Normalized neutral state spectra of cast polymer films on ITO coated glass in 0.2 M LiBTI/PC electrolyte solution.

In the solid state, the trend is comparable to solution and as expected there is a red shift in the film absorption profiles. The notable exceptions are polymers that contain dimethoxyphenylene, these exhibit considerable red shifted spectra in the solid state relative to their solution forms. Random copolymer P2.5 has the third lowest E_g, indicating that there is an increase in conjugation along the backbone, facilitated by the methoxy groups on the phenylene cores inducing S-O interactions with their ProDOT neighbors. The second lowest E_g is for P2.4, slightly lower than P2.5; little change in the E_g. However, due to dimethoxy substituted phenylene replacing unsubstituted phenylene, P2.4 has a narrower absorption profile, lacking high energy transitions imparted by phenylene neighbors that would induce strain in the backbone. P2.6 exhibits an absorption profile of similar shape to that of P2.1, but is red shifted by ~40 nm giving it a vibrant peach color.

4.2.3. Colorimetric Properties, Improvement with ProDOT-Cbz

To gain a greater understanding of the breadth of colors achieved in the neutral and oxidized states, a colorimetric (L*, a*, b*) comparison of all polymers studied, based on the spectroelectrochemistry for each polymer is presented in Figure 4.2.3.1. All neutral state colors range from vibrant yellows very similar to P2.1 (P2.3 possessing nearly the

same a*b* values during switching) to colors bordering on or falling into the orange region of the L*a*b* color space such as the case for P2.6. Many of the polymers exhibit transmissive oxidized states at potentials lower than P2.1 (ECP-Yellow-1) with the exceptions of P2.7 and P2.8.

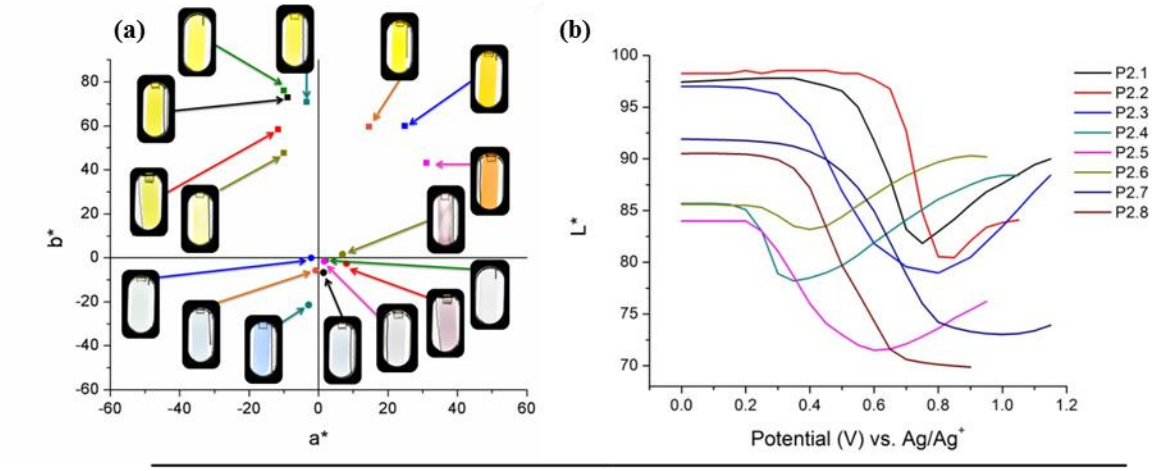

(c)

Polymer	Neutral State L*, a*, b* color coordinates	Oxidized State L*, a*, b* color coordinates
P2.1	97, -9, 73	90, 1, -7
P2.2	98, -12, 58	84, 8, -3
P2.3	97, -10, 76	88, 2, -1
P2.4	86, 25, 60	88,-2, 0
P2.5	84, 15, 60	76, -1, -6
P2.6	86, 31, 43	90, 2, -2
P2.7	92, -10, 48	74, 7, 2
P2.8	91, -3, 70	70, -3, -22

Figure 4.2.3.1: Colorimetry of all polymers in the neutral and oxidized states. Squares represent neutral states, Circles represent most oxidized states. P2.1 (Black), P2.2 (Red), P2.3 (Green), P2.4 (Blue), P2.5 (Orange), P2.6 (Pink), P2.7 (Brown), P2.8 (Dark Cyan) (a). Plots of L* versus Potential for all polymers (b). Tabulation of extreme state color values (c). All films are sprayed to an optical density of ~0.8 *a.u.*

A comparison of P2.3, P2.5, and P2.1 in the neutral and most oxidized transmissive states is shown in Figure 4.2.3.2. These three polymers were chosen as they display a true yellow color as defined by Munsell (L*=82, a*=4, b*=80)[6] while also achieving the highest transmission in the oxidized state of the family reported. Of the three polymers one can see that P2.3 is able to acquire the most transmissive oxidized state and is the most transmissive of all of the polymers studied in this chapter. This is possible due to

lower absorption of residual long wavelength visible light with an oxidation potential that is 50 mV less than P2.1. It is worthy to point out the importance of accuracy when spraying films as the data presented in Figure 4.2.3.2 is not normalized.

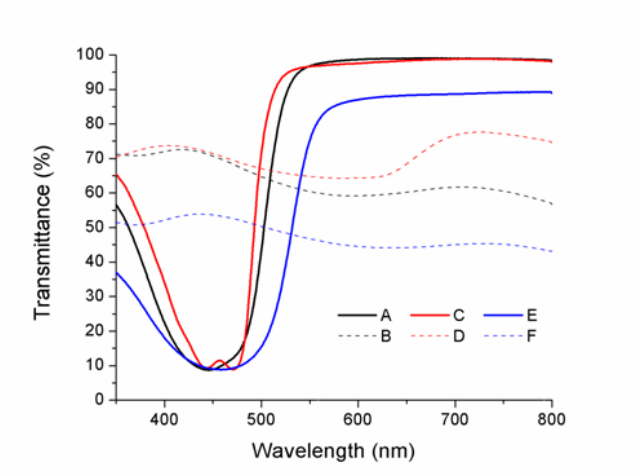

Figure 4.2.3.2: Comparison between the Transmittance (%) of the neutral and oxidized forms of P2.1, P2.3 and P2.5. Films were sprayed to an absorbance of ~1.0 a.u. A.) P2.1 at 0 mV B.) P2.1 at 1150 mV C.) P2.3 at 0 mV D.) P2.3 at 1100 mV E.) P2.5 at 0 mV F.) P2.5 at 950 mV.

4.3. Use of Dioxythiophene Dimers to Enhance Yellow Contrast

Of the materials studied thus far, P2.3 shows the most improvement in lowering the oxidized state potential and E_{ox} while maintaining a yellow neutral state color but the potential in the bleached state remained above 800 mV, greater than the typical maximum stable redox potential of many ECPs. Thus optimization of yellow ECPs needed to be continued.

4.3.1. The Inspiration from ECP-Peach

Looking back, P2.6 was peach in its neutral state but exhibited a bleached state potential that was more compatible with other ECPs. Drawing inspiration from P2.6 (ECP-Peach), a new structure was proposed: using bulky but electron rich dioxythiophene dimers to increase steric hindrance in the back bone, pushing the band gap to higher energy from 2.23 eV to 2.32 eV while maintaining a facility towards oxidation. Rather than using BiProDOT, more sterically strained BiAcDOT (where AcDOT is 3,4-(2-ethylhexyl)-

oxythiophene) was chosen. The structure of this new polymer, P2.9 (ECP-Yellow-2) is shown in Figure 4.3.1.1 and from the normalized broken-in neutral state spectra and photographs, the desired affect was realized; a vibrant yellow neutral state ECP with a low bleached state potential, compatible with other ECPs.

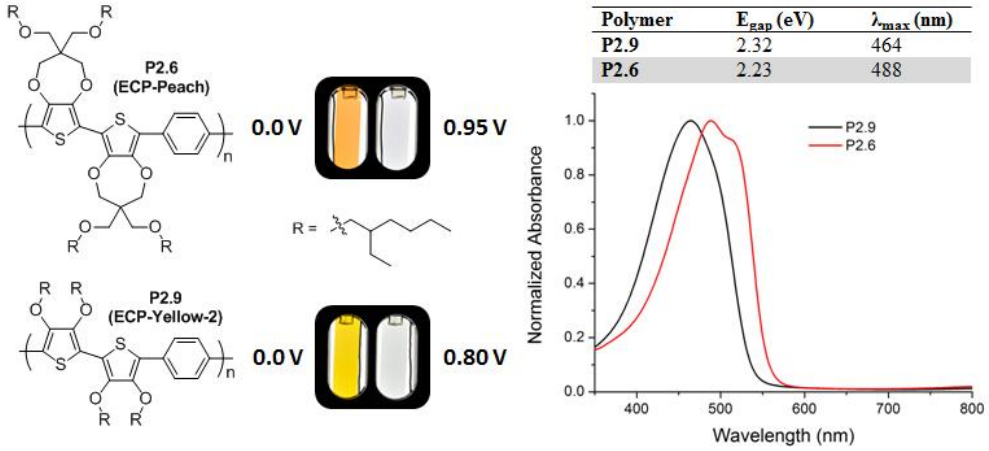

Figure 4.3.1.1: Structural (left), extreme state photographical (center), and normalized spectral comparison (right) for P2.6 and P2.9.

4.3.2. Comparison to ECP-Yellow-1 (P2.1) and ProDOT-Cbz (P2.3)

When comparing the spectra of the neutral and oxidized states of ECP-Yellow-2 to ECP-Yellow-1, and ProDOT-Cbz, ECP-yellow-2 shows substantial improvement in the oxidized state transmittance while maintaining a neutral yellow colored state with values that differ minimally. Direct spectral, colorimetric, and photographical comparisons can be seen in Figure 4.3.2.1. In the neutral state each polymer has L*,a*,b* values as follows: 96,-6,86 (P2.1), 97,-10,82 (P2.3), and 90,12,79 (P2.9). Once fully oxidized to the transmissive state the color values are: 82,1,-8 (P2.1), 86,2,-2 (P2.3), and 87,1,2 (P2.9). With regards to contrast upon switching the polymers exhibit the following values of Δ%T at λ_{max}: 62% (P2.1), 60% (P2.3), and 57% (P2.9). Though P2.9 has the lowest Δ%T at its λ_{max}, it possesses significantly less residual absorption of light across the visible at 800 mV, as evident by the oxidized state curves in Figure 4.3.2.1a. This results in oxidized states with the least amount of color as evident by the color values in Figure 4.3.2.1c,d and exemplified in the photographs in Figure 4.3.2.1b.

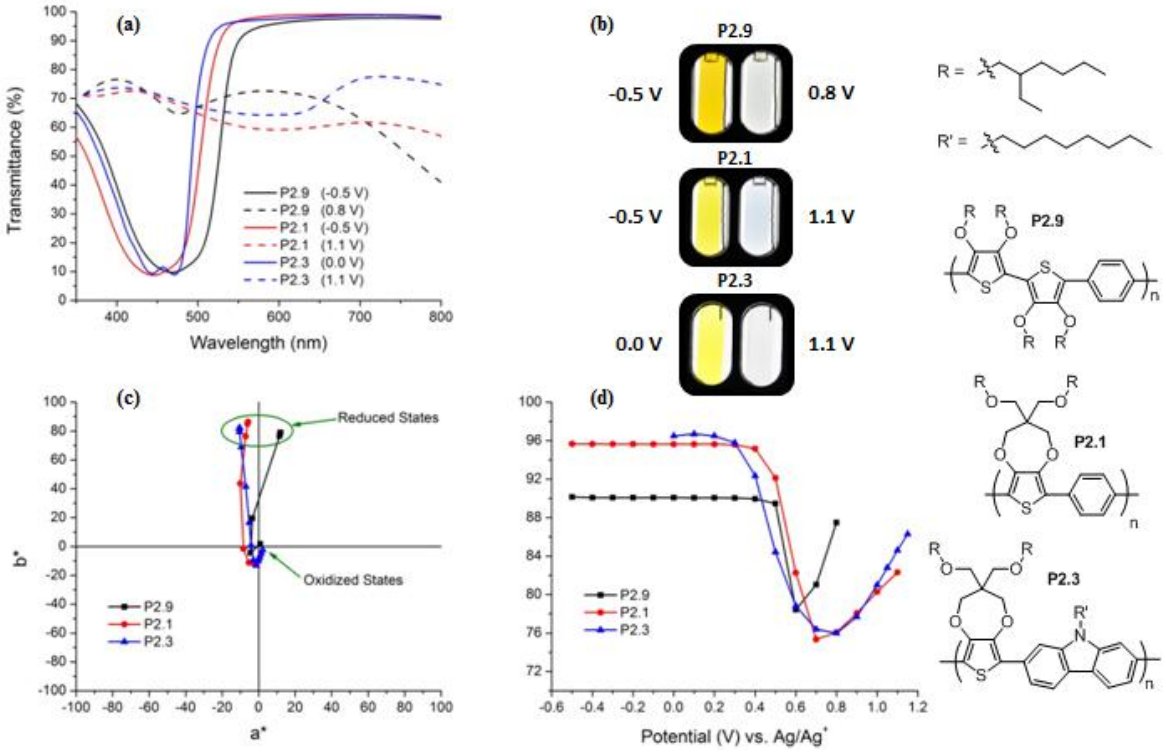

Figure 4.3.2.1: Colored and transmissive state spectra of P2.9 (ECP-Yellow-2), P2.1 (ECP-Yellow-1), and P2.3 (ProDOT-Cbz) (a). Photographs of films of each polymer in their extreme potential states (b). Color values (a*, b*) of all polymers (c). Color values (L*) at potentials (d).

4.4. Summary of Yellow ECPs

The use of torsional strain along the conjugated backbone imposed by subtle C-H *ortho* interactions from phenylene moieties neighboring DOTs accesses materials with high gaps (>2.25 eV) to give yellow neutral states and using this, P2.1 completed the color palette of ECPs, realizing full color ECDs. The ProDOTs impart the polymer with the ability to oxidize at low potentials. Unfortunately, this increase in strain and aromaticity from phenylene moieties makes P2.1 difficult to oxidize and fully bleach.

Through the studies conducted with P2.2-8 it was shown that by varying the electronic content of arylenes neighboring ProDOTs the oxidation potential could be tuned while maintaining yellow color neutral states. Through the knowledge gained by P2.6, P2.9 was

developed using additional strain, pushing the band gap to higher energies to give the desired yellow neutral state color while the high electron richness imparted by DOT dimers allowed more transmissive and colorless bleached states. With P2.9, the optimization of yellow ECPs and this chapter is concluded.

CHAPTER 5

TUNING THE PAINTERS PALETTE

As we saw in Chapter 4, high strain in conjugated polymer backbones is used to achieve high band gaps which give yellow neutral state colors. In this chapter we will examine the effects of subtle steric interactions in the form of relaxation and strain to tune new colors across the visible without the use of acceptors. These techniques were then applied in attempts to produce new black or brown ECPs (dark, as noted by low L*) where it was desired to improve upon neutral state broadly absorbing materials across the visible but with improved transmission in the oxidized states.

5.1. Subtle Strain and Relaxation Changes for New ECP Hues

Numerous techniques have been employed to control the visible absorption spectra and color of the neutral state in ECPs. These range from utilizing donor-acceptor (D-A) effects, vinylene and azomethine[160] linkers, interchanging atoms that constitute heterocycles or reside on the β positions, the augmentation of comonomer feed ratios or modification of pendant groups,[161] and varying the design of the metal-ligand in metallo-supramolecular polymers.[162,163,164,165] The D-A method has proven particularly useful as the donor moiety positions the HOMO while the acceptor positions the LUMO, retaining low oxidation potentials required for long term redox switching.[49,47,48]

If we examine the spectra for the transmissive oxidized states of D-A ECPs, they show tailing of charge carrier absorption in the near infrared back into the visible, giving some residual visible absorption which induces a blue tint in the films. This effect is minimal in all donating PEDOT[166] and PProDOT[33] ECPs with long and bulky alkyl substituents. In retaining the highly electron rich nature of XDOT polymers (X = ethylene, propylene, butylene, etc.), I hypothesized that steric control could be a sole "handle" for tuning color

while maintaining exceptional electrochromic switching to highly transmissive states without using acceptors.

In this section, we will discuss EDOT, ProDOT, and AcDOT (acyclic dioxythiophene, 3,4-(2-ethylhexyloxy)thiophene) containing copolymers, that are soluble and electron rich (all donating) with alternating repeat units, as shown in Scheme 5.1.1. The polymers were synthesized using direct arylation techniques. All of the polymers were isolated in high yield (>60%) with the exception of ProDOT-EDOT as it was difficult to solubilize. The solubility of the polymers that are composed of EDOTs is relatively low (ca. <2 mg/mL) but sufficient enough to conduct spray casting of solutions at room temperature. Neutral colors can be varied from bright pink, to magenta, purple, periwinkle, and blue by using only steric control, no acceptors. These polymers can switch rapidly and reproducibly to highly transmissive oxidized states that give greater transmittance and less residual color than previously reported polymers. These ECPs also address the issue of color break-in, by comparing as sprayed films to those that have been electrochemically cycled, as steric hindrance eliminates the break-in effect making for more color consistency. Table 5.1.1 facilitates the comparison of the electrochromic properties of these polymers throughout this section.

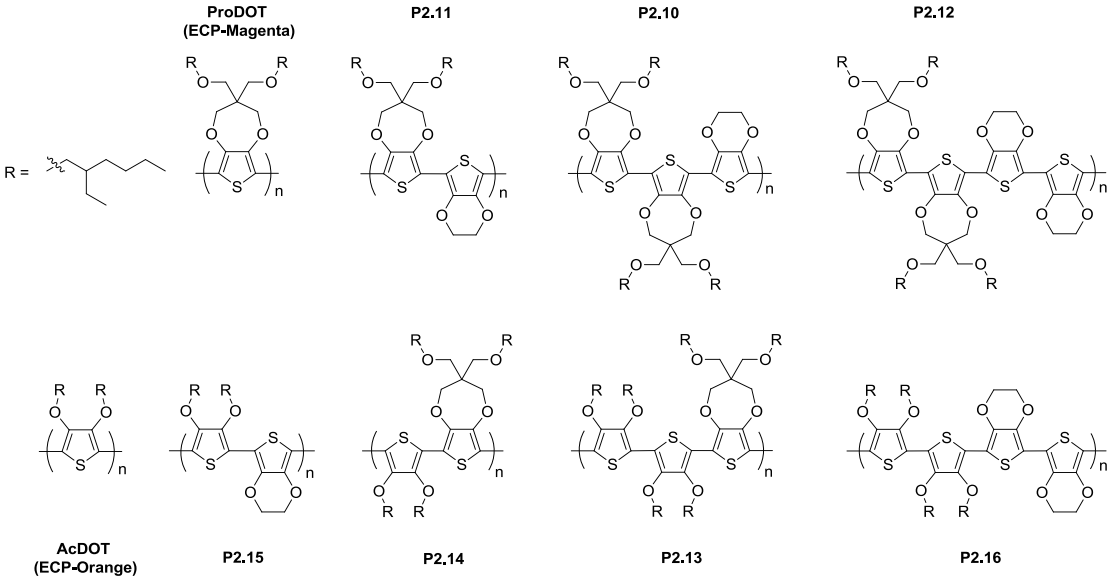

Scheme 5.1.1: Family of EDOT-, ProDOT-, and AcDOT-based ECPs prepared using direct arylation.

Table 5.1.1: Electrochromic properties for the family of EDOT-, ProDOT-, and AcDOT-based ECPs after break-in.

Polymer	Absorption Onset (eV)	λ_{max} (nm)	Δ%T (at λ_{max})	Neutral State L*,a*,b*	Oxidized State L*,a*,b*
ProDOT	1.97	555, 606	71	50, 51, -37	88, -1, -2
P2.10	1.81	590	71	33, 32, -63	90, -2, -3
P2.11	1.75	597	68	40, 16, -43	85, -4, -5
P2.12	1.74	606	75	37, 12, -63	92, -3, -3
AcDOT	2.10	490	48	72, 42, 53	81, -2, -7
P2.13	2.01	536, 579	73	56, 59, -16	91, -2, -1
P2.14	2.00	541, 587	72	47, 70, -36	91, -2, -3
P2.15	1.84	553	63	49, 41, -35	88, -3, -4
P2.16	1.81	557	70	38, 38, -44	91, -2, -4

5.1.1. New Hues of Blue and Magenta ECPs: Electrochemistry and Break-in Effects

The polymers are divided into two families: the blues comprising P2.11 (ProDOT-EDOT), P2.10 ($ProDOT_2$-EDOT), P2.12 ($ProDOT_2$-$EDOT_2$), and the magentas with P2.14 (AcDOT-ProDOT), P2.13 ($AcDOT_2$-ProDOT), and P2.15 (AcDOT-EDOT) while ProDOT (ECP-Magenta), AcDOT (ECP-Orange), and P2.13 ($AcDOT_2$-$EDOT_2$) stand as comparisons between the two families. The families of blue and magenta ECPs were designed and synthesized with the goal of examining the effects of subtle relaxation and torsional strain (energy towards planarization of two neighboring rings) on electronic absorption transitions to explore color control. This is presented as a cartoon in Scheme 5.1.1.1. The theoretical AcDOT-AcDOT system (left most structure) shows the highest degree of strain, breaks conjugation, giving the shortest wavelength absorption transitions. As backbone strain is decreased, conjugation is enhanced and moderate wavelength absorption transitions are achieved, giving bright magentas and purple neutral state colors.

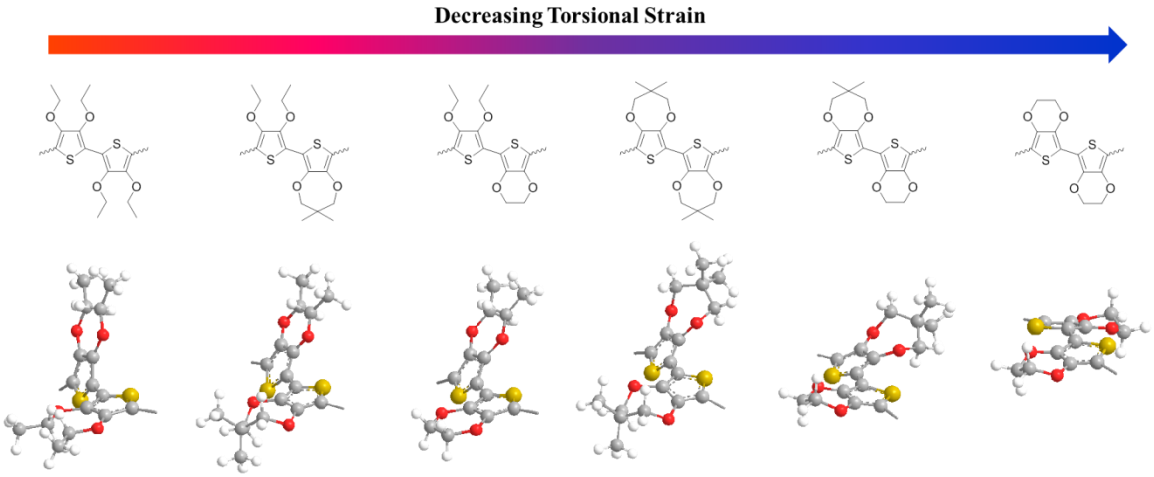

Scheme 5.1.1.1: General model in steric interactions to achieve new neutral state hues.

As relaxation is further induced, a greater extent of conjugation is reached and long wavelength transitions are attained giving purple to blue colors. The use of dimers (such as $ACDOT_2$, $EDOT_2$, or $ProDOT_2$) over monomers (only AcDOT, ProDOT, or EDOT) in the repeat unit also induces longer wavelength absorption transitions.

The structures shown in Scheme 5.1.1.1 are based on torsional angles acquired from previously reported X-ray crystal structures of dioxythiophenes.[35,167,168] For those not reported, the order of strain was estimated by calculating the energy barrier towards planarization using the program default energy minimizations performed in ChemBio3D Ultra 14.0 by CambridgeSoft.

Before the spectroelectrochemistry could be analyzed, the films were electrochemically conditioned (we refer to such processes and films as "break-in" and "broken in" respectively) with 25 cycles *via* cyclic voltammetry (CV) until the current stabilized and became reproducible (as discussed in Chapter 3.2.3). Looking at Figure 5.1.1.1 and Figure 3.2.3.2, there is a considerable change between the first and second cycle, after which the current stabilizes to become fully reproducible in all polymers by the 25^{th}.

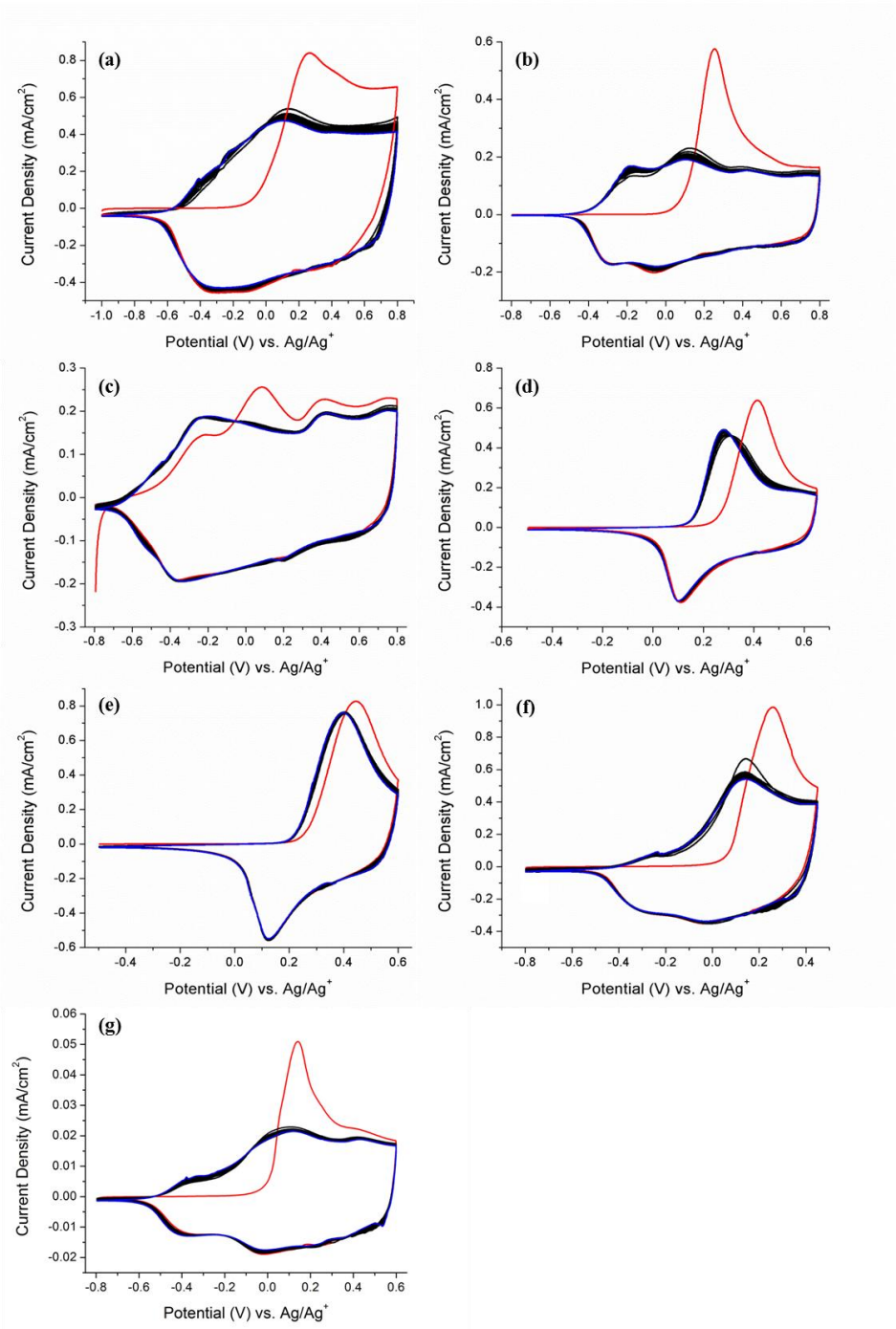

Figure 5.1.1.1: Break-in CV for all polymers. 1st cycle (red), 2nd-24th cycles (black), and 25th cycle (blue). P2.11 (a), P2.10 (b), and P2.12 (c); P2.14 (d), P2.13 (e), P2.15 (f), and P2.16 (g).

The induction of steric relaxation along the conjugated backbone from alternating EDOT moieties presents drastic changes between the pristine and broken in film states. As strain

is introduced through AcDOT incorporation, this effect is minimized with little change between the pristine and broken in state exhibited by P2.13. This indicates that strain reduces electrochemical break-in effects.

All of these polymers oxidize easily as shown by differential pulse voltammetry (DPV) with the current normalized in Figure 5.1.1.2. The onset of oxidation potentials range from -490 to 206 mV. AcDOT however, has the highest oxidation potential of 260 mV, due to pendant group bulkiness.[32] Expectedly, the increase in strain raises oxidation potential onsets while relaxation lowers them.

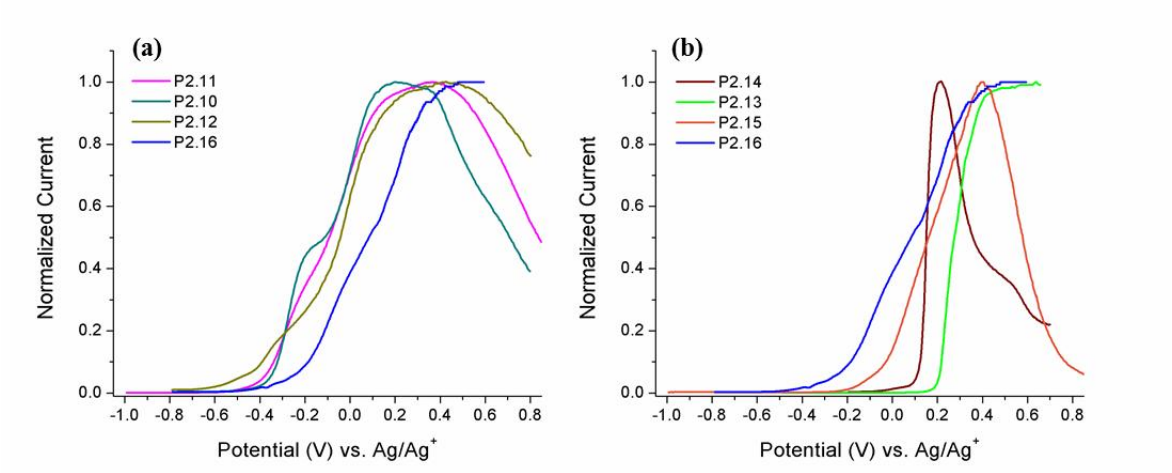

Figure 5.1.1.2: Oxidation DPV for all polymers where current is normalized for new blue (a) and magenta (b) ECPs. The oxidation potentials (E_{ox}, in mV, reference calibrated to 80 mV vs. Fc/Fc^{+}) are as follows: P2.11 (-390), P2.10 (-340), and P2.12 (-490); P2.14 (125), P2.13 (206), P2.15 (-50), and P2.16 (-235).

5.1.2. New Hues of Blue and Magenta ECPs: Electrochromism and Colorimetry

For films, the break-in effect observed results in an alteration of the spectra as exemplified in Figure 5.1.2.1. Concurrent with the changes observed during CV, the film spectra redshift and intensify as strain is reduced, while the changes in the spectra are reduced with increasing strain.

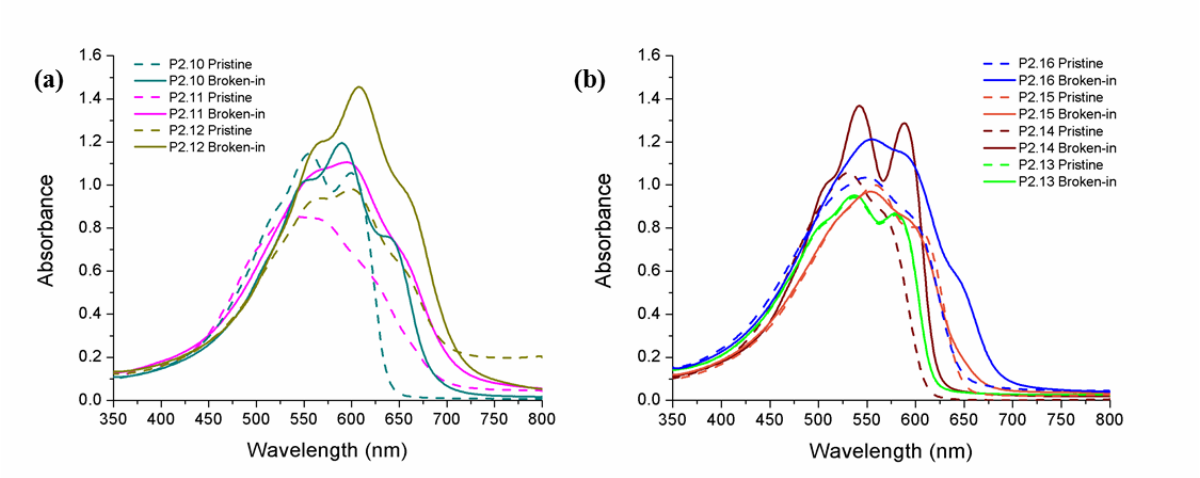

Figure 5.1.2.1: Comparison between spectra of wet, pristine and broken-in states for blue (a) and magenta (b) hue ECPs.

To examine the optical properties of the broken-in films held at their neutral state voltages, the normalized absorption spectra for the two families of the all donor polymers are shown in Figure 5.1.2.2 with the absorption onsets and λ_{max} values in Table 5.1.1. Looking at Figure 5.1.2.2a, as relaxation is subtly induced through increasing the EDOT content, long wavelength (low energy) absorption transitions, relative to ProDOT and AcDOT, arise. The family of blue ECPs possesses lower band gaps relative to ProDOT, absorbing longer wavelength light, making the materials appear periwinkle-blue to the eye. With this red-shifted absorption onsetting at ~700-750 nm, these polymers can be thought of as organic soluble analogues of PEDOT. Now examining Figure 5.1.2.2b, as steric strain is increased with AcDOT addition, shorter wavelength transitions arise relative to ProDOT. These materials with greater strain absorb more of the shorter wavelengths of the visible spectrum, reducing the amount of blue light that reaches the eye, thus making the materials appear as “hotter” or “reddened” magentas and pinks.

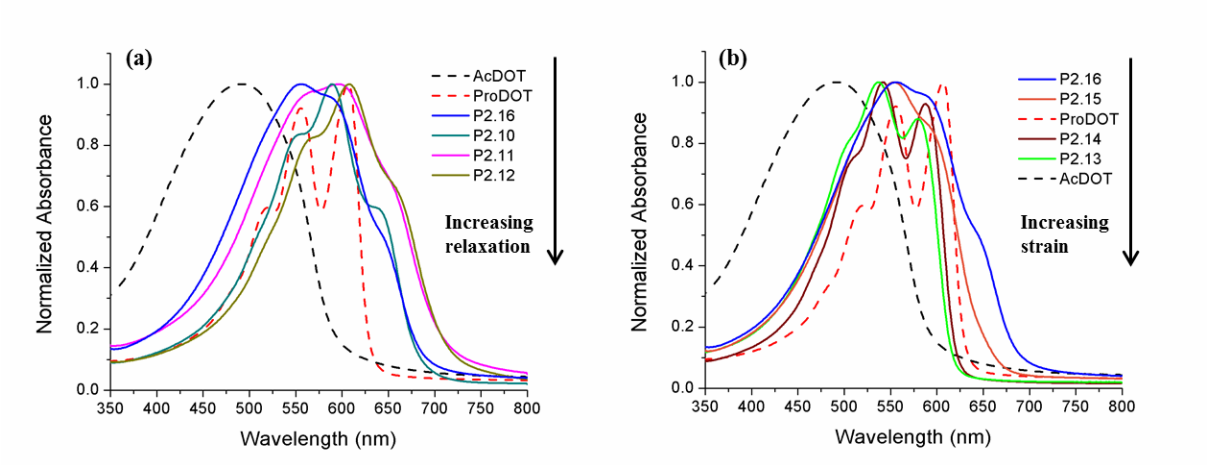

Figure 5.1.2.2: Normalized neutral state spectra of blue (a) and magenta (b) hued ECPs spray cast as films after break-in cycling.

The polymer repeat unit structure affects the presence, or lack thereof, vibronic coupling in the solid state spectra. The increasing amount of strain *via* shifting from P2.14 to P2.13 shows only a slight decrease in the degree of vibronic coupling, as evidenced by the lower definition in the multiples of peaks, relative to ProDOT which exhibits a high degree of order.[166,168,169] Following this, a decrease in the extent of vibronic coupling is observed for the EDOT containing polymers. This indicates that, although AcDOT is considerably more bulky than EDOT, the low steric hindrance of the latter allows the propylene bridge on neighboring ProDOT rings to have more freedom in conformational changes. This induces greater degrees of disorder in the polymer backbone, reducing the extent of vibronic coupling and broadening the spectra.[43,170, 171]

These blue and magenta hued all-donor polymers exhibit desirable electrochromic contrast, switching from a vibrant colored state to highly transmissive. This is best illustrated in Figure 5.1.2.3 for P2.12 and P2.13, along with the remaining polymers in Figure 5.1.2.4. The entire family of polymers studied exhibit changes in contrast (Δ%T) above 60% at the λ_{max} as shown in Table 5.1.1. P2.12 and P2.13 exhibit the highest contrast values, 75% and 73% at λ_{max} respectively. They also possess the least residual absorption tailing into the visible from the fully oxidized transmissive state, even for

thicker films. Those that incorporate EDOT broaden the potential range over which the polymer's switch with subtle changes during progressive oxidation while those that utilize AcDOT narrow the potential window considerably, presenting more drastic changes with each potential step. This phenomena has been attributed to twiston effects, which can be considered delocalized conformational defects, seen in previous polymer systems.[32,172,173] Due to the higher twist in P2.14 and P2.13, there is a resistance to planarization on initial oxidation. However, at increasing oxidation steps, localized planarization begins to occur, which has a rapid domino effect on neighboring repeat units. This may also explain the unusually narrow switching window for P2.9 discussed at the end of Chapter 4.

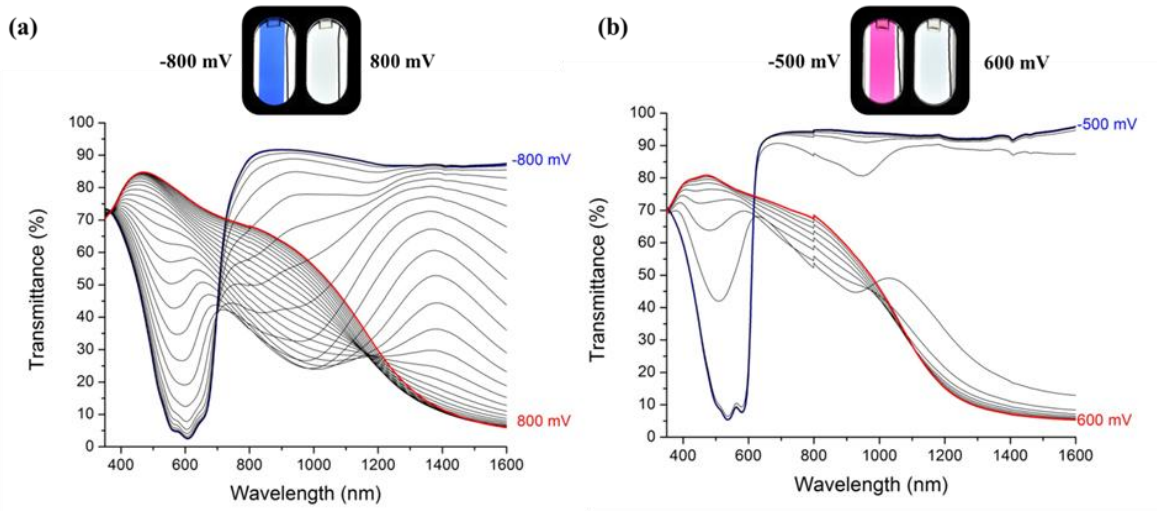

Figure 5.1.2.3: Electrochromic properties of thick films (~1.2 *a.u.*) of P2.12 (a) and P2.13 (b). Spectroelectrochemistry performed at potential steps of 50 mV.

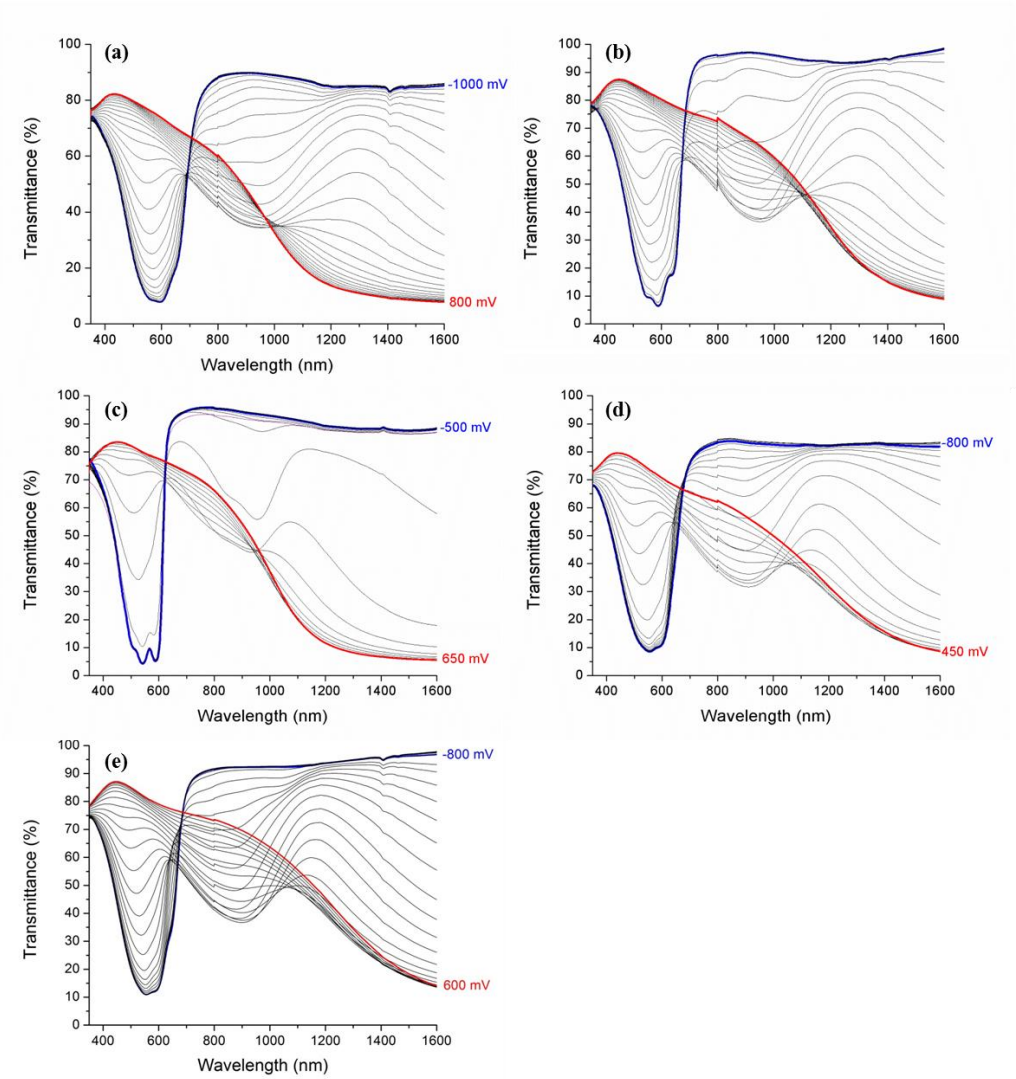

Figure 5.1.2.4: Spectroelectrochemistry of P2.11 (a) and P2.10 (b); P2.14 (c), P2.15 (d), and P2.16 (e).

All of the polymers are able to switch rapidly with minimal losses in contrast shown by the switching kinetics *via* chronoabsorptometry in Figure 5.1.2.5. They undergo the full neutral colored to oxidized transmissive change with switch times as fast as 1 second. Upon switching at fast speeds with ½ and ¼ second cycles, the polymers exhibit an expected decrease in contrast through diffusion limiting processes of electrolyte migration. After cycling at high speeds, the polymers can regain high levels of contrast

with no apparent negative effects (delaminating, blistering, etc.), demonstrating robustness during rapid changes in switching speeds.

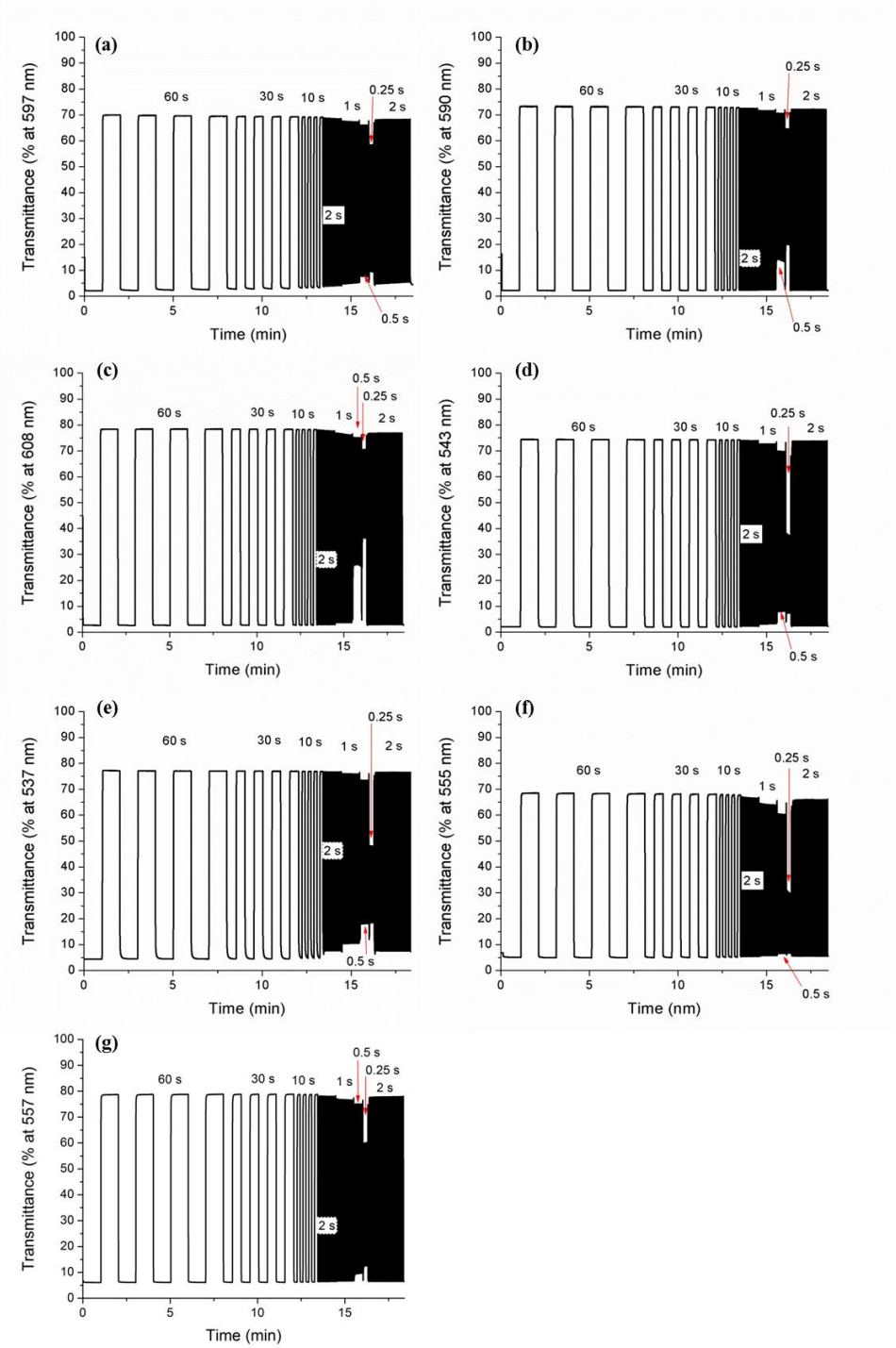

Figure 5.1.2.5: Chronoabsorptometry for P2.11 (a), P2.10 (b), and P2.12 (c); P2.14 (d), P2.13 (e), P2.15 (f), and P2.16 (g).

To better relate the influence of spectra on color, the colorimetric properties (a*b*) and extreme state photographs of each polymer is in Figure 5.1.2.6, with the color values of each in their neutral and most oxidized states shown in Table 5.1.1.

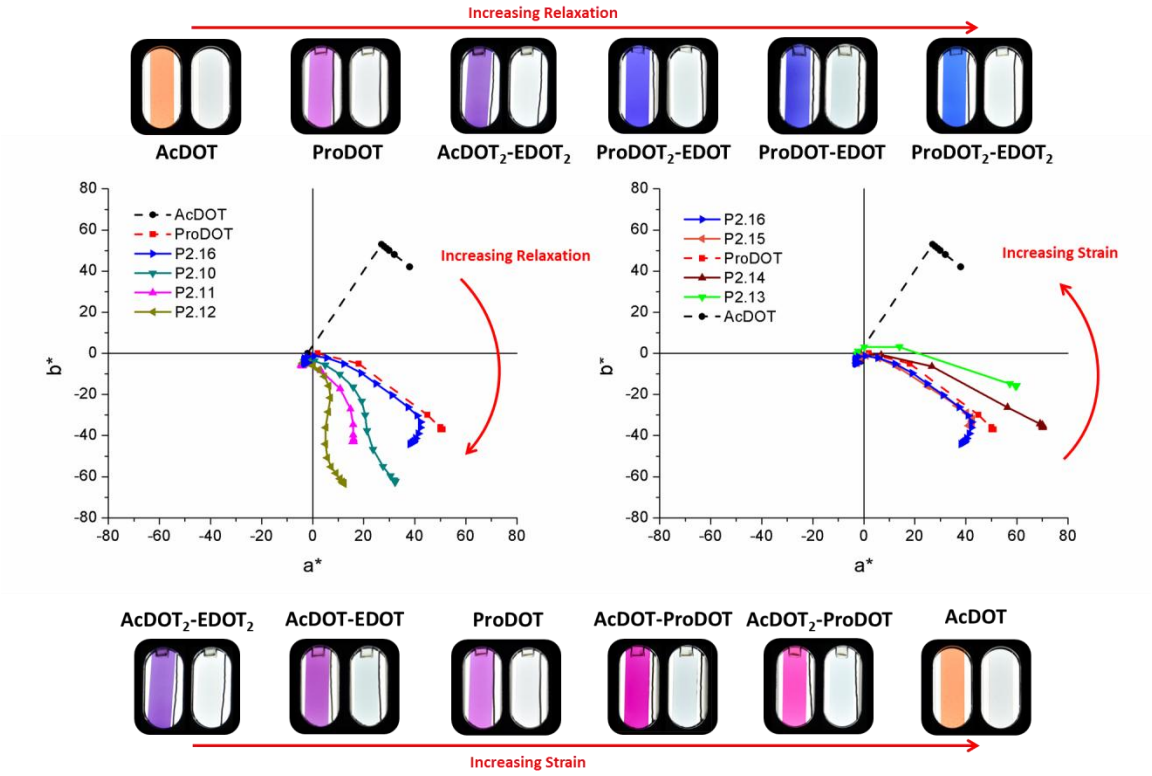

Figure 5.1.2.6: Colorimetry (a*b*) of the blue and magenta hued ECPs. Films sprayed to ~1.0 *a.u.* Direction of the arrows indicate increasing relaxation or strain.

The color trend for the blue hued ECPs with increasing relaxation progressing from orange, through purple, to blue a*b* values are as follows:

AcDOT (42, 53) → ProDOT (51, -37) → $AcDOT_2$-$EDOT_2$ (38, -44) →

$ProDOT_2$-EDOT (32, -63) → ProDOT-EDOT (16, -43) → $ProDOT_2$-$EDOT_2$ (12, -63)

If we connect back to the neutral state spectra in Figure 5.1.2.2a, as long wavelength absorption transitions are produced through the increase in relaxation from the raised content of EDOT, the neutral state color values progress to lower a*. This indicates less

purple color and more blue hue due to the progressive transmittance of shorter wavelength (blue) and less long wave (red) light. For the magenta hued ECPs, the color trend with increasing strain transitioning from purple, through pink, to orange a*b* values are as follows:

$AcDOT_2$-$EDOT_2$ (38, -44) → AcDOT-EDOT (41, -35) → ProDOT (51, -37) → AcDOT-ProDOT (70, -36) → $AcDOT_2$-ProDOT (59, -16) → AcDOT (42, 53)

Again, looking back to the neutral state spectra provided in Figure 5.1.2.2b, as moderate and short wavelength absorption transitions are induced through the increase in strain from the addition of AcDOT, color values in the neutral state progress to higher b*. This decreases "purpleness" and yields truer magenta and pink colors from more absorption of blue light and increasing transmission of red light. P2.13 is of particular importance as this polymer nearly matches the color values of magenta as defined by Munsell (L*, a*, b* = 52, 50, -15)[6] whereas ProDOT is a bit too "purple" after break-in. P2.13 will allow for more accurate color mixing in the cyan-magenta-yellow (CMY) subtractive regime using these soluble polymers.[87] The as processed (pristine) state color values for P2.14 are also close to the Munsell magenta, but after break-in its color shifts to more purple values. This color shift was prevented upon the incorporation of increased strain with P2.13, eliminating break-in changes that give rise to lower energy absorption transitions. For a better understanding of the color values at three different thicknesses, the complete colorimetry and photographs for each polymer is shown in Figure 5.1.2.7.

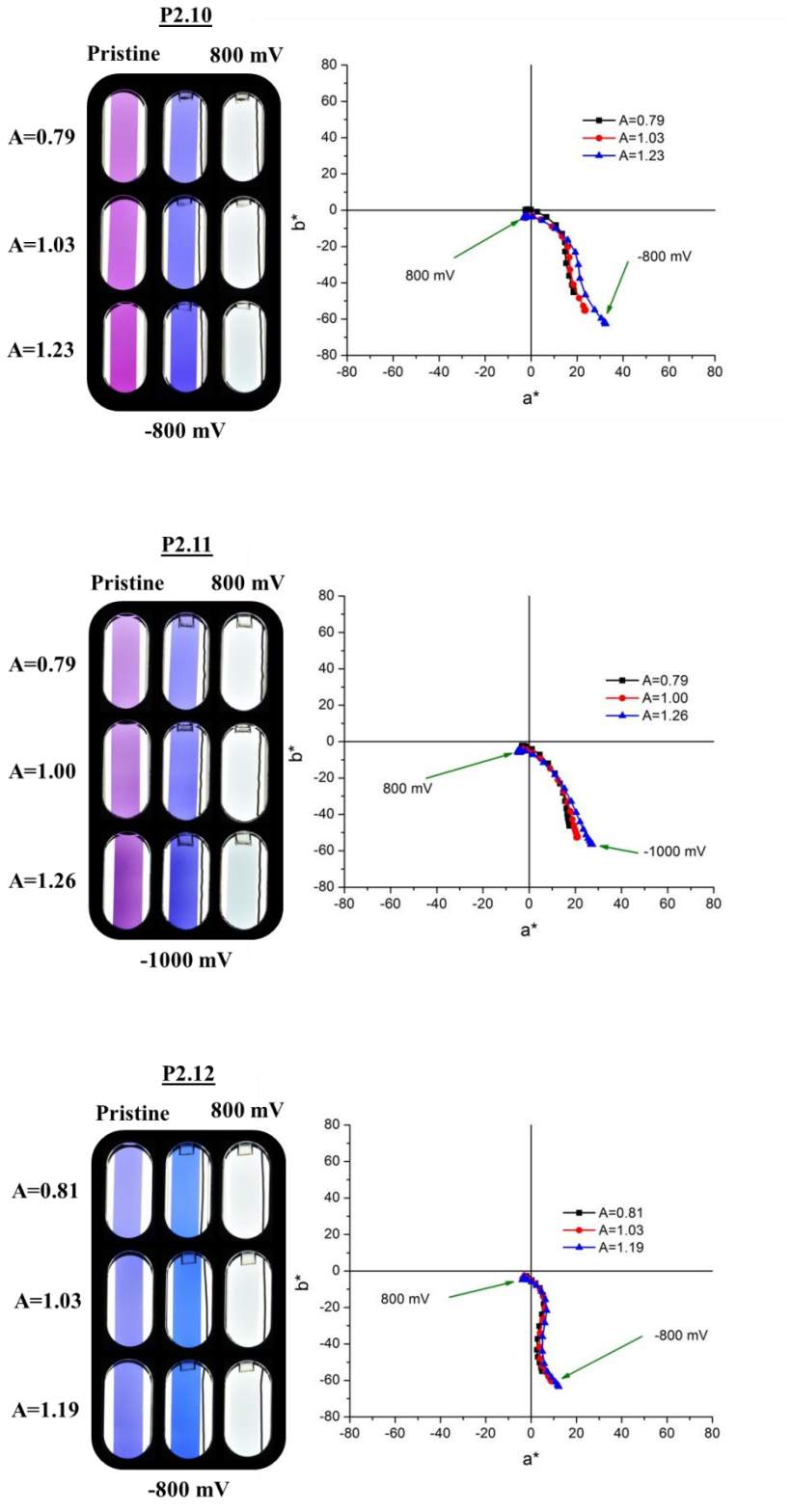

Figure 5.1.2.7: Photographs and a*b* color coordinated for all polymers at various thicknesses for this section.

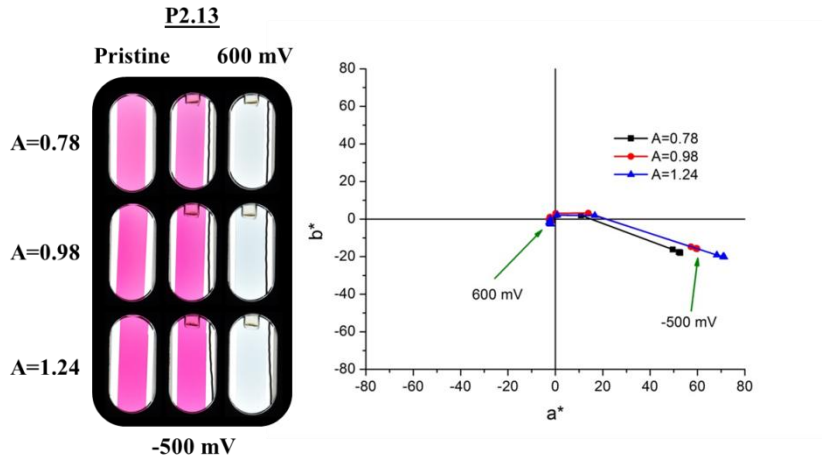

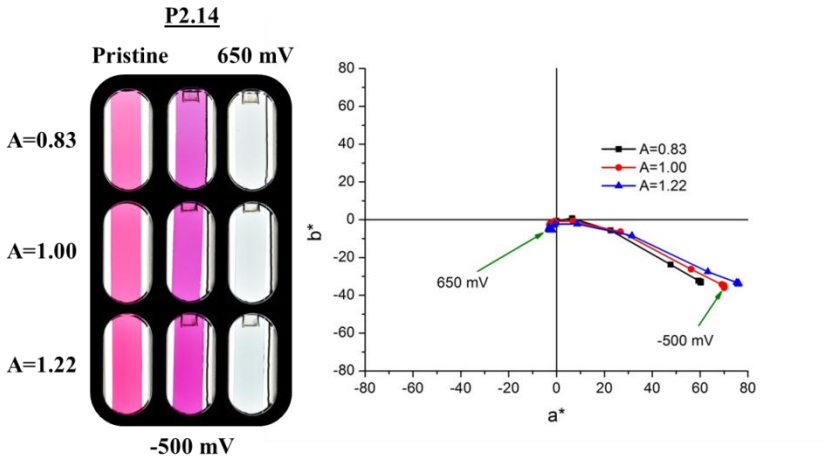

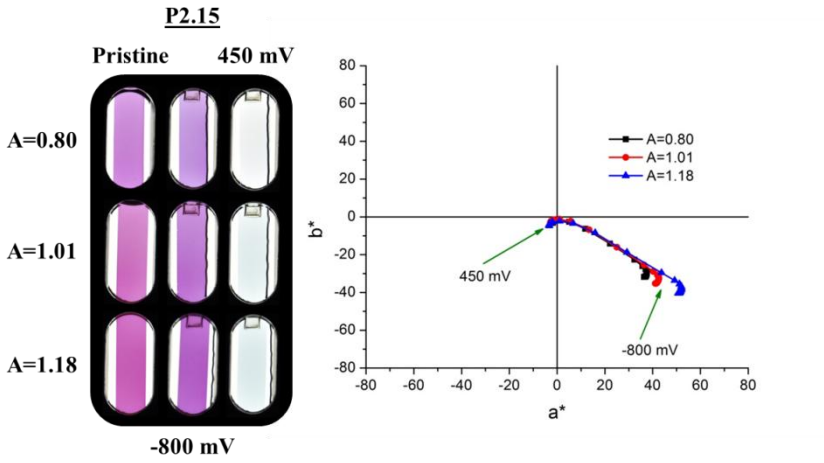

Figure 5.1.2.7: Continued.

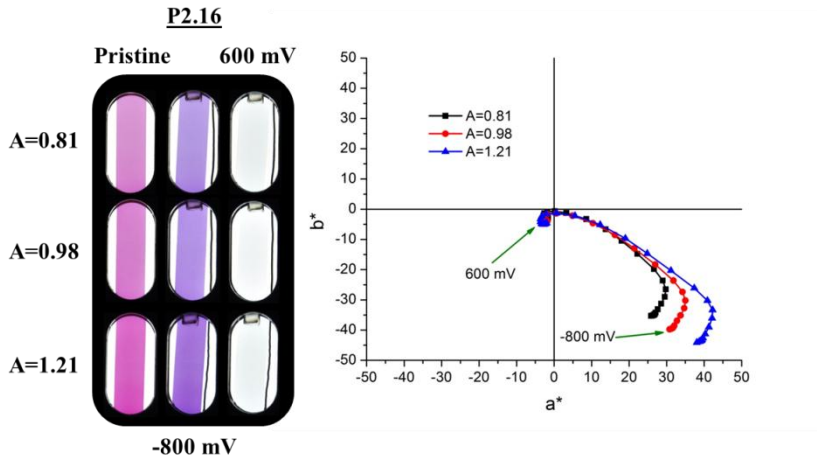

Figure 5.1.2.7: Continued.

In all of the copolymers most oxidized transmissive state, the a*b* values are close to the origin with high L* (Table 5.1.1) which indicates a distinct lack of color with high transmissivity and no other special trend evident during electrochromism. This color neutrality comes from these polymers exhibiting minimal residual absorption into the visible spectrum because of their electron rich all donating character, as shown by Figure 5.1.2.8a, discussed further in Section 5.1.3. The L* for all synthesized polymers as a function of voltage during switching can be seen in Figure 5.1.2.8b

.

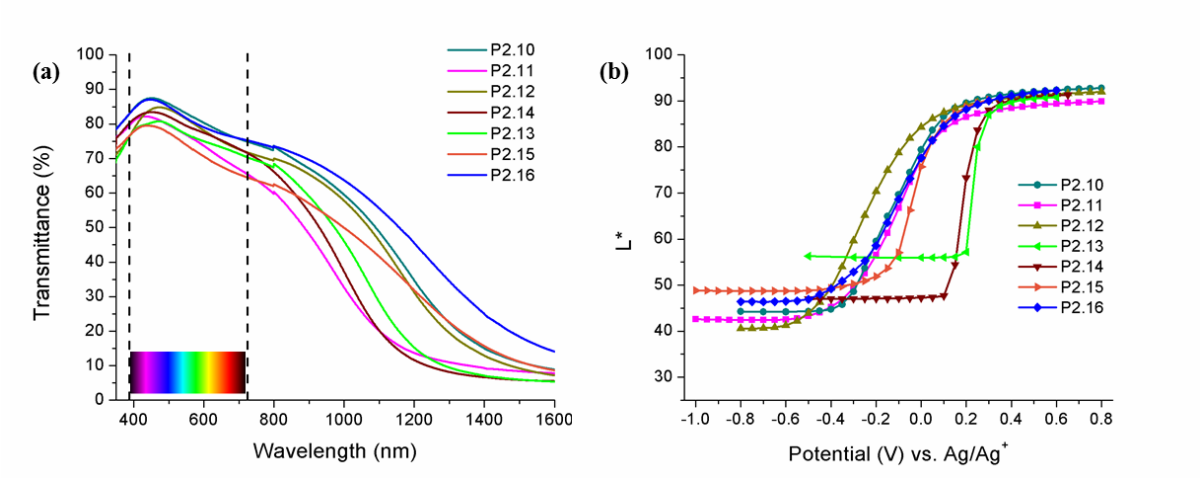

Figure 5.1.2.8: The most transmissive oxidized state absorption for all polymers where the visible spectrum is represented within the boundaries between the dotted lines (a). Lightness values (L*) for all polymers discussed in this study (b). All films were sprayed to ~1.0 *a.u.*

5.1.3. Comparison to ECP-Blue (Donor-Acceptors)

This subtle steric tuning through relaxation in all donor polymers is able to yield materials with low band gaps (P2.12) that are blue colored in the neutral state with color values that are comparable to those of a blue-to-transmissive ECP designed by donor-acceptor (D-A) methods.[47] Let's concern ourselves with a comparison between the neutral states for P2.12 and the previously reported ECP-Blue (ProDOT-BTD) in Figure 5.1.3.1a. This comparison was chosen because the two materials possess similar color values while employing distinctly different structures to tune optical transitions and color. From Figure 5.1.3.1a, using the D-A approach between alternating ProDOT and BTD (benzothiadiazole) produces a dual band absorption where the shorter wavelength absorption is attributed to the π to π* and the longer wavelength absorption is from the donor-acceptor charge transfer (CT) interactions.[48] From the method of steric relaxation in P2.12, a similar long wavelength absorption was attained with an onset at shorter wavelengths (1.74 eV), remaining at the edge of the visible spectrum. The D-A approach produced a much lower onset (1.53 eV) with a trench at 431 nm between the two bands.

The difference in the two spectra affects the neutral state color whereas shown earlier; P2.12 allows a majority of blue light to pass while minimizing the amount of transmitted red light, giving a saturated blue color. With ECP-Blue, the more redshifted onset from the CT absorption allows more green than red light to transmit however, the higher energy π to π* actually filters out a portion of blue and violet light, making it a less saturated sky-blue color. Though they have similar numerical color values, P2.12 appears more saturated because more blue light is reaching the highly sensitive S cones in the human eye.

The electron rich character of the all donor polymers discussed above allow them to be fully bleached (oxidized to a point where a*b* color values approach zero and L* is high) at lower potentials than those exhibited by donor-acceptor systems. In the fully oxidized transmissive states, for the all donor polymer P2.12, the π-electron donating character of the oxygen's residing on the β-position of thiophene impart a stabilization to their oxidized forms, red-shifting the overall absorption (see Figure 5.1.3.1a) and leading to a repression of the absorption between 700-1,000 nm relative to the donor-acceptor system (ECP-Blue). The ability for S and O to interact between neighboring DOTs and induce planarization may also assist the redshift.[43, 171] The red-shifting of the spectra for the fully oxidized transmissive forms results in less residual absorption tailing into the visible, improving contrast in all donor polymers relative to the D-A system ECP-Blue. In Figure 5.1.3.1a it can be seen that at ECP-Blue's most transmissive oxidized state there is a significant absorption continuing to tail into the long wavelength portion of the visible (600-720 nm) with a peak in the NIR at ~1460 nm, resulting in a blue tint when oxidized (Figure 5.1.3.1c) while P2.12 exhibits minimal tailing in the same portion with a peak beyond 1600 nm, being nearly colorless when oxidized.

From the comparison presented in Figure 5.1.3.1, we can see that lower gaps are attained with donor-acceptor effects, but at the cost of electrochromic contrast as a consequence of tailing absorption due to the incorporation of electron deficient acceptors. To do the

same with all donor systems would require significant synthetic design of exotic new relaxed rings to achieve comparably low gaps. So as the state of the art stands with DOTs, the attainable gaps are sufficient for color applications with high electrochromic contrast from all donor structures nearly eliminating residual visible absorption when fully oxidized. Based on this, it is wise to avoid using D-A interactions in ECP color control when possible.

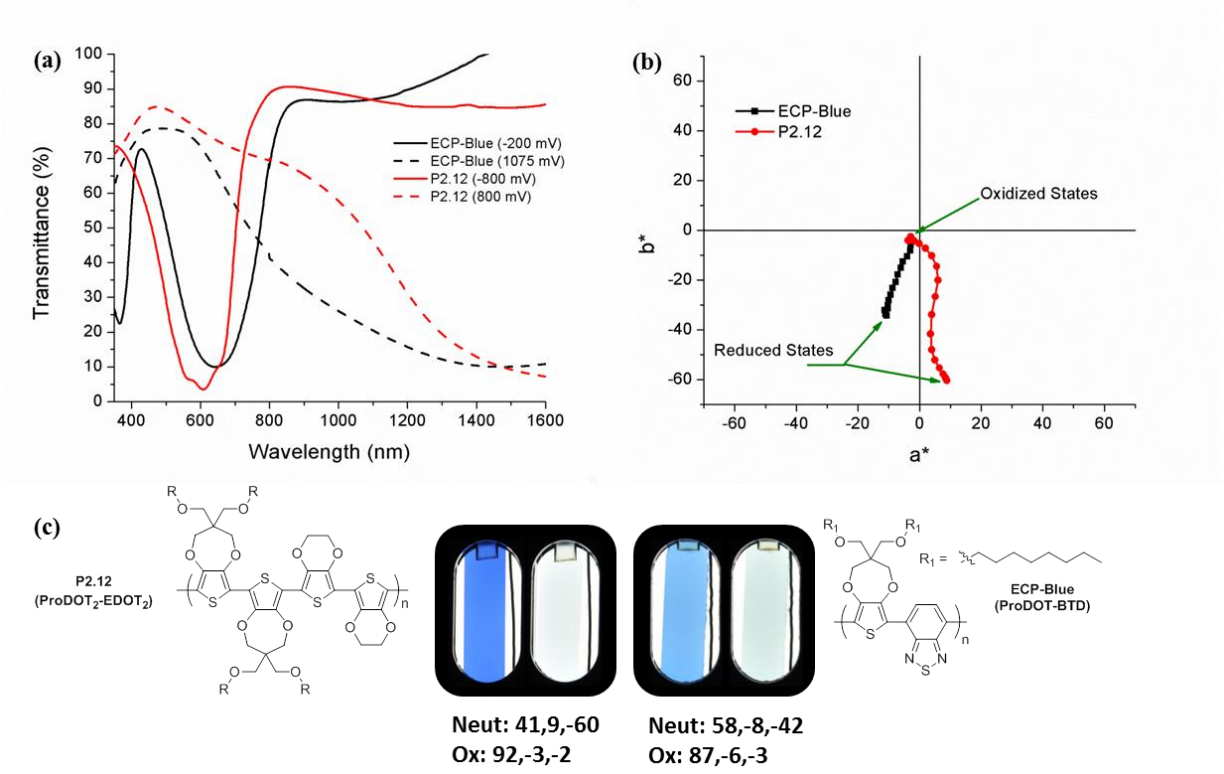

Figure 5.1.3.1: Comparison between P2.12 and ECP-Blue (ProDOT-BTD). Spectra of the extreme states (a), colorimetry (b), and structurally and photographically (L*a*b* color values below photos, Munsell Blue: 29, 14, -50) (c). Both polymers sprayed to ~1.0 *a.u.*

5.2. Progress in Achieving All Donor Broadly Absorbing Polymers

Because of the ability for all donating polymers to achieve highly transmissive oxidized states, architectures to achieve black-to-highly transmissive ECPs without acceptors is most desirable. This need for improvement in visible broadly absorbing ECPs is due to the inability for the present ECP-Black to achieve high contrast during electrochromic

switching as shown in Figure 5.2.1.[42] With a Δ%T < 50 across the visible (380-780 nm), this material would not be suitable for applications in windows or eyewear due to residual color in the oxidized state. A similar structure by Beaujuge *et al* for another black ECP exhibits the same tailing with a less broad absorption spectrum.[51] Concerning the discussion on photography in Chapter 3, note the difference in the photographs of ECP-Black between Figure 1.3.5.2 and Figure 5.2.1b as the latter is shot using a camera calibrated to the standard illuminant (D50) used for quantification of color and better represents the true nature of the color properties.

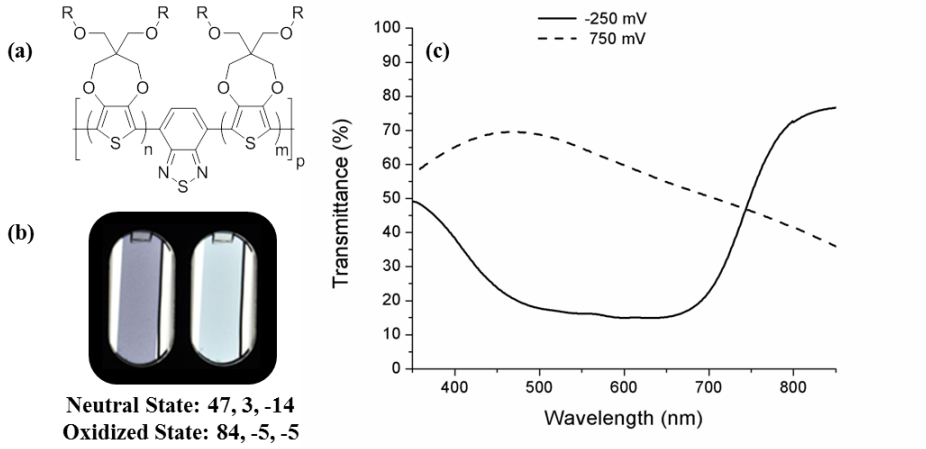

Figure 5.2.1: Structure (a), extreme state photographs (b) and neutral and oxidized state spectra (c) for ECP-Black. Color values are provided beneath the photographs as L*a*b*.

In this section we will discuss two different random copolymer architectures as randomness is needed to achieve varying lengths of conjugation to target broadly absorbing spectra. Two systems were designed using the structure-property relationships gained from the previous section: ProDOT-AcDOT/EDOT and ProDOT-EDOT/Ph. These materials did not achieve the intended broadness or contrast but are important in the development of the materials discussed in Chapter 6.

5.2.1. Lessons in the Design of a ProDOT-AcDOT/EDOT System

In an attempt to exploit the energy transitions produced in Section 5.1 to achieve a broadly absorbing material that could be black or brown in color, a random all donor polymer utilizing an even ratio of EDOT and AcDOT coupled to a ProDOT monomer was produced. In theory, through the random incorporation of the monomers EDOT and AcDOT with ProDOT, varying conjugation lengths would be formed leading to a broadly absorbing material with all donor character. The structure of P2.17 is shown in Scheme 5.2.1.1.

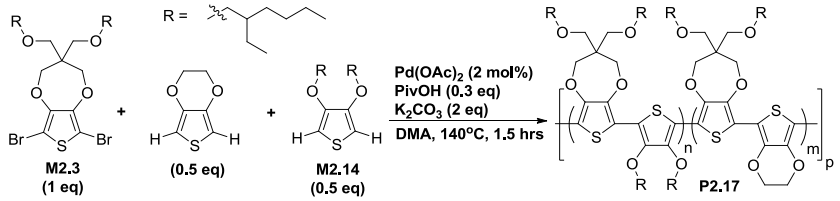

Scheme 5.2.1.1: Polymerization scheme to achieve P2.17.

In broken in films of P2.17 however, there was little increase in long wavelength absorption relative to P2.10-12 with the onset redshifting from 1.94 (pristine) to 1.84 eV (broken in). As shown in Figure 5.2.1.1, the polymer maintained a narrow absorption in the middle of the visible. This indicates that the random all DOT architecture was not leading to the desired broadness, though it was expected that varying lengths of ProDOT-ACDOT interactions would lead to moderate to short wavelength transitions and ProDOT-EDOT runs would give long wavelength transitions. In the oxidized state, P2.17 was exceptionally transmissive with a Δ%T at 551 nm of 77%. It is of interest to note that as films of P2.17 were produced with greater optical density (thickness), the reduced state color became darker (as noted by the decrease in L*) but in the oxidized state, the films remained highly transmissive (as noted by the minimal change in L*). The spectrum of P2.17 in the pristine state lead to the film having an appearance similar to that of ECP-Magenta (ProDOT with respect to discussions in section 5.1).

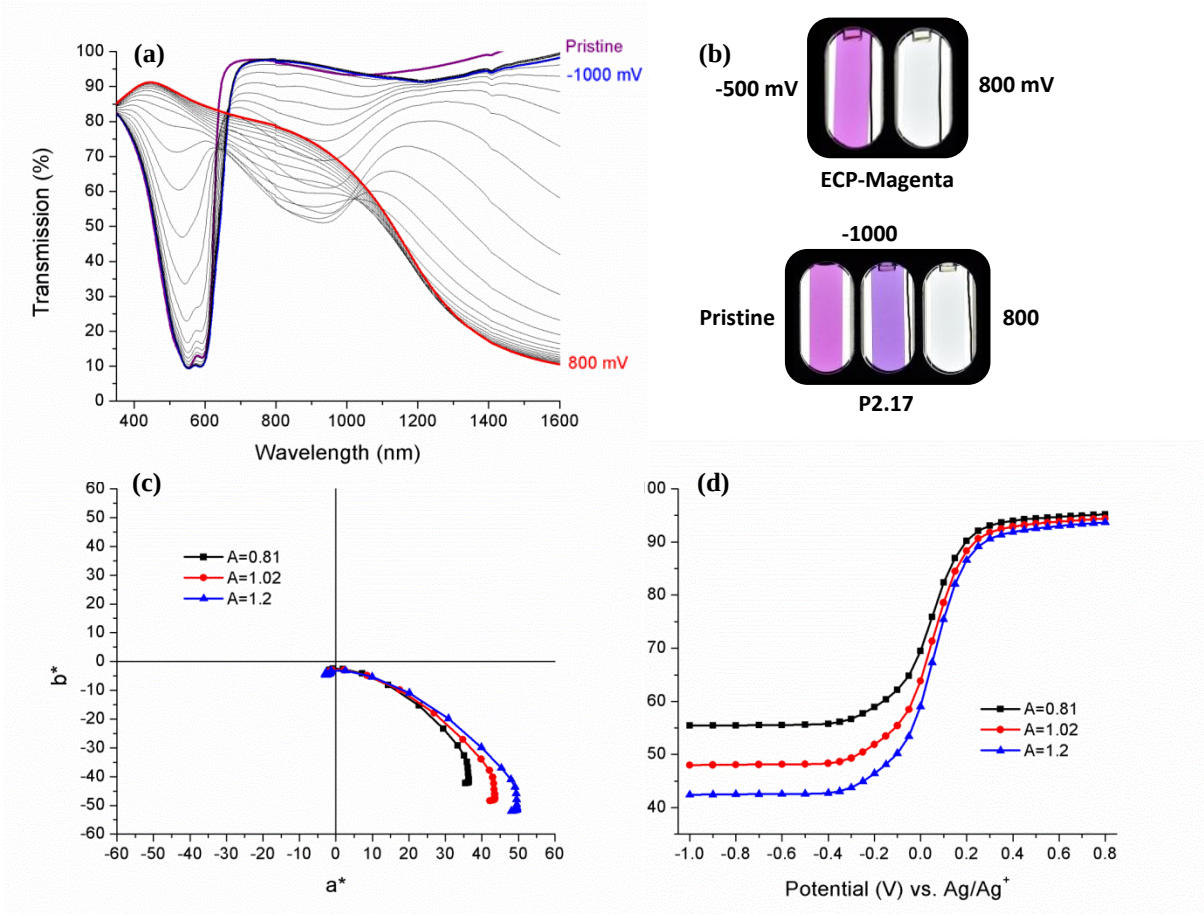

Figure 5.2.1.1: Spectroelectrochemistry of P2.17 (a). Photographical comparison between P2.17 and ECP-Magenta (b), color value comparison in a*b* (c), and photographical and L* comparison (d) different optical densities for P2.17.

5.2.2. Design and Ultimate Failure of ProDOT-EDOT/Ph Systems

Unexpectedly, a broad distribution of energy transitions across the visible did not develop upon break-in for P2.17. To achieve a visibly broad absorption towards enhancing black (or dark)-to-transmissive ECPs, a new route needed to be investigated. P2.17 may not have been able to yield the desired optoelectronic results because of the ability for sulfur and oxygen atoms to interact, making a uniform extent of conjugation leading to a narrow absorption spectrum. The design of ProDOT-EDOT/Ph systems sought to break up the extent of conjugation along the backbone, giving a random distribution of short to long runs of conjugation and in theory, give a broader neutral state spectrum by absorbing more high energy light, producing brown or near black-to-transmissive ECPs without

acceptors. The method is shown in Scheme 5.2.2.1 where the ratio of EDOT and Phenylene were varied in alternation with to a ProDOT monomer. The direct arylation polymerizations forming P2.18-20 were high yielding (> 85 %) after soxhlet.

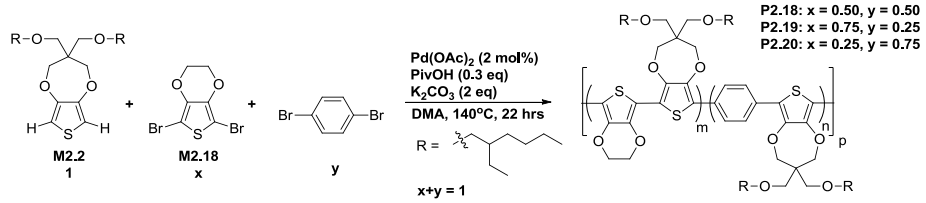

Scheme 5.2.2.1: Method to produce ProDOT-EDOT/Ph polymers and with monomer equivalencies.

Upon electrochemical break-in, the onset of the spectra between the pristine and broken in state redshifted from 1.92 to 1.85 eV for P2.18, 1.88 to 1.78 eV for P2.19, and 1.99 to 1.94 eV for P2.20. The extent of the change between the pristine and broken in state is greatest for P2.19, which has the highest EDOT content, while the least change is observed for P2.20 due to high phenylene content, preventing backbone relaxation minimizing development of low energy transitions. Concerning the spectroelectrochemistry of Figure 5.2.2.1, all polymers exhibit the trend that as oxidation progresses, there is a shift towards intermediate spectra at shorter wavelengths in the visible. This is due to the oxidation of ProDOT-EDOT runs before ProDOT-Ph due to the large difference in oxidation potential.

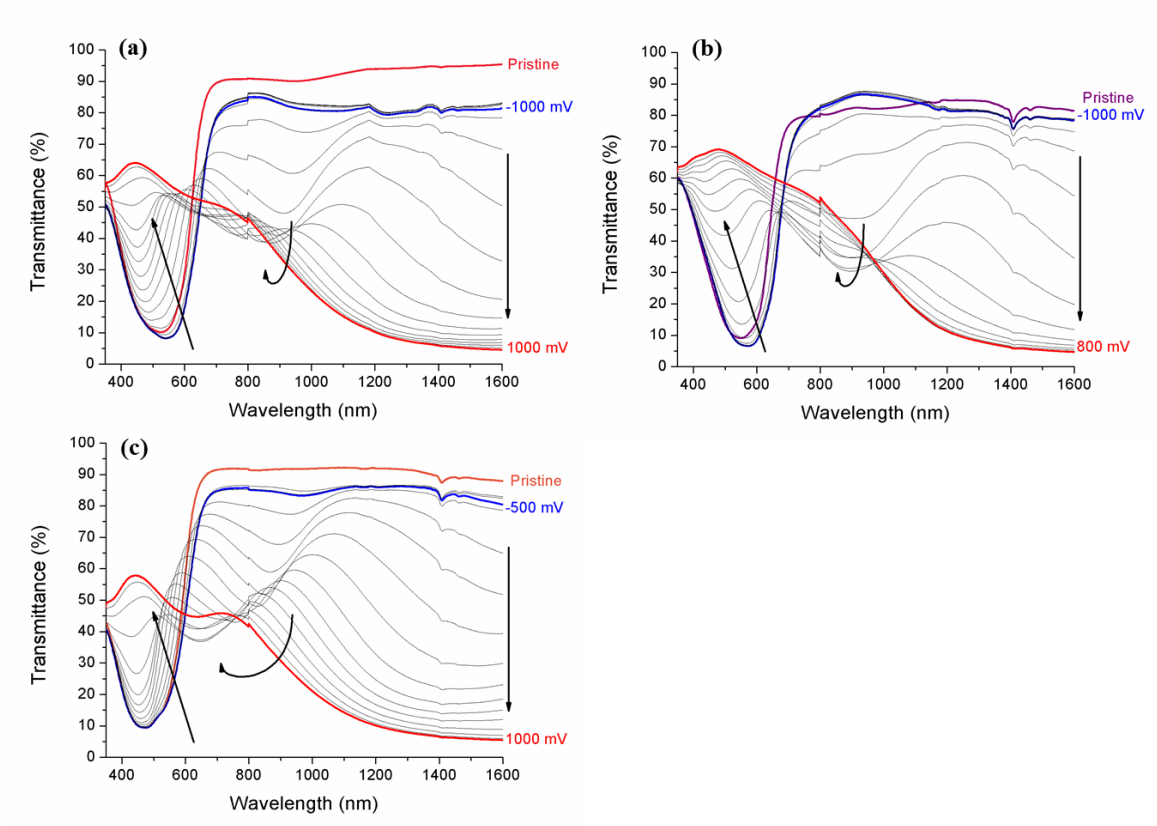

Figure 5.2.2.1: Spectroelectrochemistry of ProDOT-EDOT/Ph polymers including pristine states for P2.18 (a), P2.19 (b), and P2.20 (c). Arrows dictate the transition of spectra upon voltage changes.

Unfortunately, P2.18-20 exhibit rather poor contrast at the λ_{max}. The Δ%T for each polymer at their own λ_{max} is as follows: P2.18 with 50% at 542 nm, P2.19 with 57% at 570 nm, and P2.20 with 47% at 471 nm. P2.19 is able to achieve the greatest contrast due to high content of sterically relaxed and electron rich EDOT while P2.20 exhibits the poorest contrast because of the high level of randomly dispersed phenylenes which, as we learned in Chapter 4, introduce a higher degree of strain and twisting in the backbone, making it difficult to achieve uniform delocalization of charge carriers leaving much absorption tailing into the visible giving it significant residual color as exemplified in Figure 5.2.2.2b. A similar phenomenon was observed for P2.5 in Chapter 4.

The spectra of these random copolymers are broad but unfortunately, not sufficient to produce black or brown neutral state colors and demonstrating unwanted degrees of color

saturation which is evident from the L*a*b* track and photographs in Figure 5.2.2.2b and Figure 5.2.2.3. The addition of phenylenes randomly and at different contents for each polymer do allow the materials to absorb more short wavelength light but comparing P2.19 to P2.11, at the cost of long wavelength absorption. However, comparing P2.20 to P2.1, P2.20 with random incorporation of EDOT affords much more absorption of longer wavelengths of light.

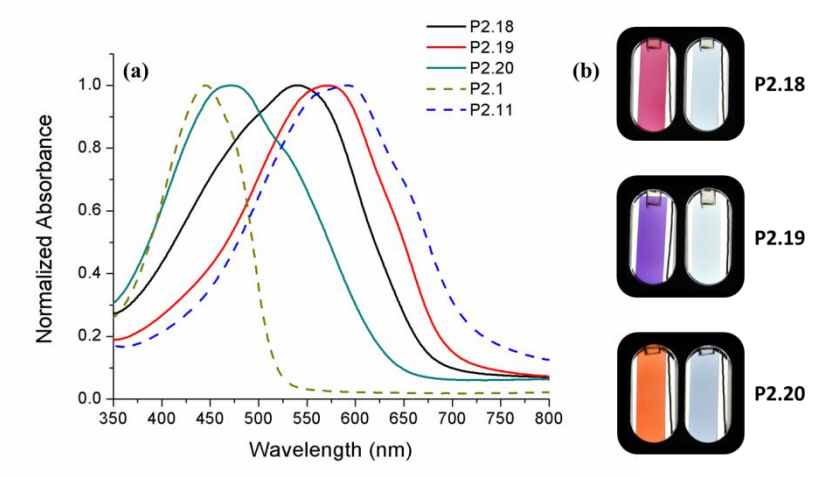

Figure 5.2.2.2: Normalized spectral comparison between P2.18-20 with P2.1 and P2.11 as standards due to alternating backbones of ProDOT-Ph or ProDOT-Ph respectively (a). Extreme state photographical comparison (b).

An interesting artifact in the colorimetry can be connected to the spectroelectrochemistry. As the random copolymers are gradually oxidized, the subsequent intermediate spectra occur at shorter wavelengths. This loss in long wavelength absorption transitions give rise to the strongly pronounced “loop” in the color track where there is a maintenance of high b* values which is eventually suppressed at higher voltages when the random lengths of ProDOT-Ph’s (which give rise to short wavelength transitions) are oxidized.

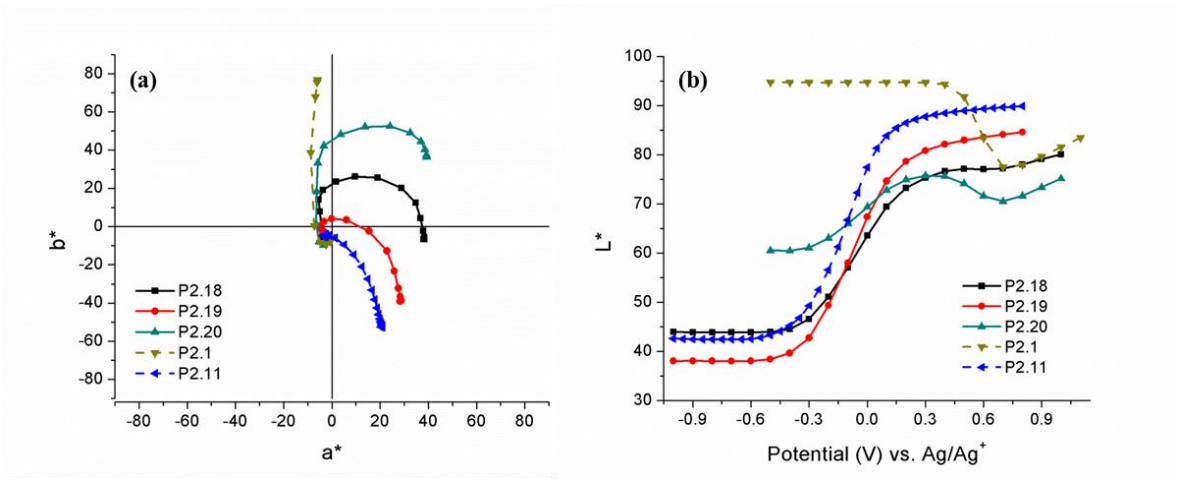

Figure 5.2.2.3: Colorimetric comparison in a*b* (a) and L* (b).

5.3. Summary of All Donor ECPs

The use of controlled torsional strain or relaxation along the conjugated backbone results in an induction of short wavelength (high energy) transitions or long wavelength (low energy) transitions respectively. In section 5.1 several alternating, all donor copolymers were produced in an effort to control color based on steric interactions. These polymers exhibited changes in contrast that were greater than 70 % at their λ_{max} except for P2.15. The ECPs with the most desirable electrochromic properties were P2.12 and P2.13 where P2.12 gave a vibrant blue-to-transmissive color change with no acceptor and P2.13 gave a truer magenta-transmissive switch. The magenta color of P2.13 is closely related to the Munsell definition of magenta, allowing for more accurate color mixing in ECDs and this color was not lost upon break-in. P2.12 achieves color properties very similar to ECP-Blue but without using an acceptor and because of this, it has a much higher level of transmittance at lower voltages.

The structure-property relationships gained from P2.10-16 were used in an attempt to obtain more broadly absorbing, high contrast ECPs with the ultimate goal of attaining an all-donor black or brown (in essence dark, noted by low L*) colored ECPs as the acceptor moieties are believed to cause the poor contrast in ECP-Black. A ProDOT-

AcDOT/EDOT system (P2.17) was developed with the idea of deploying random all donors to give a broad distribution of absorbance transitions with what were hoped to be exceptionally transmissive oxidized states. Though a highly transmissive oxidized state was achieved, the backbone was unable to acquire the desired broad absorption. In an attempt to broaden the spectra by breaking up the extent of conjugation, building higher energy absorption transitions to produce black or brown ECPs, ProDOT-EDOT/Ph systems (P2.18-20) were synthesized and characterized. These did give broader absorptions, but there still remained high degrees of color saturation with poor transmittance when oxidized due to the randomly dispersed phenylenes rings. It appears that acceptors are necessary for broadly absorbing black-to-transmissive ECPs and augmentation of the acceptor is needed to improve contrast.

CHAPTER 6

BROADENING THE PAINTERS PALETTE

As demonstrated in Chapter 5, the ProDOT-AcDOT/EDOT (P2.17) and ProDOT-EDOT/Ph (P2.18-2.20) polymer systems gave too narrow of absorptions to improve upon black-to-transmissive ECPs. We learned that donor-acceptor interactions are required at the same time to give sufficient long wavelength or low energy absorption transitions needed to access broad neutral state spectra. The donor-acceptor interactions however, give reduced transmission when fully oxidized when compared to all donor composed polymers. Thus, Chapter 6 develops the use of a relaxed donor-acceptor motif and the modulation of strain to improve the contrast of the fully oxidized states in broadly absorbing ECPs.

6.1. Catching Higher Energy Light for a Broader Spectrum

ECP-Black[42] and the previously reported black-to-transmissive ECP produced by Beaujuge *et al* (dubbed Inky-Black)[51] as discussed in Chapter 5 and shown in Figure 6.1.1, demonstrate low contrast during electrochromic switching due to significant absorption of the fully oxidized states tailing into the long wavelength portion of the visible. This tailing gives transmissive state color values of L*= 84, a*= -5, b*= -5 for ECP-Black (Figure 6.1.1a) and L*= 85, a*= -5, b*= -5 for Inky-Black (Figure 6.1.1b) (films cast at ~1.0 *a.u.*). These both also exhibit rather weak absorption of short wavelength light in the neutral state, imparting them with a subtle blue hue as noted by the color values of L*= 47, a*= 3, b*= -14 for ECP-Black (Figure 6.1.1a) and L*= 45, a*= 0, b*= -18 for Inky-Black (Figure 6.1.1b). This section concerns a method of increasing torsional strain along the backbone to capture this unabsorbed blue light to increase the overall contrast across the visible.

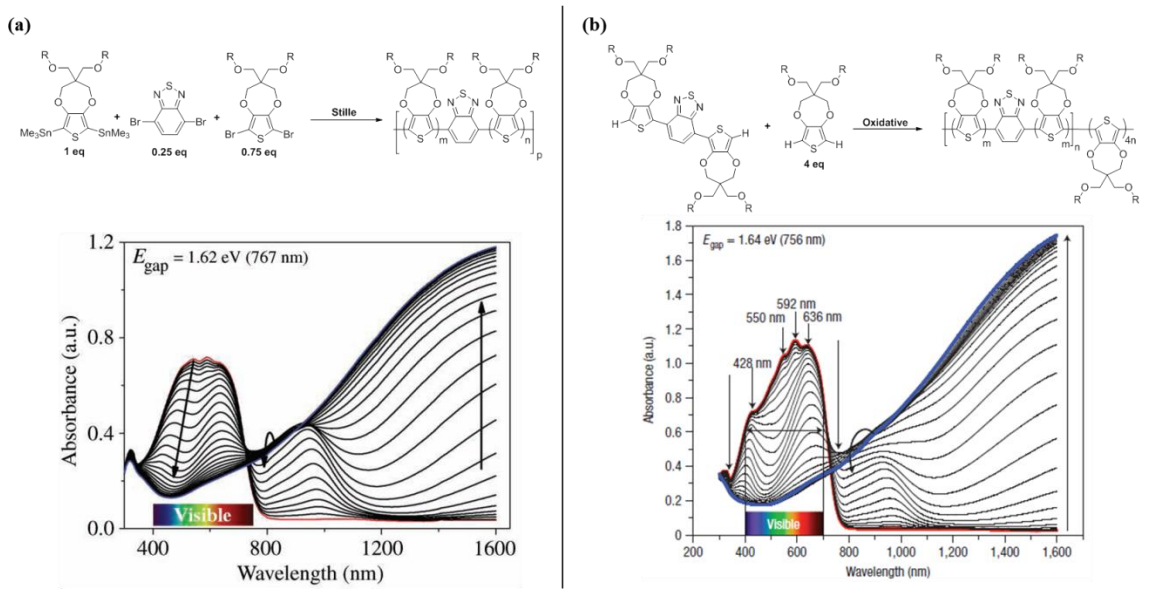

Figure 6.1.1: Polymer structure, polymerization scheme (top), and specEchem (bottom) for ECP-Black formulated by Pengjie Shi (a)[42] and Inky-Black prepared by Pierre Beaujuge (b).[51] Where R= 2-ethylhexyl.

6.1.1. Introducing Strain to Absorb High Energy Light

To increase the overall contrast, I sought to adopt Dr. Shi's synthetic method as it gave polymers with a more even absorption across the visible. Using this method and gradually increasing steric strain along the back bone relative to ECP-Black allows the absorption of the blue light that was not captured in the structures mentioned previously. This was accomplished with the synthesis of the P2.21 and P2.22 shown in Scheme 6.1.1.1 where strain was increased *via* AcDOT incorporation.

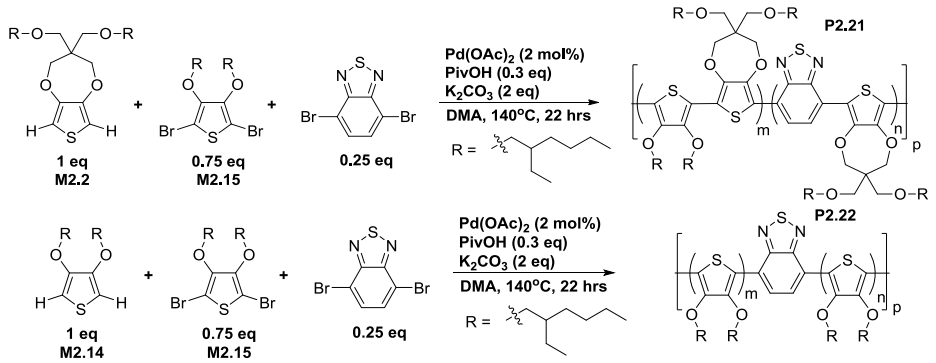

Scheme 6.1.1.1: Polymer structures with increased strain for shorter wavelength light absorption.

Upon electrochemical break-in, P2.21 and P2.22 exhibit notable differences in their redox properties. P2.21 is able to be broken in with little issue within 5-6 cycles, exhibiting good stability. P2.22 however, requires extensive cycling to completely break-in the film evenly across the electrode surface (> 25 cycles). This is demonstrated in Figure 6.1.1.1b where there is a progressive growth in the current with each cycle. Due to the increased strain from all AcDOT incorporation in a random copolymer with BTD, P2.22 has a higher oxidation potential relative to P2.21 as shown by the DPV curve in Figure 6.1.1.1c and d. Because of the poor electrochemical characteristics, P2.22 already does not appear to be a viable system for improvement.

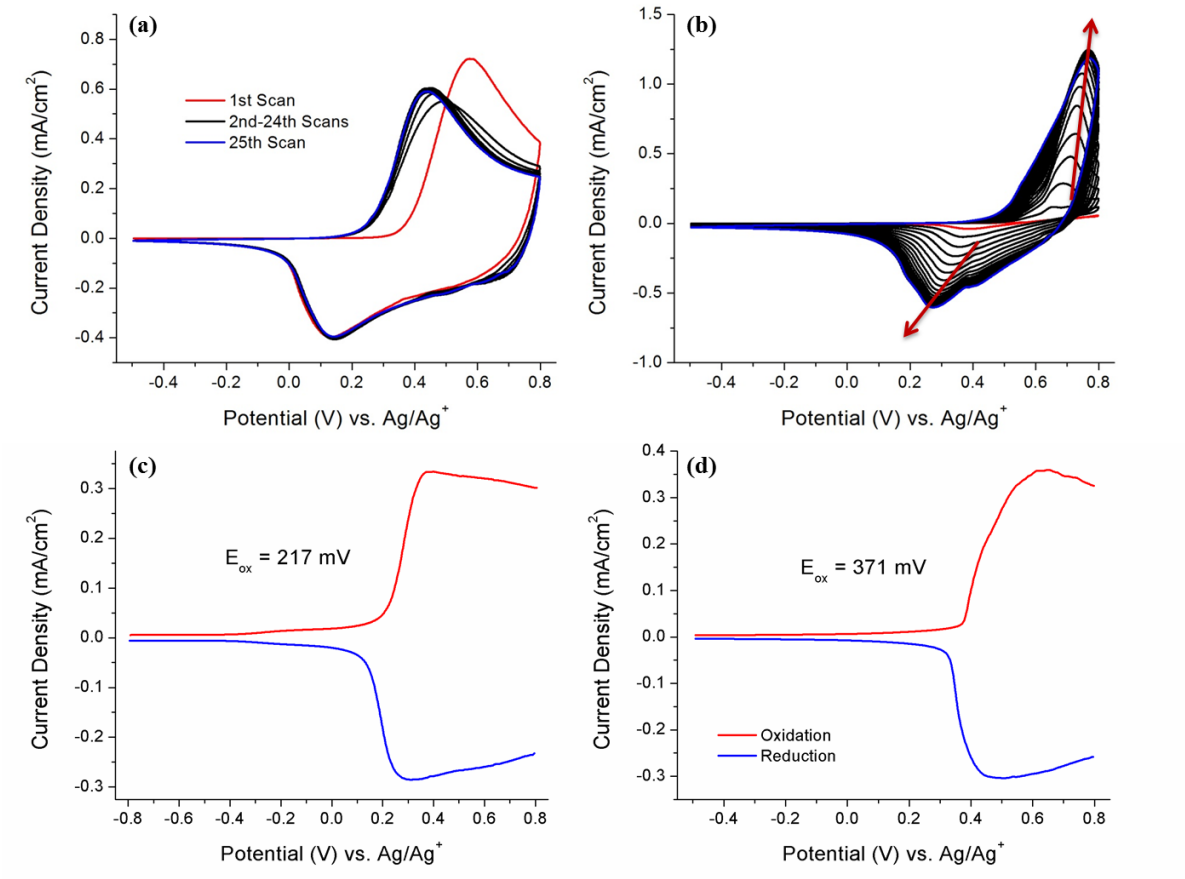

Figure 6.1.1.1: Break-in CV curves for P2.21 (a) and P2.22 (b), where the arrows show the progression of current growth and DPV curves for P2.21 (c) and P2.22 (d) with oxidation potentials (E_{ox}) inset.

Films of P2.21 and P2.22 exhibit minimal red-shifting of the absorption onsets upon break-in where the pristine and broken states shift from 1.64 to 1.60 eV for P2.21 and 1.75 to 1.71 eV for P2.22 respectively. P2.22 has a considerably higher energy onset due to the strain from all AcDOT moieties. Looking to the spectroelectrochemistry in Figure 6.1.1.2, P2.21 demonstrates an even absorption across the visible while P2.22 exhibits a dual band absorption with peaks at 434 and 602 nm and a trench at 526 nm. Films of P2.22 also showed a degree of cracking and hazing, and thus scattered light, upon repeated cycling, owing to the increase in absorption from 780 to 1600 nm.

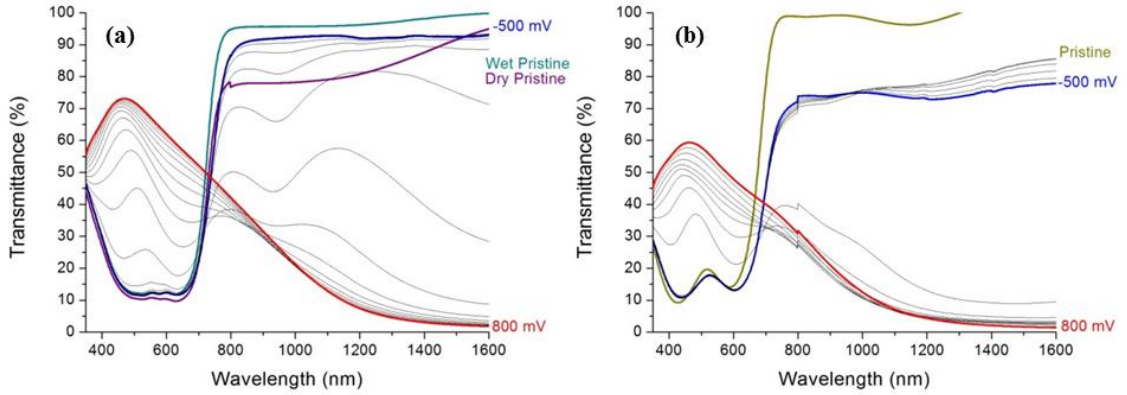

Figure 6.1.1.2: Spectroelectrochemistry of P2.21 (a) and P2.22 (b). Films sprayed to ~1.0 *a.u.*

Both polymers switch from dark neutral to transmissive oxidized states at low voltages (< 900 mV) but P2.22 exhibits poor switching stability over time. When comparing the integrated Δ%T (Δ%T_{int} across the visible: 380-780 nm), P2.21 has a higher contrast with a value of 39.1 % while P2.22 shows a lower contrast across the visible with a Δ%T_{int} of 22.6 %. This low contrast is a result of high steric strain preventing adequate delocalization of charged states, giving a significant degree of residual absorption in the visible portion of the fully oxidized state spectrum, severely reducing contrast upon switching. Compare these with the Δ%T_{int} for ECP-Black shown above, 34.2 %. By subtly increasing the strain in the form of AcDOT, the contrast across the visible exhibited a minor improvement of 4.9 % with P2.21. This overall enhancement of contrast is exemplified in Figure 6.1.1.3. We can see that the increase in strain has led to the higher contrast by absorbing more high energy visible light, making P2.21 appear blacker to the eye (supported by Figure 6.1.1.3b), evidenced by a*b* values that are closer to the origin and with a lower L*. For P2.22, the dual band absorption with a trench at 526 nm imparts the polymer with an unsaturated pale green color. Both ECP-

Black and P2.21 have similar oxidized state spectral profiles, which leads to color vales that are nearly identical.

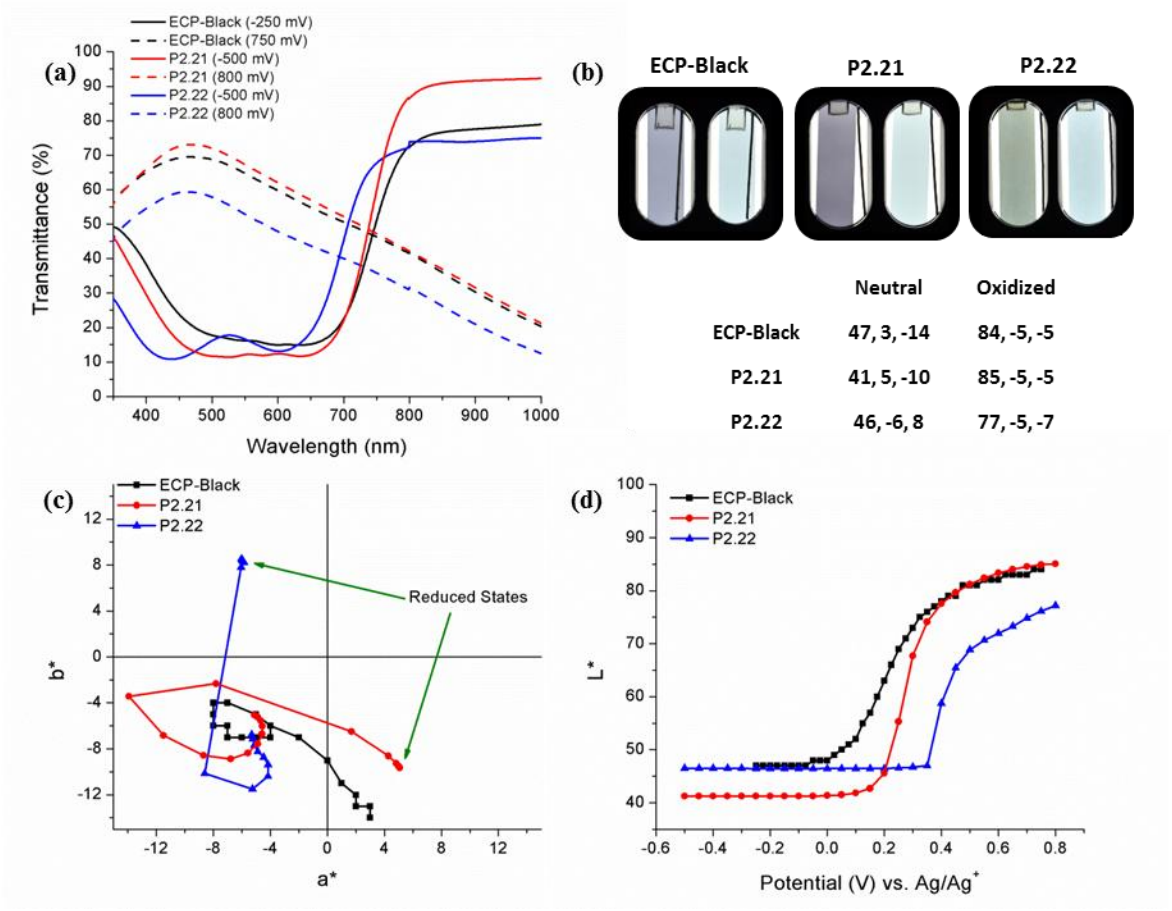

Figure 6.1.1.3: Spectral comparison of the extreme states for black ECPs (a). Photographical comparison between black ECPs (b), a*b* colorimetric comparison (c), and L* comparison (d).

Though the subtle increase in strain with P2.21 has improved contrast relative to ECP-Black through absorbing more short wavelength visible light, the limit to contrast still appears to be the current acceptor architecture and steric tuning alone of the main chain DOTs will not complete the augmentation.

6.2. Relaxation Modification to the Acceptor

Based on a report concerning the synthesis and characterization of green-to-transmissive ECPs,[50] it was noticed that by flanking a BTD acceptor with sterically relaxed EDOT, high electrochromic contrast was achieved at the peak of a dual band absorption that is the result of donor-acceptor charge transfer interactions. In this section we will explore this EDOT flanked BTD acceptor (EDOT-BTD-EDOT, EBE) and the trimer incorporation into random copolymers to improve the contrast of black-to-transmissive ECPs. The general method of producing these polymers is shown in Scheme 6.2.1 where x and y represent the starting monomer ratios and m & n describe random lengths of DOTs in the final polymer structure. The blue or green DOT balls can be either ProDOT or AcDOT but color only notes a difference.

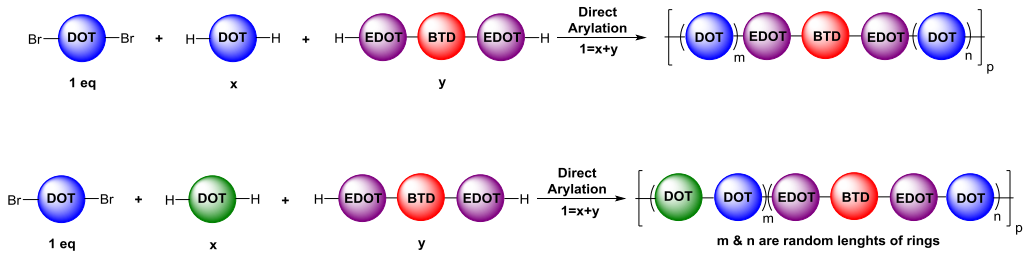

Scheme 6.2.1: General polymerization scheme to produce new broad absorbers using relaxed donor-acceptors.

Using EBE, we ensure that the BTD acceptor will always be flanked by the less torsionally strained EDOTs in random copolymerizations. It is believed that once fully oxidized, this would allow greater planarization, improving delocalization of charge carriers, giving higher transmittance to the oxidized forms. The EBE (monomer M2.20) trimer was synthesized using direct arylation coupling methods followed by purification using sublimation and washing the resulting red solid with methanol. The relaxed donor-acceptor monomer was used in 0.25 equivalencies while only tuning the strain of the DOTs during polymerization; increasing strain *via* raising AcDOT content from P2.23 to P2.25 to P2.24. Then with strain fixed, polymerizations were conducted where the equivalencies of EBE was increased from 0.25 to 0.35 starting from P2.25 to P2.26 to

P2.27. The final structures are shown in scheme 6.2.2 (specific schemes used can be found at the end of Chapter 2).

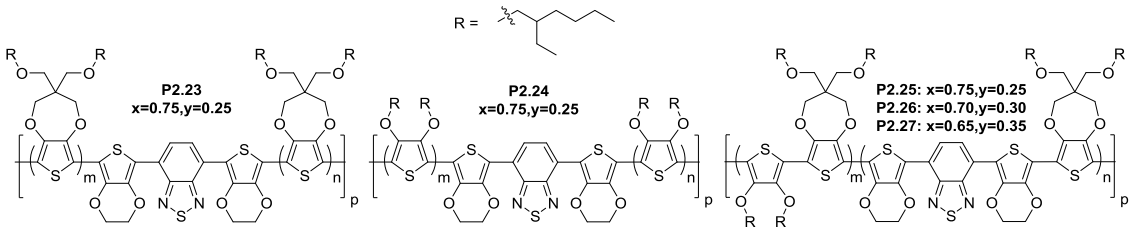

Scheme 6.2.2: Polymers to produce new broad absorbers using relaxed donor-acceptors.

The steric interactions were tuned to broaden the overall neutral state spectrum in the following manner: the steric strain in the backbone of the random copolymers increases from P2.23 to P2.25 to P2.24 from increasing AcDOT content. In solid films, these polymers produce dual band absorptions where the D-A peak was relatively fixed and the π to π* peak was moved to shorter wavelengths with increasing backbone strain from AcDOT. To examine the effect of the relaxed EBE on the neutral and most oxidized state spectrum, the content of EBE was steadily increased from P2.25 to P2.26 to P2.27 (0.25 to 0.30 to 0.35 equivalencies respectively). This change in strain and then EBE content is illustrated in Figure 6.2.1. Because P2.25 was able to absorb the most light across the visible spectrum with the highest contrast, this ProDOT-AcDOT/EBE architecture was used to measure changes in EBE content. To easily compare optoelectronic properties of these polymers, their relevant data has been compiled into Table 6.2.1.

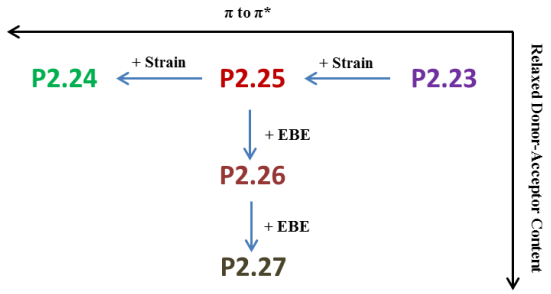

Figure 6.2.1: Model to produce broad absorbers with higher contrast through increasing steric strain and then increasing relaxed donor-acceptor content.

Table 6.2.1: Optoelectronic properties of each polymer in the series. For films sprayed to an optical density of ~1.0 *a.u.*

Polymer	π to π^* Peak (nm)	D-A peak (nm)	E_{onset} (eV), Pristine	E_{onset} (eV), Broken in	Integrated Contrast (%)[a]
ECP-Black	--[b]	--[b]	---[c]	1.61	34.2
P2.23	543	675	1.59	1.50	52.8
P2.24	457	674	1.47	1.45	45.6
P2.25	505	671	1.54	1.50	51.0
P2.26	495	677	1.50	1.49	51.2
P2.27	487	680	1.49	1.48	51.7

[a]$\Delta\%T_{int}$ across 380-780 nm. [b]634 nm for ECP-Black λ_{max}, peaks are not resolved in this spectrum, see Figure 6.1.1a. [c]ECP-Black exhibited no changes upon break-in.

6.2.1. Electrochemical Break-in and Behavior

The polymer films all demonstrated reversible break-in cycling with electrochemical differences between the first and second scan, stabilizing over subsequent scans as shown in Figure 6.2.1.1. Exploring the oxidation potential onsets *via* DPV (see Chapter 3 for details) in Figure 6.2.1.2 gave an increasing trend of 13 mV to 110 mV to 180 mV for P2.23 to P2.25 to P2.24 respectively which correlates to lower strain to higher strain. As the content of relaxed acceptor was increased there was a decrease in oxidation potential from 110 mV to 50 mV to -45 mV for P2.25 to P2.26 to P2.27 respectively and is attributed to increasing EDOT content.

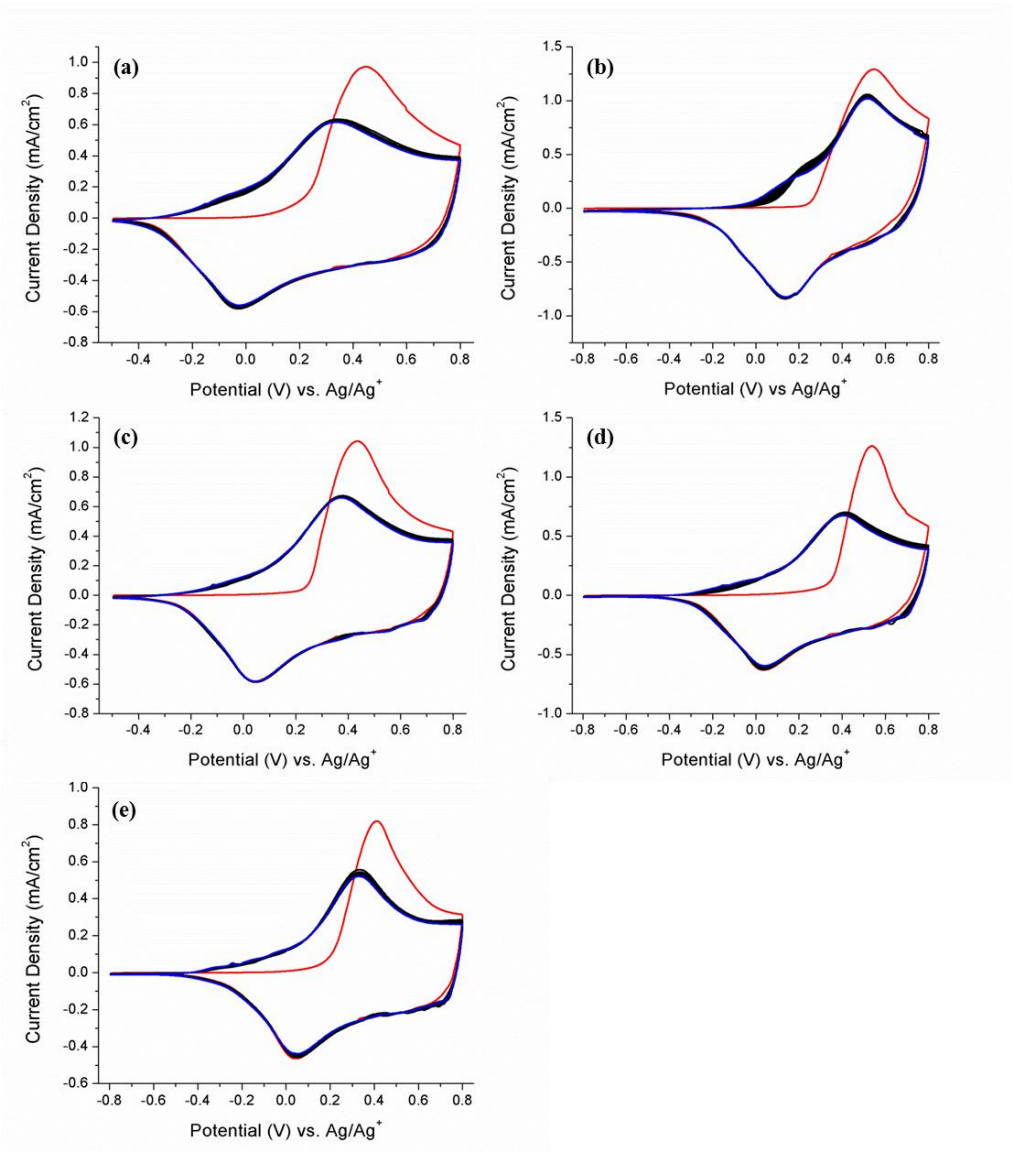

Figure 6.2.1.1: Break-in CV for all polymers. 1st cycle (red), 2nd-24th cycles (black), and 25th cycle (blue). P2.23 (a), P2.24 (b), P2.25 (c), P2.26 (d), P2.27 (e).

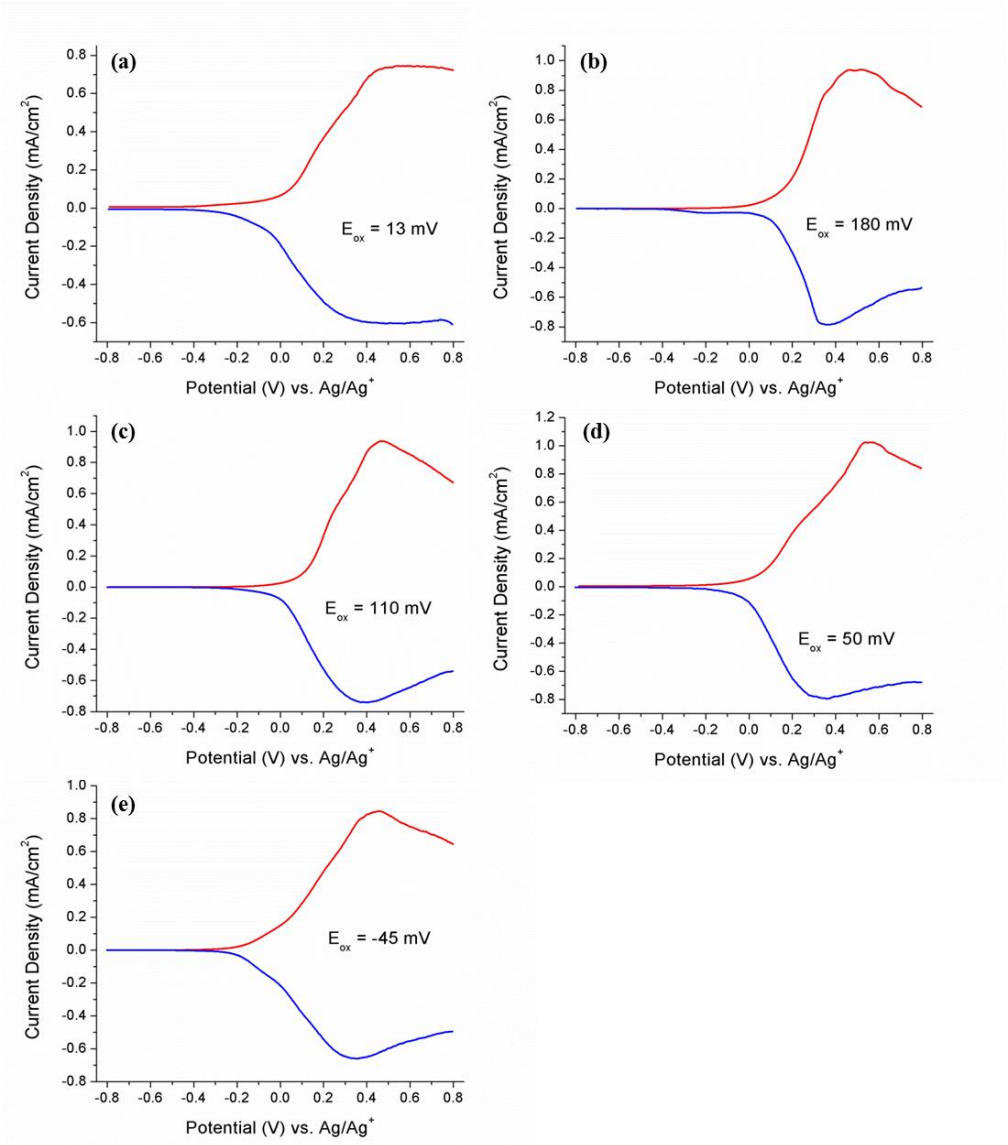

Figure 6.2.1.2: DPV curves for all polymers. Oxidation (red) from low to high potentials and reduction (blue) from high to low potentials. P2.23 (a), P2.24 (b), P2.25 (c), P2.26 (d), P2.27 (e).

With a relaxed acceptor architecture of BTD flanked by EDOTs, lower onsets of absorption are achieved that are ~0.10 eV less than ECP-Black. As the films were electrochemically conditioned for break-in, there was a slight change in the spectra upon going from the pristine to broken in states, as shown in Figure 6.2.1.3. The shorter wavelength peak corresponding to the π to π* transition exhibits minimal change upon break-in except for an increase in intensity seen with P2.23. For the lower energy peak

attributed D-A CT interactions however, there is a redshift in the onset of absorption as well as a slight increase in intensity, absorbing longer wavelength light. Changes upon break-in are minimized with increasing strain. As strain increases from P2.23 to P2.25 to P2.24, the band gap change from break-in is reduced respectively and as the relaxed acceptor content is raised from P2.25 to P2.26 to P2.27, the onset changes minimally. When dry films are cast and then immersed in electrolyte, there is a decrease in absorption intensity likely due to index matching. Then, the as sprayed or dry pristine intensity is regained upon break-in; this does not occur in ECP-Black. The changes between the pristine and broken-in spectra are likely due to backbone reorganization in the form of relaxation from the added EDOTs flanking the acceptor. This is supported by the changes in CV cycles 1 and 2 in Figure 6.2.1.1, a similar effect discussed in Chapter 5.1.

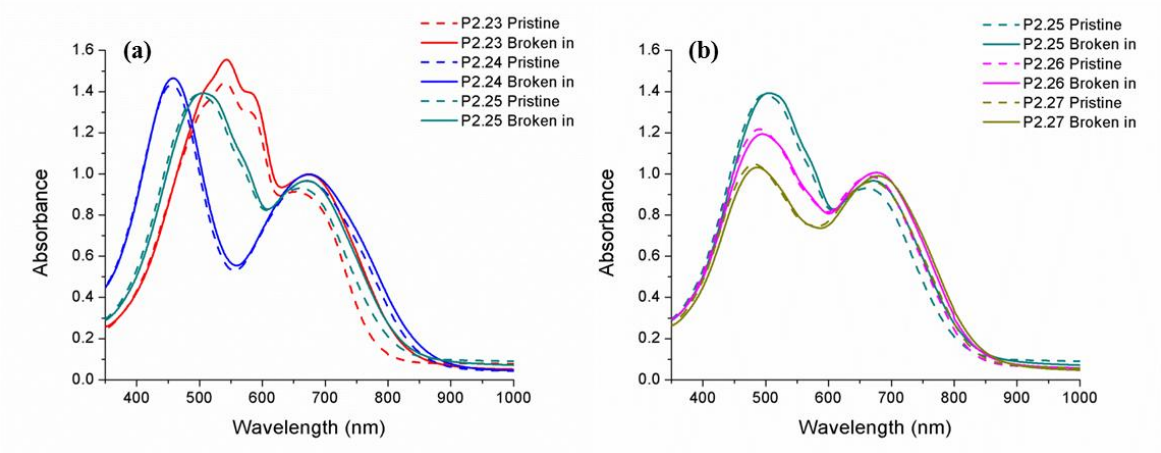

Figure 6.2.1.3: Spectral differences for films between the electrolyte wetted pristine and broken in states. Polymers where π to π* was tuned (a) and where content of relaxed D-A was varied (b). Films sprayed to ~1.0 *a.u.*

6.2.2. Spectroelectrochemical and Colorimetric Behavior

With the films broken in, the spectral properties were examined further in Figure 6.2.2.1. The peaks were normalized to the longer wavelength D-A band, as we are concerned with the effect on contrast from relaxed D-A CT interactions even though for most of the polymers, the dominant absorption is at the π to π* transition. From Figure 6.2.2.1a, as steric strain is increased from P2.23 to P2.25 to P2.24, the λ_{max} blue shifts from 543 to 505 to 457 nm respectively with a window of transmission gradually becoming more pronounced with additional strain until the window is positioned at 558 nm for P2.24. In Figure 6.2.2.1b, as the EBE content is increased from P2.25 to P2.26 to P2.27, the high energy peak λ_{max} exhibits a less extensive blue shift from 505 to 495 to 487 nm respectively, but the ratio of the two peaks decreases until being nearly equal (Absorption ratio: π to π*/D-A) from 1.44 (P2.25) to 1.18 (P2.26) to 1.04 (P2.27). P2.27 exhibits shallow dual band absorption with a window at 586 nm. For all of these polymers, the D-A absorption band remains relatively fixed from 671-680 nm.

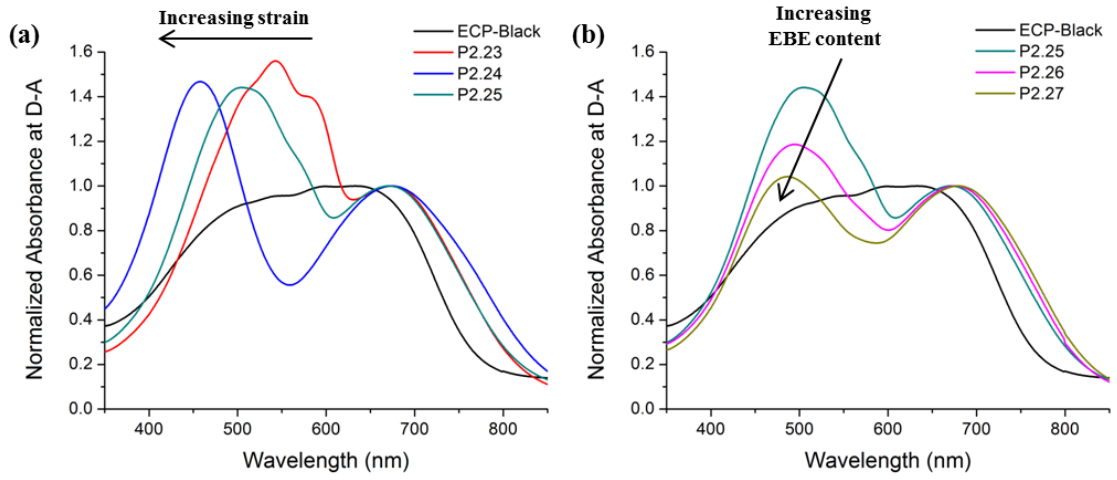

Figure 6.2.2.1: Spectra of broken in films that are normalized at the long wavelength peak with variations of the π to π* transition (a) and the EBE content (b).

Spectroelectrochemistry was performed to examine the electrochromic contrast between the extreme neutral and most oxidized states for P2.23-27 and are presented in Figure 6.2.2.2. In general, at the long wavelength peak (due to D-A interactions), all polymers have fully oxidized states with high transmittance (Δ%T > 50%) with the exception of P2.24, likely due to strain from all AcDOT. However P2.24 exhibits a Δ%T at the long wavelength peak of 44%, still greater than the Δ%T of ECP-Black at 634 nm which is 41%. P2.24 also has the highest transmittance when compared to previously reported green-to-transmissive ECPs.

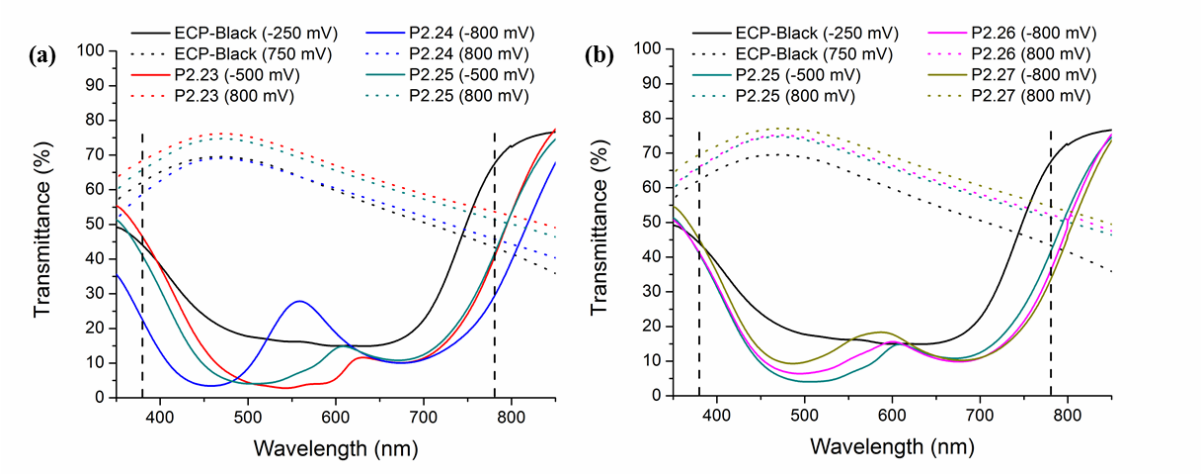

Figure 6.2.2.2: Extreme state spectra for polymers where π to π* was tuned through strain (a). Extreme state spectra for polymers where EBE content was varied (b). Films sprayed to ~1.0 *a.u* and then broken in. Visible range of 380-780 nm is bound by the black dotted lines.

To more accurately quantify the contrast for these broadly absorbing polymers, the Δ%T was integrated across the visible (380-780 nm). The method of using a relaxed donor-acceptor system substantially enhances the overall contrast across the visible relative to ECP-Black, as shown from the calculated values in Table 6.2.1. The values for all polymers with the exception for P2.24, have integrated contrast values ($\Delta\%T_{int}$) > 50%. P2.24 has the lowest integrated contrast possibly due to it having the highest degree of

strain and preventing enhanced delocalization of charged states, analogous to P2.22. It is important to note that as the EBE content in P2.25-P2.27 is increased there is minimal reduction in contrast.

P2.27 absorbs the most evenly across the visible, appearing black-brown to the eye when neutral. When fully oxidized, it exhibits improved transmission over ECP-Black and its full spectroelectrochemical series is shown in Figure 6.2.2.3. The general spectroelectrochemical properties are the same across the family of polymers. As the polymers are progressively oxidized, there is an uneven rate of loss in the intensity of the two peaks present in all polymers as demonstrated by the green spectrum corresponding to 150 mV in Figure 6.2.2.3 where the D-A peak appears to oxidize more rapidly than the π to π^*. This results in a "loop" of color values that will be discussed in colorimetry later. The spectroelectrochemistry for P2.23-26 can be found in Figure 6.2.2.4.

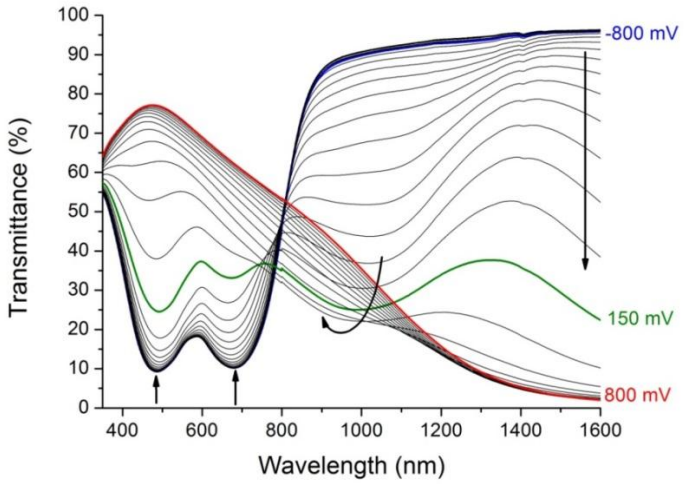

Figure 6.2.2.3: Spectroelectrochemistry of P2.27 where neutral, intermediate and oxidized states are represented by the blue, green, and red traces respectively.

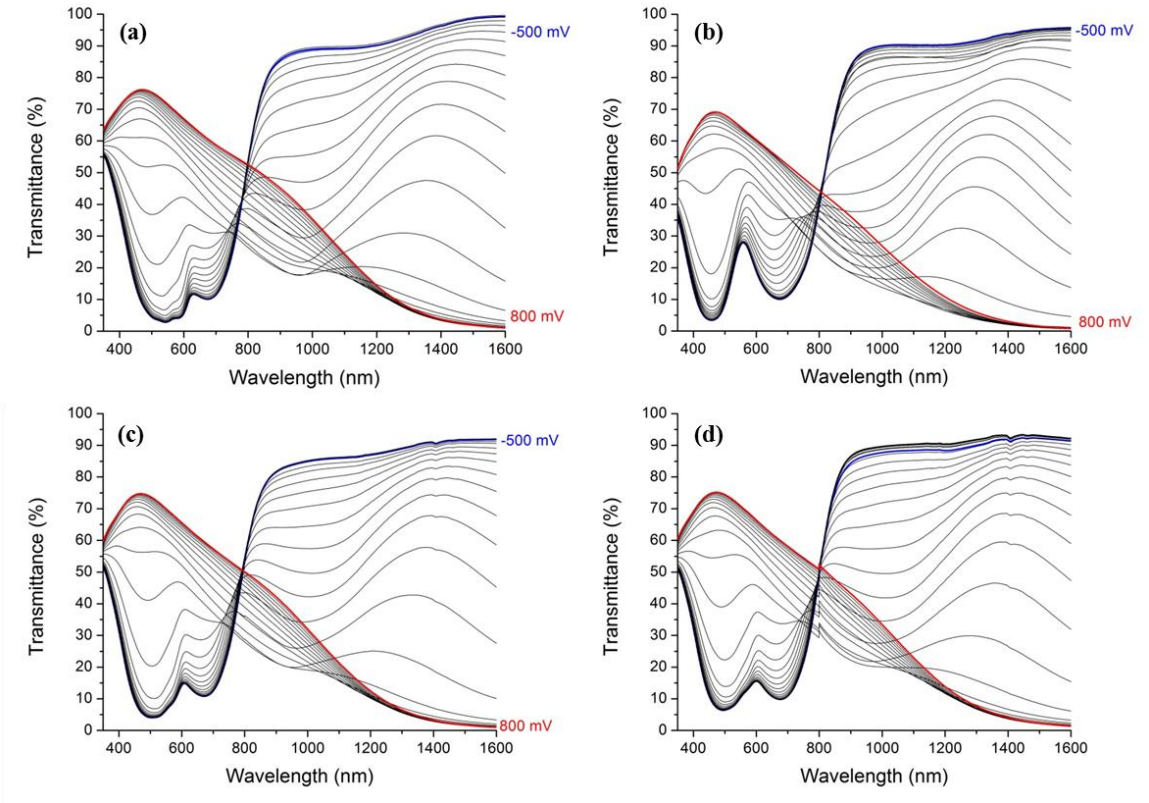

Figure 6.2.2.4: Spectroelectrochemistry of P2.23 (a), P2.24 (b), P2.25 (c), and P2.26 (d).

Though P2.23-27 exhibit improved contrast over ECP-Black, in the oxidized state there is still a considerable degree of visible light absorption tailing from 600-780 nm when compared to all donor polymers. This persistent tailing needs to be addressed in future development of high contrast, broad absorbers.

With respect to switching kinetics, all polymers in this family are able to switch with their highest contrast at the highest speed of 2 seconds. Due to diffusion limiting processes, as the rate of switching increases, there is an overall loss in contrast but is always recoverable at 2 seconds or greater. The chronoabsorptometry for all polymers is shown in Figure 6.2.2.5. The contrast has been enhanced using a relaxed donor acceptor

architecture in random copolymers but, the Δ%T at the D-A peak is less than the higher energy π to π*, a testament to the inability to fully bleach D-A systems.

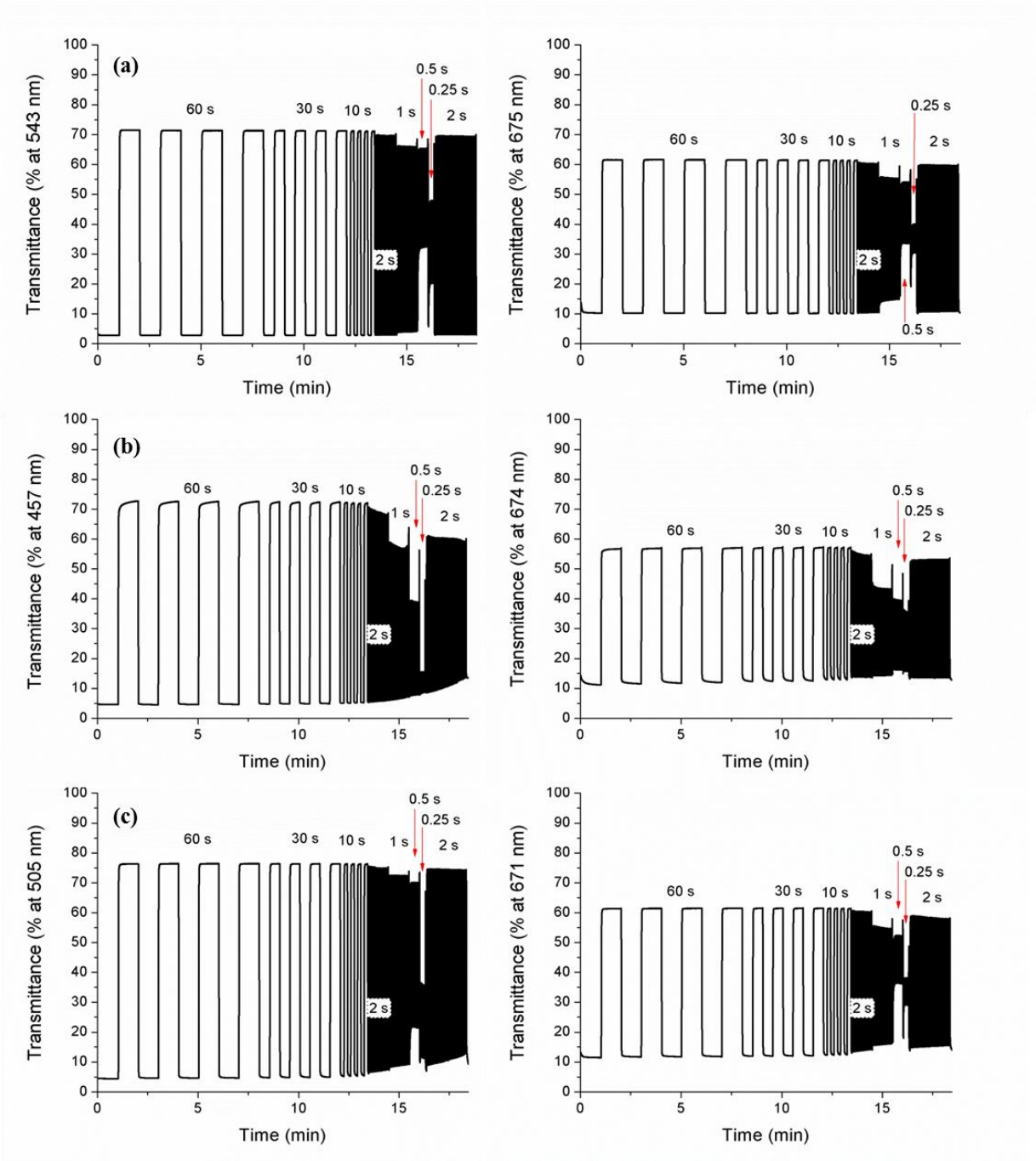

Figure 6.2.2.5: Chronoabsorptometry of P2.23 (a), P2.24 (b), P2.25 (c), P2.26 (d), and P2.27 (e). Plots on left are taken at the π to π* transition while those on left are at the D-A peak.

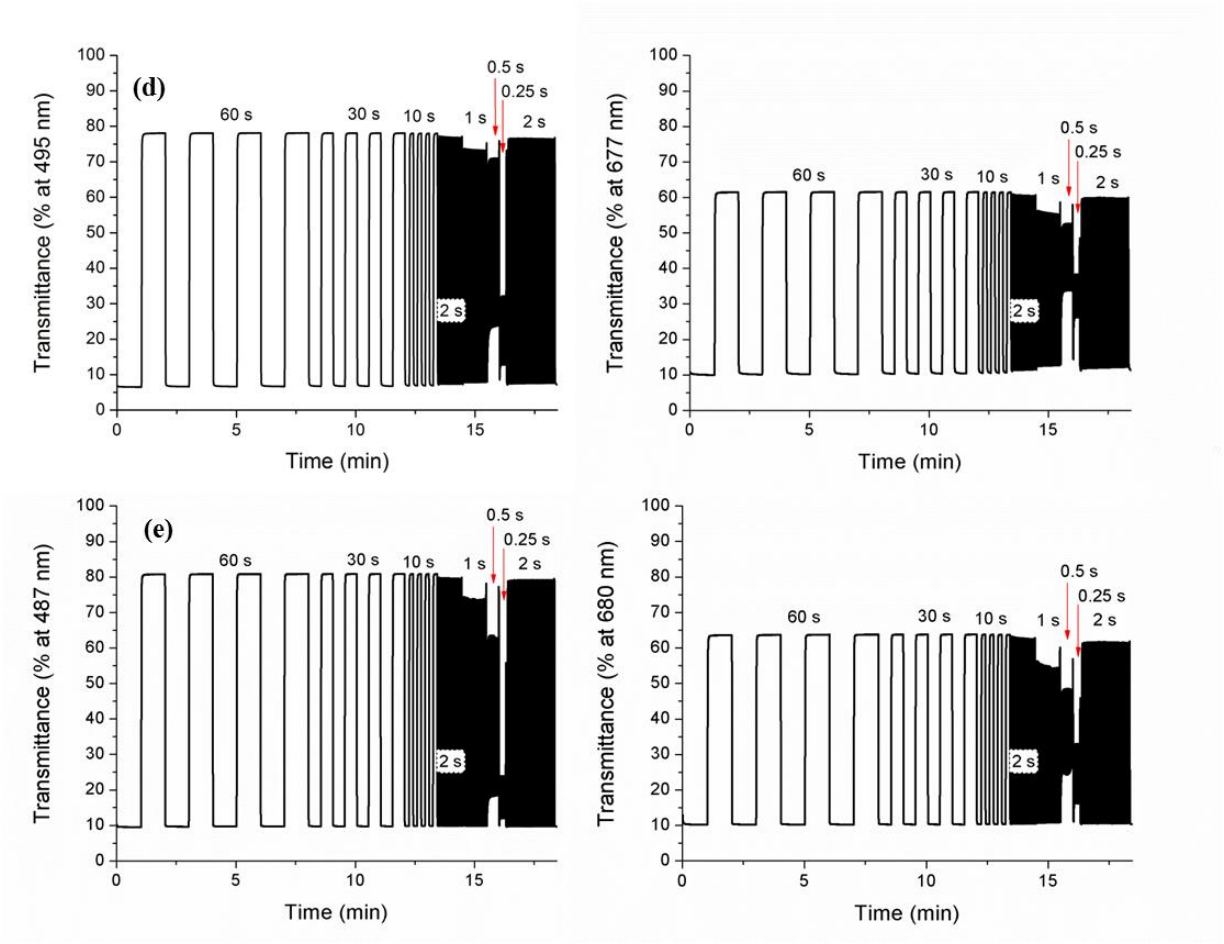

Figure 6.2.2.5: Continued.

6.2.3. Colorimetry

The family of polymers discussed in this section are broadly absorbing and, as such, they have color values that are lower or closer to origin than what has been discussed previously in this dissertation. The family composed P2.23-27 has been able to control color through two routes using a relaxed donor-acceptor to enhance the transmittance of the fully oxidized states, and the color values are presented in Figure 6.2.3.1. In the first route to control neutral state color (a*, b*), it can be tuned through increasing the steric strain of the donors along the main chain from P2.23 (-31, 30), P2.25 (23, -4), to P2.24 (-14, 44). P2.23 has a broad absorption that is centered in the visible spectrum allowing unequal amounts of blue and red (less) light to pass and so it appears purple to the eye.

P2.25 absorbs much of the blue and green light from its short-wavelength positioned π to π* while letting through a portion of red light appearing a dark, brick-red color. Both of these polymers absorb strongly where the $\bar{y}$ standard observer is most stimulated, giving them the lowest L* of the series. Due to their uneven absorption, they possess a degree of color saturation. P2.24, with its highly blue shifted π to π* band absorbs more blue than red light but with a deep window centered at 556 nm, it allows green light to pass. Because it also lets some red light through it gives a lime-green color with a high b* value. Its spectrum is also the reverse of what is observed in previous green ECPs[49,50] where P2.24 has a greater absorbance of short wavelength light than long giving its neutral state color values.

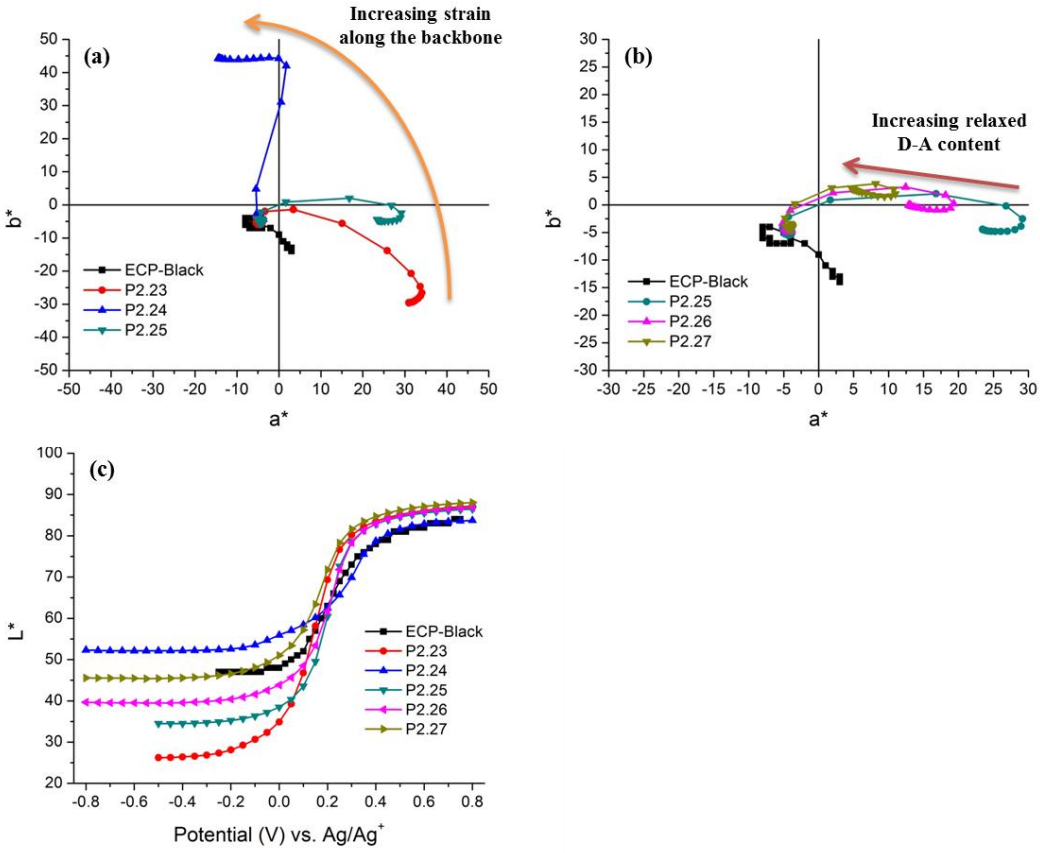

Figure 6.2.3.1: Colorimetry values (a*b*) for relaxed D-A polymers where the π to π* transition was tuned through strain (a) and the relaxed D-A content was varied (b). Lightness values for all polymers in this section (c).

Because P2.25 gave neutral state color values that were closest to the origin with a high contrast across the visible, it was decided to use it as a starting point to study the effect of increasing content of the relaxed donor-acceptor EBE on color and contrast, this is the second route to control color. As the content of EBE is raised from P2.25 (23, -4), to P2.26 (13, 0), to P2.27 (5, 3), the saturation is progressively sapped and the colors become muted. Due to the more even absorption (and shallow window that it ever present in these systems) more light is able to overlap with the $\bar{\mathbf{y}}$ standard observer, raising the lightness. P2.26 now absorbs more red light than P2.25 and so it's a*b* color values decrease over all, putting it within the lower b* region of what Munsell defines as brown, making P2.26, the world's first brown-to-transmissive ECP. Following P2.26, P2.27 absorbs even more red light, reducing the saturation further to appear black-brown. Though it has such low a*b* values, the positive magnitude is a result of residual red and orange light transmitting due to the window at 586 nm. All of the color values at a variety of thicknesses as well as photographs can be found below in Figures 6.2.3.2 and 6.2.3.3 respectively. Before we move on, let's discuss the "loop" that was described earlier concerning the spectroelectrochemistry. This loop can be seen in any of the a*b* color plots in Figure 6.2.3.1a and b or Figure 6.2.3.2 and is a result of the longer wavelength D-A band bleaching faster upon oxidation than the π to π^*. This allows more red light to reach the eye with increasing voltage and so the a* becomes more positive and the polymers go through reddened intermediate states with the exception of P2.24 which passes through a yellow intermediate state because more red light along with green light is stimulating both the M and L cones respectively, making you see yellow.

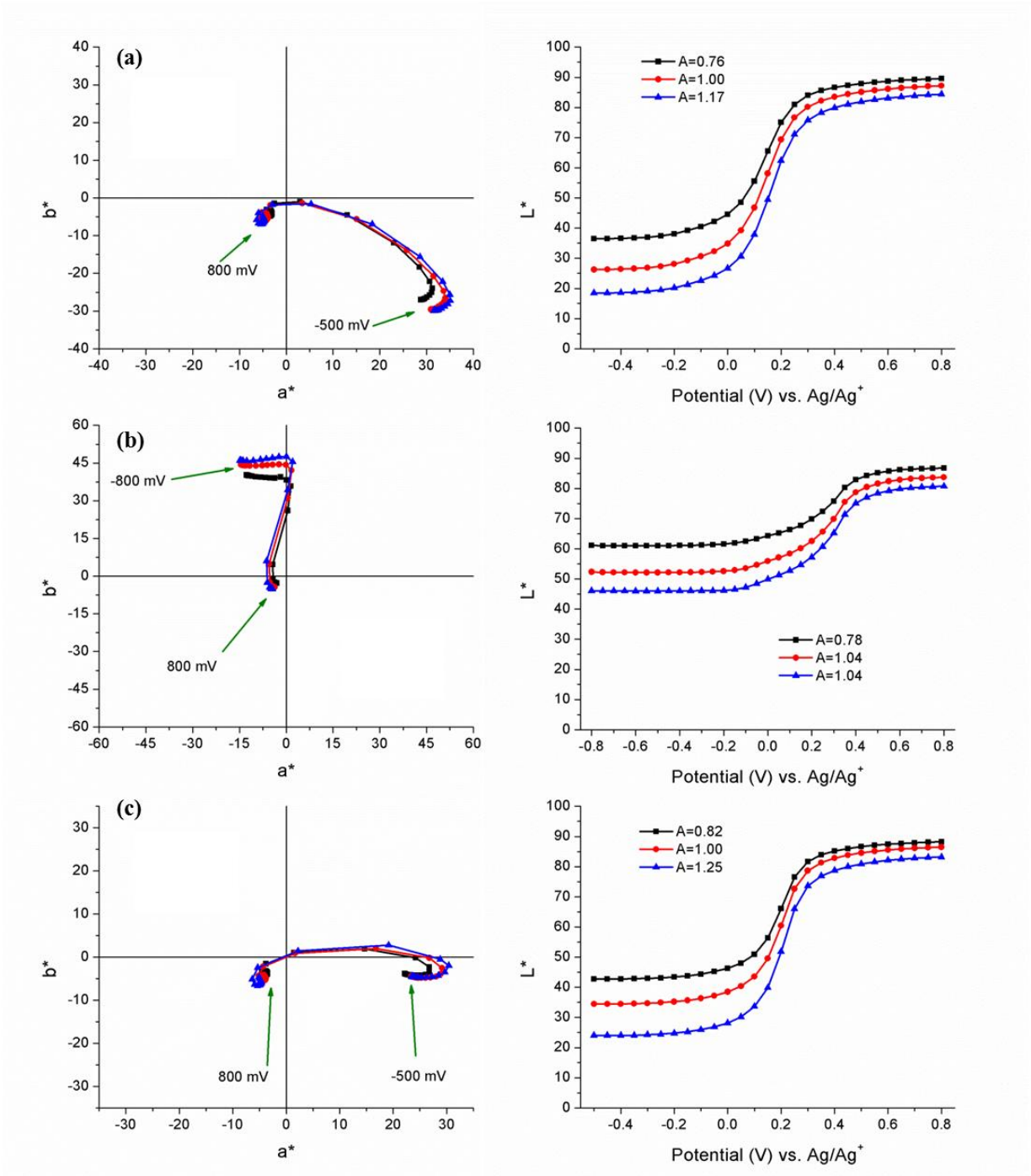

Figure 6.2.3.2: Colorimetry (a*b* values on left, lightness on right) of P2.23 (a), P2.24 (b), P2.25 (c), P2.26 (d), and P2.27 (e).

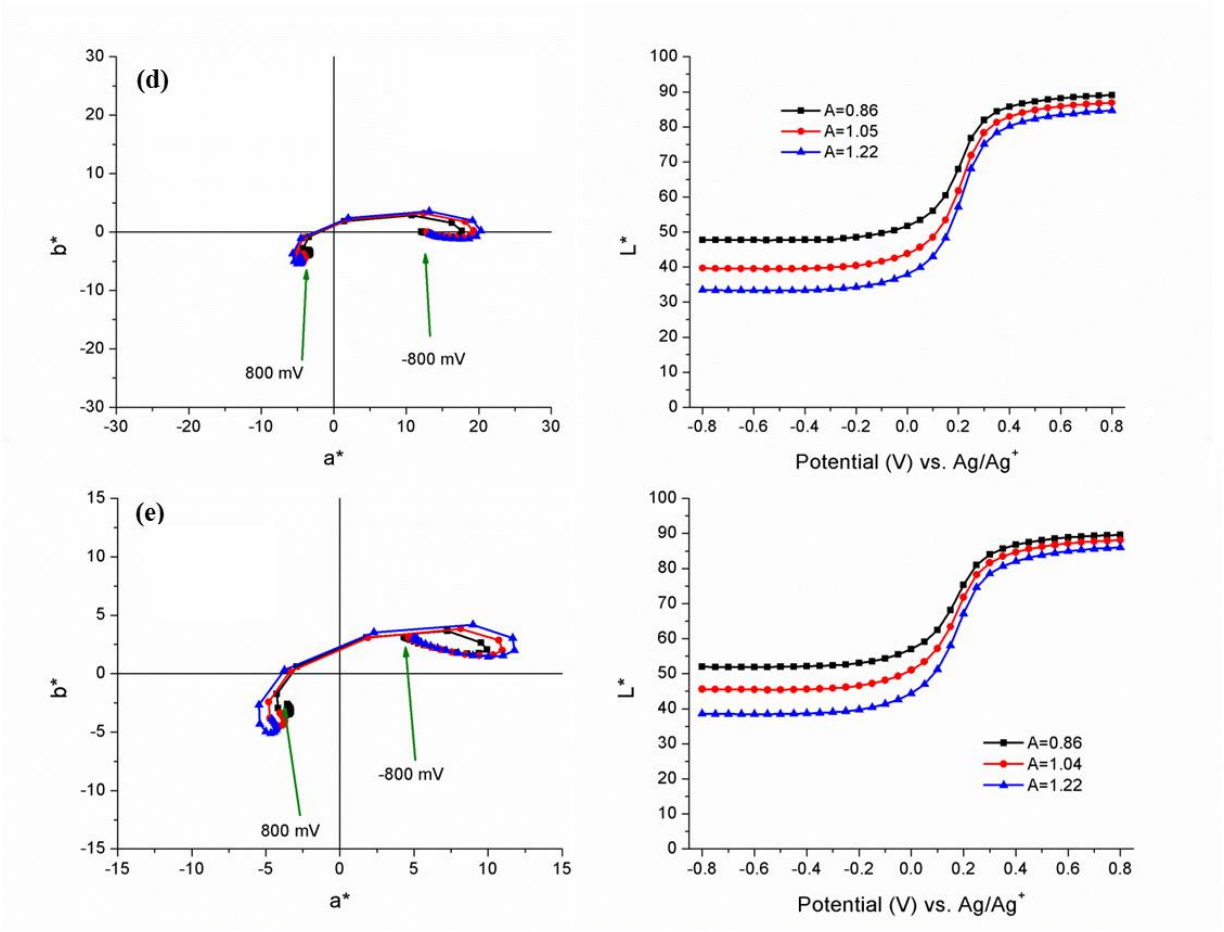

Figure 6.2.3.2: Continued.

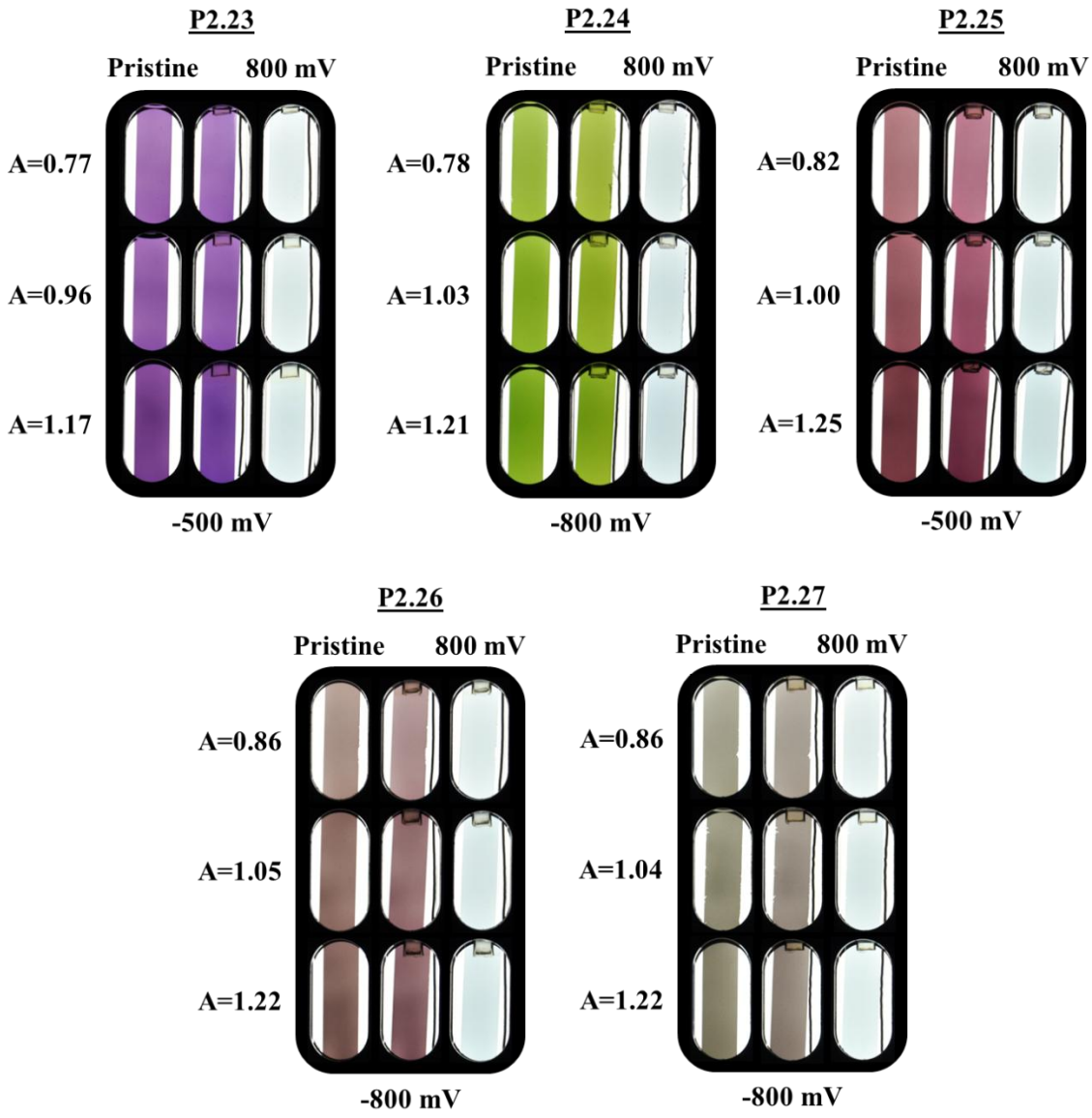

Figure 6.2.3.3: Photography of all polymers at various thicknesses (as measured by difference in optical density, as sprayed).

Looking to Figure 6.2.3.4 we close this section and chapter with a final comparison of the neutral and oxidized state color values. We are able to tune through a variety of neutral color states by manipulating steric interactions then, to reduce saturation by increasing the content of acceptor. As the synthetic ratio of EBE is increased, there is minimal reduction in contrast. But how different are the color values of the fully oxidized

transmissive states, particularly between ECP-Black and P2.27? We can calculate what CIE calls a *just noticeable difference* (JND) in color by determining the distance between color points using Equation 6.2.3.1.

$$\Delta \boldsymbol{E}^{*}_{\boldsymbol{ab}} = \sqrt{(\Delta \boldsymbol{L}^{*})^{2} + (\Delta \boldsymbol{a}^{*})^{2} + (\Delta \boldsymbol{b}^{*})^{2}}$$

Equation 6.2.3.1: Equation to calculate the just noticeable difference (JND) for the human eye between color points.

Where $\Delta \boldsymbol{E}^{*}_{\boldsymbol{ab}}$ represents the JND and studies have found that values or differences in color points below 2.3 mean that it is not noticeable to the eye.[174] Comparing the fully oxidized color states between ECP-Black and P2.27, we calculate a JND of 4.8 so indeed there is a noticeable difference with P2.27 having the least color once fully oxidized.

	ECP-Black	P2.23	P2.24	P2.25	P2.26	P2.27
Neutral Color (L*, a*, b*)	47, 3, -14	26, 31, -30	52, -14, 44	34, 23, -4	39, 13, 0	45, 5, 3
Oxidized color (L*, a*, b*)	84, -5, -5	87, -4, -4	84, -4, -4	86, -4, -4	87,-4, -4	88, -4, -3

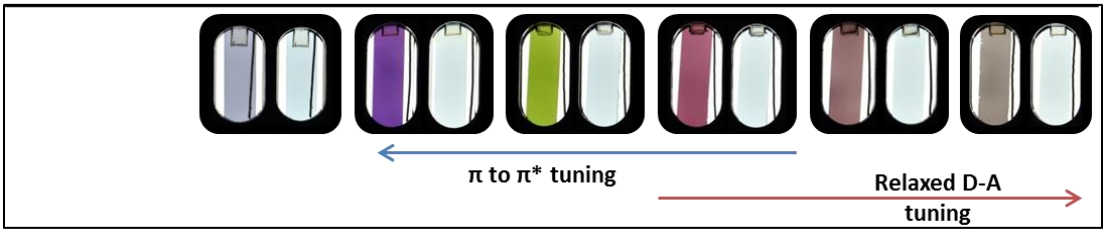

Figure 6.2.3.4: Photographical and numerical comparison of colors achieved with the polymers described herein this section.

P2.23 would have been ideal due to it having the shallowest window in its neutral state spectrum and the highest contrast but because it allows uneven stimulation of the eye, it appears purple. Based on what has been shown above with increasing relaxed acceptor

content, this could be amended to give a material that would be black with the most transmissive state to date.

6.3. Summary of Broadly Absorbing Polymers Containing Relaxed Acceptors

In section 6.1 we examined how increasing backbone strain in random copolymers can give absorption of shorter wavelength light, making the neutral state absorption broader across the visible, as seen with P2.21. This increase in broadness gave higher contrast across 380-780 nm ($\Delta\%T_{int}$: 39.1 %) but it was a minimal improvement over ECP-Black ($\Delta\%T_{int}$: 34.2%). To increase the contrast further, the relaxed donor-acceptor trimer EBE was used as this would allow greater delocalization of charge carriers of fully oxidized states, giving higher transmittance as covered in section 6.2. With this EBE system and tuning steric strain through AcDOT incorporation, new, high contrast hues of purple (P2.23), dark red (P2.25), and green (P2.24) ECPs were produced from lower to higher strain respectively. Increasing the content of the EBE moiety gave high contrast dark red (P2.25), brown (P2.26), and black/brown (P2.27)-to-transmissive ECPs from lower to higher EBE equivalencies respectively. Increasing EBE content did not deplete contrast. P2.27 gave a material that appeared black/brown to the eye in the neutral state (L*, a*, b* of 45, 5, 3) that once fully oxidized, switched to a highly transmissive state (88, -4, -3) with dramatically improved contrast across the visible ($\Delta\%T_{int}$: 51.7 %). P2.27 closes this chapter and the relaxed donor-acceptor model leads the way in continuing to enhance contrast in broadly absorbing ECPs.

CHAPTER 7

OUTLOOK AND PERSPECTIVE

The materials discussed in this thesis excel in their performance for electrochromic applications. As demonstrated, the properties can be modulated in a facile manner using synthetic approaches to tune the steric or D-A CT interactions along the backbone to achieve desired electrochromic functionality. The three main foci of work accomplished in this dissertation are illustrated in Figure 7.1

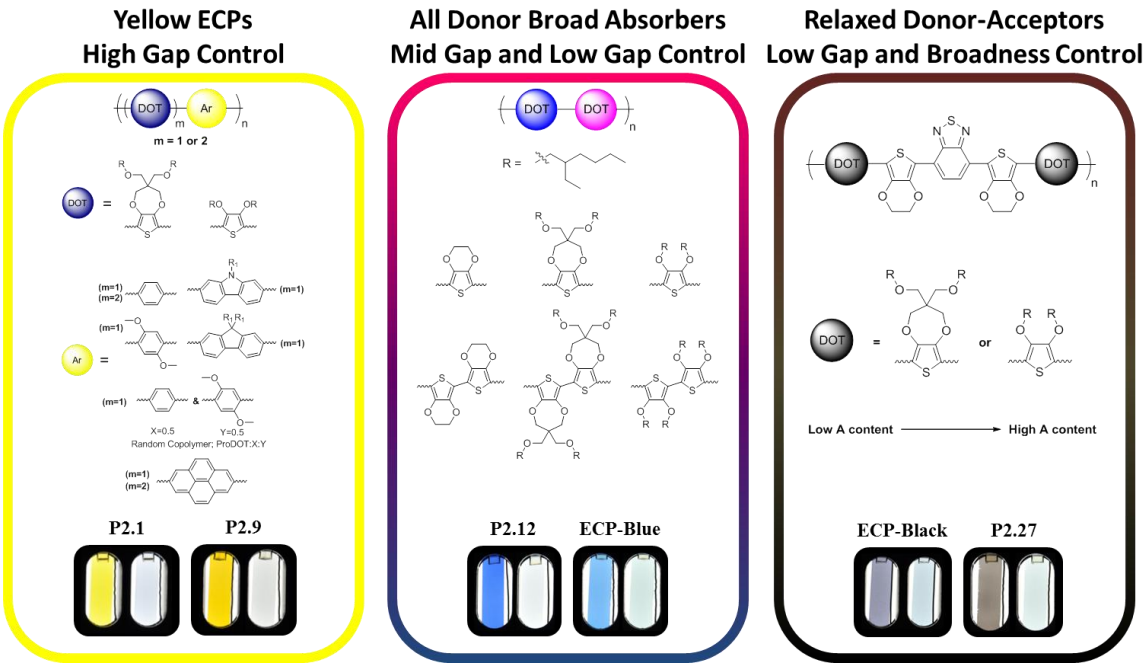

Figure 7.1: Three complete stories summarizing the work of this dissertation.

Through synthetic control of high gaps in Chapter 4, the palette of colored-to-transmissive ECPs was completed with P2.1, allowing full color devices to be realized and then fully optimized with P2.9. In Chapter 5, steric interactions in the form of strain and relaxation were explored in all donor dioxythiophene-alternating copolymers to

explore synthetic color control. When compared to donor-acceptor based polymers, the all donors exhibit higher contrast in the fully oxidized states. This observation was utilized in a variety of attempts to produce high contrast broadly absorbing polymers to enhance ECP-Black. Though this was not successful it was discovered that acceptors are needed to achieve the desired broad absorption, leading to chapter 6. Based on the revelations in Chapter 5 and previous ECP-Greens, a relaxed donor-acceptor architecture was used to achieve broadly absorbing polymers with considerably higher contrast than ECP-Black. This is exemplified with P2.27, a polymer with the highest contrast across the visible while being the darkest neutral state polymer to date thus enabling the applications of ECPs in eyewear or windows.

The future of these materials now lies in addressing the photooxidation that has plagued these ECPs,[144] processing from aqueous solvents or alcohols to avoid chlorinated solvents, and continuing studies into new methods achieve even higher contrast broadly absorbing ECPs to create better performing polymers for dark-to-transmissive device applications.

REFERENCES

1. Tipler, P. A.; Mosca, G., *Physics For Scientists and Engineers, Volume 2B, Electrodynamics and Light.* 2004.

2. Lekner, J., *Theory of Reflection of Electromagnetic and Particle Waves.* 1987.

3. Craig, F. B.; Donald, R. H., *Absorption and Scattering of Light by Small Particles.* 1983.

4. Kaihovirta, N.; Larsen, C.; Edman, L., "Improving the Performance of Light-Emitting Electrochemical Cells by Optical Design," *ACS Appl. Mater. Interfaces* **2014**, *6* (4), 2940.

5. Bhuvana, T.; Kim, B.; Yang, X.; Shin, H.; Kim, E., "Reversible full-color generation with patterned yellow electrochromic polymers," *Angew. Chem. Int. Ed.* **2013**, *52* (4), 1180.

6. Berns, R. S., *Billmeyer and Saltzman's Principles of Color Technology*. 3rd ed.; John Wiley & Sons: New York, 2000.

7. Ohta, N.; Robertson, A. R., CIE Standard Colorimetric System. In *Colorimetry*, John Wiley & Sons, Ltd: 2006; pp 63-114.

8. [Online] http://micro.magnet.fsu.edu/primer/lightandcolor/humanvisionintro.html (accessed 20 May 2014).

9. Ohta, N.; Robertson, A. R., Light, Vision and Photometry. In *Colorimetry*, John Wiley & Sons, Ltd: 2006; pp 1-38.

10. Mortimer, R. J.; Varley, T. S., "Quantification of colour stimuli through the calculation of CIE chromaticity coordinates and luminance data for application to in situ colorimetry studies of electrochromic materials," *Displays* **2011**, *32* (1), 35.

11. McNeill, R.; Siudak, R.; Wardlaw, J.; Weiss, D., "Electronic Conduction in Polymers. I. The Chemical Structure of Polypyrrole," *Aust. J. Chem.* **1963**, *16* (6), 1056.

12. Heeger, A. J., "Semiconducting and metallic polymers: The fourth generation of polymeric materials," *Reviews of Modern Physics* **2001**, *73* (3), 681.

13. Shirakawa, H.; Louis, E. J.; MacDiarmid, A. G.; Chiang, C. K.; Heeger, A. J., "Synthesis of electrically conducting organic polymers: halogen derivatives of polyacetylene," *J. Chem. Soc., Chem. Commun.* **1977**, 578.

14. Salzner, U.; Lagowski, J. B.; Pickup, P. G.; Poirier, R. A., "Comparison of geometries and electronic structures of polyacetylene, polyborole, polycyclopentadiene, polypyrrole, polyfuran, polysilole, polyphosphole, polythiophene, polyselenophene and polytellurophene," *Synth. Met.* **1998**, *96* (3), 177.

15. Street, J. L. B. a. G. B., "Polarons, Bipolarons, and Solitons," *Acc. Chem. Res.* **1985**, *18*, 309.

16. Bubnova, O.; Khan, Z.U.; Wang, H.; Braun, S.; Evans, D. R.; Fabretto, M.; Hojati-Talemi, P.; Dagnelund, D.; Arlin, J-B.; Geerts, Y. H.; Desbief, S.; Breiby, D. W.; Andreasen, J. W.; Lazzaroni, R.; Chen, W. M.; Zozoulenko, I.; Fahlman, M.; Murphy, P.J.; Berggren, M.; Crispin, X., "Semi-metallic polymers," *Nature Materials* **2014**, *13*, 190.

17. Street, G. B.; Clarke, T. C.; Geiss, R. H.; Lee, V. Y.; Nazzal, A.; Pfluger, P.; Scott, J. C., "Characterization of Polypyrrole," *J. Phys.* **1983**, *44*, 599.

18. Garnier, F.; Tourillion, G.; Gazard, M.; Dubois, J. C., Organic Conducting Polymers Derived from Substituted Thiophenes as Electrochromic Material," *Electroanal. Chem.* **1983**, *148*, 299

19. Hyodo, K., "Electrochromism of Conducting Polymers," *Electrochim. Acta* **1994**, *39* (2), 265.

20. Mortimer, R. J., "Electrochromic Materials," *Chem. Soc. Rev.* **1997**, *26*, 147.

21. Roncali, J., "Conjugated Poly(thiophenes): Synthesis, Functionalizatlon, and Applications," *Chem. Rev.* **1992**, *92*, 711.

22. Skotheim, T. A.; Reynolds, J. R., *Hand Book of Conducting Polymers*. 3rd ed.; CRC Press, Taylor and Francis: Florida, 2007.

23. Mitchell, G. R.; Davis, F. J.; Legge, C. H., "The effect of dopant molecules on the molecular order of electrically-conducting films of polypyrrole," *Synth. Met.* **1988**, *26* (3), 247.

24. Heywang, G.; Jonas, F., "Poly(alkylenedioxy-thiophene)s-New, Very Stable Conducting Polymer," *Adv. Mater.* **1992**, *4* (2), 116.

25. Merz, A.; Rehm, C., "Improved Preparation of 3,4-Dimethoxythiophene" *J. Prakt. Chem. /Chem-Ztg* **1996**, *338* (1), 672.

26. Groenendaal, L.; Jonas, F.; Freitag, D.; Pielartzik, H.; Reynolds, J. R., "Poly(3,4-ethylenedioxythiophene) and Its Derivatives: Past, Present, and Future," *Adv. Mater.* **2000**, *12* (7), 481.

27. Kieseritzky, v. F.; Allared, F.; Dahlstedt, E.; Hellberg, J., "Simple one-step synthesis of 3,4-dimethoxythiophene and its conversion into 3,4-ethylenedioxythiophene (EDOT)," *Tetrahedron Lett.* **2004**, *45* (31), 6049.

28. Janda, M.; ŠRogl, J.; Stibor, I.; NĚMec, M.; VopatrnÁ, P., "Polylithiothiophenes and a Convenient Synthesis of Polymethylthiophenes," *Synthesis* **1972**, 545.

29. Gronowitz, S., "New Syntheses of 3-Bromothiophene and 3,4-Dibromothiophene," *Acta Chem. Scand.* **1959**, *13*, 1045.

30. Keegstra, M. A.; Peters, T. H. A.; Brandsma, L., "Copper(I) halide catalyzed synthesis of alkyl aryl and alkyl heteroaryl ethers," *Tetrahedron* **1992**, *48* (17), 3633.

31. Beaujuge, P. M.; Amb, C. M.; Reynolds, J. R., "A side-chain defunctionalization approach yields a polymer electrochrome spray-processable from water," *Adv. Mater.* **2010**, *22* (47), 5383.

32. Dyer, A. L.; Craig, M. R.; Babiarz, J. E.; Kiyak, K.; Reynolds, J. R., "Orange and Red to Transmissive Electrochromic Polymers Based on Electron-Rich Dioxythiophenes," *Macromolecules* **2010**, *43* (10), 4460.

33. Reeves, B. D.; Grenier, C. R. G.; Argun, A. A.; Cirpan, A.; McCarley, T. D.; Reynolds, J. R., "Spray Coatable Electrochromic Dioxythiophene Polymers with High Coloration Efficiencies," *Macromolecules* **2004**, *37* (20), 7559..

34. Dey, T.; Invernale, M. A.; Ding, Y.; Buyukmumcu, Z.; Sotzing, G. A., "Poly(3,4-propylenedioxythiophene)s as a Single Platform for Full Color Realization," *Macromolecules* **2011**, *44* (8), 2415.

35. Lin, C.; Endo, T.; Takase, M.; Iyoda, M.; Nishinaga, T., "Structural, optical, and electronic properties of a series of 3,4-propylenedioxythiophene oligomers in neutral and various oxidation States," *J. Am. Chem. Soc.* **2011**, *133* (29), 11339.

36. Song, I. Y.; Park, S.-H.; Lim, J.; Kwon, Y. S.; Park, T., "A novel hole transport material for iodine-free solid state dye-sensitized solar cells," *Chem. Commun.* **2011**, *47* (37), 10395.

37. Kumar, A.; Reynolds, J. R., "Soluble Alkyl-Substituted Poly(ethylene-dioxythiophenes) as Electrochromic Materials," *Macromolecules* **1996**, *29* (23), 7629.

38. Miomandre, F.; Audebert, P.; Zong, K.; Reynolds, J. R., "Adsorption-Assisted Electro-oxidation of Dioxypyrrole and Dioxythiophene Monomers Probed by Fast Cyclic Voltammetry," *Langmuir* **2003**, *19* (21), 8894.

39. Estrada, L. A.; Deininger, J. J.; Kamenov, G. D.; Reynolds, J. R., "Direct (Hetero)arylation Polymerization: An Effective Route to 3,4-Propylene-dioxythiophene-Based Polymers with Low Residual Metal Content," *ACS Macro Letters* **2013**, *2* (10), 869.

40. Zhao, H.; Liu, C.-Y.; Luo, S.-C.; Zhu, B.; Wang, T.-H.; Hsu, H.-F.; Yu, H.-h., "Facile Syntheses of Dioxythiophene-Based Conjugated Polymers by Direct C–H Arylation," *Macromolecules* **2012**, *45* (19), 7783.

41. McEntee, G. J.; Skabara, P. J.; Vilela, F.; Tierney, S.; Samuel, I. D. W.; Gambino, S.; Coles, S. J.; Hursthouse, M. B.; Harrington, R. W.; Clegg, W., "Synthesis and Electropolymerization of Hexadecyl Functionalized Bithiophene and Thieno[3,2-

b]thiophene End-Capped with EDOT and EDTT Units," *Chem. Mater.* **2010**, *22* (9), 3000.

42. Shi, P.; Amb, C. M.; Knott, E. P.; Thompson, E. J.; Liu, D. Y.; Mei, J.; Dyer, A. L.; Reynolds, J. R., "Broadly Absorbing Black to Transmissive Switching Electrochromic Polymers," *Adv. Mater.* **2010**, *22* (44), 4949.

43. Spencer, H. J.; Skabara, P. J.; Giles, M.; McCulloch, I.; Coles, S. J.; Hursthouse, M. B., "The first direct experimental comparison between the hugely contrasting properties of PEDOT and the all-sulfur analogue PEDTT by analogy with well-defined EDTT-EDOT copolymers," *Mater. Chem.* **2005,** *15* (45), 4783.

44. Dyer, A. L.; Thompson, E. J.; Reynolds, J. R., "Completing the Color Palette with Spray-Processable Polymer Electrochromics," *ACS Appl. Mater. Interfaces* **2011,** *3* (6), 1787.

45. Kerszulis, J. A.; Amb, C. M.; Dyer, A. L.; Reynolds, J. R., "Follow the Yellow Brick Road: Structural Optimization of Vibrant Yellow-to-Transmissive Electrochromic Conjugated Polymers," *Macromolecules* **2014,** *47* (16), 5462.

46. Amb, C. M.; Kerszulis, J. A.; Thompson, E. J.; Dyer, A. L.; Reynolds, J. R., "Propylenedioxythiophene (ProDOT)–phenylene copolymers allow a yellow-to-transmissive electrochrome," *Polym. Chem.* **2011,** *2* (4), 812.

47. Amb, C. M.; Beaujuge, P. M.; Reynolds, J. R., "Spray-Processable Blue-to-Highly Transmissive Switching Polymer Electrochromes via the Donor–Acceptor Approach," *Adv. Mater.* **2010,** *22* (6), 724.

48. Beaujuge, P. M.; Amb, C. M.; Reynolds, J. R., "Spectral Engineering in π-Conjugated Polymers with Intramolecular Donor−Acceptor Interactions," *Acc. Chem. Res.* **2010,** *43* (11), 1396

49. Beaujuge, P. M.; Vasilyeva, S. V.; Liu, D. Y.; Ellinger, S.; McCarley, T. D.; Reynolds, J. R., "Structure-Performance Correlations in Spray-Processable Green Dioxythiophene-Benzothiadiazole Donor–Acceptor Polymer Electrochromes," *Chem. Mater.* **2012,** *24* (2), 255.

50. Beaujuge, P. M.; Ellinger, S.; Reynolds, J. R., "Spray Processable Green to Highly Transmissive Electrochromics via Chemically Polymerizable Donor–Acceptor Heterocyclic Pentamers," *Adv. Mater.* **2008,** *20* (14), 2772.

51. Beaujuge, P. M.; Ellinger, S.; Reynolds, J. R., "The donor-acceptor approach allows a black-to-transmissive switching polymeric electrochrome," *Nat. Mater.* **2008,** *7* (10), 795.

52. Knott, E. P.; Craig, M. R.; Liu, D. Y.; Babiarz, J. E.; Dyer, A. L.; Reynolds, J. R., "A minimally coloured dioxypyrrole polymer as a counter electrode material in polymeric electrochromic window devices," *J. Mater. Chem.* **2012,** *22* (11), 4953.

53. Walczak, R. M. "Synthetic methodology as a basis for conducting polymer design," Dissertation, University of Florida, 2006.

54. Arroyave, F. "Methodologies for the Synthesis of 3,4-Dioxypyrrole-based pi-Conjugated Materials," Dissertation, University of Florida, 2011.

55. Granqvist, C. G., "Electrochromics for smart windows: Oxide-based thin films and devices," *Thin Solid Films* **2014**, *564*, 1.

56. Mortimer, R. J., "Electrochromic Materials," *Annual Review of Materials Research* **2011,** *41* (1), 241.

57. Corr, D.; Fay, D.; Ryan, M.; Walder, L.; Moller, M.; Asaftei, S., "High Resolution Electrochromic Displays for E-Readers," *SID Symposium Digest of Technical Papers* **2012,** *36* (1), 750.

58. Periyat, P.; Leyland, N.; McCormack, D. E.; Colreavy, J.; Corr, D.; Pillai, S. C., "Rapid microwave synthesis of mesoporous TiO_2 for electrochromic displays," *J. Mater. Chem.* **2010,** *20* (18), 3650.

59. Forgette, J. A.; Byker, H. J.; Tonar, W. L.; Bauer, F., T.; Cammenga, D. J.; Roberts, J. K. "Electrochromic rearview mirror incorporating a third surface metal reflector and a display/signal light," US6356376 B1, 2000.

60. Bonhote, P.; Gogniat, E.; Campus, F.; Walder, L.; Gratzel, M., "Nanocrystalline electrochromic displays," *Displays* **1999,** *20*, 137.

61. Dyer, A. L.; Grenier, C. R. G.; Reynolds, J. R., "A Poly(3,4-alkylene-dioxythiophene) Electrochromic Variable Optical Attenuator with Near-Infrared Reflectivity Tuned Independently of the Visible Region," *Adv. Funct. Mater.* **2007,** *17*, 1480.

62. Cirpan, A.; Argun, A. A.; Grenier, C. R. G.; Reeves, B. D.; Reynolds, J. R., "Electrochromic devices based on soluble and processable dioxythiophene polymers," *J. Mater. Chem.* **2003,** *13*, 2422.

63. Dyer, A. L. "Conjugated Polymer Electrochromic and Light-Emitting Devices," Dissertation, University of Florida, 2007.

64. Vasilyeva, S. V.; Beaujuge, P. M.; Wang, S.; Babiarz, J. E.; Ballarotto, V. W.; Reynolds, J. R., "Material Strategies for Black-to-Transmissive Window-Type Polymer Electrochromic Devices," *ACS. Appl. Mater. Interfaces* **2011,** *3* (4), 1022.

65. Byker, H. J. G. C. "Single-Compartment, self-erasing, solution-phase electrochromic devices, solutions for use therein and uses thereof," EP0240226 A3, 1990.

66. Byker, H. J., "Commercial developments in electrochromics," *Proc. Electrochem. Soc.* **1994,** *94* (2), 1.

67. Hoekstra, E. J.; Schierbeck, K. L. "Digital electrochromic mirror system," US 6595649 B2, 2000.

68. Baucke, F. G. K., "Reflecting electrochromic devices-construction, operation, and application," *Proc. Electrochem. Soc.* **1990,** *20* (4), 298.

69. Gesheva, K.; Ivanova, T.; Hamelmann, F., "Optical coatings of CVD-transition metal oxides as functional layers in smart windows and X-ray mirrors," *J. Optoelectronics Adv. Mater.* **2005,** *7*, 1243.

70. Svensson, J. S. E. M.; Granqvist, C. G., "Electrochromic coatings for 'smart windows'," *Sol. Energy. Mater.,* **1985,** *12*, 391.

71. Rauh, R. D., "Electrochromic windows: an overview," *Electrochim. Acta.* **1999,** *44*, 3165.

72. Lee, E. S.; DiBartolomeo, D. L., "Application issues for large-area electrochromic windows in commercial buildings," *Sol. Energy. Mater. Sol. Cells* **2002,** *71*, 465.

73. Azens, A.; Granqvist, C. G., "Electrochromic smart windows: energy efficiency," *J. Solid State Electrochem.* **2003,** *7*, 64.

74. Zinzi, M., "Office worker preferences of electrochromic windows: a pilot study," *Buildings and Environment* **2005,** *41*, 1262.

75. Baetens, R.; Jelle, B. P.; Gustavsen, A., "Properties, requirements and possibilities of smart windows for dynamic daylight and solar energy control in buildings: A state-of-the-art review," *Sol. Energy. Mater. Sol. Cells* **2010,** *94* (2), 87.

76. [Online] http://viewglass.com/portfolio/. (accessed 15 May 2014).

77. [Online] http://sageglass.com/portfolio/. (accessed 15 May 2014).

78. [Online] http://www.Gentex.com. (accessed 15 May 2014).

79. John Barratt, K. D., "A New Airplane for a New World: The 787 Dreamliner," *Design Management Review* **2006,** *17* (4), 25.

80. Kallman, W. R.; Roberts, M. B.; Baretich, D. F.; Dorfman, L. M.; Ahern, J. F. "Electrochromic eyewear system, rechargeable eyewear and external charger therefor," US5455637 A, 1995.

81. [Online] Karp, A. "The Well-Adjusted Spectacle," http://www.2020mag.com/l-and-t/37492/ (accessed 16 May 2014).

82. [Online] http://www.ashwin-ushas.com/EleHome/Electrochromic_Sunglasses_-Vid/index.html, (accessed 16 May 2014).

83. Xu, C.; Ma, C.; Taya, M. "Smart sunglasses, helmet faceshields and goggles based on electrochromic polymers," US7874666 B2, 2011.

84. Byker, H. J., "Electrochromics and Polymers," *Electrochum. Acta* **2001,** *46*, 2015.

85. Möller, M.; Leyland, N.; Copeland, G.; Cassidy, M., "Self-powered electrochromic display as an example for integrated modules in printed electronics applications," *The European Physical Journal Applied Physics* **2010,** *51* (3), 33205.

86. Corr, D., “Coloured electrochromic “paper-quality” displays based on modified mesoporous electrodes,” *Solid State Ionics* **2003,** *165* (1-4), 315.

87. Bulloch, R. H.; Kerszulis, J. A.; Dyer, A. L.; Reynolds, J. R., “Mapping the Broad CMY Subtractive Primary Color Gamut Using a Dual-Active Electrochromic Device,” *ACS Appl. Mater. Interfaces* **2014,** *6* (9), 6623.

88. Watanabe, Y.; Nagashima, T.; Nakamura, K.; Kobayashi, N., “Continuous-tone images obtained using three primary-color electrochromic cells containing gel electrolyte,” *Sol. Energy Mater. Sol. Cells* **2012,** *104*, 140.

89. Kondo, Y.; Tanabe, H.; Kudo, H.; Nakano, K.; Otake, T., “Electrochromic Type E-Paper Using Poly(1H-Thieno[3,4-d]Imidazol-2(3H)-One) Derivatives by a Novel Printing Fabrication Process,” *Materials* **2011,** *4* (12), 2171.

90. Schoot, C. J.; Ponjee, J. J.; van Dam, H. T.; van Doorn, R. A.; Bolwijn, P. J., “New electrochromic memory device,” *Appl. Phys. Lett.* **1973,** *23*, 64.

91. [Online] www.napa.ufl.edu/2001news/colors.htm, (accessed 16 May 2014).

92. Reynolds, J. R.; Zong, K.; Schwendeman, I.; Sonmez, G.; Schottlant, P.; Argun, A. A.; Aubert, P. H. “Controlling color, brightness and environmental stability; poly-3,4-alkylenedioxyheterocycles,” US6791738 B2, 2004.

93. Tadashi, N. “Cash card having electrochromic indicator,” JP59197980, 1984.

94. Baloukas, B.; Lamarre, J. M.; Martinu, L., “Active metameric security devices using an electrochromic material,” *Appl. Opt.* **2011,** *50* (9), 41.

95. [Online] http://www.mobileread.com/forums/showthread.php?threadid=3375, (accessed 16 May 2014).

96. Puodziukynaite, E.; Oberst, J. L.; Dyer, A. L.; Reynolds, J. R., “Establishing dual electrogenerated chemiluminescence and multicolor electrochromism in functional ionic transition-metal complexes,” *J. Am. Chem. Soc.* **2012,** *134* (2), 968.

97. Reynolds, J. R.; Dyer, A. L. “Interdigitated electrode dual electroemissive/electrochromic devices,” WO2009129275 A1, 2012.

98. Liu, H.; Crooks, R. M., "Paper-based electrochemical sensing platform with integral battery and electrochromic read-out," *Anal. Chem.* **2012,** *84* (5), 2528.

99. Ding, Y.; Invernale, M. A.; Sotzing, G. A., "Conductivity trends of PEDOT-PSS impregnated fabric and the effect of conductivity on electrochromic textile," *ACS Appl. Mater. Interfaces* **2010,** *2* (6), 1588.

100. Tehrani, P.; Hennerdal, L. O.; Dyer, A. L.; Reynolds, J. R.; Berggren, M., "Improving the contrast of all-printed electrochromic polymer on paper displays," *J. Mater. Chem.* **2009,** *19*, 1799.

101. Imamura, A.; Kimura, M.; Kon, T.; Sunohara, S.; Kobayashi, N., "Bi-based electrochromic cell with mediator for white/black imaging," *Sol. Energy Mater. Sol. Cells* **2009,** *93*, 2079.

102. Monk, P. M. S.; Mortimer, R. J.; Rosseinsky, D. R., *Electrochromism and Electrochromic Devices*. 2007.

103. Ten-Hoeve, W.; Wynberg, H.; Havinga, E. E.; Meijer, E. W., "Substituted 2,2':5',2":5",2"':5"',2"":5"",2""':5""':2""":5""",2"""":5""",2""":5""",2""":5""",2""":5""",2""":5""",2""":5""",2""":5"""-undecithiophenes, the longest characterized oligothiophenes," *J. Am. Chem. Soc.* **1991,** *113* (15), 5887.

104. Gowri, R.; Mandal, D.; Shivkumar, B.; Ramakrishnan, S., "Synthesis of Novel Poly[(2,5-dimethoxy-p-phenylene)vinylene] Precursors Having Two Eliminatable Groups: An Approach for the Control of Conjugation Length," *Macromolecules* **1998,** *31* (6), 1819.

105. Ferron, C. C.; Delgado, M. C. R.; Gidron, O.; Sharma, S.; Sheberla, D.; Sheynin, Y.; Bendikov, M.; Navarrete, J. T. L.; Hernandez, V., "α-Oligofurans show a sizeable extent of π-conjugation as probed by Raman spectroscopy," *Chem. Commun.* **2012,** *48* (53), 6732.

106. Jin, X.-H.; Sheberla, D.; Shimon, L. J. W.; Bendikov, M., "Highly Coplanar Very Long Oligo(alkylfuran)s: A Conjugated System with Specific Head-To-Head Defect," *J. Am. Chem. Soc.* **2014,** *136* (6), 2592.

107. Meier, H.; Stalmach, U.; Kolshorn, H., "Effective conjugation length and UV/vis spectra of oligomers," *Acta Polym.* **1997,** *48* (9), 379.

108. Izumi, T.; Kobashi, S.; Takimiya, K.; Aso, Y.; Otsubo, T., "Synthesis and Spectroscopic Properties of a Series of β-Blocked Long Oligothiophenes up to the 96-mer: Revaluation of Effective Conjugation Length," *J. Am. Chem. Soc.* **2003,** *125* (18), 5286.

109. Nakanishi, H.; Sumi, N.; Aso, Y.; Otsubo, T., "Synthesis and Properties of the Longest Oligothiophenes: The Icosamer and Heptacosamer," *J. Org. Chem.* **1998,** *63* (24), 8632.

110. Ng, S. C.; Xu, J. M.; Chan, H. S. O., "Synthesis and Characterization of Regioregular Polymers Containing Substituted Thienylene/Bithienylene and Phenylene Repeating Units," *Macromolecules* **2000,** *33* (20), 7349.

111. Heinze, J.; Frontana-Uribe, B. A.; Ludwigs, S., "Electrochemistry of Conducting Polymers—Persistent Models and New Concepts," *Chem. Rev.* **2010,** *110* (8), 4724.

112. Yang, C.; Orfino, F. P.; Holdcroft, S., "A Phenomenological Model for Predicting Thermochromism of Regioregular and Nonregioregular Poly(3-alkylthiophenes)," *Macromolecules* **1996,** *29* (20), 6510.

113. Leclerc, M.; Diaz, F. M.; Wegner, G., "Structural analysis of poly(3-alkylthiophene)s," *Die Makromolekulare Chemie* **1989,** *190* (12), 3105.

114. Carsten, B.; He, F.; Son, H. J.; Xu, T.; Yu, L., "Stille Polycondensation for Synthesis of Functional Materials," *Chem. Rev.* **2011,** *111* (3), 1493.

115. Chang, L. W., 2-1. "The neurotoxicology and pathology of organomercury, organolead, and organotin," *The Journal of Toxicological Sciences* **1990,** *15*, 125.

116. Amatore, C.; Jutand, A.; Le Duc, G., "Kinetic Data for the Transmetalation/Reductive Elimination in Palladium-Catalyzed Suzuki–Miyaura Reactions: Unexpected Triple Role of Hydroxide Ions Used as Base," *Chem. Eur. J.* **2011,** *17* (8), 2492.

117. Amatore, C.; Jutand, A.; Le Duc, G., "The triple role of fluoride ions in palladium-catalyzed Suzuki-Miyaura reactions: unprecedented transmetalation from [$ArPdFL_2$] complexes," *Angew. Chem. Int. Ed.* **2012,** *51* (6), 1379.

118. d'Orlyé, F.; Jutand, A., "In situ formation of palladium(0) from a P,C-palladacycle," *Tetrahedron* **2005,** *61* (41), 9670

119. Amatore, C.; Jutand, A., "Anionic Pd(0) and Pd(II) Intermediates in Palladium-Catalyzed Heck and Cross-Coupling Reactions," *Acc. Chem. Res.* **2000,** *33* (5), 314.

120. Giovannini, R.; Knochel, P., "Ni(II)-Catalyzed Cross-Coupling between Polyfunctional Arylzinc Derivatives and Primary Alkyl Iodides," *J. Am. Chem. Soc.* **1998,** *120* (43), 11186.

121. Brookins, R. N.; Schanze, K. S.; Reynolds, J. R., "Base-Free Suzuki Polymerization for the Synthesis of Polyfluorenes Functionalized with Carboxylic Acids," *Macromolecules* **2007,** *40* (10), 3524.

122. Walczak, R. M.; Brookins, R. N.; Savage, A. M.; van der Aa, E. M.; Reynolds, J. R., "Convenient Synthesis of Functional Polyfluorenes *via* a Modified One-Pot Suzuki−Miyaura Condensation Reaction," *Macromolecules* **2009,** *42* (5), 1445.

123. Stalder, R.; Mei, J.; Subbiah, J.; Grand, C.; Estrada, L. A.; So, F.; Reynolds, J. R., "n-Type Conjugated Polyisoindigos," *Macromolecules* **2011,** *44* (16), 6303-6310.

124. Liu, M.; Chen, Y.; Zhang, C.; Li, C.; Li, W.; Bo, Z., "Synthesis of thiophene-containing conjugated polymers from 2,5-thiophenebis(boronic ester)s by Suzuki polycondensation," *Polym. Chem.* **2013,** *4* (4), 895.

125. Hitosugi, S.; Tanimoto, D.; Nakanishi, W.; Isobe, H., "A Facile Chromatographic Method for Purification of Pinacol Boronic Esters," *Chem. Lett.* **2012,** *41* (9), 972.

126. Rossi, R.; Bellina, F.; Lessi, M.; Manzini, C., "Cross-Coupling of Heteroarenes by C-H Functionalization: Recent Progress towards Direct Arylation and Heteroarylation Reactions Involving Heteroarenes Containing One Heteroatom," *Adv. Synth. Catal.* **2014,** *356* (1), 17.

127. Ackermann, L.; Vicente, R.; Kapdi, A. R., "Transition-Metal-Catalyzed Direct Arylation of (Hetero)Arenes by C-H Bond Cleavage," *Angew. Chem. Int. Ed.* **2009,** *48* (52), 9792.

128. Mercier, L. G.; Leclerc, M., "Direct (Hetero)Arylation: A New Tool for Polymer Chemists," *Acc. Chem. Res.* **2013,** *46* (7), 1597.

129. Kowalski, S.; Allard, S.; Zilberberg, K.; Riedl, T.; Scherf, U., "Direct arylation polycondensation as simplified alternative for the synthesis of conjugated (co)polymers," *Prog. Polym. Sci.* **2013,** *38* (12), 1805.

130. Grenier, F.; Berrouard, P.; Pouliot, J.-R.; Tseng, H.-R.; Heeger, A. J.; Leclerc, M., "Synthesis of new n-type isoindigo copolymers," *Polym. Chem.* **2013,** *4* (6), 1836.

131. Berrouard, P.; Najari, A.; Pron, A.; Gendron, D.; Morin, P.-O.; Pouliot, J.-R.; Veilleux, J.; Leclerc, M., "Synthesis of 5-Alkyl[3,4-c]thienopyrrole-4,6-dione-Based Polymers by Direct Heteroarylation," *Angew. Chem. Int. Ed.* **2012,** *51* (9), 2068.

132. Rudenko, A. E.; Wiley, C. A.; Tannaci, J. F.; Thompson, B. C., "Optimization of direct arylation polymerization conditions for the synthesis of poly(3-hexylthiophene)," *J. Polym. Sci., Part A: Polym. Chem.* **2013,** *51* (12), 2660.

133. Rudenko, A. E.; Wiley, C. A.; Stone, S. M.; Tannaci, J. F.; Thompson, B. C., "Semi-random P3HT analogs via direct arylation polymerization," *J. Polym. Sci., Part A: Polym. Chem.* **2012,** *50* (18), 3691.

134. Lu, W.; Kuwabara, J.; Iijima, T.; Higashimura, H.; Hayashi, H.; Kanbara, T., "Synthesis of π-Conjugated Polymers Containing Fluorinated Arylene Units via Direct Arylation: Efficient Synthetic Method of Materials for OLEDs," *Macromolecules* **2012,** *45* (10), 4128.

135. Kuwabara, J.; Nohara, Y.; Choi, S. J.; Fujinami, Y.; Lu, W.; Yoshimura, K.; Oguma, J.; Suenobu, K.; Kanbara, T., "Direct arylation polycondensation for the synthesis of bithiophene-based alternating copolymers," *Polym. Chem.* **2013,** *4* (4), 947.

136. Lu, W.; Kuwabara, J.; Kanbara, T., "Synthesis of π-Conjugated Polymer Consisting of Pyrrole and Fluorene Units by Ru-Catalyzed Site-Selective Direct Arylation Polycondensation," *Macromol. Rapid Commun.* **2013,** *34* (14), 1151.

137. Lafrance, M.; Fagnou, K., "Palladium-Catalyzed Benzene Arylation: Incorporation of Catalytic Pivalic Acid as a Proton Shuttle and a Key Element in Catalyst Design," *J. Am. Chem. Soc.* **2006,** *128* (51), 16496.

138. Lafrance, M.; Lapointe, D.; Fagnou, K., "Mild and efficient palladium-catalyzed intramolecular direct arylation reactions," *Tetrahedron* **2008,** *64* (26), 6015.

139. Wang, Q.; Takita, R.; Kikuzaki, Y.; Ozawa, F., "Palladium-Catalyzed Dehydrohalogenative Polycondensation of 2-Bromo-3-hexylthiophene: An Efficient Approach to Head-to-Tail Poly(3-hexylthiophene)," *J. Am. Chem. Soc.* **2010,** *132* (33), 11420.

140. Gorelsky, S. I.; Lapointe, D.; Fagnou, K., "Analysis of the Palladium-Catalyzed (Aromatic)C–H Bond Metalation–Deprotonation Mechanism Spanning the Entire Spectrum of Arenes," *J. Org. Chem.* **2011,** *77* (1), 658.

141. Mccullough, R. D.; Iovu, M. C., "Purification methods and purified conjugated polymers," WO2008063731 A3, 2008.

142. Nielsen, K. T.; Bechgaard, K.; Krebs, F. C., "Removal of Palladium Nanoparticles from Polymer Materials," *Macromolecules* **2005,** *38* (3), 658.

143. [Online] http://anestiwata.com/product-category/airbrushes/. (accessed June 6th 2014).

144. Jensen, J.; Madsen, M. V.; Krebs, F. C., "Photochemical stability of electrochromic polymers and devices," *J. Mater. Chem. C* **2013,** *1* (32), 4826.

145. Kumar, A.; Otley, M. T.; Alamar, F. A.; Zhu, Y.; Arden, B. G.; Sotzing, G. A., "Solid-state electrochromic devices: relationship of contrast as a function of device preparation parameters," *J. Mater. Chem. C* **2014,** *2* (14), 2510.

146. Padilla, J.; Seshadri, V.; Sotzing, G. A.; Otero, T. F., "Maximum contrast from an electrochromic material," *Electrochem. Commun.* **2007,** *9* (8), 1931.

147. Inzelt, G., "Charge Transport in Conducting Polymer Film Electrodes," *Chem. Biochem. Eng. Q.* **2007,** *21* (1), 1.

148. Odin, C.; Nechtschein, M.; Hapiot, P., "Kinetics of the charge-discharge process in conducting polymers: slow relaxation and hysteresis effects. Investigations on polyaniline by millimetric and ultramicroelectrodes," *Synth. Met.* **1992,** *47* (3), 329.

149. Odin, C.; Nechtschein, M., “Slow relaxation in conducting polymers: the case of poly(3-methylthiophene),” *Synth. Met.* **1991,** *44* (2), 177.

150. Pavlishchuk, V. V.; Addison, A. W., “Conversion constants for redox potentials measured versus different reference electrodes in acetonitrile solutions at 25°C,” *Inorg. Chim. Acta* **2000,** *298* (1), 97.

151. Urano, H.; Sunohara, S.; Ohtomo, H.; Kobayashi, N., “Electrochemical and spectroscopic characteristics of dimethylterephthalate,” *J. Mater. Chem.* **2004,** *14* (15), 2366.

152. Liou, G.-S.; Lin, H.-Y., “Synthesis and Electrochemical Properties of Novel Aromatic Poly(amine−amide)s with Anodically Highly Stable Yellow and Blue Electrochromic Behaviors,” *Macromolecules* **2008,** *42* (1), 125.

153. Nielsen, C. B.; Angerhofer, A.; Abboud, K. A.; Reynolds, J. R., “Discrete Photopatternable π-Conjugated Oligomers for Electrochromic Devices,” *J. Am. Chem. Soc.* **2008,** *130* (30), 9734.

154. Oguzhan, E.; Bilgili, H.; Baycan Koyuncu, F.; Ozdemir, E.; Koyuncu, S., “A new processable donor–acceptor polymer displaying neutral state yellow electrochromism,” *Polymer* **2013,** *54* (23), 6283.

155. Xu, C.; Zhao, J.; Yu, J.; Cui, C., “Ethylenedioxythiophene derivatized polynapthalenes as active materials for electrochromic devices,” *Electrochim. Acta* **2013,** *96*, 82.

156. İçli-Özkut, M.; Öztaş, Z.; Algi, F.; Cihaner, A., “A neutral state yellow to navy polymer electrochrome with pyrene scaffold,” *Org. Electron.* **2011,** *12* (9), 1505.

157. Imaizumi, K.; Watanabe, Y.; Nakamura, K.; Omatsu, T.; Kobayashi, N., “Multicolored electrochromism in 4,4'-biphenyl dicarboxylic acid diethyl ester,” *Phys. Chem. Chem. Phys.* **2011,** *13* (25), 11838.

158. Lu, G.; Shi, G., “Electrochemical polymerization of pyrene in the electrolyte of boron trifluoride diethyl etherate containing trifluoroacetic acid and polyethylene glycol oligomer,” *J. Electroanal. Chem.* **2006,** *586* (2), 154.

159. Tang, C.; Liu, F.; Xia, Y.-J.; Xie, L.-H.; Wei, A.; Li, S.-B.; Fan, Q.-L.; Huang, W., "Efficient 9-alkylphenyl-9-pyrenylfluorene substituted pyrene derivatives with improved hole injection for blue light-emitting diodes," *J. Mater. Chem.* **2006,** *16* (41), 4074.

160. Barik, S.; Navarathne, D.; LeBorgne, M.; Skene, W. G., "Conjugated thiophenoazomethines: electrochromic materials exhibiting visible-to-near-IR color changes," *J. Mater. Chem. C* **2013,** *1* (35), 5508.

161. Gunbas, G.; Toppare, L., "Electrochromic conjugated polyheterocycles and derivatives-highlights from the last decade towards realization of long lived aspirations," *Chem. Commun.* **2012,** *48* (8), 1083.

162. Hu, C.-W.; Sato, T.; Zhang, J.; Moriyama, S.; Higuchi, M., "Multi-colour electrochromic properties of Fe/Ru-based bimetallo-supramolecular polymers," *J. Mater. Chem. C* **2013,** *1* (21), 3408.

163. Hu, C.-W.; Sato, T.; Zhang, J.; Moriyama, S.; Higuchi, M., "Three-Dimensional Fe(II)-based Metallo-Supramolecular Polymers with Electrochromic Properties of Quick Switching, Large Contrast, and High Coloration Efficiency," *ACS Appl. Mater. Interfaces* **2014,** *6* (12), 9118.

164. Hossain, M. D.; Zhang, J.; Pandey, R. K.; Sato, T.; Higuchi, M., "A Heterometallo-Supramolecular Polymer with Cu(I) and Fe(II) Ions Introduced Alternately," *Eur. J. Inorg. Chem.* **2014**, 3763.

165. Schott, M.; Lorrmann, H.; Szczerba, W.; Beck, M.; Kurth, D. G., "State-of-the-art electrochromic materials based on metallo-supramolecular polymers," *Sol. Energy Mater. Sol. Cells* **2014,** *126*, 68.

166. Kumar, A.; Welsh, D. M.; Morvant, M. C.; Piroux, F.; Abboud, K. A.; Reynolds, J. R., "Conducting Poly(3,4-alkylenedioxythiophene) Derivatives as Fast Electrochromics with High-Contrast Ratios," *Chem. Mater.* **1998,** *10* (3), 896.

167. Sotzing, G. A.; Reynolds, J. R.; Steel, P. J., "Poly(3,4-ethylenedioxythiophene) (PEDOT) prepared via electrochemical polymerization of EDOT, 2,2′-Bis(3,4-ethylenedioxythiophene) (BiEDOT), and their TMS derivatives," *Adv. Mater.* **1997,** *9* (10), 795.

168. Welsh, D. M.; Kloeppner, L. J.; Madrigal, L.; Pinto, M. R.; Thompson, B. C.; Schanze, K. S.; Abboud, K. A.; Powell, D.; Reynolds, J. R., "Regiosymmetric Dibutyl-Substituted Poly(3,4-propylenedioxythiophene)s as Highly Electron-Rich Electroactive and Luminescent Polymers," *Macromolecules* **2002,** *35* (17), 6517.

169. Grenier, C. R. G.; "Synthetic Control of Order in Soluble Dioxythiophene Polymers," Dissertation, University of Florida: 2006.

170. Reeves, B. D.; Thompson, B. C.; Abboud, K. A.; Smart, B. E.; Reynolds, J. R., "Dual Cathodically and Anodically Coloring Electrochromic Polymer Based on a Spiro-Bipropylenedioxythiophene [(Poly(spiroBiProDOT)]," *Adv. Mater.* **2002,** *14* (10), 717.

171. Elschner, A.; Kirchmeyer, S.; Lovenich, W.; Merker, U.; Reuter, K., *PEDOT: Principles and Applications of an Intrinsically Conductive Polymer*. Taylor & Francis: 2010.

172. Turbiez, M.; Frère, P.; Allain, M.; Videlot, C.; Ackermann, J.; Roncali, J., "Design of Organic Semiconductors: Tuning the Electronic Properties of π-Conjugated Oligothiophenes with the 3,4-Ethylenedioxythiophene (EDOT) Building Block," *Chem. Eur. J.* **2005,** *11* (12), 3742.

173. Leclerc, M., "Optical and Electrochemical Transducers Based on Functionalized Conjugated Polymers," *Adv. Mater.* **1999,** *11* (18), 1491.

174. Leclerc, M.; Fréchette, M.; Bergeron, J.-Y.; Ranger, M.; Lévesque, I.; Faïd, K., "Chromic phenomena in neutral polythiophene derivatives," *Macromol. Chem. Phys.* **1996,** *197* (7), 2077.

175. Mahy, M.; Van Eycken, L.; Oosterlinck, A., "Evaluation of Uniform Color Spaces Developed after the Adoption of CIELAB and CIELUV," *Color Research & Application* **1994,** *19* (2), 105.

VITA

JUSTIN A. KERSZULIS

Justin A. Kerszulis was born in Wintersprings, Florida where he became an aquatic athlete and swim instructor. In 2004, he began his undergraduate career at Florida State University in Tallahassee, Florida where he spent many years finding a profession that was enjoyable. After switching between several majors while taking part in prolonged outreach in the sciences, he graduated in 2009 with a bachelor's of science in chemistry and an unexpected minor in mathematics. In the fall of 2009 he moved down to Gainesville to attend the rival school, University of Florida where he was promptly attracted to the group of Professor John R. Reynolds with a strong desire to learn polymer and electrochemistry with a focus on how molecules produce color. While working in the field of electrochromics, he serendipitously moved with the Reynolds group to the Georgia Institute of Technology in Atlanta. He is planning to graduate at the end of 2014 with a doctoral degree from the Georgia Institute of Technology.